Characterization of Rpn10 monoubiquitination as a novel way of proteasome regulation

Marta Isasa Catalán

Characterization of Rpn10 monoubiquitination as a novel way of proteasome regulation

Marta Isasa Catalán

TESI DOCTORAL UB / ANY 2012

DIRECTOR DE LA TESI

Dr. Bernat Crosas Navarro (Institut de Biologia Molecular de Barcelona – CSIC)

Caracterització de la regulació del proteasoma mitjançant la monoubicüitinació de la subunitat Rpn10

Memòria presentada per Marta Isasa Catalán per obtar a grau de doctor per la Universitat de Barcelona.

Universitat de Barcelona

Departament de Bioquímica i Biologia Molecular

Programa de Doctorat de Biomedicina

Institut de Biologia Molecular de Barcelona

Doctorand: Marta Isasa Catalán

Director: Dr. Bernat Crosas Navarro

Poc sovint una té una excusa tan clara per asseure's amb l'únic objectiu d'expresar la seva gratitud, així que em dono la plena llibertat d'utilitzar la paraula *gràcies* fins a desgastar-la. Aquest ha estat un procés llarg, amb molta gent involucrada, una etapa única de la meva vida que m'ha permès desenvolupar tant a nivell personal com professional. La principal conclusió que n´he extret és que si podés tornar a enrera, escolliria exactament el mateix camí. Han estat uns anys fantàstics.

Gràcies Pare i *gràcies* Mare. Vosaltres sou el meu nucli i empenta, sou els meus valors, sou el que jo voldria ser. *Gràcies* per deixar-me descubrir lliurement. Per a vosaltres no hi han prou *gràcies*, sinó un constant procés d'autosuperació. *Gràcies* Mireia, una germana no es pot escollir però els amics sí. Sé que amb tu tinc les dues coses, moltes *gràcies* per ser-hi sempre. *Gràcies* a la meva Josepeta, la teva generositat i estima són infinites, *gràcies* pels millors estius. *Gràcies* als meus dos avis, l´herència ha estat enorme.

Gràcies Laia, fas que tot sempre sigui molt més fàcil, impossible agrair l'amistat d'aquests últims 27 anys. Perquè et respecto i t'estimo com a ningú, perquè encara ens queda molt per a compartir, i més per a somiar. *Gracias* Marta, mi gran COMPAÑERA. Contigo, Marta, lo he aprendido y compartido todo. Te voy a echar demasiado de menos.

Moltes *gràcies* Bernat, per a mi, no pot haver-hi un millor supervisor. *Gràcies* per transmetre aquest infinit optimisme, aquesta harmonia, passió i entusiasme. *Gràcies* per no jutjar i confiar. Gràcies per deixar-me aprendre i treballar al meu ritme, n´he après molt al teu costat. En el sentit més ampli de la paraula, *gràcies*. *Gràcies* fucking weird Gringo, aquest doctorat és tan meu com teu. Guardo a la memòria tots i cadascun dels moments que vam compartir al lab i a la nostra estimada BCN. *Gràcies* perquè no recordo haver anat mai tan feliç a treballar, sense tu aquest procés hagués estat totalment impossible.

M´ho posaré fàcil i seguiré un ordre cronològic.

Gràcies a tots els Timothies.

Gràcies Marta Soler, hauria d´haver absorbit molt més de la teva meticulositat i rigurositat. Va ser un plaer compartir l'any Centelles amb tu. *Gràcies* Raquel, contagies felicitat i bon rotllo. *Gràcies* Johanna per introduir-me a l'apassionant món del llevat. *Gracias*, muchas *gracias* Marta Guerra. Dibujo una gran sonrisa tan sólo escribir tu nombre. Eres sinónimo de bondad, constancia, transparencia, honestidad. Sencillez. De tí he aprendido mucho en todos los aspectos. Has sabido aguantar como nadie mis subidones de media tarde y mis agobios permanentes. *Gracias* porqué me lo he pasado jodidamente bien trabajando contigo. Al Toni, moltíssimes *gràcies*. Vam començar aquest procés plegats i no teníem ni idea de què ens quedava per davant. Després de 5 anys crec que hi continuem creient. *Gràcies* per mantenir aquella il·lusió i curiositat intactes. *Gràcies* Toni per la teva serenitat i enorme capacitat de treball. *Gràcies* per ser tan desgraciat ☺. A mi Pinky German, *gracias* por ser tan auténtica. *Gracias* por compartir conmigo tu fuerza y alegría. Ése fue un año increíble. *Gràcies* Oscar per donar-nos els millors moments del lab. *Gràcies* perquè ets una imparable caixa de sorpreses, *the show must go on*. *Gràcies* Lourds, no tens mai un no per resposta, ets una eterna aventurera. *Gracias* Alexia por la calma que transmites, me ha gustado mucho conocerte. *Gràcies* Paqui, admiro en profunditat la teva capacitat de

treball i organització. *Gràcies* Tim per acollir-nos al teu lab. En definitiva, gràcies a tots amb qui vaig compartir excel·lents moments al lab d'en Tim.

Moltíssimes gràcies a totes les Bernis.

Muy especialmente, *gracias* a tí Vero. Eres brutal. Tu trabajo y enorme capacidad de organización han hecho que todo sea mucho más fácil. Pilar, estic TAN contenta d´haver-te conegut! Em va ser terriblement fácil connectar amb tu. Moltes *gràcies* per la teva inacabable creativitat i entusiasme. Desprens felicitat. Guardo com un tresor la teva llibreteta de Boston. *Gràcies* Ali perquè sempre tens temps per ajudar, remirar-te bé les coses i xerrar. Amb una mica de sort, encara estic a temps d'absorbir un pèl del teu perfeccionisme i pulcritud. En definitiva, *gràcies* a les tres per iniciar tot això, *gràcies* perquè feu que em mori de ganes de tornar al nou lab. *Thanks* Marie for your advices. *Thanks* for introducing me to the cell culture room. *Thanks* Anne, I bet you will learn perfect Spanish (even Catalan) with your new notebook.

Thanks to all Bostonians.

Thanks to Steve and to all members of the Gygi´s lab for introducing me to the mass spec world. Specially, I am very grateful to Woong, Noah, Lily, Fiona, Stephan and all the computer guys. *Thanks* for your endless patience. I am looking forward to starting this new period of my life, I will learn so much from all of you! Moltes *gràcies* als catalans que vau fer de Boston una experiència molt més agradable. Molt especialment, *gràcies* a tu Marc. Em sento terriblament afortunada d'haver-te conegut. Tinc la ferma intuició de què anirà tot molt bé.

Gràcies als meus amics.

Els amics és una de les poques coses que encara tenim plena llibertat d'escollir. No tinc cap dubte de què he fet la millor elecció. Moltíssimes *gràcies* Irene, se´t troba massa a faltar. *Gràcies* als meus amics de sempre, sou absolutament insubstituïbles. *Gràcies* perquè no ens hem de justificar per res, pels petits grans moments compartits, per les noves il·lusions. Gràcies per les millors farres, heu estat la meva millor escapatòria. Moltes *gràcies* Jaume, *gràcies* per estimar tantíssim a la Laia i saber-ho compartir amb tots nosaltres, sou el millor equip. Moltíssimes *gràcies* Cristian, perquè és impossible no estimar-te. Sempre ens quedarà Formentera. *Gracias* pequeña Vane, eres imparable, me fascinas. Per a tu Sergi, les *gràcies* se´m queden curtes, vals un imperi. *Gràcies* pel teu infinit recolzament, sobretot aquest últim any. *Gràcies* a tots els químics per compartir amb mi aquest llarg procés, guardo un gran record d'aquells anys de pràctiques, informes i campanes al pàrquing. Molt especialment, *gràcies* a l'Albert, en Jaume i al Sant Pol. *Gracias* Rafa por ser el mejor compañero de piso, tus cocktails han sido la mejor terapia.

Finalment, gràcies a...

La Isabel Fernandez. Durant aquests anys has estat la meva màxima referència, *gràcies* per la teva increïble capacitat de superació, per aixecar-te tan ràpid, però sobretot, *gràcies*, per aixecar-te sempre amb un somriure. *Gràcies* Maribel Geli i Gemma Marfany pel vostre seguiment i recolzament

desinteressats. *Gràcies* a aquells professors del Químic que van despertar en mi la curiositat científica, molt especialment en Santi Nonell i en Toni Planas. *Gràcies* Magda Faijes per donar-me l'oportunitat d'anar a Holanda i introduir-me en la Biologia Molecular. Realment ha estat el punt d'inflecció més important en la meva carrera professional. Finalment, *gràcies* a l'Ayrton Senna, per ser el millor, per creure-hi, pel seu carisma i força.

Gràcies, gràcies i més gràcies.

Som-hi!

Targeted protein degradation plays a central role in eukaryotic cell regulation and homeostasis. The ubiquitin proteasome system (UPS) is involved in a large number of cellular events, being, day by day, more difficult to find pathways without links with the system. Proteins are marked for degradation by ubiquitin ligases that append polyubiquitin signals, which can recruit the targeted protein to the 26S proteasome for degradation. In the process, polyubiquitin chains appended to the target protein are disassembled into free monoubiquitin for subsequent rounds of substrate tagging by means of deubiquitinating enzymes.

Rpn10 is a proteasome receptor that recognizes the Lys^{48}-linked polyubiquitin degradation signal by means of a ubiquitin-interacting motif (UIM). Mutation of the UIM domain of Rpn10 significantly ablates the proteolytic capacity of the proteasome. Rpn10 also contains a Von Willebrand factor A (VWA) domain which is responsible of Rpn10 interactions inside the proteasome. Rpn10 is in equilibrium with a pool of free protein so that it functions as both, a receptor at the proteasome, and an extraproteasomal adaptor.

In the present work, we have shown that Rpn10 is monoubiquitinated (Rpn10-mUb) *in vivo* and that Rpn10-mUb is found in both proteasomal and non-proteasomal pools. Levels of Rpn10-mUb are regulated *in vivo* by Rps5, a NEDD4 ubiquitin-ligase protein family, and Ubp2, a deubiquitinating enzyme. Our observations link for first time monoubiquitin signal with proteasome regulation. Monoubiquitination strongly inhibits Rpn10 to interact with ubiquitin conjugates by a specific interaction *in cis* between Rpn10 UIM domain and the linked monoubiquitin. By means of genetic and proteomics tools we found that four sites of Rpn10 sequence are subjected to monoubiquitination by Rsp5 (Lys^{71}, Lys^{84}, Lys^{99} and Lys^{268}), but Lys^{84} within its VWA domain is the preferred one. Ubiquitination of Rpn10 inhibits its ability to bind polyubiquitinated substrates, thus functioning as mechanism of inactivation of this receptor. Interestingly, our findings suggest that Rpn10 monoubiquitination could decrease proteasome activity.

The UIM of Rpn10 also strongly interacts with the ubiquitin-like domain (Ubl) of Dsk2, a polyubiquitin-binding protein. Furthermore, extraproteasomal Rpn10 plays a critical role in filtering Dsk2 and its substrates from the proteasome. We evaluated the affinity of several forms of Rpn10-mUb to Dsk2 and found that Ub-UIM interaction *in cis* of Rpn10-mUb impairs the binding of Dsk2 *in trans*. These results suggest that in an extraproteasomal context, Rpn10 monoubiquitination could regulate the Dsk2-Rpn10 interaction.

Notably, the proteasomal pool of Rpn10-mUb is suppressed under perturbations that promote the proteolytic pathway, such as stress by temperature and oxidative stress, whereas the extraproteasomal pool remains fairly constant. To assess whether the distinct behavior of the Rpn10-mUb pools correlated with the modification of different lysine residues of Rpn10, we set up assays of absolute quantification of the two major ubiquitination sites, $\mathbf{Lys^{84}}$ and $\mathbf{Lys^{268}}$, by mass spectrometry (AQUA). The obtained results clearly indicate that Lys^{84} is the main target of Rsp5 ligase in both pools of Rpn10, enhancing the role of the VWA domain in Rpn10 ubiquitination.

Finally, we have combined ubiquitin remnant profiling with quantitative proteomic approaches to identify ubiquitinated species that are increased in RPN10-RAD23 deletion, under standard growth conditions and cold-shock stress. Enriched conjugates have been distributed across different biological functions being proteins involved in RNA processing and transport metabolism accounting for the biggest fractions. Further molecular biology approaches and informatic analysis are required to address which proteins are likely to be true UPS substrates as opposed to proteins regulated by ubiquitination in a non-proteolytic manner.

Overall, our results provide a novel evidence of involvement of monoubiquitin signals in the regulation of the availability of substrates to bind proteasomal surfaces. Considering that substrate binding is the first event in the multicatalytic process promoted by the proteasome, the control of the accessibility of proteasome receptors is a crucial level of proteasome regulation. Thus, if the NEDD4 enzyme catalyzed monoubiquitination of Rpn10 inhibits proteasome activity, the control of this reaction could be an interesting target. Classical proteasome inhibitors, such as Bortezomib, which target the proteolytic activity of the core particle of the proteasome, are used as anticancer drugs. We propose that Rpn10 monoubiquitination could be considered as a new target in cancer research.

Introduction

Ubiquitin: A Highly Versatile And Conserved Signaling Molecule In The Cell

Proteins in eukaryotic cells are subjected to a wide variety of post-translational modifications, which greatly extend the functional diversity and dynamics of the proteome. Proteins can be modified by small molecules, such as phosphate, methyl or acetyl groups, or by certain proteins (Hochstrasser, 2000; Pickart, 2001). The first such protein-based modification to be described was ubiquitin at late 70's – beginning of 80´s- when a reticulocyte proteolytic system was described (Ciechanover et al., 1980). Since then the research devoted to ubiquitin (Ub) -and ubiquitin-like proteins (Ubls)- field in the last three decades has uncovered complex and diverse regulatory roles of ubiquitin in multiple processes, making ubiquitin one of the most versatile signaling molecules in the cell. Remarkably, to perform its broad functional repertoire, ubiquitin utilizes two molecular mechanisms: covalent attachment to other proteins or to itself (process known as ubiquitination), and specific binding to surfaces (ubiquitin-binding domains – UBD) that form transient, non-covalent interactions either with ubiquitin moieties or with the linkage regions in their chains (Dikic et al., 2009).

The ubiquitin system is found in all eukaryotes and involved in the regulation of multiple and divers cellular processes, such as proteasomal-dependent protein degradation, antigen processing, apoptosis, biogenesis of organelles, cell cycle and division, DNA transcription and repair, differentiation and development, immune response and inflammation, neural and muscular degeneration, morphogenesis of neural networks, modulation of cell surface receptors, the secretory pathway, response to stress and extracellular modulators, ribosome biogenesis or viral infection (Deshaies and Joazeiro, 2009; Raiborg and Stenmark, 2009; Ulrich and Walden, 2010). The range of ubiquitin signaling in protein homeostasis can be illustrated by the following numbers: in *Saccharomyces cerevisiae*, ubiquitin has been suggested to modify around a thousand different proteins (Peng et al., 2003), and recent studies have shown that, in the human ubiquitin-modified conjugated proteome, there are more than four to five thousand proteins that are modified by ubiquitin at the steady state (Kim et al., 2011b; Wagner et al., 2011).

Ubiquitin is a 76-residue polypeptide that is highly conserved among all different kingdoms. A multiple sequence alignment among distant species illustrates the high conservation between ubiquitin gene products (Figure 1). For instance, only three amino acid differences between the yeast and human polypeptides at positions 19, 24 and 28 clearly illustrates that, during evolution, Ub has been extremely refractory to amino acid changes.

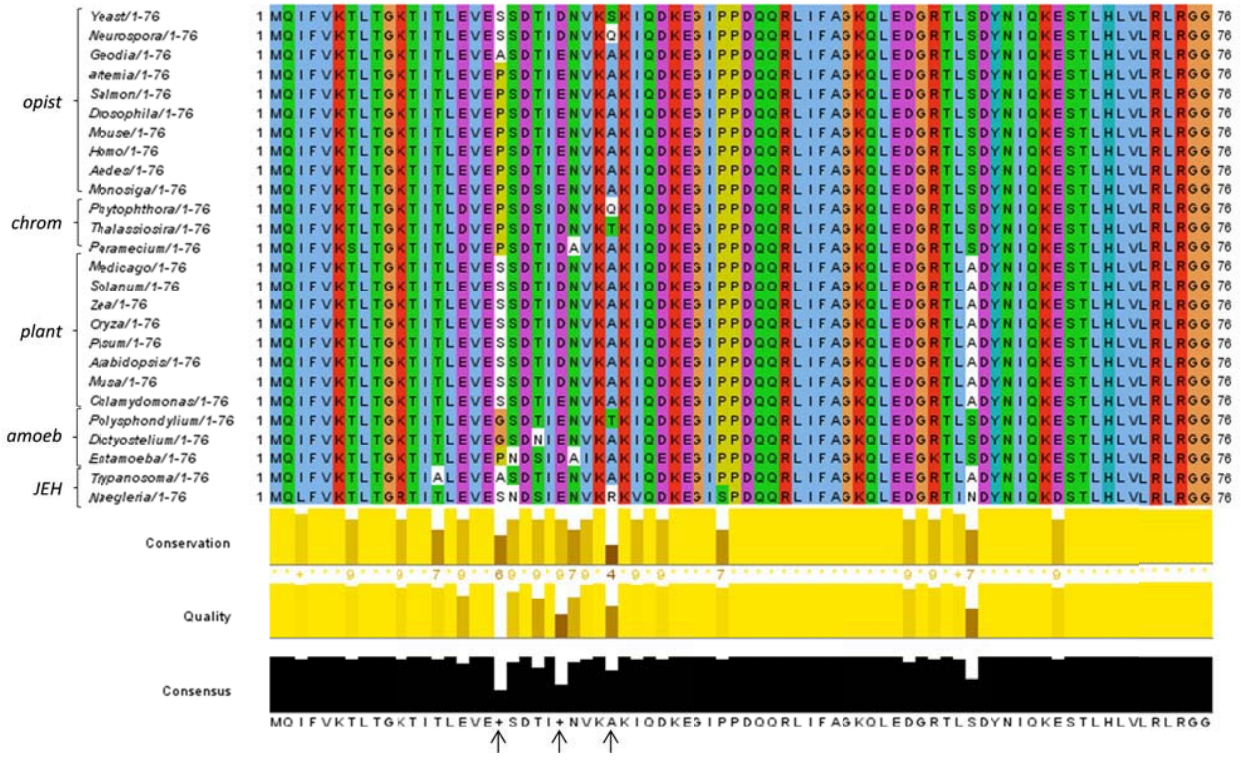

Figure 1: Extreme Conservation of Ubiquitin Through Evolution.
The ubiquitin sequence of species of distinct kingdoms is shown. *opist* = opisthokonts, *chrom* = chromalveolates, *amoeb* = amoeba and *JEH* = Jakobids, Euglenozoans, and Heteroloboseans group. Residues 19, 24 and 28 are marked with an arrow. The alignment is visualized with JalView Java editor (www.jalview.org) (Clamp et al., 2004).

Ubiquitin belongs to the superfamily of beta-grasp folded (βGF) proteins, consistent in 4 or 5 β strands forming an anti-parallel sheet and one α helix region. A common feature of βGF is the adjacent and parallel orientation of the N- and C-terminally located strands, crossed by the helical group, defining the centre of the molecule (Figure 2A). This structural pattern of ubiquitin is stabilized by hydrophobic interactions, providing a compact architecture, highly resistant to proteolytic processing, stable to temperature and pH changes (Ibarra-Molero et al., 1999; Lenkinski et al., 1977; Schlesinger et al., 1975). The βGF is a very robust fold which tolerates amino acid substitutions with no major effect in structure (Burroughs et al., 2007). In agreement with that, ubiquitin preserves its function when single mutations are carried out at 60% of its positions (Sloper-Mould et al., 2001), suggesting a low restriction to amino acid substitutions. Importantly, only two regions in Ub surface are essential for cell viability: the Ub-tail and two distinct functional faces of the Ub globular domain (Sloper-Mould et al., 2001). Gly^{75} and Gly^{76} at the C-terminal are subjected to a series of reactions that result in the conjugation of ubiquitin to target proteins (see next sections for detailed information). The first essential surface cluster includes Leu^{8}, Ile^{44} and Val^{70} and consists of nine amino acids that extend from the base of the Ub tail up to Gly^{47} and Lys^{48} (Figure 2B). Leu^{8}, Ile^{44} and Val^{70} , known as the hydrophobic patch, are critical for proteasomal degradation and endocytosis (see next sections for detailed information) (Shih et al., 2000; Sloper-

Mould et al., 2001). The second essential cluster on the globular domain surface consists of residues Gln^{2}, Phe^{4}, and Thr^{12}. Phe^{4} which are critical for endocytosis (Figure 2B).

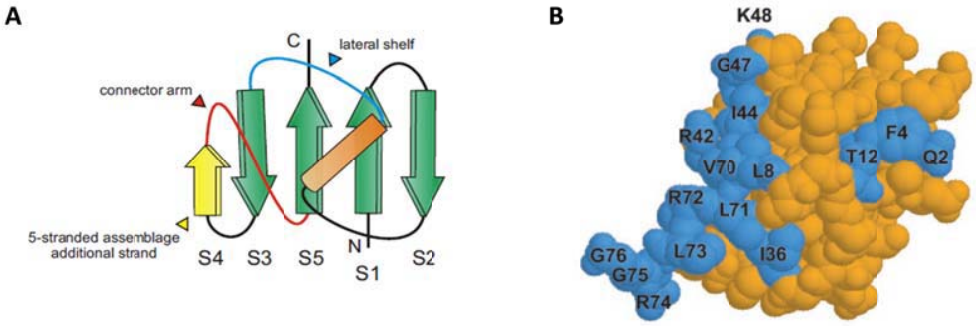

Figure 2: The Ubiquitin Molecule.
(**A**) A generalized topology diagram of the beta-grasp folded members with the key structural features. Adapted from Burroughs et al., 2007. (**B**) A three-dimensional structure of the ubiquitin molecule is shown. The essential ubiquitin residues for life in yeast are shown in blue. Adapted from Sloper-Mould et al., 2001.

For decades the paradigm that prevailed was that ubiquitin signaling system was only found in eukaryotes. The discoveries that prokaryotes and archaea contain ubiquitin-like systems are drawing a new map of ubiquitin signaling evolution. The existence of prokaryotic sulphur-carrier proteins involved in molybdenum cofactor and thiamin biosynthesis (Moa and ThiS, respectively) structurally related to ubiquitin, sharing a beta-grasp folding and a Glycin-Glycin at the C-terminal end, suggest a common origin and a radiation in the pre-eukaryotic period. Interestingly, in Moa and ThiS pathways, sulphur-containing factors are the final product (Lake et al., 2001), whereas in eukaryotic ubiquitin and ubiquitin-like systems sulphur-conjugation is an intermediary step in the formation of a final sulphur-free protein-protein conjugate (see next sections for detailed information). The recent description of SAMPs (small archaeal modifier proteins) in the halobacterium *Haloferax volcanii* unequivocally demonstrates that protein conjugation by ubiquitin-like proteins is not exclusive of eukaryotes (Humbard et al., 2010). However, SAMPs show very low sequence identity (9%) with eukaryotic ubiquitin and multiple insertions (Bienkowska et al., 2003; Darwin, 2009). In addition to the discovery of SAMPs, a putative ubiquitin ortholog has been found in the archea species *Caldiarchaeum subterraneum* (Nunoura et al., 2011).

When analyzing the topology of archaeal and eukaryotic ubiquitin systems, remarkable differences are observed. In eukaryotes, with very few exceptions, ubiquitin is redundantly expressed in genomes, encoded as a fused protein by at least three loci (Catic and Ploegh, 2005; Sharp and Li, 1987): a polymeric head-to-tail concatamer of multiple (from 4 to 15) ubiquitin open reading frames and two fusions with L40 and S27 ribosomal proteins (Catic and Ploegh, 2005; Finley et al., 1989). In *Caldiarchaeum subterraneum*, the organization of the ubiquitin system is substantially different. The genome contains five genes encoding ubiquitin signaling factors: ubiquitin, ubiquitin activating enzyme (E1), ubiquitin conjugating enzyme (E2), ubiquitin-protein ligase (E3) and deubiquitinating enzyme (DUB) (Nunoura et al., 2011). Interestingly, these five genes are organized in an operon-like cluster,

representing the most simplified genetic arrangement encoding a ubiquitin signaling system (Nunoura et al., 2011). The existence of this redundancy in ubiquitin genes in species from all eukaryotic groups, including protists, suggests that these loci already existed in early steps of evolution of eukaryotes (Catic and Ploegh, 2005; Sharp and Li, 1987).

The Ubiquitin Signaling Pathway Is Mediated By An Enzymatic Cascade

A three-step cascade mechanism catalyzes the modification of substrate proteins with ubiquitin, process known as ubiquitination. Conjugation of ubiquitin is catalyzed by the sequential activity of ubiquitin-activating (E1), ubiquitin-conjugating (E2) and ubiquitin-ligating (E3) enzymes (Deshaies and Joazeiro, 2009; Scheffner et al., 1995; Schulman and Harper, 2009; Ye and Rape, 2009). The polyubiquitinated substrates will be subsequently recognized and degraded by the Ubiquitin Proteasome System (UPS) (Figure 3A).

Initially, the ubiquitin activating enzyme E1 activates ubiquitin in an ATP-requiring reaction to generate a high-energy thioester ubiquitin intermediate. One E2 enzyme transfers the activated ubiquitin moiety from E1, via an additional high-energy thioester intermediate, to the substrate that is specifically bound to a member of the ubiquitin-protein ligase family, E3. Although there are a number of different classes of E3 enzymes (more details are described below), all E3s specifically catalyze the covalent attachment of ubiquitin to the substrate. The ubiquitin is attached to protein substrates through an amide linkage between its C-terminal end and a primary amino group of the acceptor polypeptide (Hochstrasser, 2009; Pickart, 2001). The successive E3 activity on the substrates produces polyubiquitinated proteins containing chains of ubiquitin (Figure 3A). In some situations, a specific E3 ligase confers only initial oligoubiquitination and the chain is later extended by another type of Ub ligase. Enzymes that possess this Ub chain extending are termed E4 ligases (Crosas et al., 2006; Koegl et al., 1999). The most common type of conjugation consists in the addition of ubiquitin to the epsilon-amino group of a lysine residue (Glickman and Ciechanover, 2002), but it can also be conjugated to the amino terminus of a protein (Ciechanover and Ben-Saadon, 2004), as well as to Cys, Ser, and Thr residues of target proteins (Cadwell and Coscoy, 2005; Ravid and Hochstrasser, 2007).

The ubiquitin system follows a hierarchical structure, meaning that a much reduced number of E1 enzyme activates ubiquitin and transfers it to a higher number of E2s (Hershko and Ciechanover, 1998; Pickart, 2001). Most E2s interact with several E3s, and usually, most E3 are found to interact with several different protein substrates via similar or identical recognition motifs (Figure 3B). However, this hierarchy is more complicated and cannot be seen simply as a pyramid structure, but rather as a complex network of overlapping interactions between multiple components. A few examples are next listed to highlight the complex combinatory of different E2-E3-substrate interactions: **1.** a single E2 acts along with a single E3 to target a set of substrates. This would be the case of UBEC2 (also known as UBCH10) that acts along with the APC/C (anaphase-promoting complex/cyclosome) in cell cycle regulation (Ye and Rape, 2009), or **2.** certain substrates can be recognized by different E3s or **3.** a single E3 can interact with different E2 to recognize and ubiquitinate a set of substrates. For example, the SCF (Skp1-Cullin1-Fbox) ligase acts both with members of the E5D (UBCH5) family of E2s and with the UBC3/Cdc34 E2 (Bennett et al., 2010; Gonen et al., 1999).

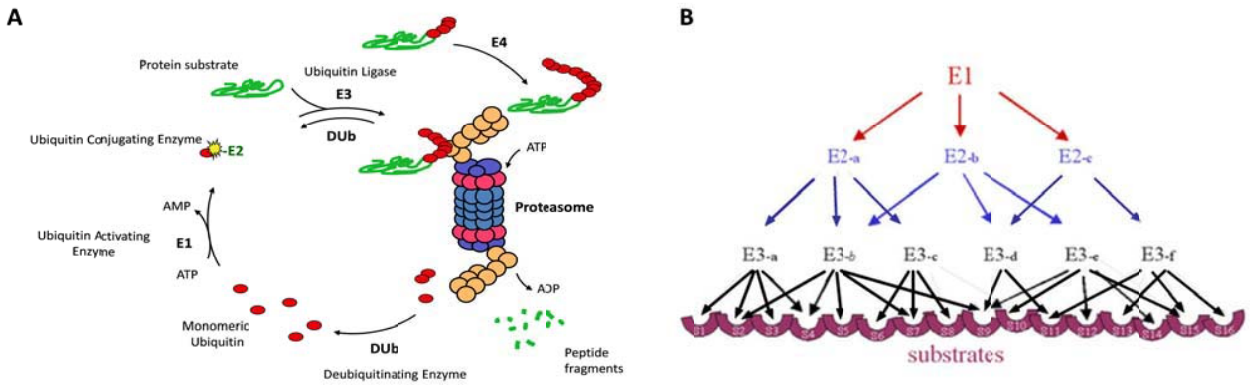

Figure 3: The Ubiquitin Signaling Pathway And Its Enzymatic Hierarchical Structure.
(**A**) Ubiquitin-tagging for proteasomal degradation is performed by a multi-enzyme cascade comprising ubiquitin-activating (E1), ubiquitin-conjugating (E2) and ubiquitin-ligating (E3 and E4) enzymes. Ubiquitinated proteins are then transported to the 26S proteasome where they undergo final degradation. The ubiquitin escort is released by deubiquitinating enzymes (DUBs) and recycled. (**B**) A simplified view of the hierarchical structure of the ubiquitin system. A single E1 interacts with several E2 and each E2 face towards a huge number of E3. Each E3 targets several targets.

Ubiquitin-Activating Enzymes, E1

The process of covalent linkage of ubiquitin to substrates requires activation of ubiquitin by E1. E1s have their origins in prokaryotic proteins molybdopterin-converting factor subunit 1 (MoaD) and thiamine biosynthesis protein S (ThiS), which carry sulphur for incorporation into molybdopterin and thiazole, respectively. In a reaction that resembles the one catalyzed by eukaryotic E1s, MoaD and ThiS are activated by C-terminal acyl-adenylation by the bacterial enzymes molybdopterin biosynthetic enzyme B (MoeB) and by ThiF, respectively (Burroughs et al., 2009; Taylor et al., 1998). Thus, MoeB and ThiF embody minimal modules that contain Ub-E1 recognition and adenylation activities (Hochstrasser, 2000).

In humans, two E1 for ubiquitin have been described, UBA1 and UBA6 (also known as UBE1L2). For more than two decades, it was believed that a single ubiquitin-activating enzyme, UBA1, charged E2s, as in lower eukaryotes. However, recent studies identified UBA6 as a second E1 enzyme for ubiquitin, challenging this dogma (Jin et al., 2007; Pelzer et al., 2007). UBA6 is uniquely responsible for transferring ubiquitin to the E2 USE1 (Jin et al., 2007) and its deletion in mouse results in embryonic lethality (Chiu et al., 2007). As regards the Ub-E1 UBA1, in the early 80s, temperature-sensitive mutations in mammalian UBA1 were identified (Finley et al., 1984). Cells with these mutations arrest the cell cycle at the G2–M phase transition and display a significant decreased in ubiquitin conjugation (Ciechanover et al., 1985). Furthermore, UBA1 is regulated by phosphorylation which increases nuclear import and/or retention and modulation of nucleotide excision repair during macrophage differentiation (Stephen et al., 1996).

The catalytic mechanism is best studied for the Ub UBA1 (Jin et al., 2007). The C-terminus of ubiquitin, invariably occupied by a glycine in all ubiquitin sequences in eukaryotes (Figure 1), is first adenylated

and the ubiquitin-AMP adducts remains bound to the enzyme (Haas and Rose, 1982). In a second step, the adenylated ubiquitin is attacked by the catalytic cysteine of UBA1, producing a covalent thioester linkage between the Cys sulphydryl of UBA1 and the C terminus of ubiquitin (Ciechanover et al., 1981). Subsequently, UBA1 catalyzes the adenylation of a second ubiquitin molecule, becoming asymmetrically loaded with two ubiquitin molecules at distinct active sites: one ubiquitin molecule is covalently linked to the catalytic Cys of the E1 enzyme through a thioester bond; and a second ubiquitin is associated non-covalently at the adenylation active site (Haas and Rose, 1982; Haas et al., 1982). Finally, UBA1 physically interacts with an E2 and a thioester transfer reaction follows, ensuring that C terminus of Ub is transferred to the catalytic Cys of the E2 enzyme (Haas et al., 1982; Pickart and Rose, 1985). The next step is driven by the release of inorganic phosphate and AMP generated in the first and second steps, respectively.

Ubiquitin-Conjugating Enzymes, E2

Central players in Ub transfer choreography are the Ub-conjugating enzymes (E2). E2s represent a conserved group of enzymes that couple activation of the Ub/Ubl molecule to downstream conjugation events (Wenzel et al., 2011). E2 enzymes are essential for adequate conjugation and are directly influencing the type of lysine used to label substrates and thereby influencing the fate of the substrate (see next section) (Ye and Rape, 2009). By contrast with E1, no E2-like activities have been identified in bacteria (Iyer et al., 2008). E2 enzymes are present in all eukaryotes, and the protein family is expanded during evolution; lower eukaryotes have lower numbers of E2 enzymes than higher ones (Michelle et al., 2009).

Members of the family of ubiquitin-conjugating enzymes (E2s) are characterized by the presence of a highly conserved 150–200 amino acid ubiquitin-conjugating catalytic (UBC) fold (Burroughs et al., 2008; Schulman and Harper, 2009). These domains of 14–16 kDa are 35% conserved among different family members and provide a binding platform for E1s, E3s, and the activated Ub/Ubl (Burroughs et al., 2008). Within this domain, a catalytic cysteine is embedded and accepts the activated Ub/Ubl via a thioester bond, prior to interaction with E3 ligases and subsequent substrate conjugation. E2s are classified based on the existence of additional extensions to the catalytic core; some E2s consist only of the catalytic domain (class I), others have additional N- or C-terminal extensions (classes II and III, respectively) or both (class IV) (Hofmann and Pickart, 2001). These extensions are involved in functional differences between E2s, which involve differences in subcellular localization, stabilization of the interaction with E1 enzymes, or modulation of the activity of the interacting E3.

Ubiquitin-Ligases Enzymes, E3

In the last step of the cascade, E2-ubiquitin associates with an E3, which is required for specific detection of protein substrates. E3 ubiquitin ligases mainly belong to two enzymatic subfamilies: HECT (Homologous to E6AP C-Terminus) and RING (Really Interesting New Gene). HECT enzymes contain an active-site cysteine, which is charged with ubiquitin by E2s prior to ubiquitin ligation to the substrate (Rotin and Kumar, 2009) (Figure 4A). By contrast, RING ligases, which do not contain an enzymatic active site, bind at the same time the E2-ubiquitin intermediate and the substrate to promote ligation (Figure 4B). Of the human E3s, most (~95%) belong to the RING family and only 28 belong to the HECT family (Li

et al., 2008).

RING E3 can be a single chain (for example, CBL ligases) or be part of multimeric complexes (for example, cullin E3s). The basic sequence expression of the canonical RING is a Cys-X_2-Cys-$X_{(9-39)}$-Cys-$X_{(1-3)}$-His-$X_{(2-3)}$-Cys-X_2-Cys-$X_{(4-48)}$-Cys-X_2-Cys, where *X* is any amino acid (Figure 4B). Three-dimensional structure of RING domains revealed that its conserved Cys and His residues are buried within the domain's core, where they help to maintain the overall structure by binding two atoms of zinc (Borden and Freemont, 1996). Additional semiconserved residues are implicated either in forming the domain's hydrophobic core or in recruiting other proteins. The Zn coordination sites in a RING "finger" are interleaved, yielding rigid, globular platform for protein-protein interaction (Deshaies and Joazeiro, 2009). Activity of RING domain ligases is posttranslationally controlled by covalent modification such as phosphorylation or conjugation with ubiquitin-like proteins, by noncovalent binding of protein or small-molecule ligands, or by competition among substrates. RING E3s are involved in multiple aspect of cellular physiology. Their involvement in many diseases is also apparent, as illustrated by findings of a large number of Parkin mutations in Parkinson´s disease and mutation or deregulation of Mdm2, VHL, Brca1, and other E3 in cancer (Hashizume et al., 2001; Mata et al., 2004).

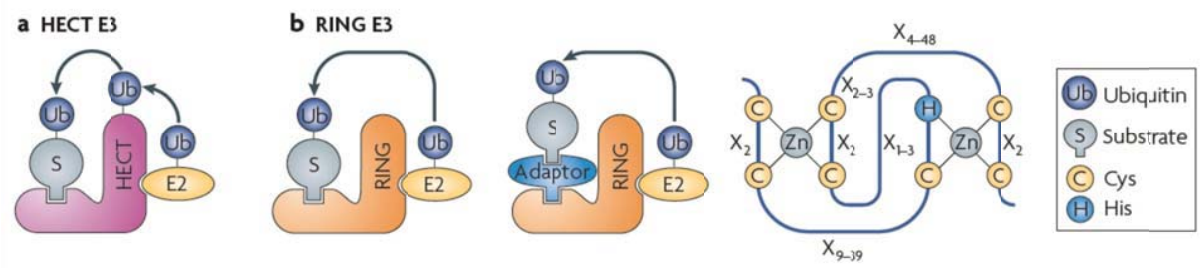

Figure 4: Two Types Of E3s Ligases: HECT And RING Enzymes.
(**A**) The HECT and the RING E3s differ in the way they transfer ubiquitin to the substrates. HECT E3s contain a conserved and catalytic cysteine, which acts as an acceptor of ubiquitin from E2 enzymes. Ub is then transferred to a specific Lys residue in the substrate. (**B**) RING E3s function as adaptors between the substrate and E2. The RING family can act in its own or be part of large multi-subunit E3 complexes. RING are characterized by a Cys-X_2-Cys-$X_{(9-39)}$-Cys-$X_{(1-3)}$-His-$X_{(2-3)}$-Cys-X_2-Cys-$X_{(4-48)}$-Cys-X_2-Cys, where X is any amino acid. This sequence produces a "crossbrace" motif that is stabilized by the binding of two Zn atoms through Cys and His residues. Adapted from Rotin and Kumar, 2009.

HECT is a C-terminal domain of approximately 350 amino acids that was first described in human papilloma virus (HPV) E6-associated protein (E6AP) (Schwarz et al., 1998). HECT domains, which contain a cysteine active site, have been found in all eukaryotes. HECT domain consists in a domain formed by two lobes (N- and C-terminal lobes) expanding approximately 350-380 amino acids. N-terminal lobe represents two thirds of the domain and is involved in E2 interaction. C-terminal lobe contains a cysteine active site and represents the region of ubiquitin interaction. Most HECT ligases contain one or more protein–protein or protein–lipid interaction domains located towards the amino terminus of the protein (Rotin and Kumar, 2009). HECT E3s are found in all eukaryotes divided in several families. In

humans, HECTs can be divided into 3 groups, based on the motifs found in the N-terminal regions: the Nedd4 family, the HERC family and other HECTs (e.g., TRIP12, HUWE1 and UBE3B) (Park et al., 2009b; Rotin and Kumar, 2009).

In addition to the HECT domain, two N-terminal domains define the Nedd4 family: C2 and WW. The C2 domain is a calcium-binding domain that is approximately 120 amino acids in length. Upon Ca^{2+} binding, the C2 domain can bind to phospholipids and inositol polyphosphates, mediating intracellular targeting to membranes (Dunn et al., 2004; Plant et al., 2000), and some other proteins, such as annexin or Grb adaptors (Morrione et al., 1999; Plant et al., 2000; Plant et al., 1997; Seo et al., 2004). The WW domains are 35–40 amino acid long containing two conserved tryptophan (W) residues spaced 21 amino acids apart. WW domains interact with PY (PPXY/PPLP) motifs or phospho-serine/threonine residues in substrate proteins (Dupre et al., 2004; Lu et al., 1999; Staub et al., 1996). Protein structures for C2, WW, and HECT domains have also been solved separately (Ingham et al., 2004). Since the original discovery of the Nedd4 gene, related proteins, including Nedd4–2/Nedd4L, WWP1/Tiul1, WWP2, AIP4/Itch, Smurf1, Smurf2, HecW1/NEDL1, and HecW2/NEDL2 have been identified in human and mouse. Although the similar structure and expression patterns of the Nedd4 family members suggest functionally redundant roles for these proteins, recent studies have begun to define specific functions for individual members (Yang and Kumar, 2010).

Distinct Ubiquitination Products Generate Diversity In Ubiquitin Signaling

Ubiquitination may involve the attachment of one single ubiquitin group to protein targets, known as monoubiquitination, or the formation of branches of ubiquitin polymers linked to targets, known as polyubiquitination. Polyubiquitination may involve all seven lysines in ubiquitin (Lys^{6}, Lys^{11}, Lys^{27}, Lys^{29}, Lys^{33}, Lys^{48} and Lys^{63}) and the amino-terminal methionine (M1) (Dikic et al., 2009) (Figure 5A). In 2003, a proteomic analysis revealed that all seven lysines were used as Ub acceptors *in vivo* providing evidence for unexpected diversity in polyubiquitin chain topology (Peng et al., 2003).

Chains formed by the conjugation of a single type of lysine residue in sequential Ub molecules are homotypic, whereas those assembled through several distinct lysines in the Ub monomers are mixed-linkage chains. As a consequence of using divergent lysines for conjugation, mixed-linkage Ub chains form bifurcations, such as chains containing two different types of linkage—$Lys^{6/11}$, $Lys^{27/29}$, $Lys^{29/48}$ or $Lys^{29/33}$ (Kim et al., 2007). Moreover, the integration of other ubiquitin-like modifiers, such as SUMO or NEDD8, into Ub chains gives rise to heterologous Ub chains (Ikeda and Dikic, 2008). Finally, monoubiquitination or multiple monoubiquitination (several independent ubiquitin molecules) are also considered as distinct signals. The model that emerges from this complexity is that the fate of modified proteins depends on the type and length of polyubiquitin signal (Husnjak and Dikic, 2012; Ikeda and Dikic, 2008) (Figure 5A). At least two evidences support this model.

The first one is that eukaryotic cells possess machineries that produce specifically all type of polyubiquitin chains and that these chains appear to show different conformations and topologies depending on the lysine residue involved in the linkage. Lys^{48}- and Lys^{11}-linked chains adopt a more rigid conformation, in which ubiquitin monomers are tightly packed against each other, alternating open and

closed conformations (Ryabov and Fushman, 2006) (Figure 5B). In contrast, Lys^{63}-linked or M1-linked chains (often referred as a linear) show a similar extended conformation, with no important contacts between ubiquitin moieties (Ikeda and Dikic, 2008; Komander et al., 2009) (Figure 5B). This creates unique modules composed of aligned ubiquitin moieties in which the hydrophobic patch containing Ile^{44} (essential for proteolytic and non-proteolytic ubiquitin functions) is either embedded or facing out towards the surface (Bremm et al., 2010; Pickart and Fushman, 2004). Conversely, Lys^{6}-linked chains form an asymmetric compact conformation distinct from any other type of Ub chain (Virdee et al., 2010).

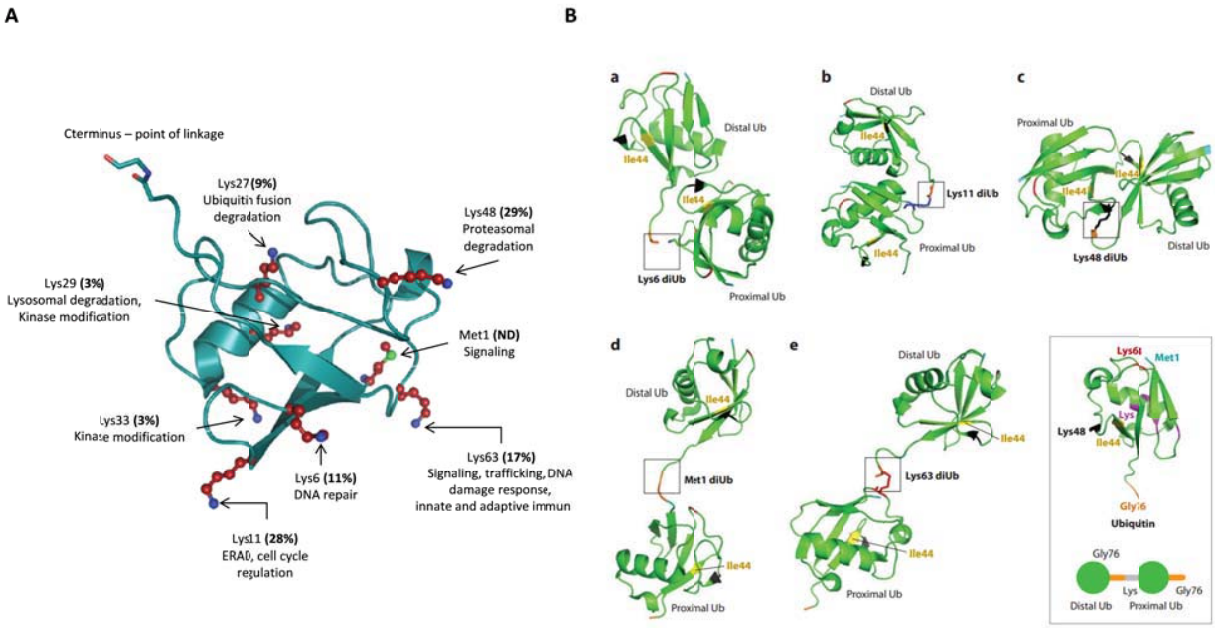

Figure 5: Diversity In Ubiquitin Signaling.

(**A**) Structure of the ubiquitin molecule. Ub can be conjugated through seven lysines (Lys^{6}, Lys^{11}, Lys^{27}, Lys^{29}, Lys^{33}, Lys^{48} and Lys^{63}) and the amino-terminal methionine (M1) resulting in various conformations of Ub chains. This creates a plethora of molecular signals in the cell. A summary of the major cellular processes whereby specific ubiquitin linkages play roles is shown (Husnjak and Dikic, 2012). The percentage of different linkages in *S. cerevisiae* is also shown ((Peng et al., 2003) (**B**) Ubiquitin (Ub) chains have different topologies, the structure of which has been solved for most of the chains: (*a*) chemically synthesized Lys^{6}-linked diubiquitin, (*b*) chemically produced Lys^{11}-linked diubiquitin, (*c*) degradative Lys^{48}-linked diUb, (*d*) Met1-linked diubiquitin chains and (*e*) Lys^{63}-linked diUb chains. The linkage is shown in a square and crucial residues in ubiquitin structure are colored: Met1 (cyan), Ile^{44} (yellow), Lys^{48} (black), Lys^{63} (red), Gly^{76} (orange). Adapted from Husnjak and Dikic, 2012.

The second evidence is that cells possess motifs and domains that recognize specifically almost each type of ubiquitin linkage, with a high level of specificity. Thus, ubiquitin conjugation generates a sophisticated code of signals in the cell, the recognition of which is carried out by specific receptors, adaptors and enzymes (Dikic et al., 2009; Harper and Schulman, 2006; Komander et al., 2009). The ubiquitin code is only partially understood and the percentage of different linkages varies between the

individual studies and might reflect technical differences in cell types and/or in the model organism employed in the study (yeast, human) (Peng et al., 2003; Ziv et al., 2011). In addition, different stages of the cell cycle or intrinsic activity of chain assembly complexes can provide cell-specific ubiquitinome patterns, as recently demonstrated for Lys^{11}-chains. These chains are highly abundant in mitotic cells at a point when the substrates of the E3 ligase anaphase-promoting complex/cyclosome are degraded (Matsumoto et al., 2010).

Several proteomic studies provide evidence for the role of ubiquitin chains in a variety of cellular functions (Figure 5A). Xu and collaborators found that in yeast all six Lys linkages, except Lys^{63}, are involved in proteasomal degradation of numerous substrates in cells *in vivo*, being Lys^{48}-linked chains (also known as "canonical" Ub chains) and Lys^{11} the most abundant type of chains (Xu et al., 2009). Another study shows that the APC polyubiquitinates cyclin B1 *in vitro* generating a mix of Lys^{48}-, Lys^{63}- and Lys^{11}-linked chains rather than Lys^{48} alone (Kirkpatrick et al., 2006). Furthermore, Lys^{63}-, Lys^{11} or M1-linked chains are associated with DNA repair regulation, cell-cycle progression, innate immunity and inflammation (Ikeda and Dikic, 2008; Wickliffe et al., 2009). Both Lys^{27} and Lys^{33} linkages can be assembled by U-box E3 ligases during the stress response (Hatakeyama et al., 2001), and Lys^{29}-linked chains play a role in ubiquitin fusion degradation (Johnson et al., 1995). Finally, to date, a single E3 ligase complex has been shown to assemble linear Ub chains, in which the terminal Gly^{76} of the proximal ubiquitin is linked to the Met1 of the distal ubiquitin (Ikeda et al., 2011). This type of chain plays a crucial role in NF-κB signaling (Gerlach et al., 2011).

Rsp5 HECT Ligase: Single Member Of The Nedd4 Family In Yeast

Rsp5p, one of the most extensively studied ubiquitin ligase in yeast, is the only HECT E3 encoded by an essential gene (Huibregtse et al., 1995). The first characterized function of Rsp5p was the ubiquitination of the Spt23p and Mga2p transcription factors, which activate transcription of the OLE1 gene (Hoppe et al., 2000), which encodes Δ9 fatty acid desaturase, an ER-bound enzyme required for the synthesis of palmitooleic and oleic acids. Thus, the essential function of Rsp5p was initially associated with providing cells with unsaturated fatty acids. However, the identification of multiple substrates in different functional contexts, and the capacity to modify substrates with distinct mono- and polyubiquitin signals (Horak, 2003; Kaliszewski and Zoladek, 2008; Rotin and Kumar, 2009), suggest a multitasking profile for Rsp5.

The role of Rsp5p (also known as Npi1p) in ubiquitination and endocytosis of yeast plasma membrane proteins was first demonstrated for Gap1p and Fur4p transporters in *npi1* mutant cells carrying a promoter mutation that expressed less than 10% of the wild-type enzyme (Springael and Andre, 1998). Subsequently, Rsp5p has been shown to affect a broad range of other ubiquitin-dependent cellular events, ranging from diverse membrane-bound as well as nuclear substrates. Thus, Rsp5 participates in several cellular functions (Figure 6A): mitochondrial inheritance, chromatin remodeling, fatty acid biosynthesis, drug resistance, regulation of transcription (Huibregtse et al., 1997; Somesh et al., 2007), regulation of endocytosis and the sorting of numerous transmembrane proteins (e.g. uracil and general amino acid permeases Fur4 and Gap1), transporters and receptors (Lin et al., 2008; Shih et al., 2007; Stamenova et al., 2004; Stawiecka-Mirota et al., 2007). In addition to its role as an internalization signal

at the plasma membrane, Rsp5-dependent ubiquitination is also required for the sorting of membrane proteins originating from the Golgi apparatus or the plasma membrane to the internal vesicles of multivesicular bodies (MVB) (Katzmann et al., 2002). Yeast MVB cargoes have been shown to undergo ubiquitination. Inhibition of this ubiquitination abolishes MVB sorting, resulting in the recovery of cargoes at the vacuolar membrane rather than in the vacuolar lumen, after the fusion of MVBs with the vacuole. Genetic analyses in yeast have led to the discovery of four protein complexes, the ESCRTs (endosomal sorting complexes required for transport) (ESCRT-0, -I, -II and -III), conserved from yeast to humans and involved in the recognition of ubiquitinated cargoes and their sorting to the internal vesicles of MVBs (Katzmann et al., 2002).

Rsp5 shares common modular domain architecture with the rest of the HECT ligases: an N-terminal C2 domain, three central WW domains and a ~ 350 amino acid C-terminal HECT domain (Figure 6B). After a number of structure-function studies of individual Rsp5 domains, it has been shown that the C2 domain of Rsp5p is not required for the vital function of this enzyme (Wang et al., 1999). In cells with the entire C2 domain deleted, a severe defect in the transport of fluid-phase markers to the vacuole has been observed (Dunn and Hicke, 2001). However, the internalization and breakdown (but not ubiquitination) of Fur4p and Gap1p is only partially impaired (Wang et al., 2001), and the rate of Ste2p internalization is not affected (Dunn and Hicke, 2001). To determine which WW domains of Rsp5p are required for its essential function *in vivo*, and endocytotic function, a variety of point mutations in conserved residues of the ligand-binding pocket of each domain have been analyzed. It has been shown that WW3 and HECT domains of Rp5p are sufficient to provide its essential function under normal growth conditions (Hoppe et al., 2000). In the same set of mutant cells, it has been also found that the WW2 and WW3 domains are required for Fur4p endocytosis (Gajewska et al., 2001) and all three WW domains for ubiquitination and internalization of the Ste2p (Dunn and Hicke, 2001). These observations illustrate that individual WW domains or their different subsets may play distinct regulatory roles in selecting proteins as endocytotic cargo.

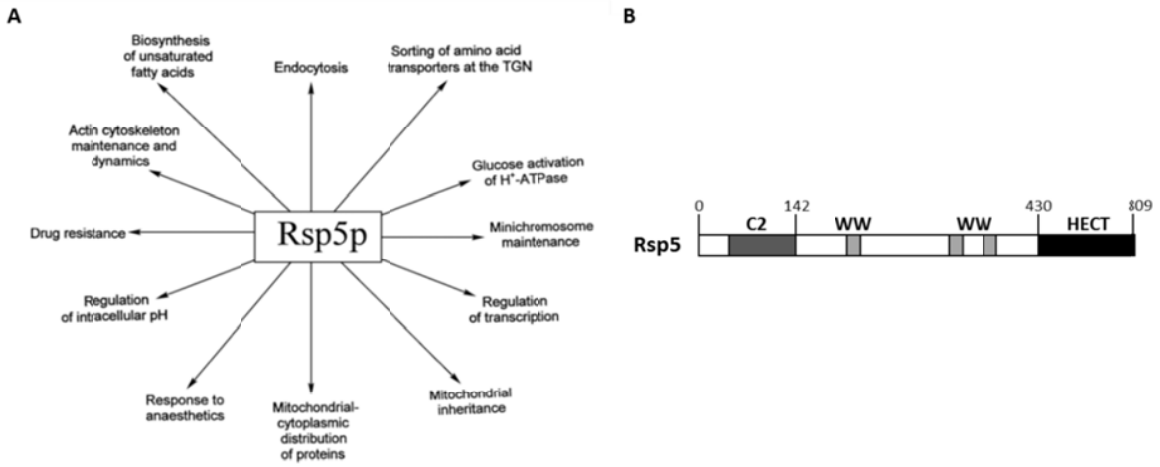

Figure 6: Examples Of Known Functions of The Rsp5 E3 Ligase And Its Structure.

(**A**) Rsp5 ubiquitin ligase regulates diverse processes in yeast cells. Adapted from Horak, 2003. (**B**) Schematic representation of Rsp5 HECT ligase indicating the position of its functional domains.

The molecular basis of Rsp5 interaction to substrates is diverse. Interactions with Rpb1 and with Vps9 are clear examples of this diversity. In the first case, Rsp5 binds the C-terminal domain (CTD) of the RNA polymerase II subunit Rpb1, and efficiently synthesizes Lys^{63}-linked polyubiquitin (Somesh et al., 2007). This reaction of polyubiquitination is thought to be counteracted *in vivo* by the deubiquitinating enzyme Ubp2, which forms a complex with Rsp5. The result of Rsp5 and Ubp2 concerted activities would be monoubiquitinated Rpb1, a form observed *in vivo* (Somesh et al., 2007). The interaction between Rsp5 and Ubp2 is mediated by Rup1, a ubiquitin-associated (UBA) domain-containing protein, and Ubp2 modulates Rsp5-catalyzed substrate ubiquitination (Kee et al., 2005). Kee et al. proposed that Ubp2, through Rup1, might assist in the partial disassembly of Lys^{63}-linked Ub chains to generate monoubiquitinated targets (Kee et al., 2006). However, it remains unclear whether, in a subset of this type of substrates, Rsp5 is able to synthesize directly monoubiquitination *in vivo*, in a Ubp2 independent manner. As regards the second case, Vps9 protein, which contains a CUE domain, is monoubiquitinated by Rsp5. The CUE domain is required for Vps9 monoubiquitination, which does not produce Lys^{63} polyubiquitin (Shih et al., 2007).

A systematic identification of substrates and substrate specificity for Rsp5 was done using global proteomics and protein screenings (Gupta et al., 2007; Hesselberth et al., 2006; Kus et al., 2005; Lu et al., 2008). Gupta et al. described that, as expected, most of the high-confidence Rsp5 substrates (72%) had at least one PY motif, usually PPxY motif. However, not all known Rsp5 substrates were identified in their screen, such as Pma1 plasma membrane or Rpb1 and Hpr1 transcriptional proteins. Authors suggested that, since these substrates did not have PY motifs, could not bind Rsp5 directly and may require adaptor proteins for their interaction (e.g Bul1 or Bul2; Hellivell et al., 2001). In fact the existence of PPXY-containing arrestin-like adaptors involved in Rsp5 substrate recognition has been recently shown by several studies (Leon et al., 2008; Lin et al., 2008; Nikko et al., 2008). Surprisingly, other Rsp5 substrates involved in the ubiquitin pathway did not contain any PY motif and do not seem to require adaptors (e.g. Sgt1, Cue5) (Gupta et al., 2007). The precise role of Sgt1 is still not clear, but the association of this protein with Rsp5 is interesting, since it has been implicated as an activator of SCF E3 enzymes (Kitagawa et al, 1999; Spiechowicz and Filipek, 2005). Cue1 has a ubiquitin binding motif and its affinity for ubiquitin may facilitate its monoubiquitination (Kang et al, 2003).

Deubiquitination, A Key Regulatory Reaction In Ubiquitin Signaling

In the same way that regulation of E3 ligation controls signaling, so does the reversal of that process by the class of enzymes called deubiquitinating enzymes (DUBs). DUBs are isopeptide proteases which specifically cleave ubiquitin from Ub-conjugated protein substrates and polyubiquitin chains (Ventii and Wilkinson, 2008).

Catalysis of deubiquitination requires a nucleophylic attack to the carbonyl group of the isopeptide bond established between the C-terminal end of ubiquitin and the amino group of the accepting lysine. In

case of linear linkages, the attack is against a peptide bond that links two ubiquitin groups in a head-to-tail fashion. There are two types of DUBs according to their enzymatic mechanism: DUBs with a cysteine active site and DUBs containing a zinc active site.

Ubiquitin isopeptidases with cysteine active site contain a highly conserved catalytic triad, in which an aspartic acid polarizes a histidine residue, resulting in the cysteine deprotonation. This mechanism is found in ubiquitin C-terminal hydrolases (UCHs), ubiquitin-specific proteases (USPs), ovarian tumour proteases (OTUs) and Josephins (MJDs), which represent more than 80% of human deubiquitinating enzymes. In zinc active sites of ubiquitin peptidases, similar to other metalloenzymes, a zinc atom is attached to two histidine residues and one aspartate residue. One polarized water molecule coordinates the fourth link to the metallic atom, ensuring reactivity. This type of active site is found in JAB1/MPN/MOV34 (JAMMs) deubiquitinating enzymes.

Given the complexity of ubiquitination, deubiquitinating enzymes have the difficult task of discriminating their targets among a highly variable pool of ubiquitin-ubiquitin and protein-ubiquitin linkages in different subcellular and functional contexts. Several layers of specificity have been suggested to categorize these isopeptidases: **1.** linkage specificity (selection of ubiquitin chain topology established by lysine usage, e.g. Lys^{11}, Lys^{48}, Lys^{63}, etc), **2.** relative position of cleavage within ubiquitin chains (distal versus proximal cut), **3.** protein specificity (protein-ubiquitin versus ubiquitin-ubiquitin linkage identification), **4.** mono-deubiquitination specificity (deubiquitinating enzymes recognizing monoubiquitinated substrates) and **5.** chain recycling (selection of unanchored versus anchored chains) (Komander et al., 2009). Importantly, specificity is not restricted to particular DUBs families. USPs comprise enzymes that target particular substrates, showing little affinity to lysine linkage. By contrast, OTU family encompasses members with an exquisite linkage specificity (Bremm and Komander, 2011). For instance, A20 and OTUB1, are specific for Lys^{48}-linked chains and do not hydrolyze Lys^{63}-linked or linear chains (Komander et al., 2009; Wang et al., 2009). Similarly, Cezanne which associates with Lys^{11}-linked chain disassembly (Bremm et al., 2010; Song and Rape, 2008) or TRABID, that hydrolyzes both Lys^{29}- and Lys^{33}-linked diubiquitin (Licchesi et al., 2011).

The human genome encodes 79 deubiquitinating enzymes predicted to be active (Nijman et al., 2005), whereas 24 DUBs are encoded in *S. cerevisiae* (Reyes-Turcu et al., 2009). Although most of them have not been formally characterized, Sowa et al. applied a platform called CompPASS for proteomic and informatic analysis to human DUBs leading to the identification of candidate pathways and targets for a large fraction of DUBs (Sowa et al., 2009). It has been demonstrated that these enzymes play pivotal regulatory roles in various cellular processes, like hereditary cancer, cell-cycle regulation or neurodegeneration (Amerik and Hochstrasser, 2004), however, most of them have not been investigated yet. It will be crucial to gain further knowledge of DUBs specificity and mode of acting in choreographed events to obtain a multidimensional view of the ubiquitin code.

Ubiquitin Interacting Surfaces

The huge spectrum of functions given by ubiquitin signaling pathway it can also be explained by the network of interactions between Ub and proteins containing Ub interacting surfaces. Recognition of the

diversity of ubiquitin signals has been achieved in eukaryotes by a variety of ubiquitin-binding domains (UBDs) or ubiquitin receptors that contain at least one UBD within their structure (Dikic et al., 2009). Several pathways within the ubiquitin system have been shown to concentrate multiple factors that bind ubiquitin. In addition to proteasome pathway, which contains at least five ubiquitin receptors and four deubiquitinating enzymes (see next sections for detailed information), the endocytic pathway, DNA maintenance and damage response pathways, and NFkB signaling pathway have been shown to use a complex network of ubiquitin recognition factors (Bennett and Harper, 2008; Haglund et al., 2003; Komander et al., 2009; Lo et al., 2009; Saksena et al., 2007; Wagner et al., 2008).

Several distinct modes of UBD interaction with ubiquitin have been described so far, involving approximately 20 different families (summarized in Table 1) (Husnjak and Dikic, 2012). Although structurally different, UBDs share a feature of noncovalently binding to ubiquitin signals. UBDs can be divided into several subfamilies: **1.** single or multiple α-helices [ubiquitin associated (UBA) domain, ubiquit interacting motif (UIM), double-sided, ubiquitin interacting motif (DUIM), motif interacting with ubiquitin (MIU), coupling of ubiquitin conjugation to endoplasmic reticulum degradation (CUE), GGA and Tom1 (GAT), Vps27/Hrs/STAM (VHS), ubiquitin binding in ABIN and NEMO (UBAN) protein]; **2.** zinc fingers [nuclear protein localization 4 zinc finger (NZF), zinc-finger ubiquitin-binding protein (ZnF UBP), zinc finger in A20 protein (ZnF A20), ubiquitin-binding zinc finger (UBZ)]; **3.** a pleckstrin-homology (PH) fold [gramlike ubiquitin-binding in Eap45 (GLUE), pleckstrin-like receptor for ubiquitin (PRU)]; **4.** ubiquitin-conjugating-like structures [ubiquitin E2 variant (UEV) and UBC] and **5.** other structures [SH3, ubiquitin-binding motif (UBM), PLAA family ubiquitin binding domain (PFU), Jab1/MPN].

UBD	Structure	Ub Surface	Type of Ub binding	Proteins with specific UBDs
UBA	Three-helix bundle	Ile44	mUb; polyUb (>K48); UBL	PLIC1/2, HHR23A/B, Ddi1, p62/SQSTM1,NBR1, Cbl-b, USP5, UBC1,HERC2
CUE	Three-helix bundle	Ile44	mUb	Cue2 (monomeric), Vps9 (dimeric)
UIM	Single α-helix	Ile44	mUb; polyUb (K48, K63); UBL	S5a, Vps27, USP28, ataxin-3, EPS15, STAM, RAP80
MIU/IUIM	Single α-helix	Ile44	mUb	Rabex-5
DUIM	Single α-helix	Ile44	mUb	Hrs
VHS	Superhelix of eight α-helices	Ile44	mUb	STAM, Hrs
GAT	Three-helix bundle	Ile44	mUb	GGA3, TOM1
NZF	Zinc finger, four β-strands	Ile44	mUb; pUb (K63)	Npl4, VPS36, TAB2, TAB3, HOIP, HOIL-1L
ZnF A20	Zinc finger	Asp58	mUb (Rabex-5); Lys63 (A20)	A20, Rabex-5
ZnF UBP	Zinc finger	Leu8, Ile36	pUb (unanchored)	USP5,HDAC6, BRAP2
UBZ	Zinc finger, ββα-fold	Ile44	mUb; pUb	Polymerase η, polymeraseκ,FAN1, NDP52, TAX1BP1, WRNIP1
UBC	β-sheet	Ile44	mUb	UbcH5C
UEV	αβ-sequence	Ile44	mUb	VPS23, TSG101
UBM	Helix turn helix	Leu8	mUb	Polymerase ι , polymerase Rev1
GLUE	Split-pleckstrin homology domain	Ile44	mUb	EAP45
PRU	Pleckstrin homology domain	Ile44	mUb (Ile44); pUb (K48); UBL	Rpn13
Jab1/MPN	Inactive variant of Jab1/MPN domain	Ile44	mUb	Prp8p
PFU	Four ß-strands and two α-helices	Ile44	mUb; pUb	Doa1, PLAA
SH3	β-barrel fold	Ile44	mUb	Sla1, CIN85, amphiphysin
UBAN	Parallel coiled-coil dimer	Ile44; Phe4	Met1-diUb	NEMO, optineurin, ABIN1-3
WD40 repeat β-propeller	Top surface of WD40 repeat β-propeller	Ile44	mUb	Doa1/UFD3

Table 1: Summary Of The Different Ubiquitin-Binding Domains (UBDs).
For each UBD described so far, it is summarized: UBD abbreviation, structure, ubiquitin surface interaction, type of ubiquitin binding interaction and proteins containing the specific UBD. Adapted from Husnjak and Dikic, 2012.

The majority of identified UBDs bind to a hydrophobic patch around Isoleucine 44 of ubiquitin (Hicke and Riezman, 1996; Sloper-Mould et al., 2001) (Table 1). Adjacent binding surfaces on the large Ub hydrophobic (centered on the Leu^{8}, Ile^{44}, and Val^{70} residues) have also been shown to contribute to the

binding specificity of different UBDs. For example, the ubiquitin binding motif found in polymerases ι and Rev1 binds to the hydrophobic patch centered around Leu^{8} (Table 1) (Bienko et al., 2005), whereas the ubiquitin Asp58 residue binds the ZnF A20 domain of Rabex-5 (Table 1) (Penengo et al., 2006). In the case of DUB isopeptidase T (IsoT, USP5), the ZnF UBP domain primarily contacts the C-terminal part of ubiquitin, and the ubiquitin tail penetrates deeply into the hydrophobic pocket of the ZnF UBP domain (Table 1) (Reyes-Turcu et al., 2006). Additionally, ZnF UBP also interacts with a surface centered on Ile^{36} of ubiquitin. A comprehensive analysis of ubiquitin surface residues revealed two additional areas centered on Ile^{36}/Leu^{71}/Leu^{73} and Gln^{2}/Phe^{4}/Thr^{12} residues, which are important for vital functions in yeast (Sloper-Mould et al., 2001).

Although ubiquitin networks are involved in many cellular processes, the binding affinities of individual UBDs for Ub are generally low, with K_d values in high micromolar ranges (Fisher et al., 2003; Kang et al., 2003), especially because cellular ubiquitin concentrations can be as high as 85 μM (Kaiser et al., 2011). In many cases, protein oligomerization combined with multiple UBDs within single proteins (or within protein subcomplexes), and the presence of multiple ubiquitin-binding surfaces in single UBDs, provide the basis for a multivalent ubiquitin-binding complex. For example, many UIM-containing proteins involved in protein trafficking have been shown to associate with each other (Asao et al., 1997; Bache et al., 2003), enabling the buildup of large protein complexes. Although most UIMs bind monoubiquitin with low affinity (0.2–1 mM) (Fisher et al., 2003); the presence of multiple UIMs in UIM-containing proteins (Hofmann and Falquet, 2001) implies that cooperative binding might enhance binding affinity, where UIMs could bind to either multiple monoubiquitinated proteins or protein complexes. Different structural variations of UIM architecture have been utilized during evolution to expand the binding spectrum to diverse ubiquitin signals. In a DUIM, the UIM forms a single α-helix, which can simultaneously bind to two ubiquitin molecules on the opposite faces of the same helix (Hirano et al., 2006).

The Proteasome: A Central Element In Cell Physiology

The fate of a large fraction of cellular proteins modified by ubiquitin is the proteasome, which promotes their proteolysis (Goldberg et al., 1995; Xu et al., 2009). Like ubiquitin, proteasomes are intimately involved in multiple aspects of cell physiology. Its substrates are probably numbered in the hundreds and they are involved in diverse pathways. Therefore the proteasome functions as an integral component of many cellular regulatory mechanisms and, accordingly, its activity is under intricate control (Demartino and Gillette, 2007; Finley, 2009). The proteasome is an ATP-dependent protease of 1.4 MDa (Finley, 2009; Schrader et al., 2009; Volker and Lupas, 2002) that exists in multiple forms. It has the proteolytic and the unfolding activities in different compartments: the core particle (CP, also known as 20S particle) with peptidolytic activity, and a regulatory particle (RP, also known as 19S or PA700), with ATP-hydrolysing activity, that binds, unfolds and translocates polyubiquitinated proteins to the CP (Figure 7A). The RP is organized in 2 subparticles, the lid and the base which are distal and proximal to the CP, respectively (Figure 7A)

The 26S proteasome, although commonly considered a single entity of invariant structure and dedicated function, exists as a heterogeneous group of structures with different functional features. Moreover,

cells can regulate proteasome function in response to changing physiological demands both by altering the total number of proteasomes (Lecker et al., 2006) and by altering the subunit composition of proteasomes (Glickman and Raveh, 2005; Hanna et al., 2007).

The proteasomal activity has also been linked to the pathological states of many diseases, including inflammation, neurodegeneration and cancer, for different reasons. The increased sensitivity of malignant cells to proteasome inhibitors has resulted in proteasome inhibition emerging as a novel strategy for cancer treatment (Nalepa et al., 2006). Most proteasome inhibitors target the active sites of the CP and the chemical nature of these compounds includes peptide boronates, vinyl sulfones, epoxyketones and beta-lactones. Bortezomib, the active ingredient of velcade, is the first proteasome inhibitor to be approved as a single agent for the treatment of relapsed or refractory multiple myeloma (MM) (Jagannath et al., 2004; Richardson et al., 2003) and mantle cell lymphoma (Fisher et al., 2006). Bortezomib treatment is associated with manageable but substantial resistance (Orlowski and Kuhn, 2008) and thus, novel proteasome inhibitors are currently being developed, and several second-generation proteasome inhibitors are now entering clinical trials, including carfilzomib (PR-171) (Demo et al., 2007), marizomib (NPI-0052) (Fenical et al., 2009) and delanzomib (CEP-18770) (Piva et al., 2008). Like bortezomib, delanzomib is a reversible boronic acid-based inhibitor that suppresses NF-κB mediated transcription and induces apoptosis in human MM cell lines and patient-derived cells (Piva et al., 2008). It has a favorable cytotoxicity profile toward a variety of normal human cell lines as compared to bortezomib. In a preclinical model of human MM, delanzomib evidenced significant and sustained proteasome inhibition in tumors relative to normal tissues and antitumor efficacy, resulting in complete tumor regression in MM xenografts. On the other hand, a decline in proteasome activity, or the incapacity of the proteasome to degrade certain proteins, has been linked to the development of neurodegenerative diseases (Finley, 2009).

The Core Particle: Composition, Architecture And Function

The proteasomal core particle is a barrel-like complex of four stacked heptameric rings of 28 subunits, with the proteolytic active sites facing the interior space (Groll et al., 1997). Substrates gain entry to the core particle's interior through a gated axial channel (Groll et al., 2000; Rabl et al., 2008; Stadtmueller et al., 2010). Disruption of the gate enhances ubiquitin-dependent protein degradation in yeast (Bajorek et al., 2003). The channel is formed by the outermost subunits of the core particle, which constitute the α-rings, whereas the proteolytic sites are found in the central β-rings (Groll et al., 1997) (Figure 7B).

Even though the architecture of the CP is conserved in evolution, the composition of its subunits shows increasing levels of complexity in the range of evolution. With few exceptions, archea and eubacteria possess one alpha type and one beta type subunit, forming an homomeric ring based complex (Maupin-Furlow et al., 2006). Eukaryotic proteasomes express seven different alpha (alpha1-alpha7) and beta subunits (beta1-beta7) which occupy specific positions in the complex (Groll et al., 1997) (Figure 7B). Concerning proteolytic activity, the beta1, beta2 and beta5 subunit end termini define active sites, which contain a threonine residue that promotes nucleophylic attack in the proteolytic reaction. Higher eukaryotes contain two genes for each of these three catalytic subunits. Two of these genes (β1i and β5i) are encoded in the major histocompatibility locus and, with the third gene (β2i), are conditionally

expressed and selectively incorporated into newly synthesized proteasomes instead of their constitutive counterparts under certain physiological states, such as enhanced immune function (Baumeister et al., 1998). Proteasomes containing inducible catalytic subunits are termed “immunoproteasomes” as they participate in the production of major histocompatibility complex (MHC class I) antigenic peptides. Although antigen production also involves nonproteasomal events, immunoproteasomes display altered catalytic properties that favor production of certain class I peptides (Goldberg et al., 2002). Animals lacking genes for inducible catalytic subunits cannot produce these peptides, whereas overexpression of inducible genes enhances antigen production. Class I peptides are derived from proteins degraded by a ubiquitin-dependent process, demonstrating that catalytic features of the 26S immunoproteasome represent an important regulatory determinant of the antigen production pathway.

The cylindrical architecture of CP includes three interior chambers that are connected by a central channel. The innermost chamber is lined with the proteolytic active sites (N-termini of beta subunits) and is flanked by the two external chambers (Groll et al., 1997). The entry to the interior of the complex is composed of narrow pores, positioned at each end of the cylindrical complex. Moreover, pores are closed by extended N-termini of alpha pockets (Benaroudj et al., 2003; Groll et al., 2000; Kohler et al., 2001a; Kohler et al., 2001b; Tian et al., 2011) (Figure 7C, alpha pockets represented in blue). This design protects the cell from unregulated protein degradation and has an important consequence: the CP needs to be activated to be functional. Association of additional factors (such as subunits of the RP, in yellow in Figure 7D) to the ends of the barrel structure drives the shift of N-termini of alpha subunits and open the gate, which promotes complex activation (Groll et al., 2000; Stadtmueller and Hill) (Figure 7D). When RP binds to the cylinder end of the CP and opens a channel located centrally within the cylinder end, the axial channel opens directly onto the RP. The substrate translocation channel, even when opened, is too narrow preventing out-of-control cytoplasmatic proteins degradation. The channel also imposes another constraint on true substrates: they must be previously unfolded by the RP. Substrate entry in an unfolded state also facilitates efficient hydrolysis of substrates within the CP.

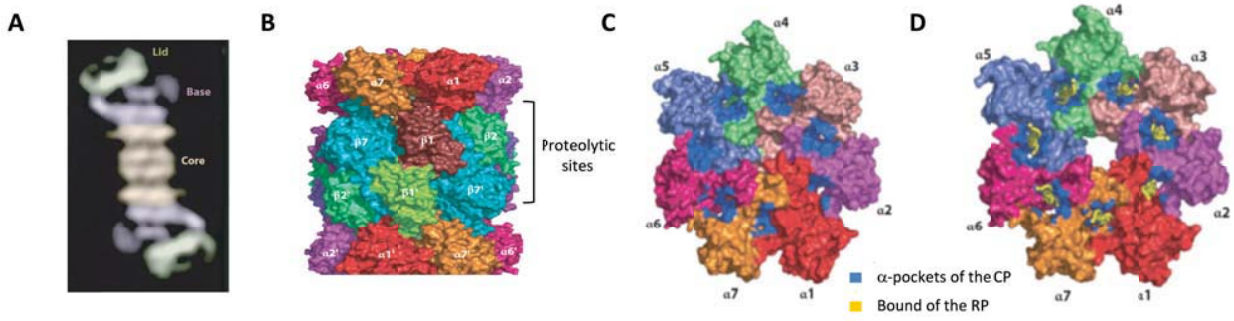

Figure 7: Structure Of The Proteasome And Its Core Particle.
(**A**) Structure of the proteasome holoenzyme. The image was generated by averaging of electron micrographs of negatively stained *Xenopus laevis* proteasomes. Adapted from Walz et al., 1998. (**B**) Surface representation of the CP, showing its organization into four heptameric rings of subunits. β-subunits constitute the proteolytic active sites. Adapted from Finley, 2009. (**C**) Close conformation of the α-ring of the free CP seen, with α-pockets of the CP

in blue. Adapted from Finley, 2009. (**D**) Open conformation of α-ring with bound RP subunits (yellow). Adapted from Finley, 2009.

The Regulatory Particle: A Nano-Machine That Binds And Processes Substrates

The RP is compound of, at least, 19 subunits in yeast (and probably the same number in other eukaryotes) and is organized in two sub-particles: the base and the lid. The ten components of the base include the six ATPases from the AAA family, named Rpt subunits, and four non-ATPase subunits, Rpn1, Rpn2, Rpn10 and Rpn13. The lid contains nine proteins (Rpn3, Rpn5-Rpn9, Rpn11-Rpn12, Sem1) (Glickman et al., 1998b) The topology of the yeast RP has been recently elucidated by electron microscopy tools, revealing the spatial rearrangement of the diverse subunits (Lander et al., 2012) (Figure 8A).

The ATPases form a ring and exhibit an activity that unfolds proteins in a process similar, but reversed, to chaperones (Braun et al., 1999). The Rpt ring pulls substrates into its central pore with sufficient force to promote unfolding of substrate structural domains that are too large to traverse the pore (Aubin-Tam et al., 2011). Therefore, the Rpts are crucial for RP-CP complex formation (Smith et al., 2007). This interface includes two aligned heteromeric rings, one formed by the six ATPase subunits of the RP and the other by the seven α subunits of the CP (Tian et al., 2011) (Figure 8B). The C-terminal segments (or tails) of the Rpt subunits are conserved in evolution and are critical for proteasome function: **1.** tails regulate the RP-CP interaction by their insertion into the α pockets of the CP (Thompson et al., 2009), resulting in the opening of the core particle channel (Rabl et al., 2008; Smith et al., 2007), and **2.** the tails also regulate RP assembly in yeast (Park et al., 2009a; Roelofs et al., 2009). There are six Rpt tails and seven α pockets. This symmetry mismatch indicates that the RP-CP interface is unexpectedly asymmetric (Tian et al., 2011) (Figure 8C). Using a cross-linking approach, Tian et al. have revealed that one side of the ring shows 1:1 contacts of Rpt2-α4, Rpt6-α3 and Rpt3-α2, whereas on the opposite side, the Rpt1, Rpt4 and Rpt5 tails each cross-link to multiple α pockets. The authors suggest that this asymmetry could lead to the existence of several interconvertible populations of proteasomes, which differ in the positioning of the unoccupied α pocket (Tian et al., 2011).

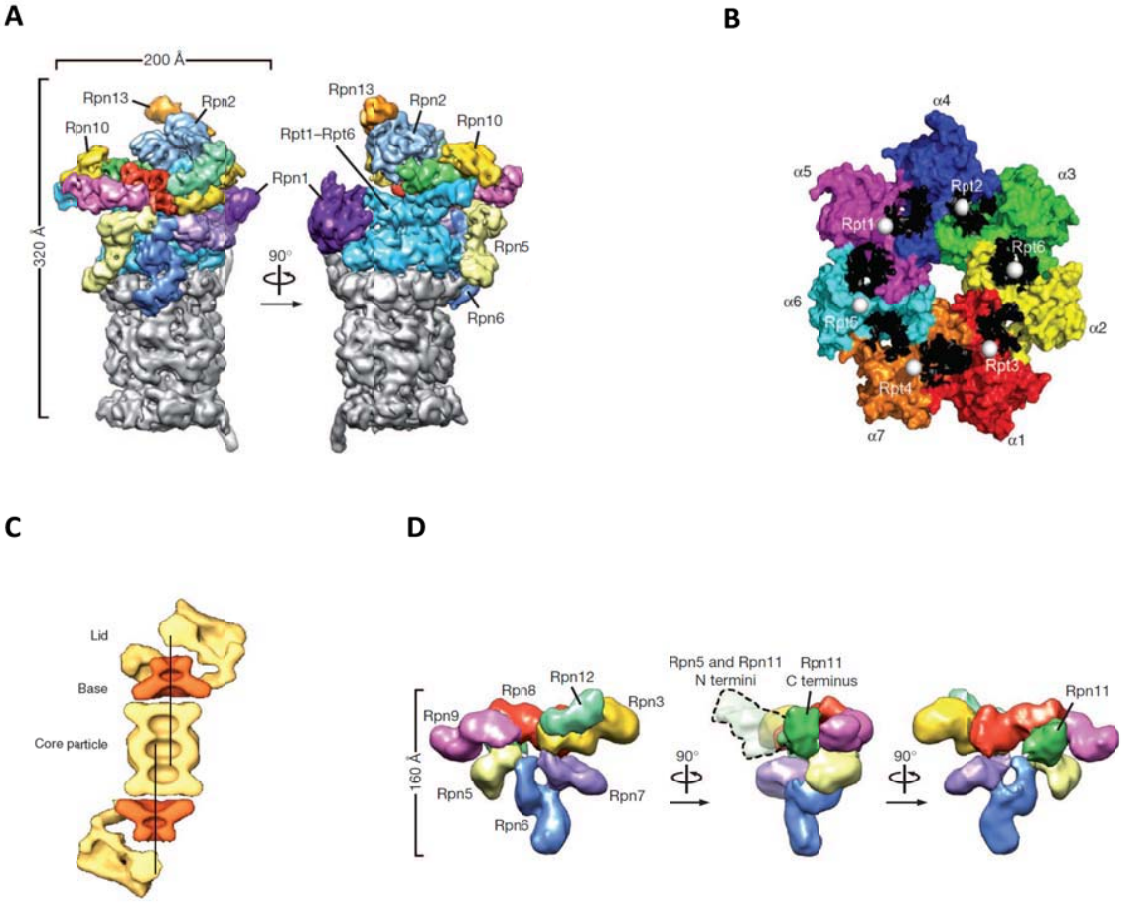

Figure 8: The Regulatory Particle Of The 26S Proteasome.

(**A**) Three-dimensional reconstitutions of the yeast 26S proteasome by electron microscopy. The CP is colored in grey and different colors are used for the lid subunits. Adapted from Lander et al., 2012. (**B**) Proposed model for mapping the six Rpt tails (ATPases of the RP) into the seven α-pockets of the CP. The pockets formed between subunits are colored black. The six Rpt C termini are represented by white spheres. Adapted from Tian et al., 2011. (**C**) Assembly of the ATPases (orange) to the CP shows a shift in the axis. Adapted from Tian et al., 2011. (**D**) A negative-stain reconstruction of the isolated lid subcomplex at 15 angstroms resolution, colored by subunit and shown from the exterior (left), the side (middle) and the interior, base-facing side (right). Adapted from Lander et al., 2012.

Other base components are the scaffolding proteins Rpn1 and Rpn2 and the ubiquitin receptors Rpn10 and Rpn13. The 19S-RP scaffolding subunits Rpn1 and Rpn2 function to engage ubiquitin receptors. Rpn1 and Rpn2 are characterized by eleven tandem copies of a 35-40 amino acid repeat motif termed the proteasome/cyclosome (PC) repeat. Rpn1 contacts the C-terminal helix of the 20S core subunit α4 and is flexible or loosely attached to the side of the base (Lander et al., 2012). The repeats of Rpn2 subunit are important to bind the ubiquitin receptor Rpn13 (He et al., 2012). Rpn10 is located above Rpt4/Rpt5, and Rpn13 above the Rpt1/Rpt2 heterodimer (Lander et al., 2012; Sakata et al., 2012).

The lid consists of nine non-ATPase proteins (Rpn3, Rpn5-Rpn9, Rpn11-Rpn12 and Sem1) including the deubiquitinating enzyme Rpn11. The Rpn11 subunit contains a highly conserved Jab1/MPN domain–associated metalloisopeptidase (JAMM) motif and its activity is essential for efficient substrate degradation and cell viability (Glickman et al., 1998b; Verma et al., 2002). Proteasome substrates, before being degraded, are first separated from some or all attached Ub groups. This step is mediated primarily by Rpn11.

Rpn3, Rpn5-Rpn7, Rpn9 and Rpn12 subunits contain a C-terminal PCI domain that is assumed to have scaffolding functions and allow inter-subunit contacts. The lid´s reconstruction provided sufficient resolution to unambiguously locate the the C-terminal PCI domains of the six Rpn subunits (Lander et al., 2012). Authors have shown that these domains interact to form a horseshoe-shaped anchor from which the amino terminal domains extend radially, demonstrating the scaffolding function of the PCI domains in the lid. Overall, Rpn3, Rpn7, Rpn6, Rpn5 and Rpn9 form the fingers of the hand-shaped lid structure (Figure 8D). Rpn8 shows and extended conformation that connects Rpn3 and Rpn9, and this closes the PCI horseshoe. In addition, it interacts with Rpn11, which lies in the palm of the hand. and makes extensive contacts with Rpn8, Rpn9 and Rpn5 (Lander et al., 2012). The assembly of the lid involves the sequential binding of pre-assembled lid subparticles. Thus, MPN subunits Rpn8 and Rpn11 form a subcomplex with PCI subunits Rpn5, Rpn9 and Rpn6 (Tomko and Hochstrasser, 2011). The latter, has the unique role of establishing contacts with the core particle (Lander et al., 2012; Pathare et al., 2012). Rpn3 and Rpn7 form another subcomplex, that also may contain Sem1. Interestingly, the total assembly of the lid requires the interaction of these two subcomplexes, and is culminated by the incorporation of Rpn12 (Tomko and Hochstrasser, 2011).

Subunits of the lid show a detailed, one-to-one correspondence to subunits of the COP9 signalosome (CSN) and of the translation factor eIF3. It has been shown that the COP9 signalosome (CSN) interacts with the ubiquitin-proteasome system to regulate protein turnover in eukaryotes (Eckardt, 2003; Harari-Steinberg and Chamovitz, 2004; Schwechheimer, 2004; Wei and Deng, 2003). The COP9 signalosome is a complex of eight subunits (Csn1 to Csn8), which are paralogs of the 19S lid subcomplex of the 26S proteasome regulatory particle. The CSN and lid subcomplex are also structurally related to the eukaryotic translation initiation factor eIF3, however, this latter complex is a more distant relative. All three complexes (CSN, 19S lid, and eIF3) contain subunits with MPN (Mov34, Pad N-terminal) and PCI (proteasome, COP9, eIF3) domains (Kim et al., 2001; Volker and Lupas, 2002).

Events Of The Degradation Process

From protein modification by polyubiquitin chains to protein unfolding by RP ATPases and actual degradation there's a number of molecular events. These events, the co-regulation of which is required for the proper proteolysis, include: **1.** mediation of substrate-proteasome interaction, either by binding to shuttling factors or direct binding to specific receptors in the proteasome, **2.** deubiquitination of substrates and **3.** the translocation of unfolded proteins to the CP which is carried out by the ATPase ring (see previous section).

1. A prerequisite for a protein-protein networking role of Ub is the existence of components that specifically recognize this post-translational modification. Five ubiquitin receptors associated to the proteasome are currently known: two proteasome subunits Rpn10 and Rpn13 and three "shuttle factors", Rad23, Dsk2 and Ddi1. These proteins are conserved through all eukaryotes. Importantly, none of these proteins is essential for yeast viability (Husnjak et al., 2008). Because these receptors are nonessential in yeast, additional Ub receptors for the proteasome probably remain to be identified. However, Rpn10 and Rad23 are both essential in mouse (Hamazaki et al., 2007; Ng et al., 2003). For more detailed information go to the below sections *Proteasomal Ubiquitin Receptors: Rpn10 and Rpn13* and *UBA-UBL Proteins*.

2. One aspect that remained unclear for many years was how the polyubiquitinated substrates are processed once they get to the proteasome. Initial observations suggested that ubiquitin was not co-degraded along with that substrate, and the presence of ubiquitin isopeptidases in the complex was postulated (Hershko et al., 1980). Later it was shown that, at least, three deubiquitinating enzymes act in the complex, and that their activities are coupled to degradation. Ubp6 (Hanna et al., 2006; Leggett et al., 2002), Rpn11 (Verma et al., 2002; Yao and Cohen, 2002), and Uch37 (Nishio et al., 2009; Yao et al., 2006). Different mechanisms of deubiquitination have been suggested for these deubiquitinating enzymes. While Ubp6 and Uch37 promote a progressive trimming of polyubiquitin, Rpn11 dissociates polyubiquitin *en bloc*, by a cleavage proximal to the substrate (Hanna et al., 2006; Nishio et al., 2009; Verma et al., 2002; Yao et al., 2006). Moreover, Ubp6 has an inhibitory effect on *en bloc* deubiquitination causing a delay in the process (Hanna et al., 2006). It has been shown that compounds that inhibit Ubp6/Usp14 have an activation effect on the proteasome (Lee et al., 2010) Hul5 is a ubiquitin ligase associated to the proteasome and intimately linked to activity and function of Ubp6 (Crosas et al., 2006; Leggett et al., 2002). Hul5 antagonizes Ubp6 by promoting the extension of polyubiquitin in substrates, resulting in the remodelling of polyubiquitin signal during the early processing of substrates in the proteasome.

3. In the last step, deubiquitinated substrates are translocated from the RP to the CP to be degraded. Because the passage between the RP and the CP is narrow, substrate translocation requires unfolding of the substrate, which is accomplished through the mechanical action of the six ATPases of the RP.

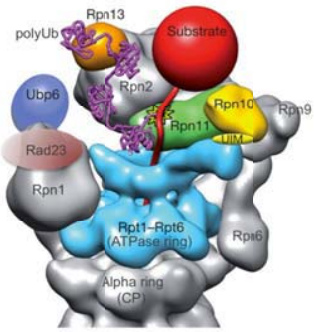

Figure 9: Model For The Recognition, Deubiquitination And Translocation Of A Polyubiquitinated Substrate By The 26S Proteasome.

A substrate conjugated with a K48-linked tetraubiquitin chain (magenta) is bound to a proteasomal ubiquitin receptor (Rpn10 and/or Rpn13). The target is then deubiquitinated by Rpn11 (green, active site indicated by a start) and translocated to the CP by ATPases subunits of the base of the RP (cyan). The "shuttle receptors", such as Rad23, are bound to base subunit Rpn1. The DUB UBp6 is localized further from the central pore, in a position to trim excess ubiquitin chains. Adapted from Lander et al., 2012.

The exact localization of both DUBs and Ub receptors inside the RP has been crucial to support the successive reactions from substrate recognition to protein unfolding and translocation. For instance, to allow cleavage without uncoupling from the receptor, the ubiquitin chain must be long enough to span the distance between receptor and Rpn11 DUB. Recent works by Lander et al. and Sakata et al. have illustrated that both Rpn13 and Rpn10 are located 70–80Å from the predicted position of the Rpn11 MPN domain (Lander et al., 2012; Sakata et al., 2012) (Figure 9). The "shuttle receptors" Rad23, Ddi1 and Dsk2 are expected to reside 80–120Å away from Rpn11, depending on where they bind Rpn1 (Elsasser et al., 2002; Gomez et al., 2011) (Figure 9). For receptor interaction, the ubiquitin chain has to be in an extended conformation with the hydrophobic patches exposed (Riedinger et al., 2010; Schreiner et al., 2008). A single ubiquitin moiety in an extended Lys^{48}-linked chain lengths approximately 30Å (Cook et al., 1992), then at least three ubiquitins are required to span the distance between Rpn10 or Rpn13 and Rpn11 (Lander et al., 2012). This model agrees with *in vitro* studies that indicate that a minimum of four Lys^{48}-linked ubiquitins is necessary for efficient substrate degradation (Thrower et al., 2000). Finally, Ubp6 is localized further from the entrance to the pore, being closer to the Rad23, Dsk2 and Ddi1 than to Rpn10 and Rpn13, suggesting that Ubp6 may act preferentially on substrates delivered by these "shuttle receptors" (Lander et al., 2012) (Figure 9).

Proteasomal Ubiquitin Receptors: Rpn10 And Rpn13

Two subunits of the RP, Rpn10 (S5a in humans) and Rpn13, are the major Ub receptors of the 26S proteasome (Deveraux et al., 1994; Husnjak et al., 2008; Schreiner et al., 2008; van Nocker et al., 1996). Rpn10, previously designated Mcb1 for multiubiquitin chain-binding protein, is a stoichiometric component of the base of the RP and it is the best characterized ubiquitin receptor. In 1996, Mcb1 was copurified with the 26S and, importantly, a significant fraction of the protein was detected in a low-molecular-mass form free of the 26S complex (van Nocker et al., 1996). Mcb1 showed high affinity to bind Lys^{48}-linked multiubiquitin chains and Δ*mcb1* deletion mutants were viable, grew at near wild type rates, degraded the bulk of short-lived proteins normally, and were not sensitive to UV radiation or heat stress (Fu et al., 1998; van Nocker et al., 1996), suggesting that Mcb1 was not an essential component of the ubiquitin proteasome pathway. However, *mcb1*Δ mutant exhibited sensitivity to amino acid analogs and showed increased steady-state levels of Ub conjugates such as ubiquitin-Pro-β-galactosidase (van Nocker et al., 1996). Although not essential in budding yeast, Rpn10/S5a is essential in mice (Hamazaki et al., 2007) and *Drosophila melanogaster* (Szlanka et al., 2003).

Rpn10 is a 37 kDa protein consisting in the N-terminal von Willebrand factor A domain (VWA) and the C-terminal ubiquitin interactif motif (UIM) (Figure 10A). *Saccharomyces cerevisiae* Rpn10 contains one UIM, whereas human and *Drosophila* S5a have two UIMs -located toward its C terminus and joined by a

flexible linker region (Kang et al., 2007)- and three UIMs, respectively (Figure 10A). The UIM region of S5a is a highly conserved hydrophobic patch that coincides with Leu-Ala-Leu-Ala-Leu motif (Leu-Ala-Met-Ala-Leu for yeast Rpn10) (Figure 10B) and has been implicated in the recognition of ubiquitinated conjugates (Deveraux et al., 1994; Fu et al., 1998; van Nocker et al., 1996). The UIM is a very short sequence motif of 20 residues and, as shown by NMR spectrometry, each UIM forms a single α-helix in which all the conserved residues are found exposed on one face (Shekhtman and Cowburn, 2002). Its tertiary structure is not well defined and it adopts a more ordered conformation upon ubiquitin binding (Wang et al., 2005).

The N terminus of Rpn10 contains a von Willebrand A (VWA) domain, whose precise function still remains to be defined (Figure 10A). It has been recently reported the VWA domain of S5a is a receptor of the UBA-UBL NUBL1 within the 26S proteasome and enables FAT10 (a ubiquitin-like modifier that can target proteins for degradation by the proteasome in a ubiquitin-independent manner) proteasomal degradation (Rani et al., 2012). Additionally, the VWA domain is known to be important for proteasome structure, stabilizing the lid-base interaction (Glickman et al., 1998a). Mutations of the VWA domain of Rpn10 promote dissociation of the RP into two modules, the base and lid (Fu et al., 1998; Glickman et al., 1998a). It has been largely reported that Rpn10´s VWA domain interact with both the base (through Rpn1) and the lid (through Rpn12) (Riedinger et al., 2010; Seeger et al., 2003). However, in Lander´s yeast RP model, the VWA domain of Rpn10 does not contact the base directly, but it bridges Rpn11 and Rpn9. This might increase the lid-base affinity indirectly by stabilizing Rpn11 (Lander et al., 2012).

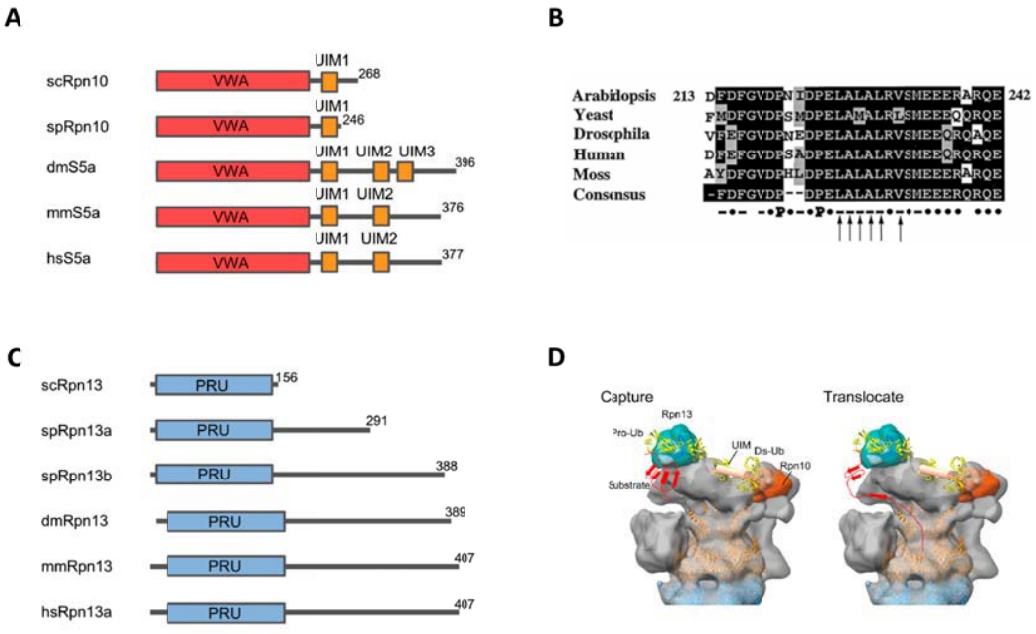

Figure 10: Rpn10 And Rpn13 Are The Main Proteasomal Ubiquitin Receptors.

(**A**) Rpn10 consists of the N-terminal von Willebrand factor A domain (red) and C-terminal UIM domain (orange). Saccharomyces cerevisiae Rpn10 contains only one ubiquitin-interacting motif (UIM), whereas human and Drosophila S5a contain two and three UIMs, respectively. (**B**). Amino acid sequence alignment of the UIM motif of

Rpn10 in different eukaryotes. The consensus sequence denotes hydrophobic residues by a dash (-), charges residues by ·, and prolines by P. Arrows indicate the hydrophobic residues which are necessary for the binding of multiubiquitin chains *in vitro*. Adapted from Fu et al. 1998. (**C**) The N-terminal pleckstrin-like receptor of ubiquitin domain of Rpn13 is generally conserved among species, whereas the C-terminal region which interacts with UCH37 is absent in *S. cerevisiae* and *S. pombe*. Adapted from Sakata et al. 2012. (**D**) Sakata´s model of substrate recognition by both Rpn10 and Rpn13 followed by translocation to the CP. *Capture*: the C terminal of the proximal (pro-) ubiquitin is suspended from Rpn13 pointing towards the central opening of the AAA-ATPase ring. The distal (dis-) Ub is associated with the Rpn10 UIM. The Ub chain spans the distance between the two receptors. *Translocate*: The substrate is grabbed by the flexible coiled coils of the ATPase ring and partially unfolded for further translocation into the CP. Adapted from Sakata et al. 2012.

Proteomic assays have been done to study the general impact of Rpn10 on proteasome´s turnover, demonstrating that Rpn10 mediates the targeting to the proteasome of a large number of ubiquitinated proteins (Mayor et al., 2005). For instance, cyclin B1, Sic1, Gic2 and Gcn4 have been shown to be targeted to Rpn10 in specific studies (Hanna et al., 2006; Seong et al., 2007; Verma et al., 2004). In addition, Rpn10 is involved in the recruitment of misfolded newly synthesized proteins produced upon proteolytic stress induced by heat shock or cadmium (Medicherla and Goldberg, 2008). When comparing wild-type and *rpn10*Δ strains, in the presence and absence of proteasome inhibitor MG132, the proportions of proteins involved in translation and DNA-associated proteins were significantly enhanced (Mayor et al., 2007). Of the proteins accumulating in *rpn10*Δ cells, only one-fifth accumulated upon the selective deletion of the UIM domain, indicating a critical role for Rpn10 other than ubiquitin receptor, localized in its N terminus. (Mayor et al., 2007). These results were in agreement with results presented by Fu et al. (1998), where authors showed that an intact UIM but a mutated N-terminal region failed to promote ubiquitin-Pro-β-galactosidase degradation and accentuated the sensitivity of the yeast Δ*rpn10* strain to amino acids analogs (Fu et al., 1998).

Different biological functions have been associated to the proteasome-unassociated pool of Rpn10 (Fu et al., 1998). The soluble pool of Rpn10, through its UIM, can alter the ubiquitination process so as to prevent the formation of nondegradable forked Ub chains (e.g., heterogeneous Lys^{48}- and Lys^{63}-linked chains) and therefore can stimulate markedly the degradation of certain substrates (Kim et al., 2009). Additionally, extra-proteasomal Rpn10 restricts the access of ubiquitin shuttle Dsk2 to the proteasome, inhibiting the flux through the proteasome, demonstrating that the biological significance of Rpn10 extends beyond the proteasome (Matiuhin et al., 2008) (Figure 12B).

Rpn13 is composed of an N-terminal pleckstrin-like receptor of ubiquitin (PRU) domain, which binds ubiquitin with high affinity (Husnjak et al., 2008; Schreiner et al., 2008) and a C-terminal extension consisting of a nine-helix bundle that binds to the deubiquitylating enzyme Uch37/UchL5 (Chen et al., 2010; Hamazaki et al., 2006) (Figure 10C). Binding to mammalian Rpn13 both facilitates the deubiquitination activity of Uch37 and links Uch37 to the proteasome. Thus, it has been suggested that Rpn13 plays a major role in Ub chain disassembly at the proteasome. However, yeast Rpn13 lacks the C-terminal extension and there is no Uch37 ortholog (Sakata et al., 2012) (Figure 10C). In yeast and mammals, Rpn13 binds to Rpn2 through its Pru domain (Chen et al., 2010; Hamazaki et al., 2006) and

this binding does not disturb the Rpn13 loops that bind ubiquitin (Schreiner et al., 2008). Rpn13 binds to Lys^{48}-linked ubiquitin chains, binding to mono- and diubiquitin at 1:1 and tetraubiquitin at 1:2 stoichiometries. NMR studies have demonstrated that Rpn10/S5a and Rpn13 bind Ub chains simultaneously with a preference of Rpn10 for distal ubiquitin and of Rpn13 for proximal ubiquitin (Zhang et al., 2009b). Sakata´s model of Rpn10 and Rpn13 proteasomal localization shows that the C terminus of the proximal ubiquitin is suspended from Rpn13 pointing toward the central opening of the ATPase ring. The distal Ub is associated with the Rpn10 UIM, so that the Ub chain spans the distance between the two receptors. Thus, the positions of both Ub receptors are suitable to support the successive reactions from substrate recognition to protein unfolding and translocation into the CP (Sakata et al., 2012) (Figure 10D).

The Ubiquitin-Like (UbL) - Ubiquitin-Associated (UBA) Family Of Ubiquitin Binding Proteins

Although polyubiquitin chains are able to bind directly to proteasome docking sites, there is a group of adaptor proteins, including Rad23, Ddi1 and Dsk2, which develop a mediation function, providing, probably, alternative anchorage sites (Elsasser et al., 2004; Verma et al., 2004) (Figure 11). These proteins, known as UBA-UBL proteins, have the dual property of binding polyubiquitin (by means of the ubiquitin-associated domain, UBA) and of interacting with the proteasome through its ubiquitin-like motif, UBL (Elsasser et al., 2002; Finley, 2009). This family of proteins is involved in a variety of additional cell processes, such as nucleotide excision repair (NER), spindle pole body duplication, and cell growth (Su and Lau, 2009). The UBL-UBA proteins are not integral proteasome subunits; they bind proteasomes transiently and they are usually substoichiometric components of purified proteasomes (Chen et al., 2001; Funakoshi et al., 2002; Wilkinson et al., 2001). UBA-UBL proteins bind proteasomes via an interaction with Rpn1, to some extent via Rpn13 (*e.g.* Dsk2) (Husnjak et al., 2008) and, in many eukaryotes, via human Rpn10 (S5a) (Leggett et al., 2002). Other proteins fulfilling diverse cellular functions are also known to bear a UBL domain, as it is the case of Ubp6 or the Ub ligase Parkin (Upadhya and Hegde, 2003). Among the UBA-UBL family, Ddi1 stands out because it contains as aspartyl protease domain. This domain is conserved from yeast to humans. Thus, Ddi1 is apparently not only a proteasomal cofactor but also a protease itself (Gabriely et al., 2008).

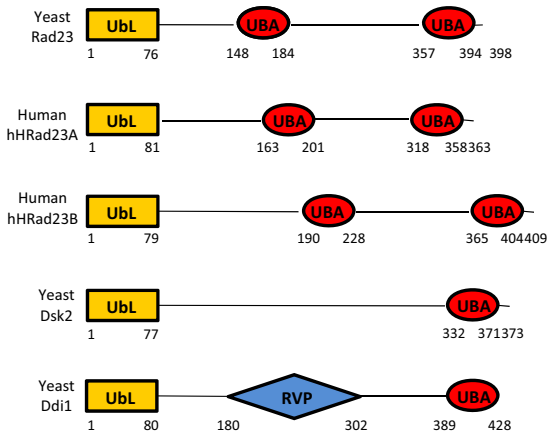

Figure 11: Schematic Diagram Of UBL-UBA Domain Containing Proteins In Yeast.

The UbL–UBA family of proteins contains an N-terminal UbL domain, one or more C-terminal UBA domain(s), and a variable central region (yeast Ddi1 contains a central RVP domain). Adapted from Su and Lau, 2009.

Rad23

Most of the conclusion of UBL-UBA´s mode of action has arisen from the research on Rad23 (Elsasser et al., 2004; Elsasser et al., 2002; Saeki et al., 2002a; Saeki et al., 2002b). It was initially identified as having a role in NER by dimerizing with Rad4, a DNA repair protein, and localizing in the nucleus (Watkins et al., 1993). Rad23 was first identified in *S. cerevisiae*, followed by the discoveries of homologues in *S. pombe* (Rhp23) (Lombaerts et al., 2000) and higher eukaryotes (HR23A and HR23B) (Masutani et al., 1994; Watkins et al., 1993). Rad23 binds tetraubiquitin and ubiquitin-conjugated cellular proteins via the UBA domains, but not monoubiquitin. The more N-terminally-located UBA1 domain may have a larger role in the latter interaction since UBA1 deletion mutants show less binding to ubiquitinated proteins than UBA2 deletion mutants (Chen and Madura, 2002; Wilkinson et al., 2001). The strong interaction with the proteasome is mediated by its UBL domain which has been shown to interact with S5a in human proteasomes (Wilkinson et al., 2001) and with Rpn1 in *S. cerevisiae* (Elsasser et al., 2002).

Overexpression or loss of Rad23 results in a significant increase in ubiquitinated proteins, with an even higher level observed in the UbL deletion mutant (Hwang et al., 2005). Overexpression of Rad23 also increases the amount of ubiquitinated protein associated with the proteasome but only in the presence of Rpn10, supporting that Rad23 is binding to ubiquitinated substrates and regulating their delivery to Rpn10 in the proteasome (Chen and Madura, 2002). This overexpression also prevents the expansion of multiubiquitin chains on model proteasomal substrates, resulting in protein stabilization (Chen and Madura, 2002; Kim et al., 2004). For example, overexpressed Rad23 reduces Rad4 multiubiquitination, and stabilizes Rad4 levels (Ortolan et al., 2004). Loss of Rad23, in conjunction with a Rpn10 mutant deleted for the UIM domain, stabilizes the CDK inhibitor, Sic1. Additionally, *rad23*Δ*rpn10*Δ double mutant exhibits growth defects, sensitivity to cellular stress, cell-cycle delays, accumulation of ubiquitinated conjugates, failure to degrade proteasome-dependent proteolytic substrates and cold sensitivity (Elsasser et al., 2004; Lambertson et al., 1999).

Dsk2

Dsk2 was initially identified in *S. cerevisiae* as having a role in spindle pole body duplication and was classified as an ubiquitin-like protein since it was 36% identical to ubiquitin (Biggins et al., 1996). Dsk2 has homologues in *S. pombe* (Dph1) and higher eukaryotes (XDRP1 in Xenopus, and Plic or Ubiquilin in mammals). Similar to Rad23, Dsk2 binds to poly -and not monoubiquitin- specifically K48-linked tetraubiquitin (not Lys^{29}- or Lys^{63}-linked) via the UBA domain (Funakoshi et al., 2002; Wilkinson et al., 2001). The Dsk2 UbL domain interacts weakly with the proteasome, and binds with lower affinity than the interaction of Rad23 with Rpn1 (Chen and Madura, 2002; Elsasser et al., 2002; Funakoshi et al., 2002; Matiuhin et al., 2008; Wilkinson et al., 2001).

Interestingly, Dsk2 association with the proteasome was found to only occur in the absence of Rpn10. Extraproteasomal Rpn10 competes for Dsk2 binding with the proteasome (Matiuhin et al., 2008). It has

also been reported the physical interaction between Rpn10 and Dsk2 (Matiuhin et al., 2008). Recent structural information has revealed that there is a hierarchy in affinities for Rpn10 association: Ub_4 > Ub_2 ≈ Dsk_2-UBL > monoUb, meaning that UIM's Rpn10 is complexed with the UBL of Dsk2 (Zhang et al., 2009a) (Figure 12A).

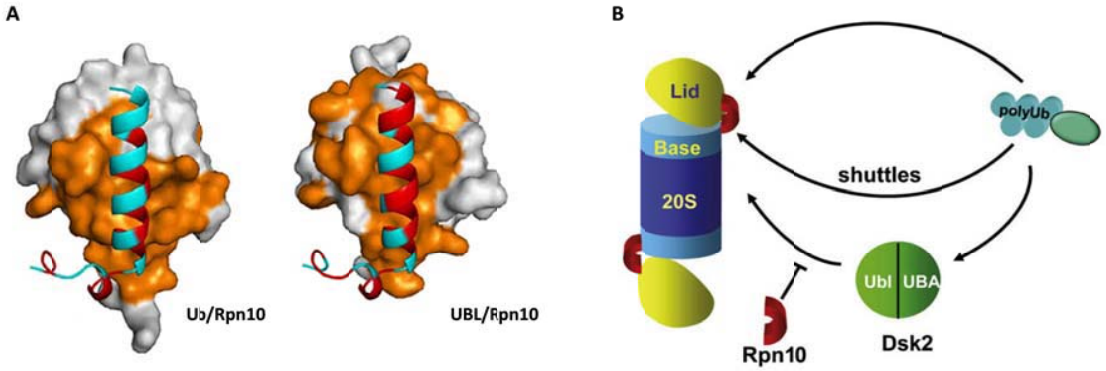

Figure 12: Physical And Functional Cooperation Between Rpn10 And Dsk2-UBL.
(**A**) Interactions between Rpn10-Ub (left panel) and Rpn10-UBL (right panel) were quantified by NMR titration and the complexes were mapped. Single-helix alpha of the UIM is represented. Orange illustrates Ub (left) and UBL (right) interaction in Rpn10 surface. Adapted from Zhang et al., 2009a. (**B**) A model describing regulation of Dsk2-escorted cargo destined for the proteasome. Ub-modified substrates may reach the 26S directly (top trajectory) or by Ub delivery proteins such as Dsk2, Rad23 and Ddi1, and possible Rpn10. Matiuhin et al. described that Dsk2-mediated trajectory is subjected to a filter in the form of extraproteasomal Rpn10 that limits the ability of Dsk2, inhibiting Dsk2-dependent substrates delivery to the proteasome. Adapted from Matiuhin et al., 2008.

Increased protein levels of Dsk2 are cytotoxic in yeast and in *Drosophila melanogaster* (Lipinszki et al., 2011). Overexpression of Dsk2 results in ~4-fold increase in the total amount of Lys^{48}-linked polyubiquitin conjugates, with the UBA domain required for this effect (Funakoshi et al., 2002; Matiuhin et al., 2008). Surprisingly, the effects of Dsk2 overexpression are relieved by Rpn10 overexpression. This relief is because extra-proteasomal Rpn10 restricts Dsk2´s access to proteasome. Dsk2´s UBL domain blocks access to the proteasomal receptor Rpn10 by interacting to its UIM to, in turn, inhibit substrate flux through the proteasome (Matiuhin et al., 2008). Altogether reveals new regulatory relationships between the proteasome´s ubiquitin receptors and functional consequences that extend beyond simple docking of substrates to the proteasome.

Signaling Through Monoubiquitination

The addition of a single ubiquitin to a substrate is defined as monoubiquitination (mUb), which implies no polyubiquitin synthesis. Moreover, several lysine residues in the substrate can be tagged with one single ubiquitin moiety, giving rise to multiple monoubiquitination. Monoubiquitination thus provides a signalling mechanism that does not promote proteasome targeting but instead regulates important cellular pathways such as endocytosis of plasma membrane proteins, the sorting of proteins to the MVB,

budding of retroviruses, DNA repair, histone activity and transcriptional regulation (Di Fiore et al., 2003; Hicke, 2001; Hoeller et al., 2007; Kirkin and Dikic, 2007).

Importantly, several ubiquitin receptors, including proteins that control endocytic membrane traffic, have been found to be monoubiquitinated themselves. This type of modification, known as "coupled monoubiquitination", requires the presence of a UBD, and most known UBD have been found to sustain this process (Di Fiore et al., 2003; Hoeller et al., 2006; Woelk et al., 2006). Monoubiquitination of UBD-containing proteins imposes an autoinhibitory conformation rendering them unable to bind *in trans* to ubiquitinated targets, thus providing an intrinsic switch-off mechanism for Ub-binding proteins.

Two different E3 ligases, the RING-type Parking ligase and the HECT-type Nedd4, have been shown to promote monoubiquitination of the endocytic protein Eps15 by mechanisms that require an intact UIM of Eps15 (Fallon et al., 2006). In the case of the HECT-type Nedd4, Eps15 UIM binds monoubiquitin attached to Nedd4 and then transfers thiolester-bound ubiquitin to Eps15 (Figure 13A). In the other case, the UIM of Eps15 interacts with the UBL domain of Parkin, which in turns mediates the Eps15 monoubiquitination (Figure 13B). Woelk et al. have shown that E3 ubiquitination is required for coupled monoubiquitination of Eps15 *in vivo* and provide a mechanistic explanation for why an intact Eps15 UIM is necessary for this process.

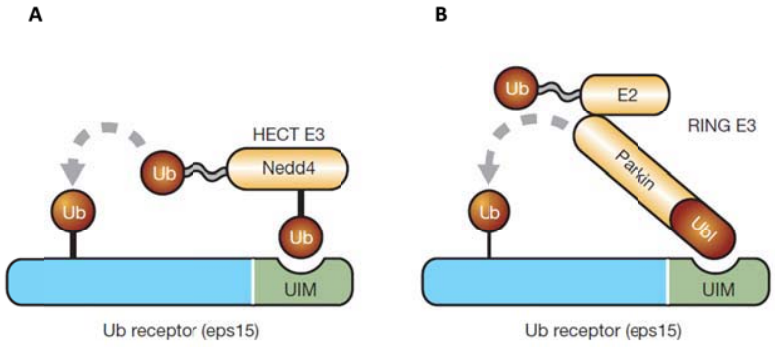

Figure 13: Representation Of Two Proposed Mechanisms For Coupled Monoubiquitination.
(**A**) A monoubiquitinated HECT-type E3 (Nedd4) interacts with the UIM of the ubiquitin receptor and transfers thioester-conjugated ubiquitin from itself to the ubiquitin receptor, which becomes monoubiquitinated. Importantly, HECT ligases form a catalytic intermediate wherein Ub is linked through a thiolester bond (in grey) to the active site cysteine of the ligase. (**B**) In an analogous manner, the UBL domain of Parkin RING ligase interacts with the UIM of the receptor and mediates the monoubiquitination by transferring the Ub from the E2 conjugating enzyme to substrate, without an intervening catalytic intermediate. Both adapted from Haglund and Stenmark, 2006.

A major unanswered question is how the ubiquitin machinery discriminates whether to mono- or polyubiquitinate specific targets. Different possibilities can be considered: **1.** Different subsets of E3 have specificity for the two different modifications; e.g. Mdm2 E3 mediates monoubiquitination of p53, whereas p300 ligase promotes p53 polyubiquitination (Grossman et al., 2003). **2.** An individual E3 might

mediate either mono- or polyubiquitination, depending on the nature of the substrate, or on other molecular specifies, such as proteins interacting with the E3 in different subcellular locations. For instance, the E3 CBL can direct polyubiquitination and subsequent proteasome degradation of cytoplasmatic proteins (e. g., Abl tyrosine kinases) and monoubiquitination of receptor tyrosine kinases. **3.** The type of Ub modification might be also determined by the UBD of the target protein, such as monoubiquitination of the CUE-domain-containing Vsp9 protein by Rsp5. **4.** Finally, in case that E3 activity generates processive polyubiquitination, the engagement of cognate DUBs would promote monoubiquitination by trimming polyubiquitin signal on substrates (Kee et al., 2005).

In the present work, a novel role of monoubiquitin signal in proteasome regulation is presented. The proteasome receptor Rpn10 is monoubiquitinated by a member of the Nedd4 ubiquitin ligase family and the UIM of Rpn10 is required for the catalysis of monoubiquitination (Isasa et al., 2010).

Mass Spectrometry-Based Proteomics: A Key Technology For Large-Scale Identification Of *In Vivo* Post-Translational Modifications

In the last decade, the genomics revolution has created an impressive amount of data based on the DNA and RNA levels (Wolfe and Li, 2003). More recently, the term proteomics has emerged as a key tool to to obtain a global view of biological function at the protein expression level, similar to what has already been possible at DNA and RNA levels. Proteomics denotes the systematic analysis of proteins for their identity, quantity and function providing an entire complement of proteins expressed in a specific state of an organism or a cell population (Wilkins et al., 1996). However, proteomics is very different from genomics in almost every aspect. Genomics measures genotype of an organism, whereas proteomics measures the phenotype, which is the consequence of both the genotype and the past and present environment of the organism (Cox and Mann, 2011).

Mass spectrometry´s (MS) characteristics have raised an outstanding position among analytical methods: unequally sensitivity, detection limits, speed and diversity of its applications. MS has progressed extremely rapidly during the last decade. As the field matures, MS-based proteomics delivers three distinct types of experimental results or data types. First, expression proteomics determines the relative or absolute amount of proteins in a sample. This is analogous to transcriptomics, mRNA measurements or deep sequencing methods. However, the main advantage to focus on proteins is that this automatically takes into account posttranscriptional and posttranslational levels. Secondly, proteomics data is accessible to the modification state of proteins. MS can identify and quantify all elements of the primary structure of the mature protein, including its posttranslational modifications (PTMs), on a near-global scale (Choudhary and Mann, 2010). Third, proteomics is exceptionally well suited for the mapping of protein interactions, which is a crucial contribution to network biology (Sowa et al., 2009). These three types of information can be applied in a myriad of different formats to dynamically study biological processes.

The Basic Principle

A mass spectrometer is an instrument that measures the masses of individual molecules that have been converted into ions. The main idea can be compared to the following ordinary situation. If something is moving and it is subjected to a sideways force, instead of moving in a straight line, it will move in a curve - deflected out of its original path by the sideways force. For instance, a jet of water from a hose-pipe would be enough to deflect a table tennis ball travelling at a given speed, but a cannonball travelling at the same speed, would hardly be deflected from its original course. Thus, the amount of deflection for a given sideways force will depend on the mass of the ball. The less the deflection, the heavier the ball. With a known speed of the ball, the size of the force and the sort of curve path it has been deflected through, the mass of the ball can be easily calculated. The same principle can be applied to atomic sized particles.

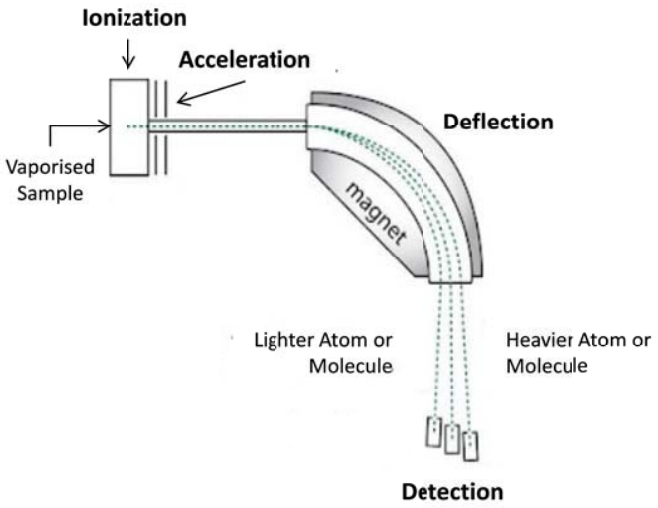

Figure 14: The Basic Principle Of A Mass Spectrometer.
A mass spectrometer is an instrument that measures the masses of individual molecules that have been converted into ions. The sequence is of what happens in a mass spectrometer is : **1.** Ionization, **2.** Acceleration, **3.** Deflection and **4.** Detection.

In order to achieve the above mentioned task, the molecules of interest need to be charged. Then the trajectories of the resulting ions are measured in vacuum to various combinations of electric and magnetic fields. The sequence of what happens in a basic magnetic mass spectrometer is next listed (Figure 14): **1.** *Ionization*. Atom are ionized by knocking one or more electrons off giving a positive ion. **2.** *Acceleration*. Ions are accelerated so that they all have the same kinetic energy. **3.** *Deflection*. Ions are then deflected by a magnetic field according to their masses. The amount of deflection depends on the mass and number of positive charges on the ion. The more the ion is charged, the more it gets deflected. **4.** *Detection*. The beam of ions passing through the machine are detected electrically.

The Instrument

Ion Sources

In the ion sources, the analyzed samples are ionized prior to analysis in the mass spectrometer. A variety of ionization techniques are used for mass spectrometry. The most important considerations are the internal energy transferred during the ionization process and the physico-chemical properties of the analyte that can be ionized. Some of them are very energetic and cause extensive fragmentation. Other techniques are softer and only produce ions of the molecular species.

Electron ionization, chemical ionization and field ionization are only suitable for gas-phase ionization and thus their use is limited to compounds sufficiently volatile and thermally stable. Electron ionization is widely used in mass spectrometry, particularly for organic molecules and it induces extensive fragmentation, so that the molecular ions are not always observed (Mora et al., 2000). However, a large number of compounds are thermally labile or do not have sufficient vapor pressure. Molecules of these compounds must be directly extracted from the condensed to the gas phase.

The direct ion sources exist under two types: liquid-phase ions sources and solid-state ions sources. In liquid-phase ions sources the analyte is in solution. This solution is introduced, by nebulization, as droplets into the source where ions are produced at atmospheric pressure and focused into the mass spectrometer through some vacuum pumping stages. Electrospray, atmospheric pressure chemical ionization and atmospheric pressure photoionization sources correspond to this type.

In solid-phase ion sources, the analyte is an involatile deposit. It is obtained by various preparation methods which frequently involve the introduction of a matrix that can be either a solid or viscous fluid. This deposit is then irradiated by energetic particles or photons that desorb ions near the surface of the deposit. These ions can be extracted by an electric field and focused towards the analyzer. Matrix-assisted laser desorption, secondary ion mass spectrometry, plasma desorption and field desorption all use this strategy to produce ions.

Mass Analyzers

Once the gas-phase ions have been produced, they need to be separated according to their masses, which must be determined. The physical property of ions that is measured by a mass analyzer (MA) is their mass-to-charge ratio (*m/z*) rather than their masses alone. As there are a great variety of sources, several types of mass analyzers have been developed. Indeed, the separation of ions according to their *m/z* ratio can be based on different principles. All of them use static or dynamic electric and magnetic fields that can be alone or combined. Most of the basic differences between the different types of MA lie in the manner in which such fields are used to achieve separation. Each MA has its advantages and limitations.

Analyzers can be divided into two broad classes on the basis of many properties. Scanning analyzers transmit the ions of different masses successively along a time scale (i.e. quadrupole instruments). Other analyzers allow the simultaneous transmission of all ions, such the dispersive magnetic analyzer,

the TOF mass analyzer and the trapped-ion mass analyzer that correspond to the ion traps, or the orbitrap instruments. Analyzers can be grouped on the basis of other properties, for example ion beam versus ion trapping types, continuous versus pulsed analysis or low versus high kinetic energies.

The five main characteristics for measuring the performance of a MA are the mass range limit, the analysis speed, the transmission, the mass accuracy and the resolution. The mass range determines the limit of *m/z* over which the MA can measure ions. The analysis speed is the rate at which the analyser measures over a particular mass range. The transmission is the ratio of the number of ions reaching the detector and the number of ions entering the MA. Mass accuracy indicates the accuracy of the m/z provided by the MA. It is the difference that is observed between the theoretical *m/z* and the measured *m/z*. Last but not least, the resolution or resolving power is the ability of a MA to yield distinct signals for two ions with small *m/z* difference.

Detectors

The ions that pass through the MA are then detected and transformed into a usable signal by a detector. Detectors are able to generate from the incident ions an electric current that is proportional to their abundance. Several types of detectors currently exist; the choice depends on the design of the instrument and the analytical applications that will be performed. However, detection of ions is always based on their charge, their mass or their speed. Detectors can be mainly divided into two classes. Some detectors are made to count ions of a single mass at a time and therefore they detect the arrival of all ions sequentially at one point. Other detectors have the ability to count multiple masses and detect the arrival of all ions simultaneously along a plane.

Tandem Mass Spectrometry

Another trend in MS is to combine different MA in sequence in order to increase the versatility and allow multiple experiments to be performed. Tandem mass spectrometry, abbreviated MS/MS, is any general method involving at least two stages of mass analyzers, either in conjunction with a dissociation process or in a chemical reaction that causes a change in the mass or charge of the ion (Donato et al., 2012). In the most common MS/MS experiment a first analyzer is used to isolate a precursor ion, which then undergoes spontaneously or by some activation a fragmentation to yield product ions and neutral fragments: $m_p^+ \rightarrow m_f^+ + m_n$. A second spectrometer analyses the product ions, allowing fragments over several generations to be observed. With MS/MS, the confidence in peptide identification it is significantly enhanced and the influence of noise in quantitative studies is reduced.

Shotgun Proteomics Workflow

Figure 15 outlines a generic shotgun proteomics workflow. The term shotgun is used when using a combination of high performance liquid chromatography (HPLC) combined with mass spectrometry. Proteomics uses a wide variety of input materials, from prokaryote or eukaryote cells through entire tissues and body fluids. Proteins are digested to peptides – preferably by a sequence-specific enzyme such as trypsin - because peptides are easier to separate and analyze by LC-MS (liquid chomatograpgy followed by mass spectrometry) than proteins and because MS is much more sensitive for low molecular-weight molecules. The peptide-based proteomics is called “top-down” proteomics (Kellie et

al., 2010; McLafferty et al., 2007). The peptide mixture is separated in high-performance liquid chromatography (HPLC) and an ionization source converts the peptides to gas phase ions. Many peptides coelute from the column and reach the mass spectrometer at the same time and in vastly different concentrations. To reduce complexity, at least one additional step of peptide separation is performed. As the peptides elute from the column and are electrosprayed, the mass spectrometer scans the entire mass range every few seconds. The acquisition software of the mass spectrometer then selects a number of peptides in the mass spectra and proceeds to isolate each one of them, to fragment them in the mass spectrometer and to measure the mass spectra of the fragments (MS/MS). The peptide mass is used together with the masses of its fragments for peptide identification. Finally, these data are scanned through an amino acid sequence database by algorithms that calculate the predicted spectrum for each possible linear peptide sequence. They return the most similar peptide according to the mass spectrum and tandem mass spectrum data one that most likely (Sadygov et al., 2004). Robust techniques for determining false discovery rates (Elias and Gygi, 2007) and stringent community requirements for peptide identification, allow unambiguous assignment of peptide sequences to more than half of all tandem mass spectra

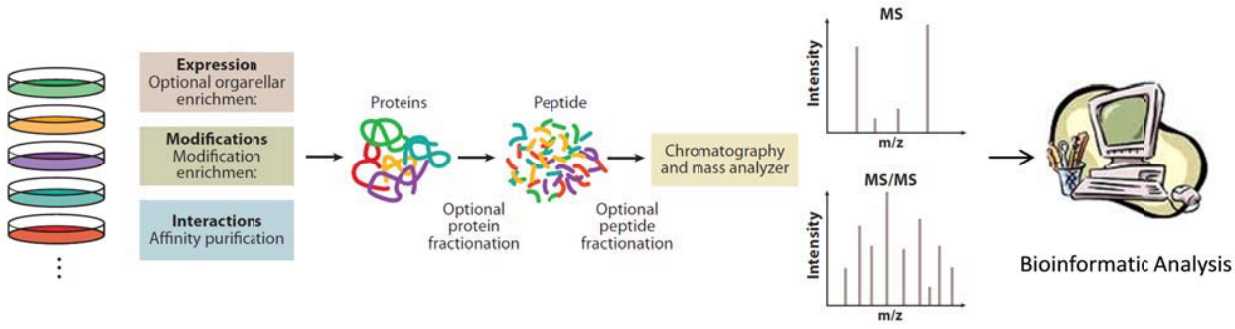

Figure 15: Generic Shotgun Proteomics Workflow.
Depending on the study, optional organellar enrichment, enrichment of modifications or affinity purification is performed up front as indicated in the colored boxes. Prefractionation at the protein or peptide level can be introduced to increase the coverage and dynamic range. Analysis with chromatography and MS then results in large data sets of MS and tandem mass spectrometry (MS/MS). Bioinformatic analysis is required for quantitative peptide information and characteristic fragmentation patterns, which are used for determining the sequence and the mass-to-charge ratio. Adapted from Cox and Mann, 2011.

Quantitative Mass Spectrometry

Quantification is of pivotal importance in MS-based proteomics. The subfield of quantitative proteomics seeks to provide information about both protein and modified protein expression levels. The absolute amount of a protein in a sample is determined by the comparison of its signal to that of a spiked in standard peptide (Steen et al., 2005) or to a protein that is isotope labeled (Everley et al., 2004; Hanke et al., 2008), using the methods described below. Usually, changes in protein amount and/or levels of particular PTM upon a defined perturbation are of biological interest. There are two main approaches for quantitative MS: stable isotope-based or label-free methods.

Isotope-based methods incorporate heavy versions of specific molecules into the peptides, either by chemical derivatization or by metabolic labeling. For example, the amide group of peptides can be methylated by light (normal isotope) or heavy (^{15}N, ^{13}C, ^{2}H) version of a chemical reagent (Boersema et al., 2009). After samples are combined and analyzed, peptides appear as pairs with a defined mass difference. Several ratios can be obtained from a single peptide as it elutes and several peptides of the same protein are usually combined. In metabolic labeling, cells are cultured in defined isotope media and SILAC (Stable Isotope Labeling by Amino acids in Cell culture) is the method of choice in mammalian and yeast systems (Everley et al., 2004). This technology has recently gained popularity for its ability to compare the expression levels of thousands of proteins in a single experiment. SILAC makes use of ^{12}C- and ^{13}C-labeled amino acids (arginine and lysine) added to the growth media of separately cultured cell lines, giving rise to cells containing either *light* or *heavy* proteins, respectively. Upon mixing lysates collected from these cells, proteins can be identified by MS/MS. The incorporation of stable isotopes also allows for a quantitative comparison between the two samples.

In 2003, Dr. Steven Gygi and his team presented an innovative strategy for the absolute quantification (termed AQUA) of proteins and their modification states (Gerber et al., 2003), which has uncovered the foundation for MS-based biomarkers validation. By using a labeled molecule as an internal standard to protein analysis, it is possible to address numerous biochemical and functional aspects that are transparent to existing molecular techniques. The strategy has two stages: peptide internal standard selection and validation, and method development and implementation (Kirkpatrick et al., 2005) (Figure 16).

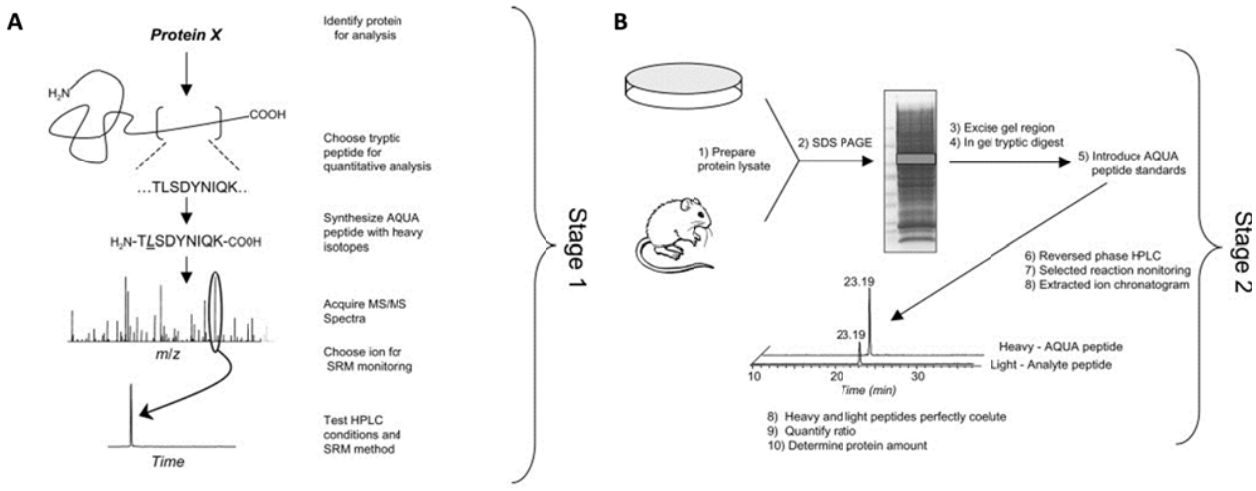

Figure 16: General Scheme for Absolute Quantification Using the AQUA Strategy.
(**A**) Methods development for absolute quantification of an exemple protein, Protein X. A representative tryptic peptide (TLSDYNIQK) is selected and an internal standard peptide is synthesized to mimic the native peptide, but which contains stable isotopes. Here, heavy leucine (6-^{13}C + 1-^{15}N = 7Da) is incorporated in the second position. LC-MS/MS analysis is performed for the purpose of selecting a high *m/z* product ion for selected reaction monitoring (SRM). LC-SRM conditions are tested for the peptide. (**B**) Application of a typical AQUA experiment. Protein lysate is prepared from cultured cells, tissue or clinical specimens. Proteins are separated by SDS-PAGE. The region

containing the target protein is excised and digested enzymatically in the presence of isotope labeled internal standard (AQUA) peptides. Extracted peptides are separated by HPLC and analyzed by tandem mass spectrometry. Extracted ion chromatograms from analyte peptides (light) are compared to coeluting internal standard peptides (heavy). Adapted from Gerber et al., 2003.

The first stage of the AQUA strategy involves the selection and standard synthesis of a peptide, which is chosen based on amino acid sequence and the protease to be used. During synthesis, stable isotopes are incorporated (e.g., ^{13}C, ^{15}N, etc) at a single amino acid residue. The result is a peptide that is chemically identical to its native counterpart formed by proteolysis, but is easily distinguishable by MS via a mass shift. The newly synthesized AQUA internal standard peptide is then evaluated by Liquid Chromatography (LC)-MS/MS to perform a Standard Reference Method (SRM). This process provides qualitative information about peptide retention, ionization efficiency and fragmentation (Figure 16A). The second stage is the implementation of the new peptide internal standard to measure the amount of a protein or modified protein from complex mixtures (Figure 16B). Whole-cell lysates are quickly fractionated by SDS-PAGE gel electrophoresis, and regions of the gel consistent with protein migration are excised. This process is followed by in-gel proteolysis in the presence of the AQUA peptides and LC-SMR. The retention time and fragmentation pattern of the native peptide formed by trypsinization is identical to that of the AQUA internal standard peptide determined previously; thus LC-MS/MS analysis results in a highly specific and sensitive measurement of both internal standard and analyte directly from extremely complex peptide mixtures. Because an absolute amount of the AQUA peptide is added, the ratio of the areas under the curve can be used to determine the precise expression levels of the protein of interest in the original cell lysate.

High-resolution mass spectrometry-based proteomics has emerged as the key technology for large-scale identification and quantification of thousands of *in vivo* PTM. Multiplex quantitative proteomics can be used to analyze relative changes in PTM abundance on a global scale, enabling the ability to determine not only the protein concentration but the stoichiometry of complexes or modifications for multiple components simultaneously and under different conditions. MS characterization of modified peptides is challenging because the modification may be labile during fragmentation or it may otherwise make the interpretation of tandem mass spectra difficult. The main challenge in PTM analysis, compared to proteome analysis, of the low abundance of modified peptides. Fortunately, this modification can often be alleviated by modification-specific enrichment.

To identify ubiquitinated proteins and the modified lysine residues it has been recently developed a mass-spectrometry-based approach known as ubiquitin remnant profiling (Emanuele et al., 2011; Kim et al., 2011b; Wagner et al., 2011). In proteomic methods for analyzing other posttranslational modifications, such as phosphorylation or acetylation, the target sequences are pulled out using antibodies specific to the modification. In contrast, ubiquitin remnant profiling relies on antibodies that recognize a protein modification generated after a ubiquitinated protein is digested with trypsin (Figure 17).

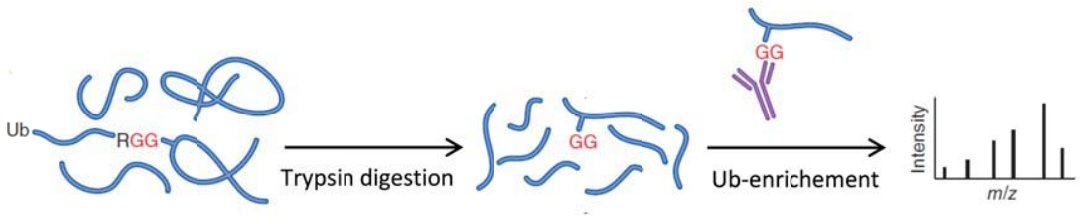

Figure 17: Ubiquitin Remnant Profiling to Identify Portein Ubiquitination Sites.
In ubiquitin remnant profiling, ubiquitin remnants are revealed after trypsin digestion of lysates. Trypsin cleaves ubiquitin after arginine residue near its C-terminus, leaving a ubiquitin-derived diglycine remnant on lysine residues in target proteins. Ubiquitin remnant-containing peptides are purified with a diglycyl-lysine-specific antibody. MS is used to sequence these peptides and identified the modified lysine residues. Adapted From Kim et al. 2011.

The C-terminal residues of ubiquitin are Arg-Gly-Gly; cleavage of ubiquitin after arginine leaves a diglycine (diGly) remnant attached to the modified lysine residues in proteins. Antibodies specific for diGly-modified lysines do not precipitate free ubiquitin but precipitate ubiquitin remnant-containing peptides from tryptic digests, allowing these peptides to be analyzed by mass spectrometry (as shown in Figure 15). In Dr. Gygi´s lab (Kim et al., 2011b), they have applied metabolic labeling together with this technology on human cells to generate the largest catalog of ubiquitination sites to date (~ 19.000). Consistent with previous studies (Peng et al., 2003), Kim et al. have revealed that a substantial number of proteins are ubiquitinated on multiple lysine residues, and that the ubiquitination status of each lysine residue can be independently regulated. A striking finding was that the majority of ubiquitination events in cells occur in newly synthesized proteins (< 70% of ubiquitinated sites dropped significantly after inhibition of protein synthesis). These results should be considered to differentiate 'quality-control' sites rather than 'regulatory' sites with roles in cellular pathways and classify ubiquitination sites as having a proteasomal-dependent or proteasomal-independent role.

Objectives

To uncover the biological significance of Rpn10 ubiquitination has been the axis of the present project. This goal has been divided into the following sections:

1. To characterize a pattern of post-translational modification of Rpn10 in cell extracts.
2. To elucidate the ubiquitin ligase and deubiquitinating enzyme involved in the regulation of Rpn10 monoubiquitination.
3. To reconstitute the enzymatic reactions of Rpn10 monoubiquitination and deubiquitination *in vitro*.
4. To determine the role of the UIM-motif in Rpn10 monoubiquitination.
5. To determine Rpn10 lysine(s) modified by ubiquitin.
6. To characterize the role and the effect of Rpn10 ubiquitination in the context of proteasome function.
7. To analyze the effect of a set of Rpn10 monoubiquitinated mutants *in vivo*
8. To assess the physiological significance and cellular distribution of Rpn10 ubiquitination under stress conditions leading to elevated protein degradation.
9. To characterize the residue-specific differential monoubiquitination according Rpn10 cellular localization.
10. To compare ubiquitinated proteins and their sites of modification of single mutant *rad23*Δ and double mutant *rad23*Δ*rpn10*Δ under normal and cold-shock growth.

Results

Rpn10 Is Monoubiquitinated In Vivo

In a recent study, it was shown that Rpn10 is degraded by the proteasome and that the ubiquitin ligase Hul5 is involved in this process (Crosas et al., 2006). To further examine the physiological significance of ubiquitination of Rpn10 we analyzed the status of Rpn10 protein in exponentially growing cultures. In direct analysis of cell extracts, an additional Rpn10 immunoreactive band with slower mobility was observed, suggestive of post-translational modification by ubiquitin (Figure 18: Rpn10 Is Monoubiquitinated In Vivo.A, band *a*). The band was not observed in cultures from cells carrying a deletion of *RPN10* gene (Figure 18: Rpn10 Is Monoubiquitinated In Vivo.B). We then purified Rpn10 expressed from an inducible vector (Figure 18C) and from its own chromosomal *locus* by means of an integrated C-terminal Tandem Affinity Purification (TAP) tag (Figure 18D). By western blot analysis of purified samples it was observed that Rpn10 showed band '*a*' again and an additional form (band '*b*') that suggested modification by two ubiquitin groups (Figure 18D).

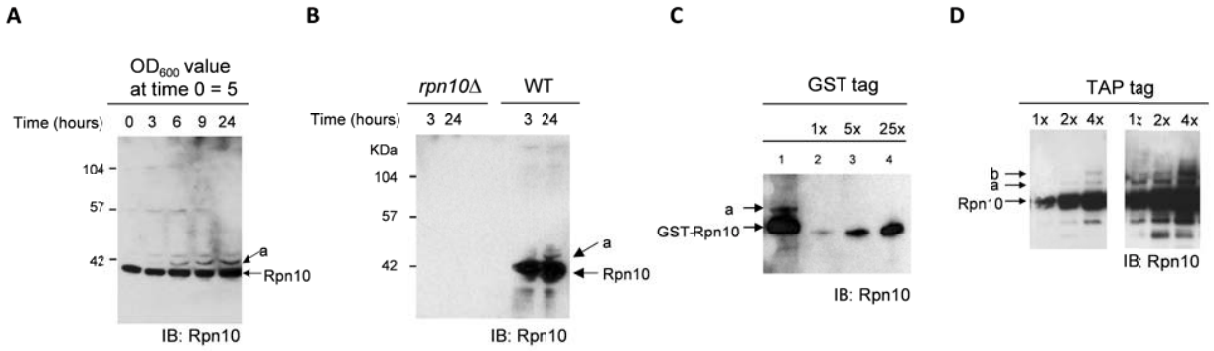

Figure 18: Rpn10 Is Monoubiquitinated In Vivo.

(**A**) Logarithmically growing wild-type yeast cells were analyzed by western blotting using Rpn10 antibody. Time points were taken as indicated. (**B**) Time points from exponentially growing cultures were taken and analyzed by western blotting. (**C**) GST-Rpn10 expressed in yeast was pulled-down and analyzed by western blot (lane 1). Different amounts of *E.coli* expressed GST-Rpn10 (lanes 2-4). (**D**) Purified TAP-tagged Rpn10 were analyzed by western blotting. Increasing amounts of fractions were visualized by short (left) and long film exposures. Asterisks, unspecific bands detected with Rpn10 antibody.

Band '*a*' of Figure 18D was analyzed by MS and two unique abundant proteins, Rpn10 and ubiquitin, were identified (Figure 19A). These approaches were not successful in detecting polyubiquitinated Rpn10, probably reflecting a relative low abundance of longer ubiquitin intermediates of Rpn10.

Using a strain that expresses ubiquitin with a 6xHIS N-terminal tag, pulldown assays of total cell ubiquitin conjugates were performed. Elution was performed by increasing concentration of imidazole (Crosas et al., 2006). When fractions were analyzed by immunobloting against Rpn10, we observed, in addition to the most abundant form corresponding to monoubiquitinated Rpn10 (mUb-Rpn10) (Figure

19B; lanes 2 to 7; Rpn10-Ub_1), diubiquitinated Rpn10 (lanes 3 to 7; Rpn10-Ub_2) and polyubiquitinated Rpn10 (lanes 6 and 7; Rpn10-Ub_n).

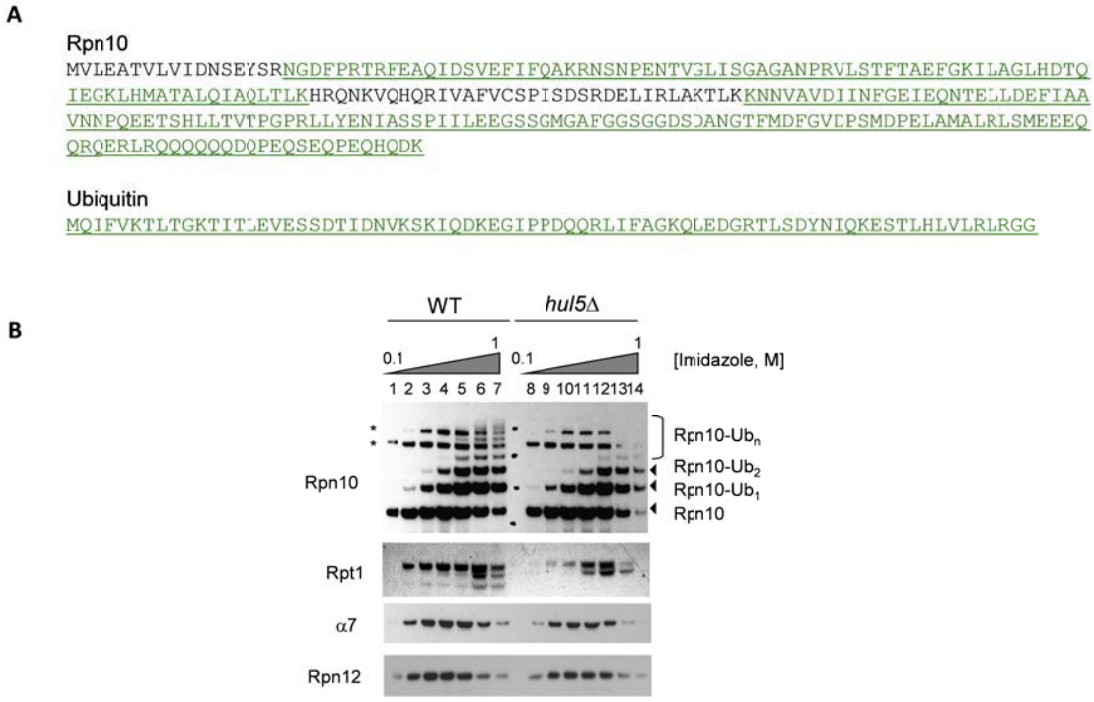

Figure 19: Mono- And Diubiquitination Are The Most Abundant Forms Of Modified Rpn10.
(**A**) Band 'a' shown in Figure 18D was analyzed by MS and two abundant proteins were found: Rpn10 and ubiquitin. Sequences of Rpn10 and ubiquitin are represented, showing in green regions covered by MS analysis. (**B**) Native 6xHIS-Ubiquitin conjugates eluted at different imidazole concentrations (lanes 1-7), analyzed by western blotting against Rpn10 antibody. The same purification and analysis procedure was performed using *hul5*Δ strain (lanes 8-14). Immunoblots against proteasome subunits Rpt1, α7 and Rpn12 are included. Asterisks, unspecific bands detected with Rpn10 antibody. The different Rpn10 forms (Rpn10; Rpn10-Ub_1; Rpn10-Ub_2; Rpn10-Ub_n) are indicated.

Synthesis of polyubiquitinated forms of Rpn10 is catalyzed by the chain elongating factor Hul5, which associates with the proteasome (Crosas et al., 2006). We performed the same ubiquitin conjugate purification procedure using a strain that carries a deletion of *HUL5* gene. We observed that, in the absence of Hul5, polyubiquitinated Rpn10 virtually disappeared (Figure 19B; lanes 13 and 14), but levels of mono and diubiquitinated Rpn10 were not affected (Figure 19B; lanes 9 to 14), suggesting that a Hul5-independent ubiquitin ligating activity is responsible for Rpn10 mono- and diubiquitination.

Monoubiquitinated Rpn10 Is Found In both Proteasomal and Non-Proteasomal Contexts

Since a significant fraction of cellular Rpn10 is not bound to the proteasome (Fu et al., 1998; Hiyama et al., 1999; Isasa et al., 2010; Kim et al., 2009; Matiuhin et al., 2008) we sought to determine the cellular context of Rpn10 monoubiquitination. Cells carrying an N-terminal 6-histidine tag on Ub were used to

isolate protein fractions rich in enzymatic factors of the ubiquitin-proteasome system, in ubiquitin-protein conjugates, and in Rpn10 (fraction UR8). As in assay shown in Figure 19, elution was performed with increasing concentrations of imidazole. Fraction 8 (called UR8) was found to be the richest in ubiquitin-protein conjugates and proteasome activity (Crosas et al., 2006) (Figure 20).

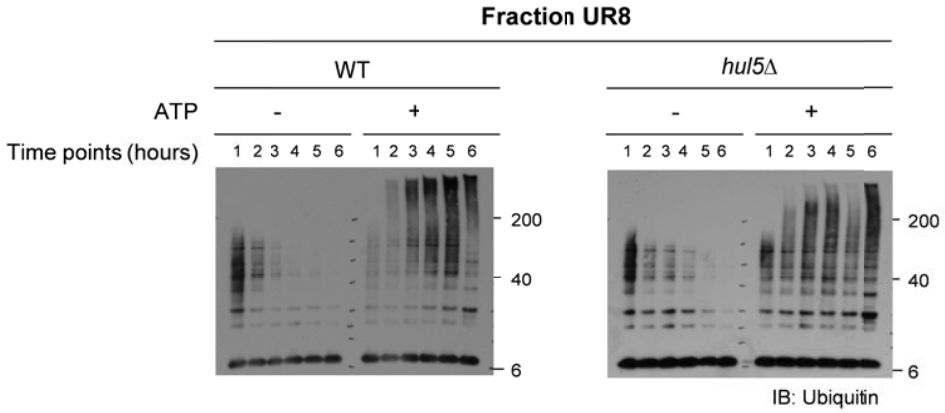

Figure 20: Bulk Of Ubiquitinating And Deubiquitinating Activities Of Fraction UR8.
Fractions containing MG132 were incubated and time points were taken as indicated.

We used fraction UR8 as a catalytically active extract. Incubations of UR8 fraction with MG132 in the absence of ATP showed that mUb-Rpn10 decreased rapidly whereas, strikingly, the rest of ubiquitin modified forms of Rpn10 remained constant (Figure 21A; lanes 1 to 4). These results suggested the involvement of a deubiquitinating enzyme highly specific for mUb-Rpn10. When the fraction was incubated in the presence of ATP, mUb-Rpn10 did not decline; instead it remained stable (Figure 21A; lanes 5 to 8), suggesting that an ATP-dependent activity was counteracting Rpn10 deubiquitination by catalyzing Rpn10 monoubiquitination or by inhibiting deubiquitination. To address this question we added to the reaction conventionally purified proteasomes, which contain unmodified Rpn10, and we observed that added proteasomal Rpn10 was robustly monoubiquitinated (Figure 21A; lanes 10 to 13). We performed the same assays shown in Figure 21A but using protein fractions and proteasomes purified from strains carrying a deletion of the *HUL5* gene. Using *hul5*Δ samples we observed the same behavior as with wild-type (Figure 21B), so we could discard a role of this protein in Rpn10 monoubiquitination regulation.

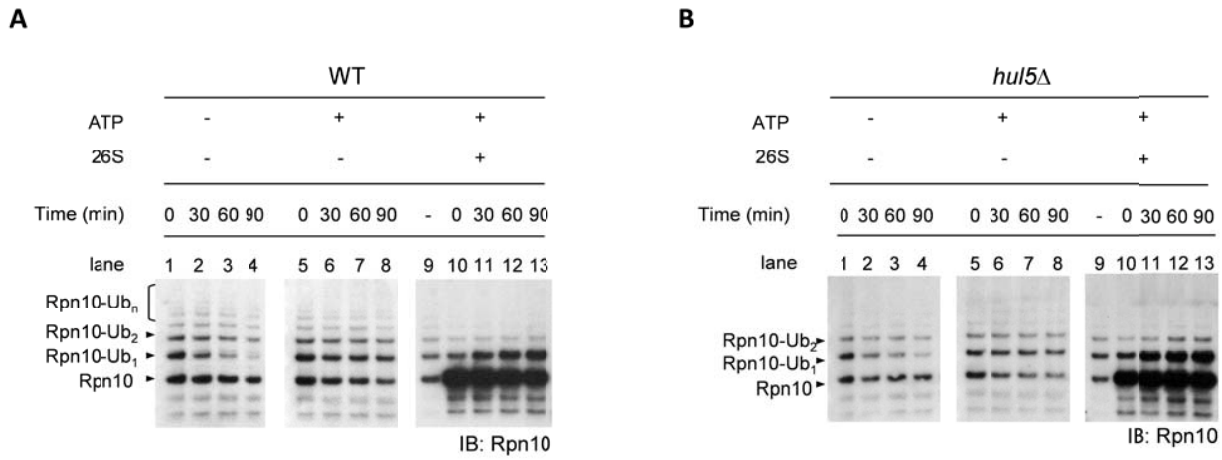

Figure 21: Monoubiquitination Of Rpn10 Is Dynamically Regulated.
(**A**) Fraction UR8 purified from a WT strain was incubated without ATP (lanes 1-4), with 5mM ATP (lanes 5-8) or with purified proteasomes (lanes 10-13). Time points were taken as shown and WB analysis was performed. (**B**) Assays as in *A* but using UR8 fraction and proteasomes from *hul5*Δ strains.

Proteasomes used in these assays were unable to catalyze Rpn10 monoubiquitination by themselves, but simply adding fraction UR8, tenfold diluted, reconstituted the reaction efficiently, indicating a high turnover rate of the Rpn10-ubiquitin ligating activity contained in this extract (Figure 22). These findings suggest that levels of mUb-Rpn10 are controlled *in vivo* by dynamically opposed ubiquitin ligase and deubiquitinating activities, and that substoichiometric amounts of the ubiquitin ligase bound to the proteasome are sufficient to promote Rpn10 monoubiquitination.

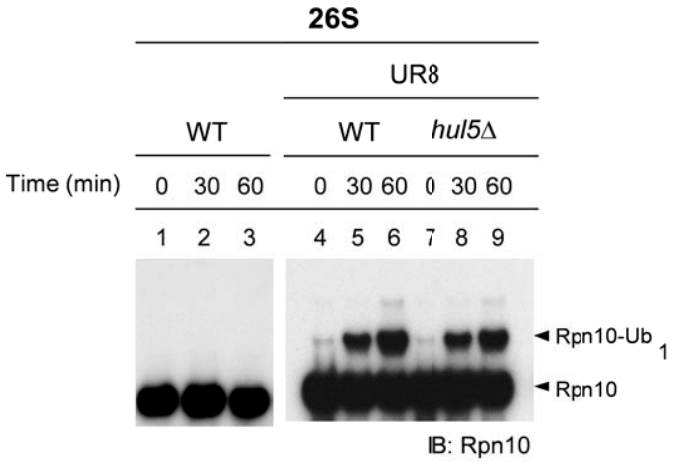

Figure 22: Monoubiquitination Reactions Using Proteasomes And Fraction UR8.

Purified proteasomes were incubated in the presence of ATP and MG132 (lanes 1-3). Reactions containing WT proteasomes and UR8 extracts (lanes 4-6). Reactions containing *hul5*Δ proteasomes and *hul5*Δ UR8 extracts (lanes 7-9).

To corroborate the observation of physiological Rpn10 monoubiquitination we performed a fractionation of a whole cell extract by Superose 6 chromatography. In this analysis, mUb-Rpn10 was present both in fractions corresponding to the proteasome elution peak, analyzed by immunodetection of Rpn12, a component of the lid of the proteasome, and α7, a core particle subunit (Figure 23A; lanes 16 and 17), and in the non-proteasomal peak of Rpn10 (Figure 23A; lanes 26 and 27).

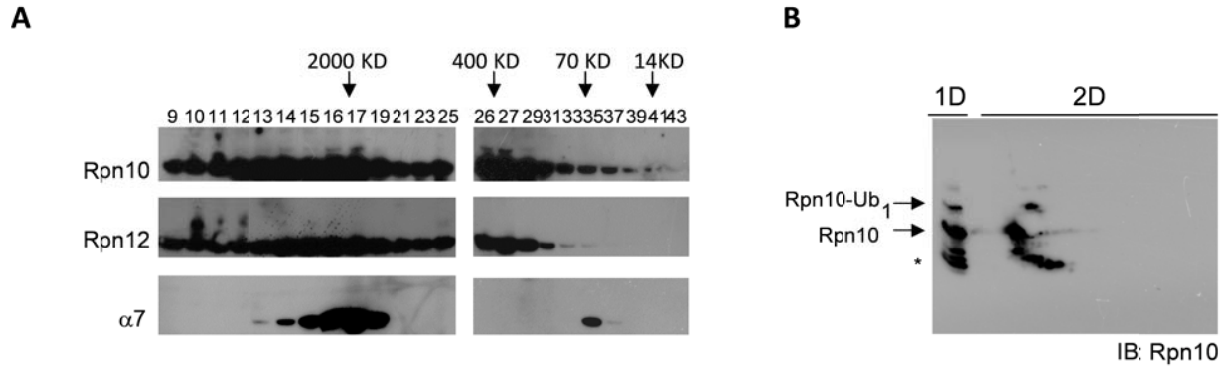

Figure 23: Rpn10 Is Modified In Both Proteaomal And Extraproteasomal Pools.
(**A**) Total cell lysates from a WT strain were applied to a Superose 6 column. Fractions were analyzed by western blotting against Rpn10, Rpn12 or α7 proteasome components. (**B**) Proteasomes purified in the presence of ATP and MG132 were analyzed by two dimensional electrophoresis followed by Rpn10 immunodetection. Asterisk, Rpn10 breakdown product.

To observe the presence of mUb-Rpn10 in affinity purified proteasomes, we set up proteasome purification conditions to stabilize this form. Proteasomes isolated using Rpn11-Protein A tag (Leggett et al., 2002), in the presence of ATP and MG132, contained mUb-Rpn10 as indicated in Figure 23B. These results provide evidence of *in vivo* Rpn10 monoubiquitination.

Rsp5 Ubiquitin Ligase And Ubp2 Deubiquitinating Enzymes Control Rpn10 Monoubiquitination

We searched for enzymatic factors involved in controlling the levels of mUb-Rpn10. Among likely candidates were ubiquitin ligases that interact with the proteasome, such as Ufd4 and Ubr1 (Xie and Varshavsky, 2000). We purified proteasomes from *ufd4Δ* and *ubr1Δ* strains and found that the levels of mUb-Rpn10 were identical to those observed in proteasomes purified from a wild-type strain (Figure 24A), suggesting that neither Ufd4 nor Ubr1 were ubiquitin ligases for Rpn10.

In addition to a functional interaction with the proteasome, a signature feature of the E3 enzyme that we were searching for might be efficient catalysis of monoubiquitination. An E3 that fits with this second

requirement is Rsp5, orthologue of NEDD4.2 mammalian enzyme (Dupre et al., 2004; Hicke, 2001), which is involved in many cellular processes in *Saccharomyces cerevisiae* and part of a large family of proteins that control analogous processes in mammalian cells. Rsp5 is forming a complex with the deubiquitinating enzyme Ubp2, which exhibits antagonistic activity (Kee et al., 2005). Rpn10 was a positive hit in a proteomic screen for Rsp5 substrates (Lu et al., 2008; Persaud and Rotin, 2011). Therefore, we analyzed the putative involvement of Rsp5 and Ubp2 in Rpn10 monoubiquitination. Wild-type, *rsp5–1* thermosensitive mutant, *ubp2*Δ mutant, and double mutant *rsp5–1 ubp2*Δ strains were used, all of them carrying a GST-Rpn10 expressing plasmid. Pulled-down fractions from cultures grown under galactose induction and restrictive temperature were analyzed by anti-Rpn10 western blotting (Figure 24B). Strikingly, the presence of mUb-Rpn10 was completely dependent on Rsp5 activity (Figure 24B; lanes 6 and 8), suggesting that Rsp5 is the major E3 for Rpn10 *in vivo*. In addition, levels of mUb-Rpn10 were strongly increased in the absence of Ubp2 (Figure 24B; lane 7).

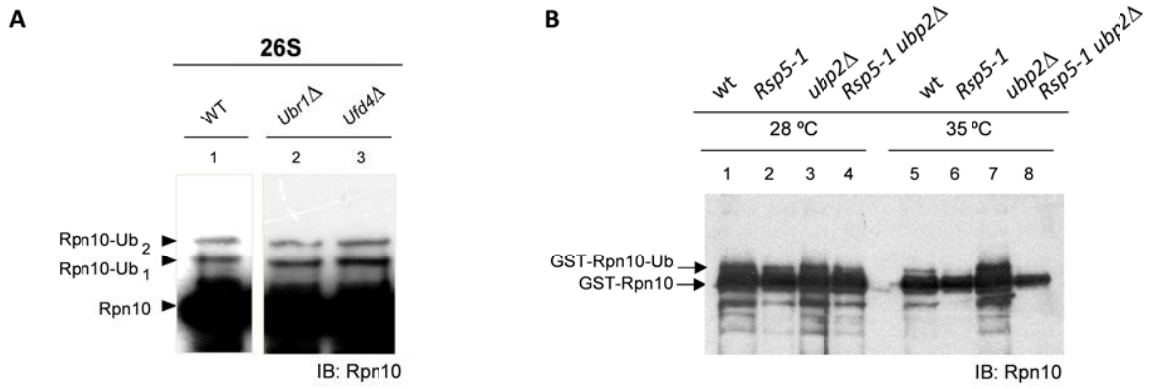

Figure 24: Levels of Monoubiquitinated Rpn10 Are Controlled by Rsp5-Ubp2 Enzymatic System In Vivo.
(**A**) Ubr1 and Ufd4 do not regulate levels of Rpn10 monoubiquitination. Purified proteasomes from WT, *ubr1*Δ and *ufd4*Δ strains in the presence of ATP and MG132, were resolved by SDS-PAGE and analyzed by immunobloting against Rpn10. (**B**) WT, *rsp5-1*, *ubp2*Δ and double *rsp5-1 ubp2*Δ strains, carrying GST-Rpn10 galactose-inducible plasmid, were expressed and shifted to restrictive temperature. GST-Rpn10 was pulled-down and analyzed by Rpn10 western blotting. Lanes 1-4, cultures grown at 28ºC. Lanes 5-8, cultures grown at 35ºC.

To characterize deubiquitination of proteasomal mUb-Rpn10, we considered, in addition to Ubp2, the putative activity of Ubp6, which is involved in substrate deubiquitination in the proteasome and is related to Hul5 (Crosas et al., 2006; Hanna et al., 2006; Leggett et al., 2002). We first isolated fractions rich in ubiquitin enzymatic factors and mUb-Rpn10 from WT and *ubp6*Δ strains (Figure 25A). Elution was performed as described in Figure 19. We then performed deubiquitinating assays by adding recombinant Ubp2, Ubp6 and the inactive mutant Ubp6^{C118A}. mUb-Rpn10 was processed by both Ubp2 and Ubp6, but Ubp2 was more efficient in the reaction (Figure 25B).

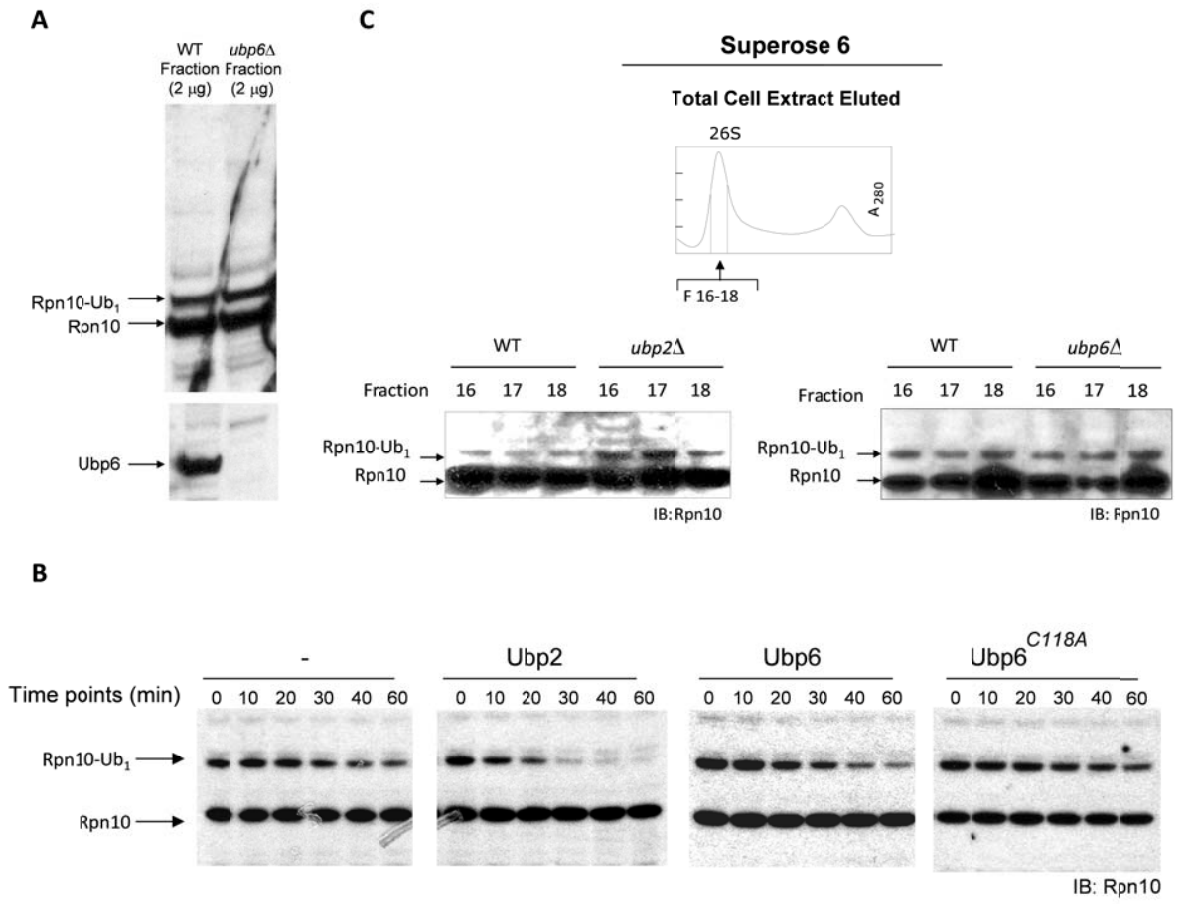

Figure 25: Ubp2 Deubiquitinates Proteasomal Rpn10-mUb.

(**A**) Fractions containing proteasomes and monoubiquitinated Rpn10. Status of Rpn10 in fractions analyzed by Rpn10 and Ubp6 western blotting. (**B**) Monoubiquitinated Rpn10 from *ubp6*Δ strain was incubated with equimolar amounts of recombinant Ubp2, Ubp6 and Ubp6^{C118A}. Reactions were analyzed by Rpn10 western blotting. (**C**) Total cell lysates from WT, *ubp2*Δ and *ubp6*Δ strains were applied to Superose 6 chromatography. Fractions that contain eluted proteasome were analyzed by Rpn10 western blotting.

To observe the effect of Ubp2 and Ubp6 on the levels of proteasomal mUb-Rpn10 *in vivo*, cellular extracts from *ubp2*Δ and *ubp6*Δ strains were fractionated by Superose 6 chromatography and the fractions corresponding to the proteasomal peak analyzed by western blotting. It was observed that mUb-Rpn10 was significantly increased in proteasomes from *ubp2*Δ cells with respect to wild-type proteasomes (Figure 25C, left panel). However, fractions from *ubp6*Δ cellular extracts showed levels of proteasomal mUb-Rpn10 identical to the ones of extracts from wild-type cells (Figure 25C, right panel). These results suggest a physiological role of Ubp2, but not of Ubp6, in Rpn10 deubiquitination. Therefore, our data suggest that the catalytic cycle that controls homeostasis of mUb-Rpn10 is largely independent of ubiquitin chain processing by Hul5 and Ubp6 in the proteasome.

Monoubiquitination Of Rpn10 *In Vitro*

To establish the direct involvement of Rsp5 in the catalysis of Rpn10 monoubiquitination we attempted to reconstitute the enzymatic reaction *in vitro*. Incubations of *free* or proteasomal Rpn10 with recombinant human E1, the E2 Ubc4, Rsp5 ligase and 6xHIS-ubiquitin showed that catalysis was promoted only in the presence of Rsp5, excluding an E3-independent monoubiquitination (Hoeller et al., 2007), and that monoubiquitination was efficiently promoted for both *free* and proteasomal Rpn10 (Figure 26A and Figure 26B; left panel). A remarkable feature of these reactions is that they are highly specific in producing mUb-Rpn10, and only synthesis of Rpn10-Ub_2 was observed secondarily (Figure 26A; long exposure).

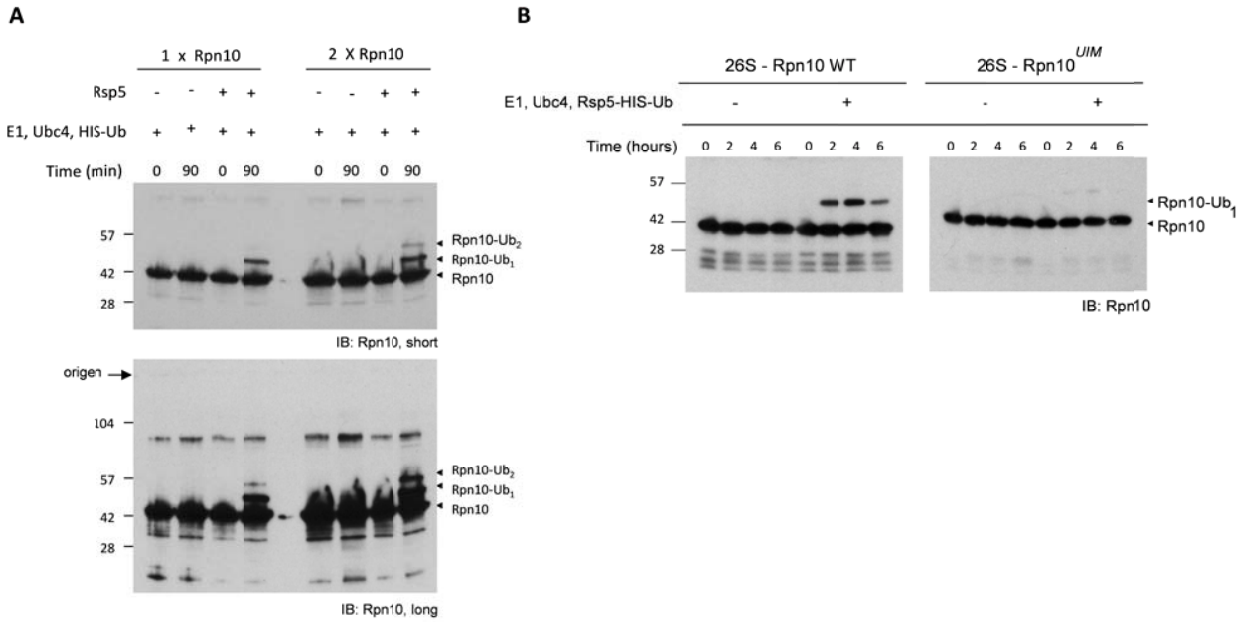

Figure 26: Reconstitution Of The Reaction Of Rpn10 Monoubiquitination In Vitro.
(**A**) Recombinant Rsp5, Rpn10, Ubc4, ubiquitin and E1 were incubated as indicated. Right lanes show a reaction in which Rpn10 input was doubled. Lower panels, longer exposures showing diubiquitinated Rpn10 more clearly. (**B**) Purified proteasomes (WT and $Rpn10^{UIM}$) were incubated with Rsp5, E1, Ubc4 and ubiquitin.

These results recapitulate the observations of Rpn10 monoubiquitination with endogenous extracts (Figure 21A and Figure 21B) and with *hul5*Δ samples *in vivo* (Figure 19B), suggesting that the reaction *in vitro* largely reproduces the physiological conditions.

Rpn10 UIM Is Required For Rpn10 Monoubiquitination

The NEDD4 ubiquitin-protein ligase family detects substrates and protein adaptors that contain PPY or UIM motifs (Dupre et al., 2004; Hicke and Dunn, 2003; Hoeller et al., 2006). The latter type of protein-protein interaction usually requires a functional UIM and promotes the so-called 'coupled' monoubiquitination (Hoeller et al., 2006; Hoeller and Dikic, 2010). Since Rpn10 is a UIM protein, we assessed whether this motif is required for monoubiquitination. We purified proteasomes from a strain

that carries the *Rpn10*^{UIM} mutant (Elsasser et al., 2004) and performed Rpn10 monoubiquitination reactions. We observed a dramatic inhibition of the synthesis of mUb-Rpn10 in *Rpn10*^{UIM} proteasomes, with respect to wild-type proteasomes (Figure 26B; right panel). We also tested the activity of cell fraction UR8 (**Figure** 20) towards wild-type and *Rpn10*^{UIM} proteasomes in the presence and absence of *o*-phenanthroline. *o*-phenanthroline is a metal chelator that strongly inhibits Rpn11-dependent deubiquitination and has been used in previous studies of deubiquitination (Guterman and Glickman, 2004). It was again observed that monoubiquitination was not promoted in the *Rpn10*^{UIM} mutant (Figure 27). These results show that the UIM is necessary for Rpn10 monoubiquitination.

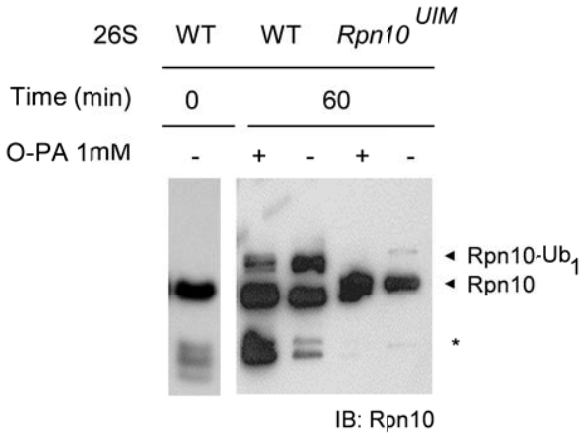

Figure 27: Rpn10 UIM Is Required For Monoubiquitination.
Purified proteasomes from WT and Rpn10UIM strains were incubated with a cell lysate fraction and Rpn10 monoubiquitination was checked by Rpn10 immunoblot analysis. An inhibitory effect of *o*-phenanthroline (PA) was observed when it was added to the reaction. Asterisk:, Rpn10 breakdown product.

Monoubiquitination Takes Place In Distinct Lysines Of Rpn10

We scaled up the *in vitro* reaction of Rpn10 monoubiquitination in order to produce higher amounts of mUb-Rpn10 for MS analysis. In optimized reactions, large amounts of mono and diubiquitinated forms of Rpn10 were produced, including tri- and tetraubiquitinated Rpn10 at lower levels, but no polyubiquitinated Rpn10 (Figure 28A). However, with this assay we could not distinguish the topology of the ubiquitin linkage formed because multi-monoubiquitination and short ubiquitin chains produce a similar electrophoretic mobility shift. To address this important issue we performed the reaction using methylated ubiquitin, which cannot form Ub chains (Hershko and Heller, 1985). Strikingly, this reaction (Figure 28B) produced the same pattern of ubiquitination observed using wild-type ubiquitin (Figure 28A), including four bands of Rpn10 modification, which is similar to the pattern observed in purified endogenous ubiquitinated Rpn10 (Figure 19B; lane 14). These results suggest that Rpn10 is multi-monoubiquitinated at four distinct lysine residues. In addition, a notable observation is that Rsp5, although inactive in the synthesis of polyubiquitinated forms of Rpn10, undergoes auto-polyubiquitination (Figure 28C), likely generating Lys^{63}-linked ubiquitin chains (Saeki et al., 2009).

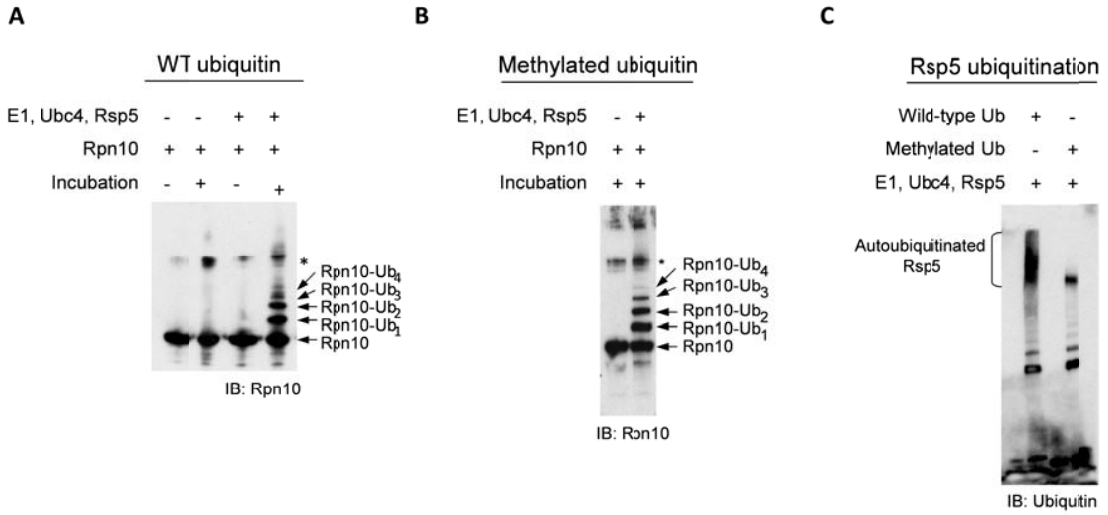

Figure 28: A Pattern Of Oligoubiquitination Is Detected In Rpn10.
(**A** and **B**) Scaled-up reactions of Rpn10 monoubiquitination using WT (**A**) or methylated (**B**) ubiquitin. Asterisk, unspecific band. (**C**) Autoubiquitinated Rsp5 using WT or methylated ubiquitin, from reactions similar to (**A**) and (**B**), respectively.

To detect the residues modified by ubiquitin in this reaction, we used proteomic technologies in collaboration with Dr. Steven P. Gygi (Harvard Medical School, USA). The two major produced bands corresponding to Rpn10-Ub_1 and Rpn10-Ub_2 (Figure 29A, framed in red) were excised from the gel and analyzed by LC-MS/MS. The analysis revealed that monoubiquitination could engage Lys^{71}, Lys^{84}, Lys^{99} and Lys^{268} (Figure 29B). Lys^{71}, Lys^{84}, and Lys^{99} are located within the VWA domain, whereas Lys^{268} is situated at the very C-terminus of the protein. In Rpn10-Ub_2 band only modifications at $Lys^{84}$and Lys^{268} were identified and, in the whole analysis, $Lys^{84}$was the most abundantly modified, representing the 52% of the GlyGly-containing peptides (Figure 29C).

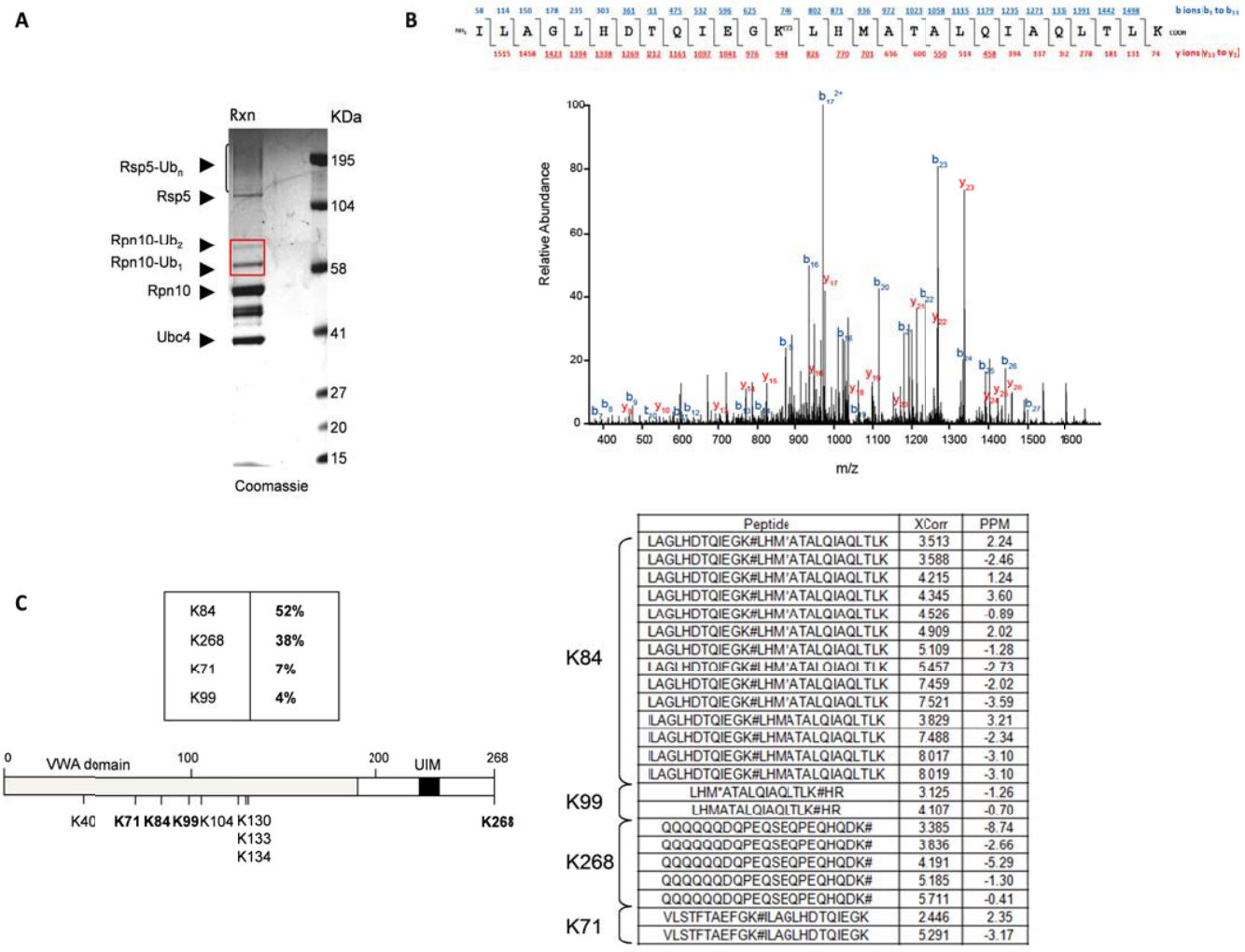

Figure 29: Proteomics Analysis Of Rpn10 Lysines Modified By Ubiquitin.

(**A**) The product of Rpn10 monoubiquitination *in vitro* was analyzed by SDS-PAGE and Coomassie staining. Bands corresponding to Rpn10-Ub$_1$ and Rpn10-Ub$_2$ (framed in red) were excised and analyzed by LC-MS/MS. (**B**) Identification of ubiquitinated lysines by MS. Above, representative MS/MS spectrum of lysines with diGlycine motif (remaining residues after tryptic digest of ubiquitinated lysines) at lysine 84 (K^{GG}). The precursor peptide ion (m/z 1047.9167) was isolated and fragmented in mass spectrometer. Fragment ions from both termini are shown (*b*- and *y*- ions respectively) where the detected ions are underlined. Below, Lysines 71, 84, 99, and 268 showed ubiquitination on Rpn10. The peptide sequence, Sequest score (XCorr) and mass deviation (PPM) are shown. Ubiquitinated lysines are indicated by K#. (**C**) Summary of MS analysis of Rpn10. Above, relative abundance of the diGlycine peptides. Below, scheme of Rpn10 protein including all lysines contained in the sequence. Lysines modified by ubiquitin are shown in bold.

To further characterize Rpn10 modification, lysine residues of Rpn10 were mutated. In GST pulldowns, forms involving Rpn10^{K84R} mutation showed a strong decrease in monoubiquitination (Figure 30A; left

panel; lanes 4, 7 and 8), while mutations in other lysines produced only mild or undetectable effects (Figure 30A; left panel). Nonetheless, our results show that additional lysines may be modified. Thus, to analyze Rpn10 forms defective in ubiquitination we prepared Rpn10^{K71,84,99,268R} and Rpn10^{NO-K} mutants, and the control mutant Rpn10^{K104,130,133,134R}. Analysis of GST pulldowns of these forms showed that the Rpn10^{K104,130,133,134R} mutant exhibited monoubiquitination to wild-type levels (Figure 30A; right panel; lanes 1 and 4), whereas Rpn10^{K71,84,99,268R} (lane 3) and Rpn10^{NO-K} (lane 2) mutants showed very low levels of modification. Rpn10^{K84R} mutant showed a decrease in monoubiquitination (lane 5) similar to that observed in the Rpn10^{K71,84,99,268R} mutant.

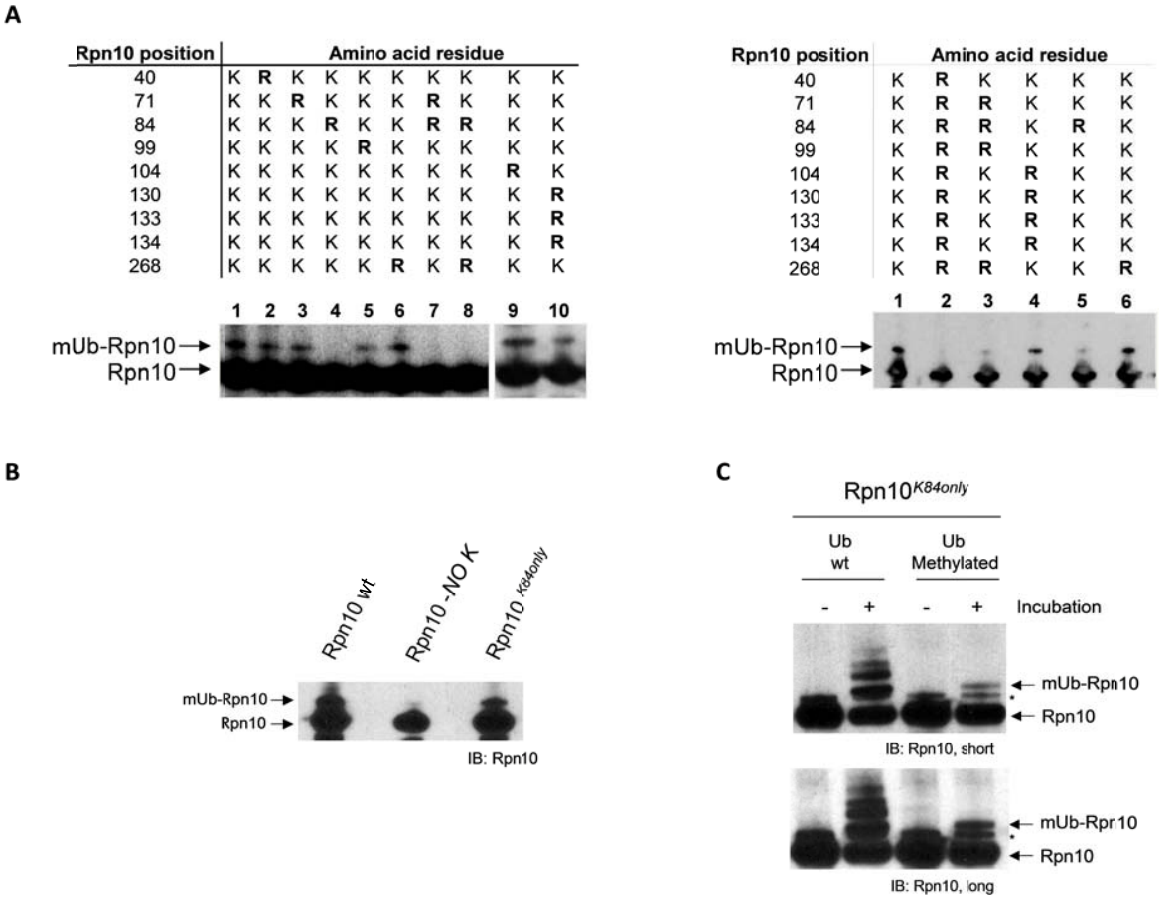

Figure 30: Genetic Analysis Of Rpn10 Lysines Modified By Ubiquitin.

(**A** and **B**) GST-Rpn10 Lys to Arg mutants including all Rpn10 lysines were expressed under galactose induction. Pulled-down GST-Rpn10 forms were analyzed by Rpn10 western blotting. (**C**) Monoubiquitination reactions of Rpn10^{K84only} using WT and methylated ubiquitin. Asterisk, electrophoretic artifact shown by the mutant, observed also in non-incubated samples.

Lys^{84} monoubiquitination was also analyzed with the Rpn10^{K84only} mutant, in which we mutated all lysine residues to arginine except for Lys^{84}. This form was expressed in yeast and showed monoubiquitination nearly to physiological levels (Figure 30B), suggesting a dominant role of Lys^{84} in the process of Rpn10

monoubiquitination. We performed reactions *in vitro* using recombinant Rpn10^{K84only} as a substrate. We observed that, while methylated ubiquitin produced one band of monoubiquitination, wild-type ubiquitin produced several bands (Figure 30C), suggesting that, secondarily (see Figure 28A and B), Rsp5 is able to build short ubiquitin chains, maybe due to the absence of additional lysine residues in the mutant Rpn10 sequence.

To assess the functional relevance of Rpn10 monoubiquitination, a complementation test was performed. Strains carrying a double deletion of *RPN10* and *RAD23* genes are strongly deficient in recruiting substrates to the proteasome and exhibit slow growth (Figure 31A) (Chen and Madura, 2002). We tested the capacity of plasmid-borne Rpn10 to rescue the absence of the *RPN10* gene. We observed that wild-type form of Rpn10 efficiently rescued growth of a *rpn10*Δ*rad23*Δ strain (Figure 31B). Similarly, the *rpn10*^{K104,130,133,134R} mutant, which shows monoubiquitination at wild-type levels, fully complemented Rpn10 function. However, the *rpn10*^{K71,84,99,268R} and the *rpn10*$^{NO-K}$ mutants, which show impaired monoubiquitination, did not rescue Rpn10 function to WT levels (Figure 31B). To our knowledge, this is the first genetic evidence linking proteasome function with monoubiquitination of a protein.

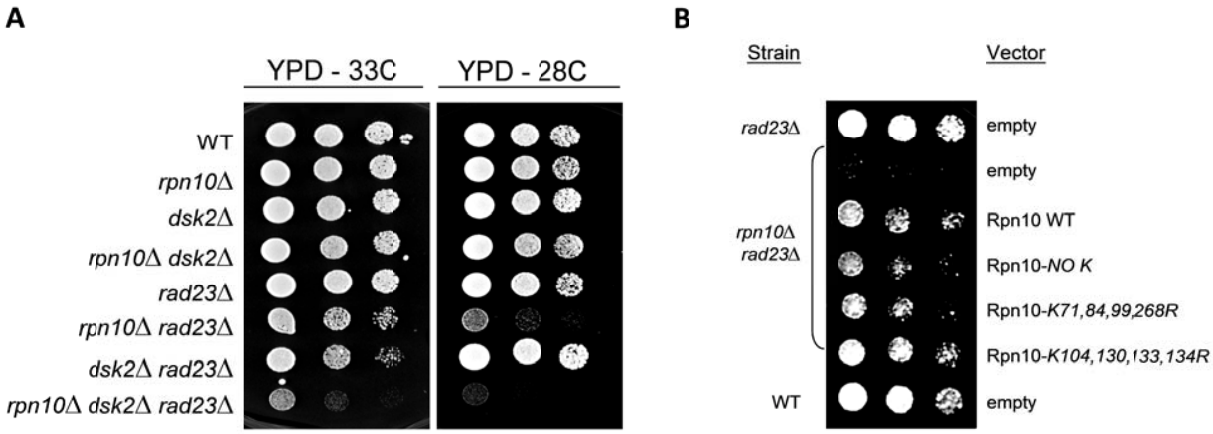

Figure 31: Functional Relevance Of Rpn10 Monoubiquitination.
(**A**) Selection of spores obtained by tetrad dissection of a diploid strain that contains *RPN10*/*rpn10*Δ, *RAD23*/*rad23*Δ and *DSK2*/*dsk*Δ heterozygotic background, kindly provided by S. Elsasser (Finley lab, HMS). Spores were genotyped and their growth at different temperatures was tested. (**B**) Ability of a set of Rpn10 mutants to rescue growth defect exhibited by *rpn10*Δ*rad23*Δ yeast strain. Rpn10 forms were expressed at 22°C using a galactose-inducible vector, selected with URA3 marker. Cells (3x10^4) were spotted in the first column, and 3/7 serial dilutions were made for the successive columns.

Monoubiquitinated Rpn10 Shows Low Affinity To Ubiquitin Conjugates

We asked what the role of monoubiquitination was in the context of proteasome function. The UIM of Rpn10 is involved in the recruitment of substrates to the proteasome (Elsasser and Finley, 2005; Fu et al., 1998; Verma et al., 2004). The interaction between ubiquitin and Rpn10 UIM relies on a hydrophobic patch on the surface of ubiquitin, composed of Leucine 8, Isoleucine 44, and Valine 70, which define a pocket for the methyl group of a strictly conserved alanine within the UIM, alanine 231 in the case of

Rpn10 (Sloper-Mould et al., 2001; Wang et al., 2005). We tested whether in mUb-Rpn10, the covalently linked ubiquitin group could impose a functional restriction to Rpn10 UIM by means of a 'fold-back' interaction (Di Fiore et al., 2003; Hoeller and Dikic, 2010; Woelk et al., 2006). We obtained a cellular fraction containing 6xHIS tagged polyubiquitin conjugates (Figure 32A). As in previous assays (Figure 20 and Figure **25**A), conjugates were obtained after a progressive elution of HIS-ubiquitin conjugates purified in the presence of MG132 and NaCl. Elution is performed by increasing concentration of imidazole. The last fraction (Figure 32A, lane 10) was used for the following binding assays. Most of the interacting proteins, including active proteasomes, have been previously eluted as assessed by measurements of protein concentration and LLVY-AMC activity (Figure 32A, graph above).

Fraction 10 was immobilized to Ni-NTA resin (Figure 32B, lane 1) and the binding capacity of Rpn10 and mUb-Rpn10 (synthesized *in vitro*, as in Figure 26A) to immobilized conjugates was challenged. We observed that unmodified Rpn10 could bind very efficiently to conjugates, but mUb-Rpn10 did not (Figure 32B, lanes 5 and 6), suggesting that monoubiquitination of Rpn10 inhibits the activity of the UIMs. In the conditions of the binding assay no Rpn10 deubiquitination was observed (Figure 32C).

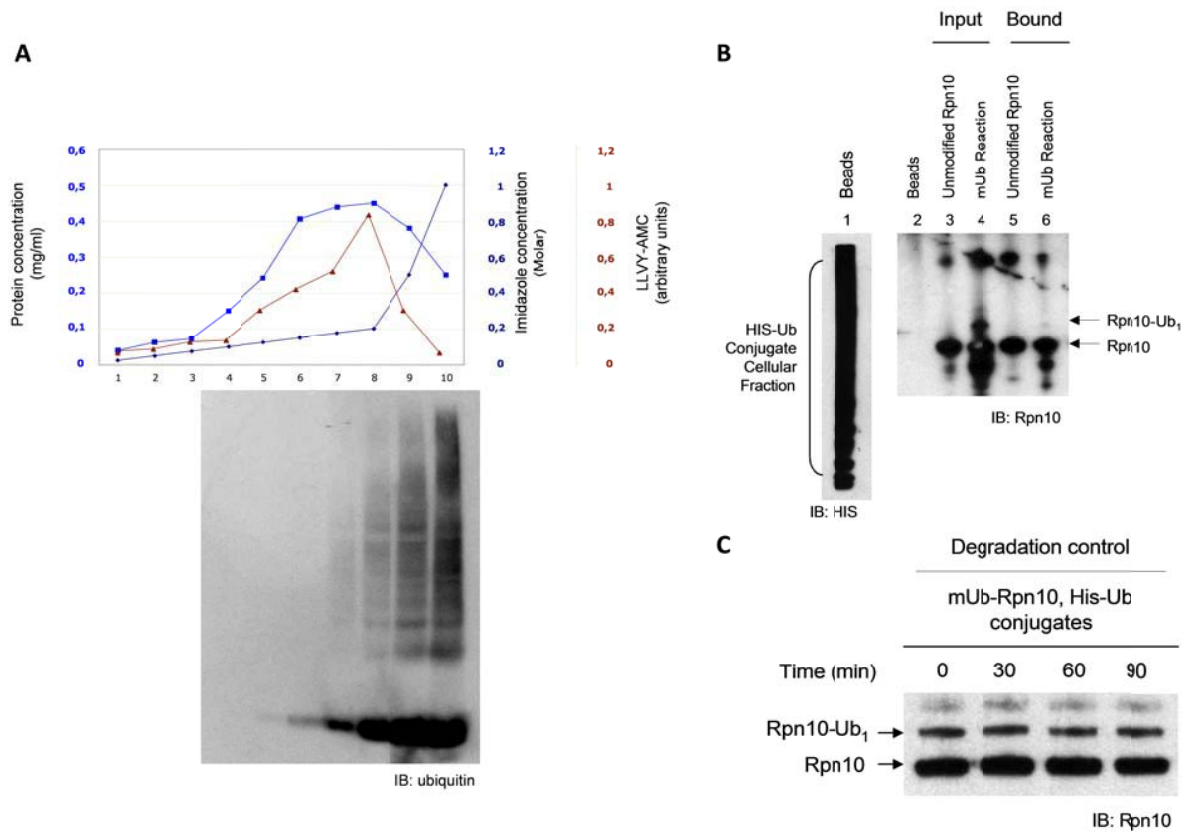

Figure 32: Binding Capacity Of Rpn10 And mUb-Rpn10 To Polyubiquitinated Conjugates.
(**A**) Fractionation of HIS-Ubiquitin cell conjugates from strain carrying an N-terminal 6-histidine tag on ubiquitin (SJR125) performed as described in Crosas *et al*., 2006. Fraction from lane 10 was used in this assay. (**B**) Binding assay of Rpn10 and mUb-Rpn10 to a fraction of endogenous HIS-ubiquitin conjugates immobilized on Ni-NTA

beads (lane 1). Liquid phase inputs include unmodified Rpn10, as a control (lane 3), and a monoubiquitination reaction sample (mUb reaction), which contains both unmodified Rpn10 and mUb-Rpn10 (Rpn10-Ub_1) (lane 4). Bound material is shown in lanes 5 and 6. (**C**) Deubiquitination control. A sample of monoubiquitinated Rpn10 *in vitro* was incubated with beads containing a fraction of cellular ubiquitin conjugates (panel A, lane 10). Samples were taken as indicated and analyzed by anti Rpn10 western blotting.

To further characterize this interaction, we generated permanently monoubiquitinated forms by appending a ubiquitin group to Rpn10 (Rpn10-Ub). We included the Rpn10-Ub^{I44A} mutant, which shows a decreased affinity of linked ubiquitin to the UIM (Hoeller et al., 2006) (Figure 33A). Thus, different forms were expressed and bound to GSH-beads (Figure 33B, lanes 1-4) and their affinity to the cellular fraction of polyubiquitin-conjugates, as the liquid phase, was tested (Figure 33B, lane 5). As in previous assay, conjugates bound strongly to Rpn10 (Figure 33B, lane 7) but not to Rpn10 linked to Ub (Figure 33B, lane 8). Interestingly, the Rpn10-Ub^{I44A} mutant partially re-established the capacity of Rpn10 to bind conjugates, showing that the non-covalent ubiquitin-UIM interaction is involved in the inhibition of the UIM.

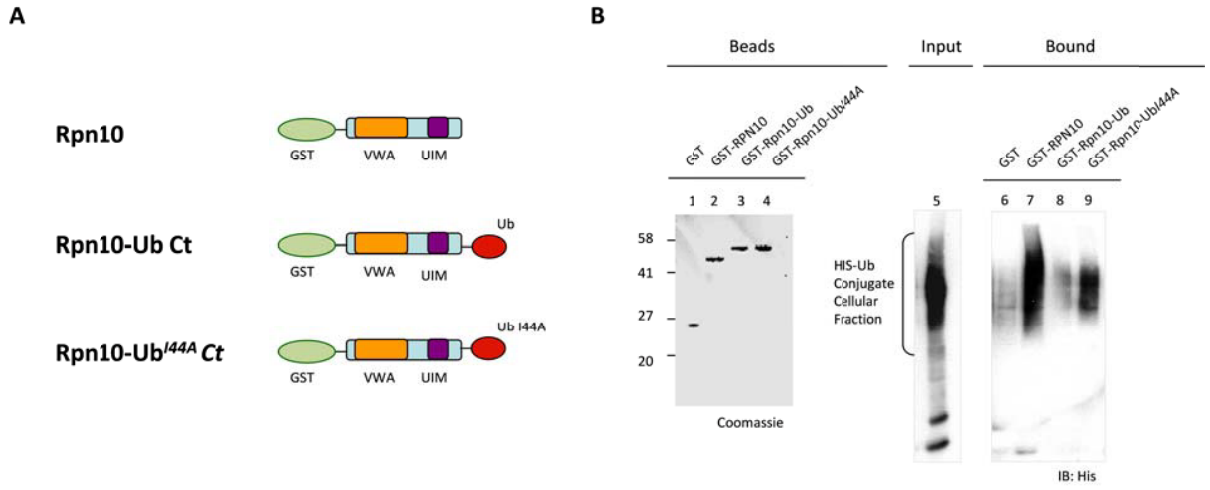

Figure 33: Binding Capacity Of Rpn10-Ub Chimeras To Polyubiquitinated Conjugates.
(**A**) C-terminal ubiquitin fusions of Rpn10. (**B**) Binding assay of Rpn10 and C-terminal ubiquitin fusions, immobilized in beads (lanes 1-4), to a fraction of endogenous HIS-ubiquitin conjugates (lane 5). Bound material was eluted and analyzed by immunoblot against HIS (lanes 6-9).

In the previous assay we used polyubiquitin conjugates isolated from cells, therefore we could not exclude the interference of cellular factors associated to ubiquitin conjugates in the binding assay. Thus, we challenged the affinity of Rpn10 and Rpn10 modified forms towards pure unanchored polyubiquitin chains. In this assay the Rpn10^{K84only} mutant was included to observe the behavior of Rpn10 modified uniquely at Lys^{84}. Again, binding assays showed that immobilized polyubiquitin chains (Figure 34A, lane 1) bound efficiently to unmodified Rpn10 (wild-type and Rpn10^{K84only} mutant) but not their respective

monoubiquitinated forms (Figure 34A, lanes 3-8). We also tested the affinity of the Rpn10-Ub fusion towards unanchored polyubiquitin chains. Consistently with the assay using cellular polyubiquitin conjugates (Figure 33B), Rpn10-Ub did not bind to ubiquitin chains (Figure 34A, lanes 9-10), whereas the Rpn10-Ub^{I44A} mutant partially re-established binding (Figure 34A, lanes 11-12). Therefore, mUb-Rpn10 synthesized by Rsp5 and the Rpn10-Ub chimera exhibit the same feature: a dramatic decrease in their affinity to ligands, suggesting that Rpn10-Ub fusion is a good approach to study the effect of monoubiquitination in Rpn10 UIM function. Moreover, the partial rescue of polyubiquitin binding capacity of the Rpn10-Ub^{I44A} mutant showed that the decreased affinity to polyubiquitin is due to an intramolecular UIM-monoubiquitin hydrophobic interaction.

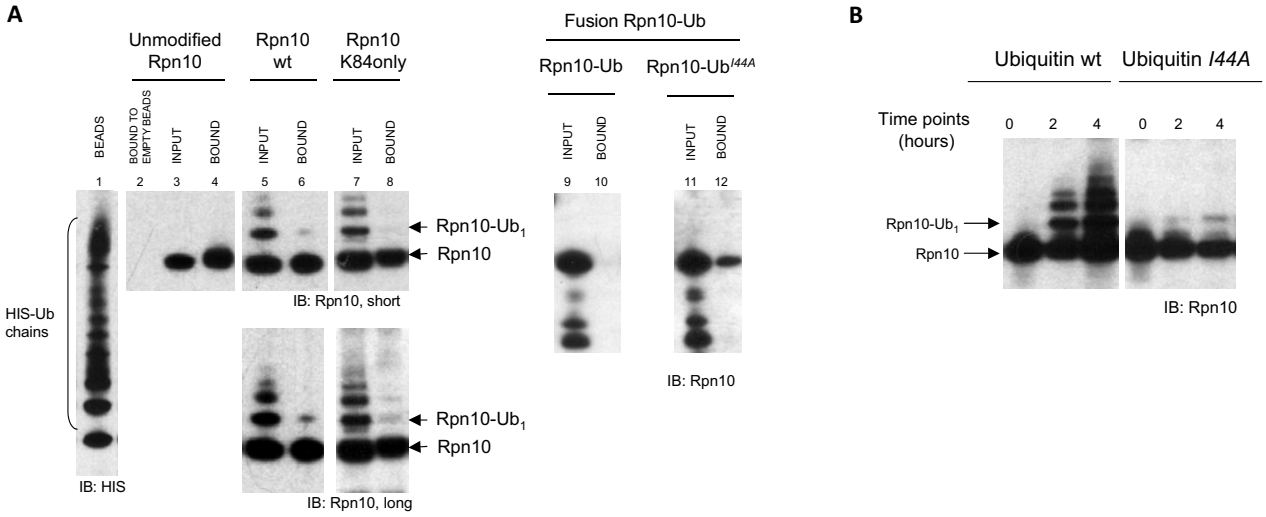

Figure 34: Binding Capacity Of Rpn10, Rpn10^{K84only} , Their Monoubiquitinated Forms, Rpn10-Ub And Rpn10-Ub^{I44A} To Pure Polyubiquitin Chains.

(**A**) Binding assay of unmodified and mUb-Rpn10 (wild-type and *K84only* mutant), Rpn10-Ub and Rpn10-Ub^{I44A} to unanchored polyubiquitin chains immobilized in beads (lane 1). Input and bound material are shown for each sample (lanes 3-12). A control of Rpn10 binding to empty beads is included in lane 2. A longer film exposure is shown for lanes 5-8. (**B**) *In vitro* ubiquitination reaction using wild-type (left panel) and mutant *I44A* ubiquitin (right panel).

According to the presented data, the interaction UIM-ubiquitin appears to be essential for both catalysis (Figure 26B and Figure **27**) and function (Figure 32B, Figure **33**B and Figure **34**A) of Rpn10 monoubiquitination. The capacity of ubiquitin^{I44A} to promote Rpn10 monoubiquitination was tested *in vitro* and very poor activity was observed, as compared to the reaction using wild-type ubiquitin (Figure 34B). These results complement the data obtained using Rpn10^{UIM} mutant (Figure 26B), and, altogether, show that Rsp5 requires the Rpn10 UIM-ubiquitin hydrophobic interaction to be active.

Monoubiquitination Of Rpn10 Reduces The Proteolytic Activity Of The Proteasome

In Figure 32B, Figure **33**B and Figure **34**A we have shown that mUb-Rpn10 exhibits low affinity to polyubiquitin and polyubiquitinated substrates but we do not show the effect in active proteasomes. To address this question, we performed cyclin B degradation tests in a time course fashion, using equimolar amounts of Rpn10 and Rpn10-Ub forms added to *rpn10*Δ proteasomes (Figure 35A). We observed that degradation rates of cyclin B were strongly accelerated when Rpn10 was added (cyclin B is degraded in less than 15 minutes), slightly accelerated when Rpn10-Ub^{I44A} was added, and substantially inhibited in absence of Rpn10 or adding Rpn10-Ub (after 60 minutes of incubation, cyclin B is not completely degraded) (Figure 35B). However, these results could also be explained by a decreased proteasome interaction of the Rpn10-Ub form. To rule out this possibility, we compared the affinity of Rpn10, Rpn10-Ub and Rpn10-Ub^{I44A} to *rpn10*Δ proteasomes by binding assays, and observed that all Rpn10 forms bound identically to the proteasome (Figure 35C), showing that degradation of cyclin B is promoted by a proteasome-bound Rpn10.

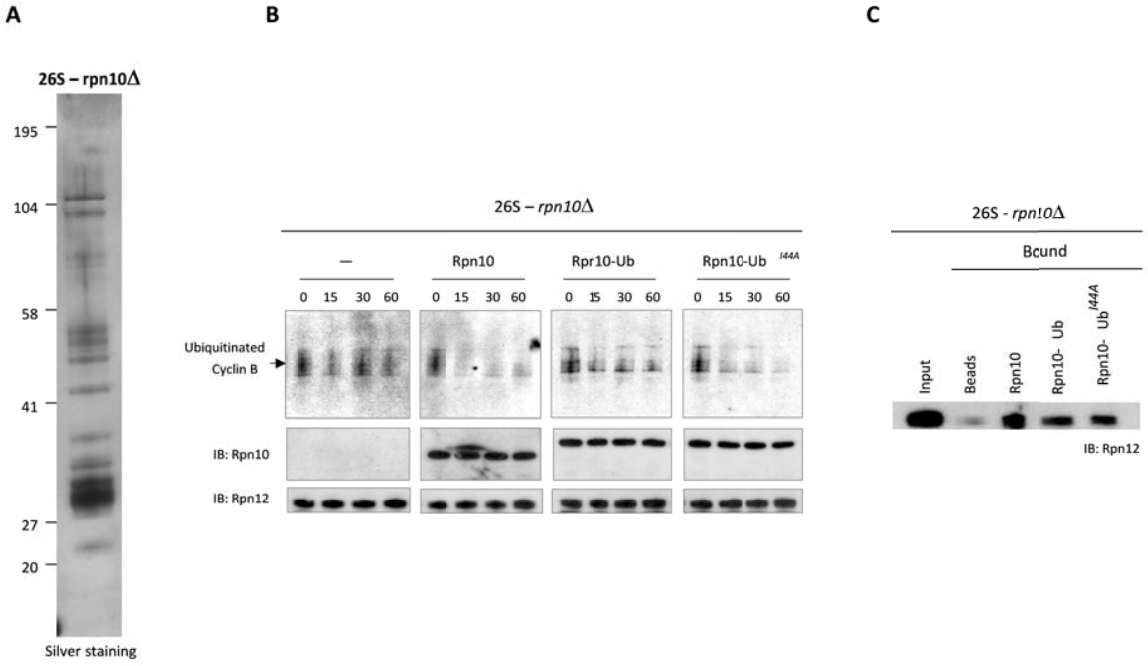

Figure 35: Monoubiquitination Of Rpn10 Reduces The Proteolytic Activity Of The Proteasome.

(**A**) Proteasomes were purified from a *rpn10*Δ strain, resolved by SDS-PAGE and visualized by silver staining to check composition. (**B**) Time course degradation assays in vitro with proteasomes deficient in Rpn10, equimolar amounts of Rpn10 forms, and ubiquitinated cyclin B. At indicated times, points were taken and analyzed by western blotting against cyclinB, Rpn10 and Rpn12. (**C**) Rpn10-Ub chimeras bound to *rpn10*Δ proteasomes. GST-Rpn10, GST-Rpn10-Ub and GST-Rpn10-Ub^{I44A} were immobilized to beads and proteasomes were applied as the soluble phase. Bound was checked by Rpn12 western blotting.

If mUb-Rpn10 shows an inactive UIM, one could expect a strong decrease of functional complementation *in vivo* of Rpn10-Ub compared to wild-type Rpn10, and an intermediate complementation of Rpn10-Ub^{I44A} (see Figure 33B, Figure 34A and Figure 35B). To check this hypothesis, we expressed these proteins in *rpn10*Δ *rad23*Δ cells and performed complementation tests. The levels of expression of plasmid-borne *RPN10* variants were similar to that of endogenous Rpn10 in all cases (Figure 36A).

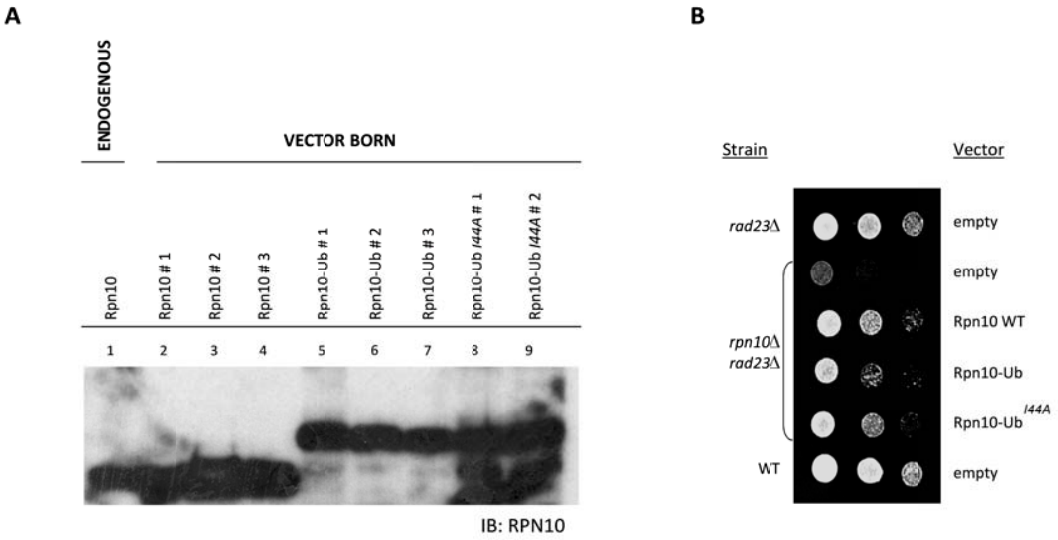

Figure 36: Rescue Of Rpn10 Function By Rpn10-Ub Forms.

(**A**) Expression levels of plasmid-borne RPN10. The *rpn10*Δ strain (SBC52), carrying plasmids (pYES2) expressing Rpn10 (lanes 2-4), Rpn10-Ub (lanes 5-7) or Rpn10-Ub^{I44A} (lanes 8-9), was grown in SGRC medium. A WT strain transformed with an empty vector was grown in parallel to evaluate endogenous levels of Rpn10 (lane 1). Protein extracts were analyzed by SDS-PAGE and immunobloted against Rpn10. (**B**) Ability of Rpn10, Rpn10-Ub and Rpn10-Ub^{I44A} to rescue growth defect exhibited by *rpn10*Δ*rad23*Δ yeast strain. Rpn10 forms were expressed at 22°C using a galactose-inducible vector (pYES2) and selected with URA3 marker. Cells (3x10^4) were spotted in the first column, and 3/7 serial dilutions were made for the successive columns.

We observed that Rpn10-Ub could not complement *rpn10rad23* null mutants efficiently, showing the strong effect of permanent monoubiquitination in Rpn10 (Figure 36B). This effect was dependent on the UIM-ubiquitin interaction of Rpn10-Ub, since *rpn10-Ub*^{I44A} mutation, in agreement with binding assays, partially re-established complementation (Figure 36B).

Rpn10 Monoubiquitination Is Reduced Under Conditions Of Proteolytic Stress

Our observations suggested that monoubiquitination of Rpn10 could regulate the capacity of this substrate receptor to bind ubiquitinated substrates. We asked whether the levels of mUb-Rpn10 could be influenced by conditions that require functional Rpn10, such as proteolytic stress (Medicherla and Goldberg, 2008). We examined the status of Rpn10 of cultures growing at 14, 28 or 37 °C (Figure 37A, B, F and G). Normalized whole cell lysates were analyzed by immunoblot against Rpn10. We observed that

Rpn10 monoubiquitination was strongly decreased in cells subjected to either cold or heat shock. In *ubp2*Δ strain, levels of modified Rpn10 were drastically diminished but not virtually disappeared (Figure 37F and G). We asked whether a similar response to stress could also be observed at 28 °C in the presence of cadmium, a compound that promotes proteolytic stress (Medicherla and Goldberg, 2008; Morano et al., 2011). We observed that, in the presence of cadmium, Rpn10 monoubiquitination was not induced (Figure 37C). We then asked whether the tight control of mUb-Rpn10 levels was a specific response to proteolytic stress or could be promoted by other kind of perturbations. To address this question we supplemented cultures with ethyl methyl sulfoxide (EMS) to cause DNA damage, or NaCl to induce osmotic stress in the same manner than in previous assays. We observed that Rpn10 monoubiquitination persisted under these conditions (Figure 37D and E).

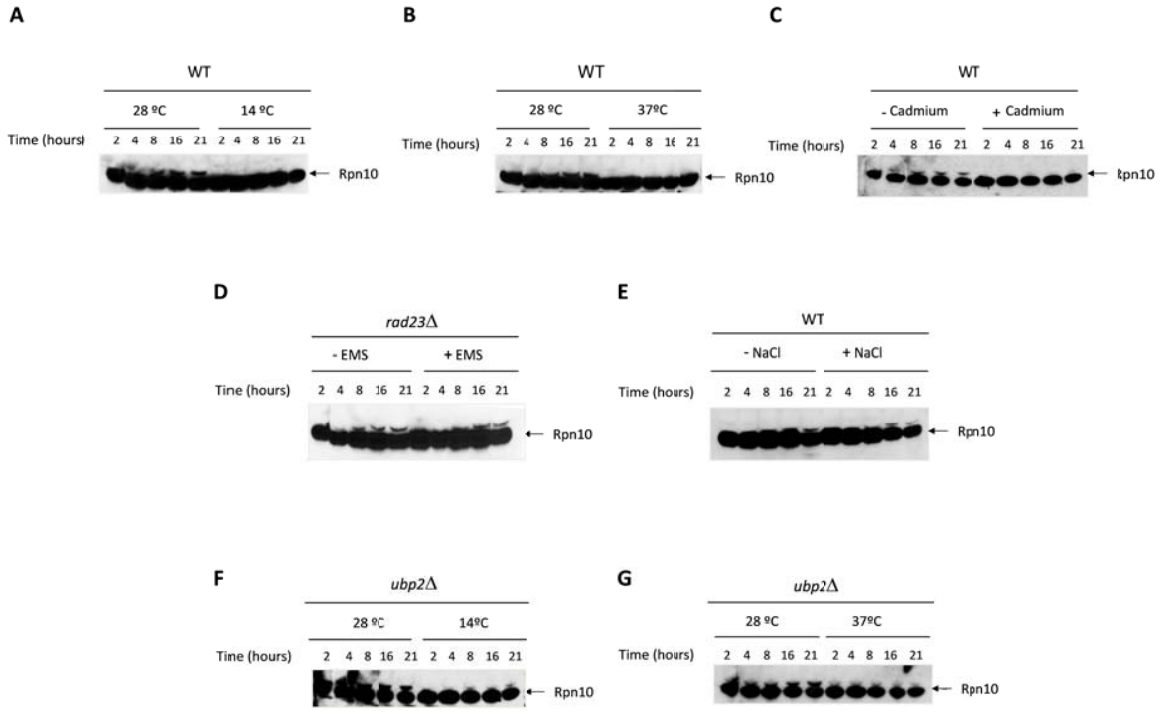

Figure 37: Monoubiquitination Of Rpn10 Is Decreased Under Certain Stress Conditions
(**A-G**) Yeast cells (WT, *rad23*Δ and *ubp2*Δ) were grown in YPD liquid media at the described conditions. Cadmium, 200mM; EMS, 0.08%; NaCl, 500 mM. Samples were taken at the indicated times and the number of cells normalized and analyzed by western blotting with Rpn10 antibody.

These results suggest that there is a strong regulatory response that downregulates Rpn10-mUb, which apparently does not affect levels of unmodified Rpn10.

The results shown so far were published in Isasa et al., 2010 (*Mol. Cell* 38: 1-13).

Only Proteasomal Rpn10-mUb Is Reduced Under Proteolytic Stress Conditions

We have shown that the monoubiquitinated form of Rpn10 is lost under certain proteolytic stress conditions, when activity of Rpn10 is required. However, it was not clear if the loss of Rpn10-mUb upon proteolytic stress affected both proteasome-bound and cytosol-free fractions of Rpn10. To analyze whether there was a pool of Rpn10 preferentially affected under proteolytic stress, we carried out fractionation assays of cell extracts from cultures upon various proteolytic and non-proteolytic stresses (as in Figure 23A). Interestingly, we observed two types of pattern. Pattern 1: standard conditions, or conditions that don't cause a major proteolytic stress (in this assay, we used NaCl 500mM to be consistent with the assay shown in Figure 37E), in which proteasomal monoubiquitinated Rpn10 appeared as the major pool (Figure 38, upper panel). Pattern 2: conditions that cause proteolytic stress, exemplified in Figure 38 (below) by a cold-shock (14°C) culture. Under these conditions, proteasomal monoubiquitinated Rpn10 is dramatically downregulated, showing a specific correlation of elevated protein degradation with low levels of proteasomal mUb-Rpn10. Importantly, the extraproteasomal pool of Rpn10-mUb, which represents a smaller fraction of modified Rpn10, is not evidently affected by proteolytic stress conditions (Figure 38, lower panel).

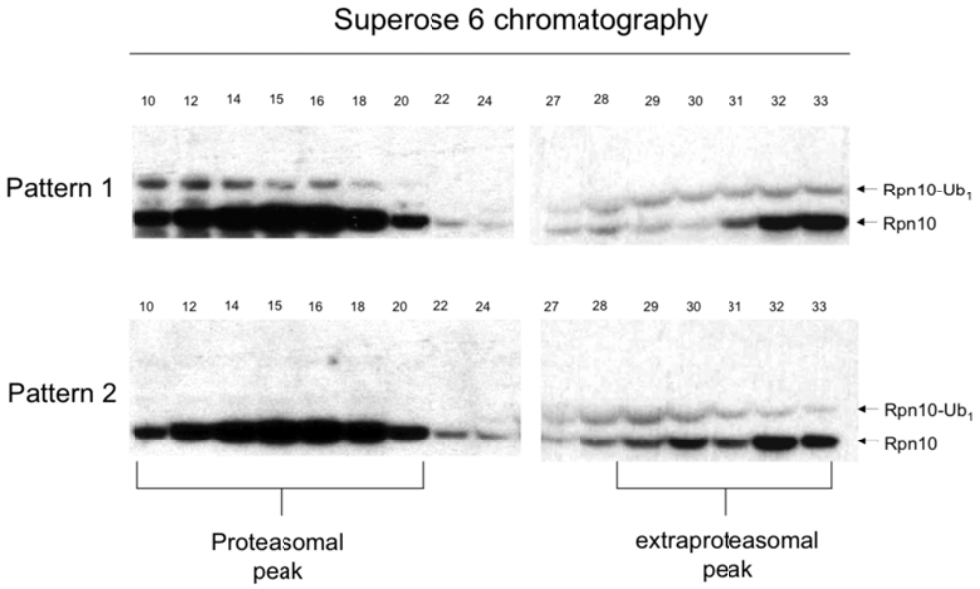

Figure 38: Proteasomal And Extraproteasomal Pools Of Rpn10-mUb Are Distinctly Regulated Upon Proteolytic Stress.

Fractionation of total cell extracts in Superose 6 chromatography and subsequent WB analysis against Rpn10. Pattern 1, non-proteolytic stress (NaCl 500 mM) (upper panel): a major peak of proteasomal Rpn10-mUb is observed. The extraproteasomal peak of Rpn10-mUb is virtually less abundant. Pattern 2, proteolytic stress (cold-shock) (lower panel): proteasomal Rpn10-mUb is drastically decreased, while the extraproteasomal pool is not affected.

These results suggested that Rpn10 monoubiquitination could be differently regulated according its cellular localization. This led us to further investigate the molecular and physiological differences of both pools of Rpn10.

Distinct *In Vitro* Activities Of Rsp5 And Ubp2 According To Rpn10 Cellular Localization

To assess differences between both pools of Rpn10-mUb we optimized the *in vitro* ubiquitination and deubiquitination reactions. Bacterial Rpn10 was used as a reference for the *in vitro* molecular characterization of the proteasomal-free pool of Rpn10.

We firstly performed ubiquitination reactions in purified proteasomes (see Figure 26B, right panel) and recombinant GST-Rpn10 (see Figure 28A). To compare ubiquitination patterns, it was crucial to add equal amounts of both substrates (400nM). An increasing amount of Rsp5 ligase (Figure 39A) was used to elucidate reaction´s stoichiometric conditions. Regardless of Rsp5 concentration, an oligoubiquitination pattern was observed in the recombinant form of Rpn10 (Figure 39B, reactions 1-3), whereas only one or two ubiquitin moieties were detected in the proteasomal pool (Figure 39B, reactions 4-6). These results suggested that different processivity and/or activity of Rsp5 could take place according Rpn10 cellular localization.

A

	GST-Rpn10			26S		
Regents	Rxn 1	Rxn 2	Rxn 3	Rxn 4	Rxn 5	Rxn 6
Buffer	-	-	-	-	-	-
Human E1	100 nM	100 nM	100 nM	100 nM	100 nM	100 nM
GST-Ubc4	400 nM	400 nM	400 nM	400 nM	400 nM	400 nM
GST-Rsp5	**400 nM**	**800 nM**	**1600 nM**	**400 nM**	**800 nM**	**1600 nM**
Ub	2mM	2mM	2mM	2mM	2mM	2mM
Substrate	**400 nM**	**400 nM**	**400 nM**	**400 nM**	**400 nM**	**400 nM**
ATP	10 mM	10 mM	10 mM	10 mM	10 mM	10 mM
DTT	1 mM	1 mM	1 mM	1 mM	1 mM	1 mM

B

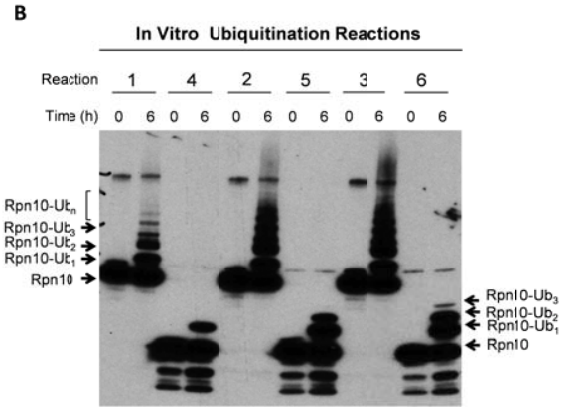

Figure 39: Different Patterns Of Ubiquitination Are Detected In Both Pools of Rpn10.
(**A**) Reagent concentration of optimized *in vitro* ubiquitination reactions. Equal amount of substrates (GST-Rpn10 and 26S) and increasing concentrations of ligase were used for each reaction. (**B**) Ubiquitination pattern *in vitro* reactions of proteasomal and recombinant Rpn10. A pattern of oligoubiquitination is observed in bacterial GST-Rpn10 (Reactions 1-3), whereas only mono- or diubiquitination is detected in proteasomal Rpn10 (Reactions 4-6).

We benefited from reactions 1 and 4 shown in Figure 39B (equimolar amounts of substrate and ligase) to assess differences in Ubp2 activity in Rpn10 cellular contexts. Kee *et al.* identified proteins that co-purified with epitope-tagged Rsp5 (Kee et al., 2005). They illustrated that Rup1, a UBA domain-containing protein, was required for binding of Rsp5 to Ubp2 both *in vitro* and *in vivo*. To focus on the characterization of Rpn10 deubiquitination *in vitro*, we used a bacterial bicistronic vector to simultaneously express Ubp2 and Rup1. We monitored enzymatic activity of Ubp2 and Ubp2-Rup1 in a

time course assay using different pools of modified Rpn10 as a substrate (Figure 40). Regardless of whether Rup1 was present in the reaction, Ubp2 was efficient in hydrolysing the oligoubiquitinated forms of monomeric Rpn10, but was unable to catalyze Rpn10 de-monoubiquitination, even after 60 minutes incubation (Figure 40A). A different activity pattern was detected in the proteasomal context. On one hand, Ubp2 was very active in diubiquitin cleavage (less than 15 minutes) and significantly removed monoubiquitin moiety (Figure 40B). On the other, co-expression of Ubp2 and Rup1 showed higher catalytic rates and was capable to precisely de-monoubiquitinate proteasomal Rpn10 (Figure 40B). This correlates with DUBs activities shown in Figure 25B and Figure 25C, where it was shown that Ubp2 is specialized in Rpn10 de-monoubiquitination in the context of the proteasome. We hypothesize that, in this context, Ubp2 activity could be strengthened by Rup1, even though Rup1 is not essential for Ubp2-dependent processing of ubiquitinated Rpn10.

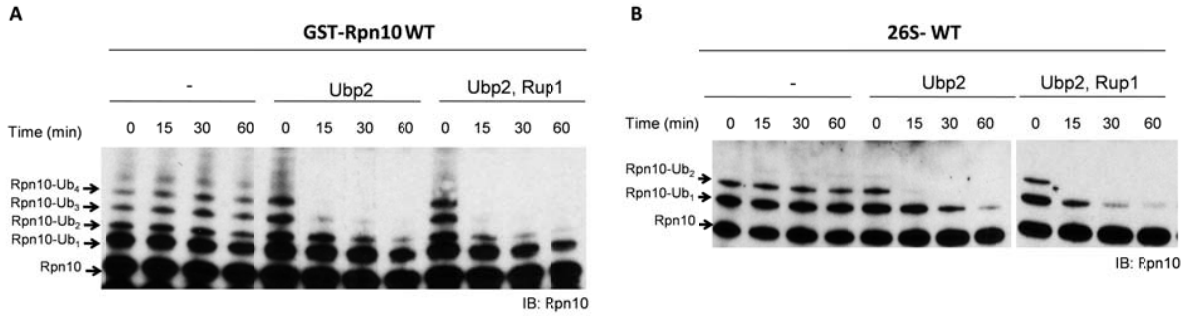

Figure 40: *In Vitro* Deubiquitination Assays Of Ubiquitinated Recombinant And Proteasomal Rpn10.
(**A**) Bacterial Ubp2 and Ubp2-Rup1 complex were incubated with ubiquitinated GST-Rpn10. Samples were taken at the indicated time points and analyzed by western blotting against Rpn10. (**B**) Bacterial Ubp2 and Ubp2-Rup1 complex were incubated with ubiquitinated purified proteasome. Samples were taken at the indicated time points and analyzed by western blotting against Rpn10.

Moreover, it is worth to remark the activity of Ubp2 on extra-proteasomal ubiquitinated Rpn10. Whereas, Ubp2 is extremely efficient with Rpn10-Ub_4 and Rpn10-Ub_3, it shows very low activity towards Rpn10-Ub_1 (Figure 40A). This pattern of DUB activity would favor the prevalence of monoubiquitinated Rpn10 against multi-monoubiquitylated or oligoubiquitylated forms.

Monoubiquitinated Rpn10 Cannot Bind To UBL-Dsk2

It has been recently obtained structural information of Rpn10 and Dsk2 alone and in complex with (poly)ubiquitin or with each other. Zhang *et al*. illustrated that a hierarchy of affinities emerges, in which Rpn10 shows higher affinity to the UBL domain of Dsk2 than to monoubiquitin, and it shows higher affinity to polyubiquitin chains than to Dsk2 UBL (Zhang et al., 2009a). It has been suggested that extraproteasomal Rpn10 restricts Dsk2 access to the proteasome, maintaining proper function of the ubiquitin-proteasome system (Matiuhin et al., 2008). In the experiment described below, we aimed to elucidate whether the Dsk2-Rpn10 interaction would be inhibited when the receptor is monoubiquitinated. We challenged the affinity of several forms of ubiquitinated Rpn10 (synthesized as

in Reaction 1 of Figure 39B) to 6xHIS-Dsk2 anchored on Ni-NTA beads. In this assay Rpn10^{K84only} and Rpn10^{K268only} mutants were added to detect differences in lysine-specific Rpn10 mutants (Figure 41A). Intrinsically, unmodified Rpn10, but not ubiquitinated forms of Rpn10, bound Dsk2, showing that Rpn10 Ub-UIM interaction *in cis* makes the UIM inaccessible to Ubl-Dsk2 domain (Figure 41B). Again, these binding assays were compatible with the 'fold-back' model previously presented in Figure 32B and Figure 34A.

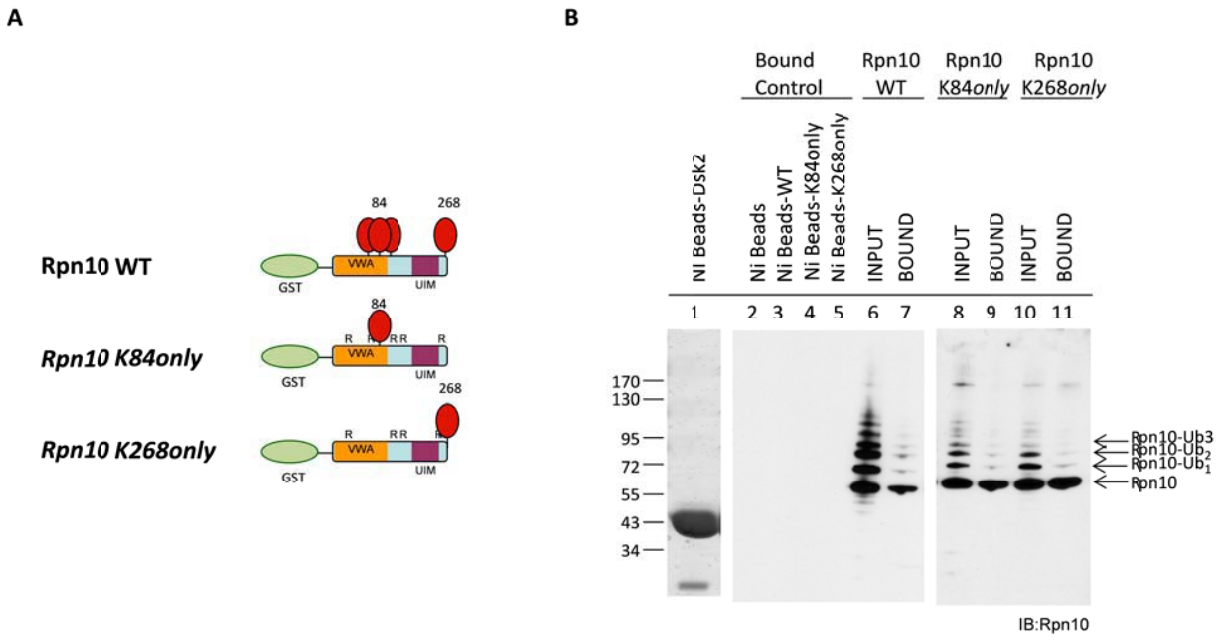

Figure 41: Monoubiquitinated Rpn10 Cannot Bind To UBL-Dsk2.
(A) Schematic representation of ubiquitinated forms of GST-Rpn10 WT, Rpn10^{K84only} and Rpn10^{K268only} mutants. (**B**) Binding assay of unmodified and mUb-Rpn10 (wild-type, *K84only*, K268only mutants) to unanchored 6xHIS-Dsk2 immobilized in Ni beads (lane 1). Input and bound material are shown for each sample (lanes 6-11). A control of different forms of Rpn10 binding to empty Ni beads is included in lanes 2-5.

Thus, Rpn10 monoubiquitination inhibits UBL-Dsk2 and UIM-Rpn10 interaction suggesting new physiological roles of Rpn10 monoubiquitination in an extraproteasomal context. We speculate that the *free* pool of Rpn10-mUb promotes Dsk2-dependent delivery of polyubiquitinated substrates to the proteasome.

Characterization Of Lysine-Specific Monoubiquitination Of Rpn10

We then asked whether differences in Rsp5 and Ubp2 activities could be reasoned by a residue-specific differential ubiquitination in Rpn10 sequence. We have confirmed that Rpn10 is modified by ubiquitin at lysines 71, 84, 99, located within the VWA domain, and in 268, located at the C terminus of the protein. The fact that Lys^{84} is located within the VWA domain suggests that this domain could be affected by Lys^{84} monoubiquitination, so it was considered the putative effect of Lys^{84} monoubiquitination, not only

on the UIM, but also on the VWA domain, involved in protein degradation in a UIM-independent manner (Verma et al., 2004). We hypothesized that modifications at Lys^{268} and at Lys^{84} inhibit protein degradation with different efficiency, probably being processed differently, maybe involving several ubiquitin ligases or deubiquitinating enzymes. Therefore, it was of our interest to assess whether there was a negative selection of the use of both lysines due to a reduced accessibility of Lys^{84} to the proteasome. This goal was approached by molecular biology techniques and quantitative proteomics methods, particularly Protein AQUA. AQUA methods allowed revealing the amount of each ubiquitinated lysine in both pools of Rpn10. This project was carried out in Dr. Steven P. Gygi lab in Harvard Medical School (Boston, USA).

The peptides labeled with heavy isotopes were complementary to Lys^{84} and Lys^{268} of Rpn10 sequence. (See Materials and Methods, Table 2). AQUA internal standards were evaluated by LC-MS/MS to perform a standard reference method, providing qualitative information about peptide retention, ionization efficiency and fragmentation (Figure 56, see Appendix).

In vitro ubiquitination reactions were then performed for recombinant and proteasomal Rpn10 as in Figure 39B, Reactions 1 and 4, respectively. Regions of the gel consistent with modified Rpn10 were excised (Figure 42A and Figure 43A), followed by in-gel trypsin proteolysis containing both internal standards (See Materials and Methods, Table 2). Lys^{84} peptide sequence contains one Met, which is easily oxidized to methionine sulfoxide. To have a uniform population to quantify, we added oxidizing agents to both internal standard and samples, displacing the reaction equilibrium towards product formation. Finally, samples were analyzed by MS. As an absolute amount of AQUA peptides was added, the ratio of areas under the curve was used to precisely quantitate the amount of each modified Lys in the original sample (Table 6, see Appendix). Accurate amounts of both GG-modified Lys were determined by AQUA tools in recombinant modified Rpn10 (Figure 42B and C). As expected, ubiquitinated Lys^{84} was largely more abundant than Lys^{268}. Of special note is that, in a non-ubiquitinated Rpn10 sample (Sample A, Figure 42A), a minor amount of modified Lys^{84} and Lys^{268} was detected (Figure 42B and C). These findings raised two possibilities: **1.** contamination from Sample B and/or **2.** reduced sensitivity and increased background, symptoms of detector glitches.

A

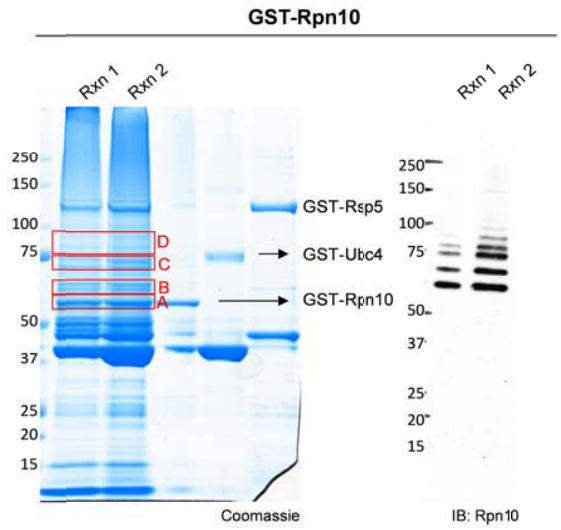

C

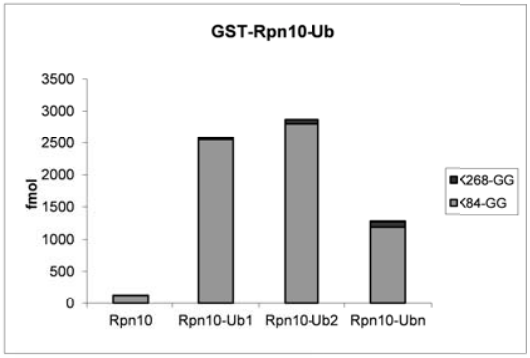

B

		K84			K268			
	Samples	Rxn1	Rxn2	Average	Rxn1	Rxn2	Average	K84/K268
A	GST-Rpn10	90.51	159.62	125.07	5.55	8.92	7.24	17.28
B	GST-Rpn10-Ub_1	2316.46	2784.22	2550.34	27.87	29.70	28.79	88.59
C	GST-Rpn10-Ub_2	2053.36	3554.38	2803.87	53.25	59.53	61.39	45.67
D	GST-Rpn10-Ub_n	876.57	1509.90	1193.24	86.77	83.50	85.14	14.02

Figure 42: AQUA Analysis Of *In Vitro* Ubiquitinated GST-Rpn10.
(**A**) Products of *in vitro* GST-Rpn10 ubiquitination were analyzed by SDS-PAGE and Coomassie staining. Western blot against Rpn10 antibody was used as a benchmark to precisely excise bands corresponding to GST-Rpn10, GST-Rpn10-Ub_1, GST-Rpn10-Ub_2 and GST-Rpn10-Ub_n (framed in red). (**B**) Samples were analyzed by mass spectrometry. Because 1 pmol of each internal standard was added, we could precisely quantify the amount (fmol) of each modified Lys. Duplicates were done for each sample and the average is given as the final result. Ratio of ubiquitinated Lys^{84} versus Lys^{268} was calculated. (**C**) Graphical representation of averages in B.

We then repeated assays shown in Figure 42, but using *in vitro* ubiquitinated proteasomes (Figure 43), and we found that native Lys^{84} was 30-fold more abundant than Lys^{268} in Sample G (Figure 43B and C). In Sample F, which was equally prepared than Sample G, we were not able to detect any signal corresponding to native Lys^{268} (Table 7, see Appendix). Altogether, these results suggested that monoubiquitination targets mainly the VWA domain of Rpn10.

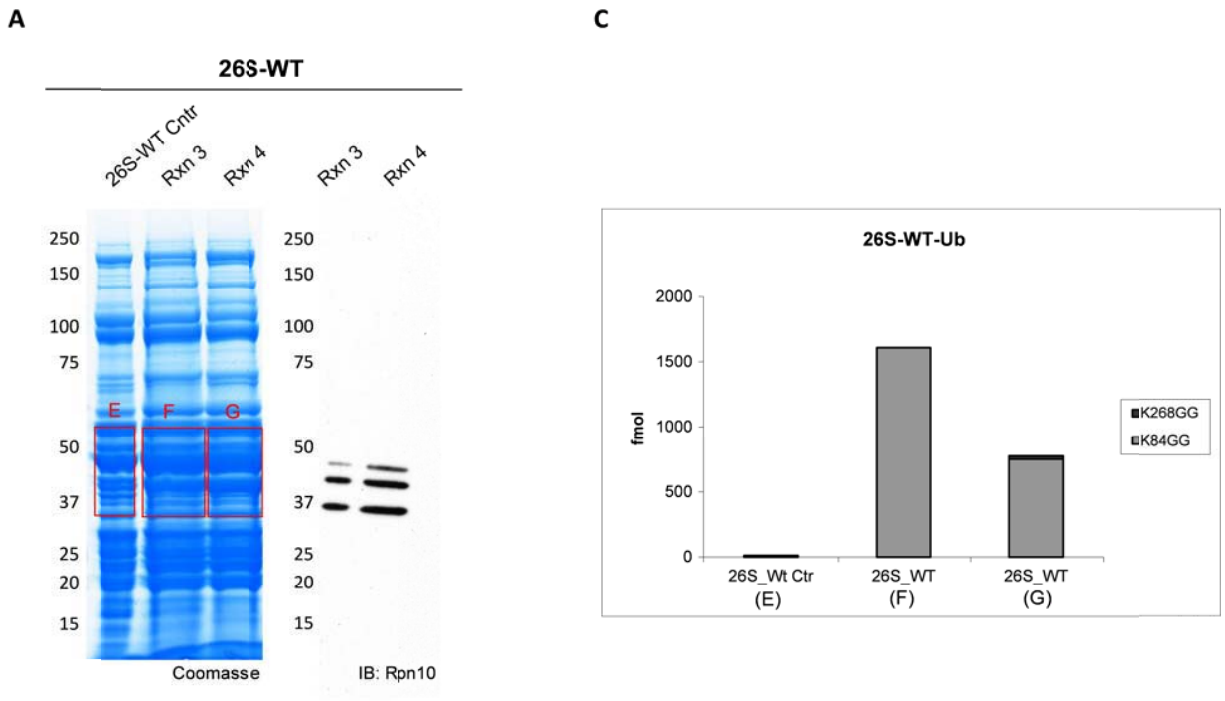

B

	Samples	K84 (fmol)	K268 (fmol)	K84/K268
E	26S WT - Cntr	12.39	-	12.39
F	26S WT	1609.08	-	1609.08
G	26S WT	751.32	25.64	29.30

Figure 43: AQUA Analysis Of *In Vitro* Ubiquitinated Proteasomal Rpn10.
(**A**) Products of *in vitro* ubiquitinated 26S were analyzed by SDS-PAGE and Coomassie staining. Western blot against Rpn10 antibody was used as a benchmark to excise the region comprising ubiquitinated Rpn10 (framed in red). (**B**) Samples were analyzed by LC-MS/MS. Because 1 pmol of each internal standard was added, we could precisely quantify the amount (fmol) of each modified Lys. Duplicates were done for each sample. Results disparity did not enable average calculation. If possible, ratio of ubiquitinated Lys^{84} versus Lys^{268} was calculated. (**C**) Total amounts of each lysine were plotted for each original sample.

At this point, an *in vivo* evidence of Lys-specific differential ubiquitination was required to achieve conclusive results. With this purpose, we fractionated a whole cell lysate and we also benefited from the whole cell lysate fractionation assay shown in Figure 25C. For both fractionations assays, proteasomal and cytosolic *free* fractions of Rpn10 were trypsinized and an absolute amount of AQUA internal standards was added (See Materials and Methods, Table 2). Since the extraproteasomal pool of Rpn10-mUb represents a small fraction of total modified Rpn10, we used polyubiquitin enrichment strategies to enhance its identification and quantification. Cellular ubiquitinome was pulled down using a monoclonal antibody that recognizes diglycine-containing isopeptides (Kim et al., 2011b). Finally, desalted and lyophilized diGly-captured peptides were resuspended and samples were used for mass spectrometry analysis (Figure 44A). Although the minor abundance of endogenous modified Rpn10,

high-resolution mass spectrometry tools enabled detection and quantification of endogenous Ub-Lys^{84} (Figure 44B and C) (Table 8, see Appendix). As shown in Figure 44B and Table 8 (see Appendix), low abundance of endogenous modified Lys^{268} made its reliable identification harder. Altogether indicated that, regardless of Rpn10 cellular localization, Lys^{84} is the preferred target of Rsp5; suggesting that there is not a negative selection of the use of Lys^{84} in the context of the proteasome.

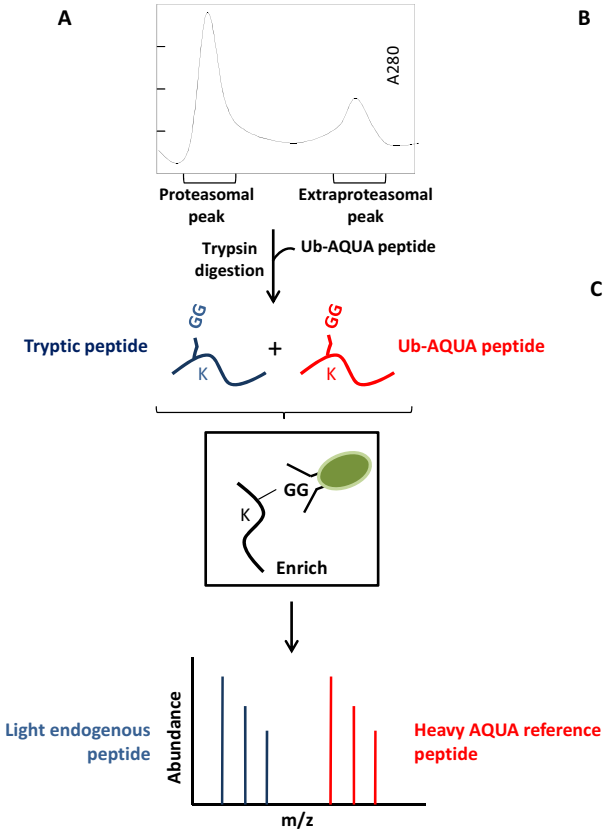

B

Samples	K84 (fmol)	K268 (fmol)	K84/K268
26S Peak	22.61	6.44	3.51
Free Peak	27.26	6.48	4.21

C

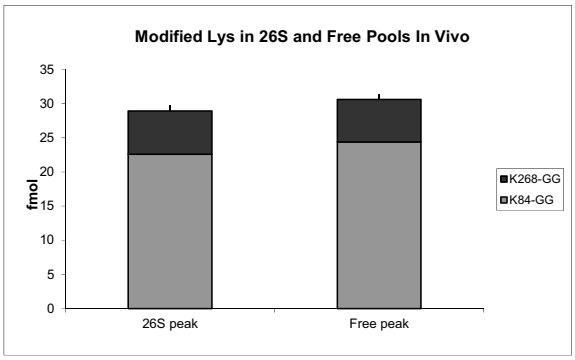

Figure 44: AQUA Analysis Of Proteasomal And Cytosolic Free Pool Of Ubiquitinated Rpn10.
(**A**) Fractions shown in Figure 25C were immunoblotted against Rpn10 and Ubp6 to decipher between both peaks of Rpn10. (data not shown). After trypsin digestion, isotope-labeled peptides were added. A polyubiquitin enrichment strategy was performed and samples were analyzed by LC-MS/MS. (**B**) Because 1 pmol of each internal standard was added, we could quantify the amount (fmol) of endogenous modified Lys in both pools of Rpn10. Ratio between Lys^{84} and Lys^{268} was calculated. (**C**) Total amounts of each lysine were plotted for both peaks of Rpn10.

In parallel, additional biochemical assays to address this point were carried out in the lab (Dr. A. Zuin , IBMB). *rpn10*Δ proteasomes were reconstituted with equimolar amounts of Rpn10 and Rpn10 lysine to arginine mutants (Rpn10^{K84R}, Rpn10^{K268R} and Rpn10^{K84,268R}). *In vitro* ubiquitination reactions were carried out using reconstituted proteasomes and GST-free Rpn10 mutants (Figure 45B and A, respectively).

Different ubiquitination profiles were observed when comparing both pools of Rpn10; but importantly, Rpn10-reconstituted proteasomes exhibited similar ubiquitination patterns to ones shown in Figure 39B. These results indicated that *in vitro* reactions of reconstituted proteasomes were a good biochemical approach to characterize residue-specificity in Rpn10 ubiquitination. Single mutation of Lys^{84} (Rpn10-K84R, Figure 45B) showed a strong decrease in proteasomal monoubiquitination. Once more, the function of Rpn10 monoubiquitination *in vitro* completely relies on Lys^{84}. These findings were in agreement with the quantitative proteomics data shown in Figure 42B, B and Figure 44B.

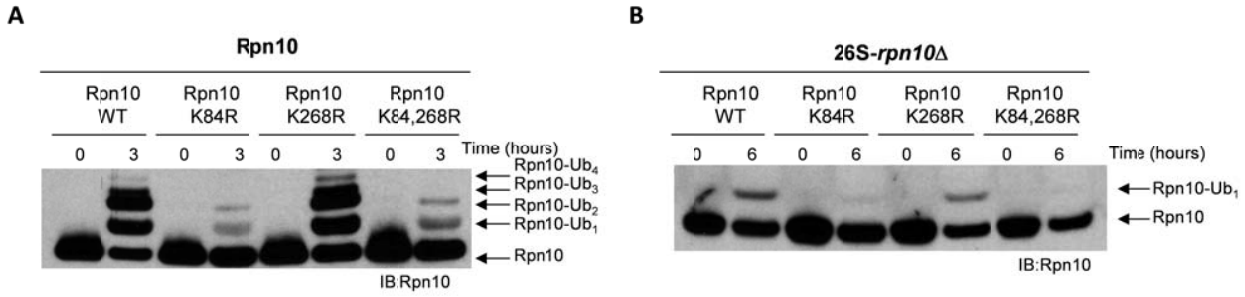

Figure 45: Lys84 Is The Main Target Of Rsp5 In Both Pools Of Rpn10.
(**A**) Purified Rpn10 WT and Rpn10 mutants ($Rpn10^{K84R}$, $Rpn10^{K268R}$ and $Rpn10^{K84,268R}$) were used as substrates for ubiquitination reactions. Oligoubiquitination was observed in WT and K268R mutant and it significantly decreased in K84R and K84,268R mutants. (**B**) *rpn10*Δ proteasomes were reconstituted with purified Rpn10 WT and Rpn10 mutants ($Rpn10^{K84R}$, $Rpn10^{K268R}$ and $Rpn10^{K84,268R}$). Monoubiquitination is observed in WT and K268R mutant but not, or in a lower extent, in Lys^{84} mutants.

Results illustrated in Figure 39B, Figure 40A and Figure 40B suggested that different enzymatic activities regulated Rpn10 monoubiquitination. We speculated that lysine residues were distinctly modified in each Rpn10 pool. However, molecular biology and MS tools of absolute quantification have corroborated that Lys^{84} and Lys^{268} are not differentially regulated, yet Lys^{84} is the main modified residue regardless of Rpn10 context.

Lys63 Is The Most Abundant Ub-Linkage In *In Vitro* Oligoubiquitinated Rpn10

Rsp5 is associated with Ubp2-deubiquitinating enzyme that removes Lys^{63}-linked chains from Rsp5 substrates, such as endocytic proteins such as Csr2 and Ecm21 (Kee et al., 2006). In this assay we used GST-Rpn10-Ub_1, GST-Rpn10-Ub_2 and GST-Rpn10-Ub_n (Figure 42A; samples B, C, and D, respectively) to assess lysine linkage-specificity in Rpn10 oligoubiquitination. As expected, ubiquitin chains were mainly assembled through Lys^{63} (Figure 46) (Table 9: Identification Of Lysine-Linkage Specificity In Rpn10 Oligoubiquitination, see Appendix), which are the type of chains usually promoted by Rsp5. Detection of minor amounts of Lys^{11}- and Lys^{48}-linked Ub chains may not have any biological significance since ubiquitin-enzymatic machinery is pushed to the limit in *in vitro* reactions.

Ub-linkage	Rpn10-Ub_1	Rpn10-Ub_2	Rpn10-Ub_n	Total	Sdev
K11	2	1	2	5	0.58
K48	1	2	2	5	0.58
K63	5	10	14	29	4.51

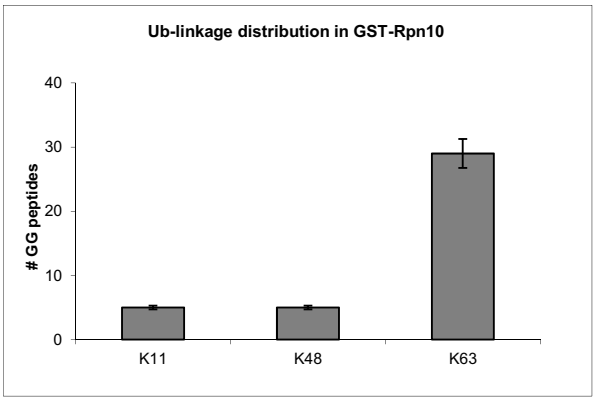

Figure 46: Lys63 Is The Most Abundant Ubiquitin-Linkage In Rpn10 Oligoubiquitination.
GST-Rpn10-Ub_1, GST-Rpn10-Ub_2 and GST-Rpn10-Ub_n products were analyzed by MS and specific Ub-linkage chains were identified through Lys^{11}, Lys^{48} and Lys^{63}. However, Lys63-linkage chains were the most abundant ones. Above, for each sample, the number of spectral counts is shown for the three detected Ub-linkage chains. Bottom, total amounts of modified Ub-lysines and its standard deviation are plotted.

Crosas et al. showed that Rpn10 was degraded by the proteasome upon Lys^{48}-linked polyubiquitination by the 19S-associated Hul5 ligase. We suggest that Rsp5-catalyzed Lys^{63}-chain formation could yield a substrate suitable for Hul5-catalyzed elongation.

Ubiquitinome Dynamics In Low-Temperature Response: Effect Of The Deletion Of Rpn10 And Rad23 Genes

A formidable challenge to decipher ubiquitin's biology is to map the networks of substrates and ligands for components of the UPS. Herein, we combined polyubiquitin-enrichment strategies with quantitative proteomic approaches to characterize the dynamics of ubiquitinated species in cells defective in proteasomal substrate receptors Rpn10 and Rad23 during cold response. As explained in the next paragraph, the experiment was designed and the controls were chosen in a way that the contribution of Rpn10 could be evaluated.

Early observations showed that *rpn10*Δ strain is viable and shows no severe phenotypes, implying that other ubiquitin receptors must exist, as reported later in the field. The discovery that, in yeast, Rad23 has the capacity to deliver ubiquitinated substrates to the proteasome in a Rpn10 independent manner (Schauber et al., 1998) suggested a complementary role of Rad23. Indeed, Rad23 function exhibits partial redundancy with respect to Rpn10. For instance, RPN10 and RAD23 mutations exhibit a slow growth defect and have additive effects in proteolysis stress phenotypes, such as accumulation of ubiquitin-protein conjugates and sensitivity to amino acid analogs (Elsasser et al., 2002; Elsasser et al., 2004; Verma et la., 2004). An additional interesting synthetic phenotype of *rad23Δrpn10Δ* cells is cold

sensitivity (Lambertson et al., 1999). Despite the fact that the role of UPS factors in heat-shock response has been extensively analyzed, the role of the UPS in cold response remains largely unexplored.

For the present study, we used two UPS-deficient strains obtained from the same tetrad dissection analysis: *rad23Δ* and *rad23Δrpn10Δ* strains. The main objective of the experiment was to compare the amount of ubiquitylated proteins, and their sites of modification, found in these two mutants, in cultures growing at standard temperature and in cold-shocked cultures. The use of the *rad23Δ* strain as a control culture (instead of the wild-type) gave us the possibility to detect and quantify those ubiquitination sites modified in a Rpn10 dependent manner.

The SILAC approach was used for MS-based quantitative proteomics. *rad23Δrpn10Δ* mutant was grown in metabolically heavy labeled medium (K8; lysine + 8 Da shift) whereas reference cells (*rad23Δ*) were cultured in light (K0) medium. Cultures were normally grown up to an OD_{600} of 1 and subjected to cold-shock stress for 4 hours. At both points (permissive temperature -PT- and 16ºC) equal amount of cells were mixed and lysed in denaturing buffer to prevent deubiquitinating enzyme activity. After protein quantification and tryptic digestion, the diGly-containing peptides were isolated by two sequential immunoprecipitations and subjected to shotgun mass spectrometry (Figure 47A). We monitored the number of cells throughout the experiment and a growth defect in *rad23Δrpn10Δ* mutant was detected when inducing cold-shock stress (Figure 47B, plotted graph), significantly increasing its doubling time (from 2.6 to 3 hours, Figure 47B, bottom panel).

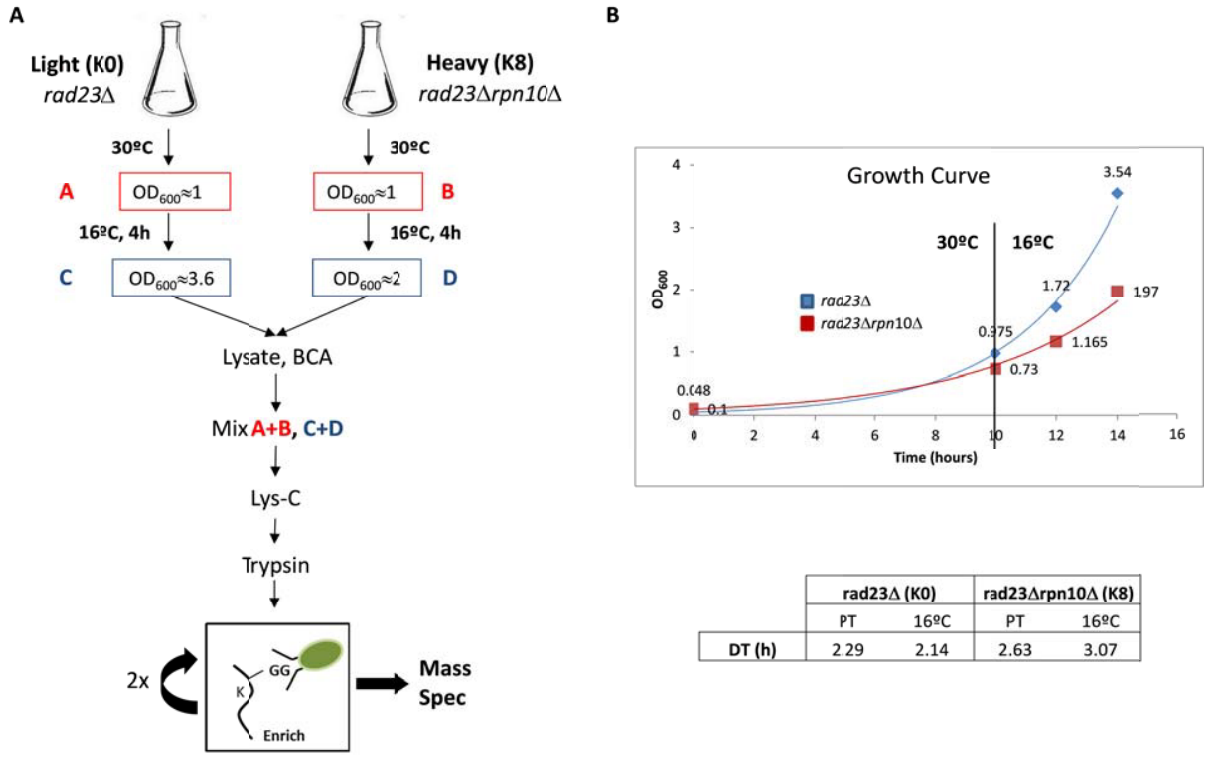

	rad23Δ (K0)		rad23Δrpn10Δ (K8)	
	PT	16ºC	PT	16ºC
DT (h)	2.29	2.14	2.63	3.07

Figure 47: Ubiquitinome Characterization Of *rad23Δ* and *rad23Δrpn10Δ* Under Normal And Cold-Shock Stress.

(**A**) Schematic overview of the methodology followed in this assay. (**B**) Cell growth was monitored by measuring the absorbance at 600 nnm at the indicated times and an exponential regression model was plotted. Doubling time of both strains under different growth conditions was calculated.

SILAC ratios were determined for each peptide and then underwent Log2 transformation for peptide normalization. Signal-to-noise ratios of both heavy and light isotopic envelopes were used for quantification of sites and proteins (Kim et al., 2011b) (for more detailed information, see Materials and Methods).

The bioinformatic analysis revealed that, at 30ºC, 688 unique sites in 318 proteins were identified, of which 478 (almost 70%) unique sites, in 238 proteins, were quantified. The number of identified and quantified sites and proteins under cold-shock stress was slightly lower: 499 ubiquitinated sites in 271 proteins were detected, of which the 75 % of sites, in 213 proteins, were quantified (Figure 48A). Interestingly, in both growth conditions multiple ubiquitylation sites were found in more than 45% of the proteins identified, with a very small fraction containing more than 4 modified sites (Figure 48B). These numbers represent a 6-fold increase with respect to a previous study analyzing ubiquitinated proteins in yeast, in which 110 diGly-modified peptides were detected (Peng et al., 2003).

A

Proteins					
PT			16ºC		
id-ed	q-ed		id-ed	q-ed	
Proteins	Proteins	%	Proteins	Proteins	%
318	238	74.8	271	213	78.6

Sites							
PT				16ºC			
id-ed		q-ed		id-ed		q-ed	
Sites	%	Sites	%	Sites	%	Sites	%
688	89.2	478	69.5	499	64.7	375	75.2

B

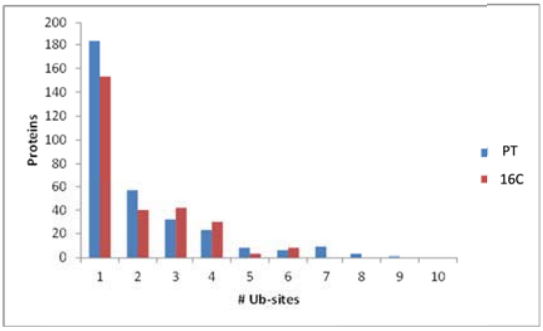

Figure 48: Overview Of The DiGly Proteomic Enrichment Strategy.
(**A**) The total number of diGly-modified lysines (sites) and proteins that have been identified and quantified in this assay. (**B**) Distribution of the sites per protein observed from diGly enrichment in both growth conditions.

On one hand, the ubiquitinated substrates were separately characterized for both growth conditions. Figure 49 and Figure 50 summarize the mass spectrometry data obtained 30ºC (hereafter, also referred as PT) and 16ºC, respectively. We firstly compared the frequency distribution of the bulk protein population with the diGly-modified proteome. For statistical analysis, the heavy to light ratios were analyzed on a base 2 logarithmic scale, meaning that a peptide is enriched in the *heavy* (*rad23*Δ*rpn10*Δ) culture when it shows values of Log2 (H:L) > 0, and enriched in the *light* (*rad23*Δ) culture when it shows Log2 (H:L) < 0. Log2 values of 0 indicate equal abundance of peptides in both cultures. So, a histogram of the Log2 heavy-to-light ratio against the spectral counting of each quantified peptide was plotted for both growth conditions (Figure 49A and Figure 50A). Using this metrics, we obtained a null distribution of Log2 (H:L) ratios when analyzing the whole protein population (> 90% of the peptides showed a Log2 (H:L) around 0) (Figure 49A and Figure 50A, plotted in the left side). However, the frequency distribution in the diGly-containing peptides was significantly shifted toward positive values (peptides more abundant in *rad23*Δ*rpn10*Δ mutant) and was more spread out (Figure 49A and Figure 50A, plotted in the right side). This tendency was more evident at cold-shock, where the median of Log2 (H:L) of all ubiquitinated sites was altered from the null value to ~1.5, indicating that most of the quantified sites showed, at least, a 2.5-fold increase when decreasing growth temperature (compare Figure 49B and Figure 50B, for PT and cold-shock, respectively). These results clearly indicated that the polyubiquitin enrichment strategy is a powerful technique to induce meaningful differences in ubiquitinated proteins abundance with evidence for a higher prevalence of enrichment (Log2 ratios > 1) than depletion (Log2 ratios < -1) (see Table 10, Table 11, Table 12 and Table 13 in Appendix for a detailed information of the most enriched and depleted ubiquitinated sites under both growth conditions).

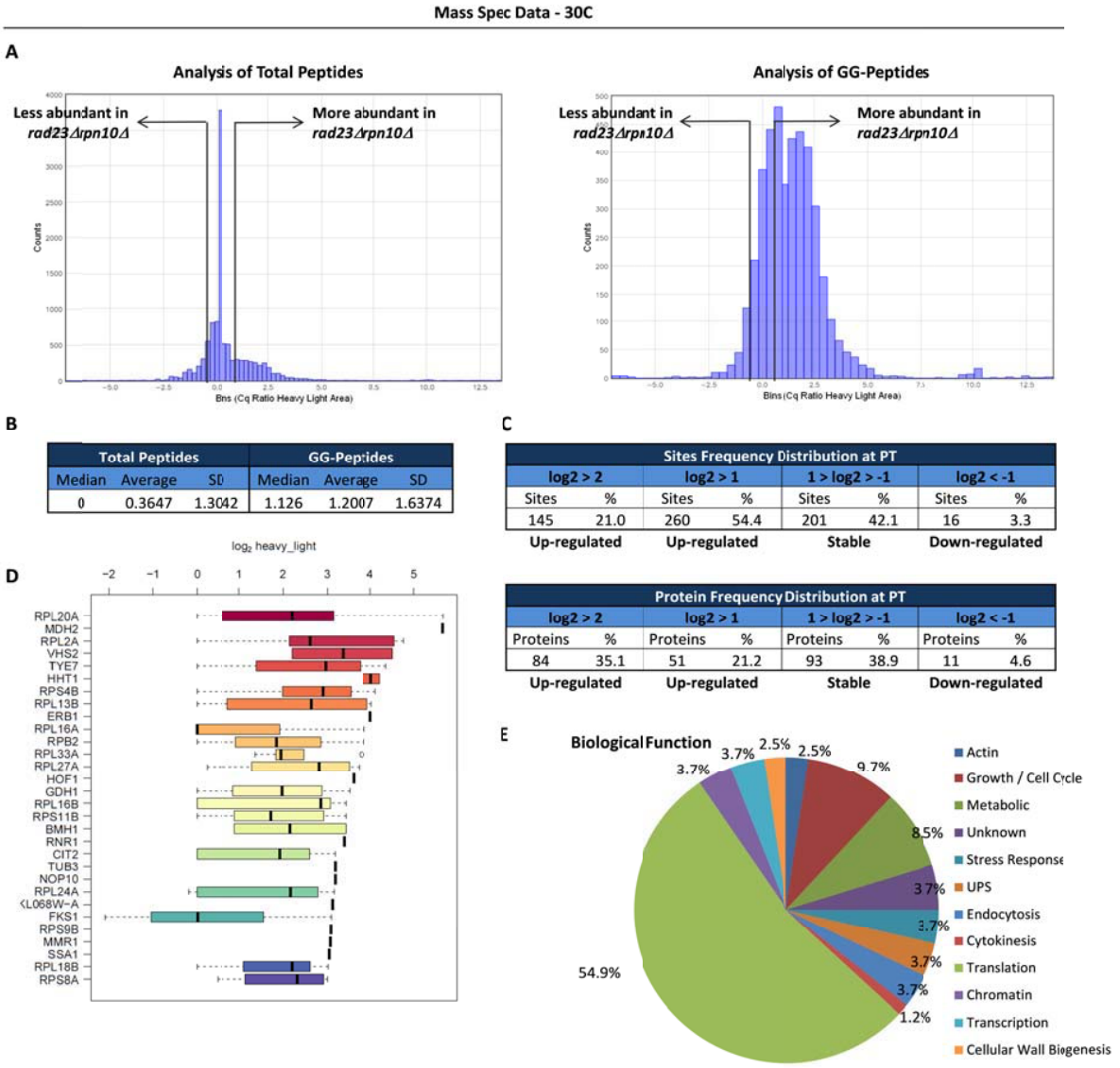

Figure 49: Mass Spec Bioinformatic Analysis Of Mutant Yeast Cells Cultured At Standard Growth Conditions.

(**A**) Frequency distributions of all quantified bulk proteins (left) and diGly-modified proteome (right). Log2 of the heavy-to-light ratios are shown in the *x* axis, the number of spectral counts is represented in the vertical axis. Proteins enriched in the double mutant (labeled with K8) show a positive Log2 (H:L), whereas the ones that are decreased (more abundant in single mutant, K0) exhibit negative ratios. (**B**) The median, the average and standard deviation of non-modified and diGly-modified peptides is calculated. (**C**) The diGly-containing peptide are clustered according their Log2 (H:L) ratio. Proteins that are modified at multiple sites have been grouped according the site with the highest Log2 (H:L) value (lower panel). (**D**) *R* software was used to statistically explore and plot the data, in collaboration with Marc Güell (Church´s lab, HMS). The quantified diGly peptides are assembled for each protein. The first 30 proteins containing at least a Log2 (H:L) > 2) are plotted in a boxplot diagram. The length of the box represents the number of quantified sites for each protein. The median of Log2 (H:L) ratio of all diGly peptides is represented by a bold black line. (**E**) Pie diagram representing the biological distribution of enriched

substrates and their percentage.

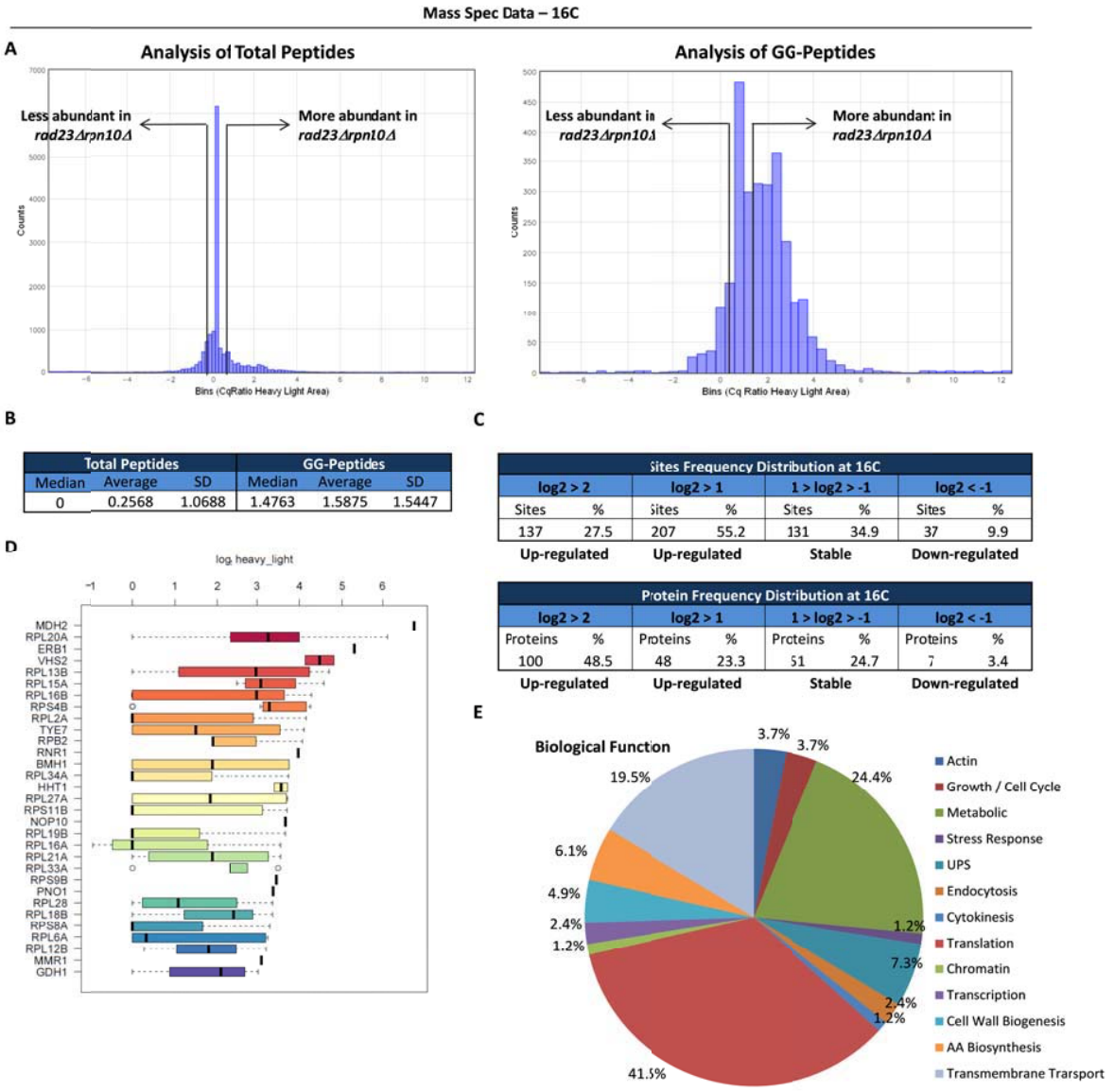

Total Peptides			GG-Peptides		
Median	Average	SD	Median	Average	SD
0	0.2568	1.0688	1.4763	1.5875	1.5447

Sites Frequency Distribution at 16C							
log2 > 2		log2 > 1		1 > log2 > -1		log2 < -1	
Sites	%	Sites	%	Sites	%	Sites	%
137	27.5	207	55.2	131	34.9	37	9.9
Up-regulated		Up-regulated		Stable		Down-regulated	

Protein Frequency Distribution at 16C							
log2 > 2		log2 > 1		1 > log2 > -1		log2 < -1	
Proteins	%	Proteins	%	Proteins	%	Proteins	%
100	48.5	48	23.3	51	24.7	7	3.4
Up-regulated		Up-regulated		Stable		Down-regulated	

Figure 50: Mass Spec Bioinformatic Analysis Of Mutant Yeast Cells Subjected to Cold-Shock Stress.
(**A**) Frequency distributions of all quantified bulk proteins (left) and diGly-modified proteome (right). Log2 of the heavy-to-light ratios are shown in the *x* axis, the number of spectral counts is represented in the vertical axis. Proteins enriched in the double mutant (labeled with K8) show a positive Log2 (H:L), whereas the ones that are decreased (more abundant in single mutant, K0) exhibit negative ratios. (**B**) The median, the average and standard deviation of non-modified and diGly-modified peptides is calculated. (**C**) The diGly-containing peptide are clustered according their Log2 (H:L) ratio. Proteins that are modified at multiple sites have been grouped according the site with the highest Log2 (H:L) value (lower panel). (**D**) *R* software was used to statistically explore and plot the data, in collaboration with Marc Güell (Church´s lab, HMS). The quantified diGly peptides are assembled for each

protein. The first 30 proteins containing at least a Log2 (H:L) > 2) are plotted in a boxplot diagram. The length of the box represents the number of quantified sites for each protein. The median of Log2 (H:L) ratio of all diGly peptides is represented by a bold black line. (**E**) Pie diagram representing the biological distribution of enriched substrates and their percentage.

To analyze in more detail the bulk data, diGly-containing peptides were clustered in four different groups: **1.** sites showing a 4-fold enhancement (Log2 (H:L) > 2) upon RPN10 deletion, **2.** sites with Log2 (H:L) >1; representing, at least, a 2-fold increase in ubiquitination enrichment, **3.** sites equally abundant in both yeast strains, considering less than 2-fold increase or decrease (-1 < Log2 (H:L) < 1) and **4.** sites that were more ubiquitinated in the single (*rad23*Δ) than the double mutant (*rad23*Δ*rpn10*Δ) (Log2 (H:L) < -1). When comparing the enriched sites at both growth conditions separately, an increase was observed in the 16ºC culture. For example, the 21% of the modified sites were highly enhanced (Log2 (H:L) > 2) at PT, whereas the 27.5% under cold-shock. A similar pattern was detected when analyzing those sites with Log2 (H:L) > 1 (Figure 49C and Figure 50C, upper panel). In both scenarios, multiple ubiquitination sites were found in a large portion of the quantified proteins. However, the effect of a cold-shock response in cellular ubiquitinome was much more evident when proteins, instead of peptides, where computed. At 16ºC, almost the 50% of the quantified proteins contained at least one site with a Log2 (H:L) ratio higher than 2, compared to the 35.5% under standard conditions (Figure 49C and Figure 50C, lower panel). These results suggested that: **1.** for those proteins containing multiple sites, all sites were not regulated similarly upon RPN10 deletion, consistent with the idea that not all ubiquitination events on target proteins are regulated identically, and **2.** proteasomal degradation mediated by the Rpn10 and Rad23 receptors could be a necessary molecular machinery to survive and adapt to cold-shock.

In both growth conditions, enriched sites were distributed across different biological functions with translational (mainly encoding ribosomal proteins) and metabolic proteins accounting for the largest fractions (Figure 49E and Figure 50E). It has been largely reported that genes related to ribosomal proteins and translation are induced after proteasomal and temperature shifts stresses (Aguilera et al., 2007; Sahara et al., 2002). However, further bioinformatic and biochemical assays are required to address which proteins in the ubiquitin proteome are likely to be true Rpn10-dependent substrates as opposed to proteins regulated by ubiquitination in a non-proteolytic manner or contaminants. A special note is that the relative amount of ubiquitinated proteins involved in cellular metabolism was significantly higher at 16ºC (24.4% *versus* the 8.5% at PT) (Figure 49E and Figure 50E). Strikingly, a novel group of enriched sites appeared under cold-shock stress: almost the 20% corresponded to integral-to-membrane proteins involved in transmembrane transport (Figure 50E), suggesting that changes in membrane fluidity could be a primary signal in the cold-shock response (Aguilera et al., 2007).

We also observed that multiple proteins, at low temperatures showed a pattern of ubiquitination distinct than at 30ºC. This change of pattern was due to a modification of the distinct Lys sites and presented and extremely interesting hypothesis. During a temperature decrease response, the ubiquitin conjugating machinery, or specific factors within this machinery, would be reprogrammed, resulting in a

dramatic change in the profile of lysine sites targeted for ubiquitin modification. This reprogramming of the ubiquitin conjugating machinery would not only involve E3 ligases, but probably also DUBs (see Discussion section).

To generate a comprehensive list of proteasome substrate candidates which are targeted to the proteasome as a response to cold-shock stress, we focused our interest on those proteins containing modified sites quantified in both growth conditions and that were significantly enhanced after a cold-shock stress induction. These results provided us with a further understanding of the physiological significance of an RPN10-RAD23-dependent cold-shock response. Figure 51 illustrates the biological function and cellular compartment of the 62 proteins which fulfill these requirements.

A

Prot. More Upregulated at 16C	E3 ligases	Prot. More Upregulated at 16C	E3 ligases
ACK1	-	GLN1	-
ACT1	Rsp5	GLY1	-
AIM44	-	GPM1	-
ASC1	-	GRX2	-
ASN2	-	HIP1	Rsp5
AVT1	Rsp5	HNM1	Rsp5
BAP2	Rsp5	HTB2	Bre1
BMH1	APCCdh1	IPP1	-
BUL1	Rsp5	ITR1	Rsp5
CAN1	Rsp5	ITR2	Rsp5
CBR1	-	KRE6	Rsp5
CCC1	Rsp5	KRS1	-
CIT2	-	LSB5	Rsp5
COS2	-	LYP1	Rsp5
COS6	-	MCH4	Rsp5
CPR1	Rsp5	MUP1	Rsp5
CPT1	Rsp5	NOP1	-
CTR1	Rsp5	NPP1	Rsp5
CUL3	SCF	NTF2	-
DSE1	-	NYV1	-
EDE1	Rsp5	OSH3	-
EFB1	-	PDC1	-
EFT2	-	PDR17	-
ENO2	-	PGK1	-
ERG11	-	PHO87	Rsp5
ERG13	-	PIN3	Hul5
FAS2	-	PMA1	Rsp5
FBA1	-	PMR1	Rsp5
FCY2	Rsp5	RPL17A	
FET4	Rsp5	RPL1B	
FKS1	Rsp5	SSH4	Rsp5

B

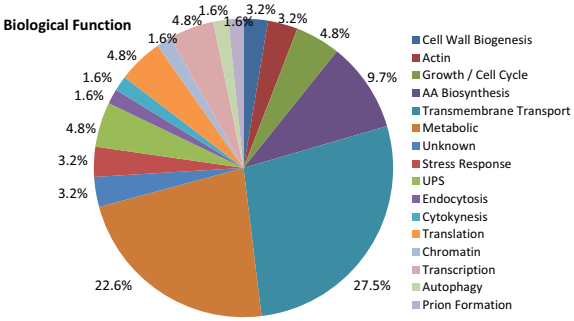

C

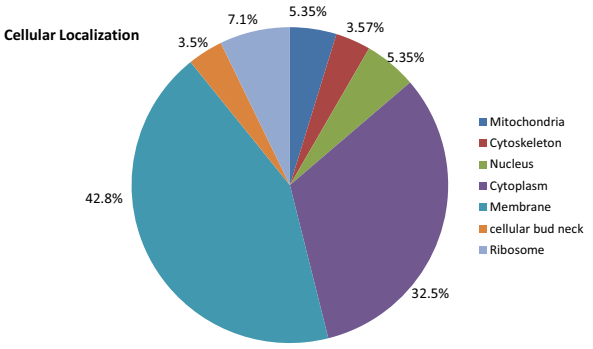

Figure 51: Bioinformatic Analysis of Ubiquitinated Proteins Significantly Increased After A Cold-Shock Stress When Compared To Standard Growth Conditions.

(**A**) List of the 62 proteins containing at least one site significantly increased after a cold-shock induction. For those proteins to which ubiquitin modification has been characterized in previous works, the proposed ubiquitin ligase is included in the right column. (**B**) and (**C**) Pie diagrams representing the biological functions and cellular localization of proteins meeting the mentioned requirement.

Most of the proteins that were significantly enriched after a decrease in temperature account for genes involved in metabolic (22.6%) or transport functions (27.5%) (Figure 51B). On one hand, these observations could indicate the need of a physiological remodeling of cell capabilities during cold-shock response. On the other, membrane proteins that would be normally degraded in a vacuolar-dependent

fashion, after a cold-shock stress, an RPN10-dependent proteasomal degradation would be highly induced. E3 ligases mainly involved in endocytosis, such as Rsp5, would modify their activity to force the newly induced proteins being degraded by the 26S. Among the proteins shown in Figure 51, some of them raised our interest. Specific examples are discussed in the next section.

Discussion

Monoubiquitination Of A Polyubiquitin Receptor

Targeted protein degradation plays a central role in eukaryotic cell regulation and homeostasis. Proteins are marked for degradation by E3 ubiquitin ligases that append polyubiquitin degradation signals to the target protein. These signals can recruit the targeted protein to the 26S proteasome for degradation. To reach a productive interaction with the proteasome, protein substrates are modified with ubiquitin chains by the action of ubiquitin ligating factors. The efficiency of the proteolytic process relies on the processivity of ubiquitin chain formation, on the topology of ubiquitin chains, and on the appropriate recruitment of ubiquitin-protein conjugates to the proteasome. The proteasome possesses several levels of control of ubiquitin-protein conjugate recruitment and processing: engagement of substrate receptors, disassembly and remodeling of ubiquitin chains, and accessing to proteolytic. In this work we show that monoubiquitination of proteasome subunit Rpn10/S5a, receptor of polyubiquitinated substrates, is a very powerful level of proteasome function regulation.

Monoubiquitination is a molecular event different from polyubiquitination. Monoubiquitination is conserved from yeast to mammals and involved in important cellular processes such as endocytosis and regulation of nuclear functions (Hicke, 2001; Dupré *et al.*, 2004; Kirkin and Dikic, 2007). Monoubiquitinated proteins are usually recognized by specific receptors that contain UBDs. For example, in the endocytic pathway, Vps9, Sts1, Sts2, Eps15 or Hrs, are UBD-containing protein adaptors that trigger protein internalization by binding to monoubiquitinated cargo. In addition, these factors are all monoubiquitinated *in vivo* (Di Fiore *et al.*, 2003; Hicke and Dunn, 2003; Hoeller *et al.*, 2006; Woelk *et al.*, 2006). In the context of the proteasome, Rpn10 binds Lys^{48}-linked polyubiquitinated substrates by means of one or two UIMs (Van Nocker *et al.*, 1996; Elsasser *et al.*, 2004; Verma *et al.*, 2004; Wang *et al.*, 2005). Mutation of the UIM of Rpn10 significantly ablates the proteolytic capacity of the proteasome. In this work we have shown that Rpn10 is regulated by 'coupled' monoubiquitination, constituting to our knowledge the first link between regulation of proteasome function and monoubiquitin signal.

Cellular levels of Rpn10 and other ubiquitin receptors are dynamically regulated in response to environmental cues (Finley, 2009; Lipinszki et al., 2009). Crosas et al. have shown that Rpn10 is degraded by the proteasome in a Hul5 dependent manner (Crosas et al., 2006). Hul5 ubiquitin ligase functions to remodel pre-existing Ub chains, in conjunction of an associated Ubp6 deubiquitinating activity to yield optimal degradation signals. *In vivo*, Rpn10 shows multi-monoubiquitination and polyubiquitination (see Figure 18), although mono- and diubiquitination are the most abundant forms of modified Rpn10 *in vivo* (see Figure 19). The formation of polyubiquitinated forms of Rpn10 depends on the presence of the ubiquitin chain elongating factor, Hul5, and correlates with Rpn10 turnover (Crosas *et al.*, 2006). We could uncouple Rpn10 monoubiquitination from polyubiquitination by deleting the *HUL5* gene (see Figure 19). Moreover, *in vivo* levels of mUb-Rpn10 are not affected in *ubp6*Δ cells (see Figure 25B and C), suggesting that the machinery involved in the process of Rpn10 monoubiquitination is essentially independent of ubiquitin chain formation and remodeling.

Rsp5/Nedd4-like Ubiquitin-Protein Ligase And Ubp2 Deubiquitinating Enzyme Regulate Rpn10 Monoubiquitination

The ubiquitin-protein ligase involved in Rpn10 monoubiquitination is Rsp5, a member of the Nedd4 HECT ligase family. Among different groups of E3, the Nedd4 family is one of the most intensely studied. One outstanding feature of Nedd4 enzymes is their involvement in multiple and diverse tasks in cell physiology, which are highly conserved in evolution. The Nedd4 representative in *Saccharomyces cerevisiae*, Rsp5, illustrates very well the multitasking profile of Nedd4 family. Rsp5 has been involved in the regulation of transcription, chromatin remodeling, mitochondrial inheritance, internalization of most -if not all- endocytic proteins, trafficking, actin cytoskeleton organization and dynamics, fatty acid biosynthesis and more recently, proteasome function (Hicke and Dunn, 2003; Isasa et al., 2010; Kaminska et al., 2011; Kirkin and Dikic, 2007). Several Rsp5 substrates have been characterized and some of them are included in the accompanying Figure 52. They include multiple proteins from the endocytic pathway, such as: Vps9, Sla1, Sna3, Gap1, Can1, Mup1, Fur4 (Lin et al., 2008; Seron et al., 1999; Shih et al., 2007; Stamenova et al., 2004; Stawiecka-Mirota et al., 2007); ER bound proteins, e. g. Spt23 and Mga2 (Hoppe et al., 2000); RNA polymerase II subunit Rpb1 (Huibregtse et al., 1997; Somesh et al., 2007) and proteasome subunit Rpn10 (Isasa et al., 2010).

Although several examples of the effects and importance of Rsp5-dependent ubiquitination have been reported, key questions of its molecular basis interaction still remains obscure. So far, four types of interaction have been characterized (depicted in Figure 52):

1. Rsp5 binds the C-terminal domain (CTD) of the RNA polymerase II subunit Rpb1, and efficiently synthesizes Lys63 linked polyubiquitin at two distinct sites of Rpb1 (Somesh et al., 2007). This reaction of polyubiquitination is thought to be counteracted *in vivo* by the deubiquitinating enzyme Ubp2, which forms a physiological complex with Rsp5. The result of Rsp5 and Ubp2 concerted activities would yield a monoubiquitinated protein, a form observed *in vivo* (Figure 52, Boxes 1 and A).
2. Rsp5 contains tryptophan-tryptophan (WW) motifs which directly recognize proteins containing proline(or leucine)-proline-x-tyrosine (PY) motifs. PY proteins are abundant in yeast and found at multiple levels of endocytosis and degradation pathways (Gupta et al., 2007). However, most membrane proteins do not contain these PY motifs, so proteins called ART (arrestin-related trafficking adaptors) display PY motifs and act as specific adaptors between plasma membrane cargo proteins and Rsp5 (Lin et al., 2008) (Figure 52, Box 2). This type of recognition usually involves synthesis of Lys^{63} chains by Rsp5. In some cases, it has been proposed that monoubiquitination is promoted by the action of Ubp2, (Kee et al., 2005) (Figure 52, Box B). However, it remains unclear whether, in a subset of this type of substrates, Rsp5 is able to synthesize directly monoubiquitination *in vivo*, in a Ubp2 independent manner (Figure 52, Box C).
3. Vps9 protein, which contains a CUE domain, is monoubiquitinated by Rsp5. The CUE domain is required for Vps9 monoubiquitination, which doesn't produce polyubiquitin (Shih et al., 2003). The reaction of deubiquitination of monoubiquitinated Vps9 has not been characterized, but Ubp2 is probably the best candidate to catalyze this reaction (Figure 52, Boxes 3 and D).

4. The proteasome subunit Rpn10 is monoubiquitinated by Rsp5. The UIM of Rpn10 is required for the catalysis of monoubiquitination. Moreover, Ubp2 is very efficient in the reaction of deubiquitination of monoubiquitinated Rpn10 (Isasa et al., 2010) (Figure 52, Boxes 4 and E).

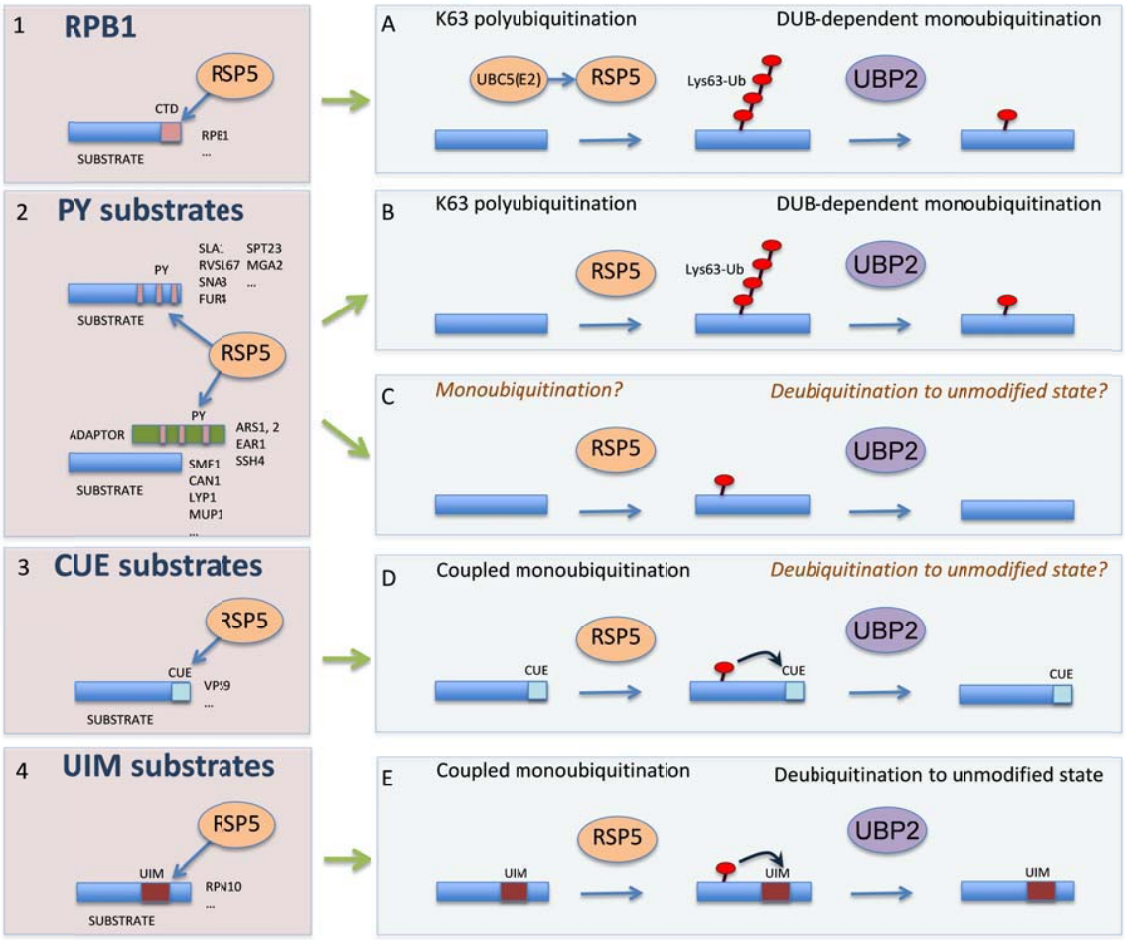

Figure 52: Models Of Rsp5 Substrate Recruitment And Processivity.
Left boxes: interaction of Rsp5 with substrates. CTD, C-terminal domain; PY, Proline (or Leucine)-tyrosine motif, CUE, coupling of ubiquitin conjugation to ER degradation domain; UIM, ubiquitin interacting motif. Several substrate and adaptor names are shown. Right boxes: Reactions catalyzed by Rsp5 and Ubp2. Uncharacterized reactions are shown in orange and italic.

It has been proposed that Rsp5-Ubp2 association provides a mechanism of monoubiquitination based on the capacity of Ubp2 to disassemble Lys^{63} ubiquitin chains synthesized by Rsp5 (Kee et al., 2006) (Figure 52, Boxes A and B). Our data shows that Rsp5 and Ubp2 exert opposed driving forces in the control of mUb-Rpn10 homeostasis *in vivo*, and that Rsp5 is sufficient for the production of mUb-Rpn10. The activity of Rsp5 on a UIM-containing protein, such as Rpn10, suggests evolutionary conservation of this type of substrate recognition by Nedd4 enzymes, since human Nedd4 members monoubiquitinate UIM-containing substrates in mammalian cells (Hoeller and Dikic, 2010). Altogether, suggests

evolutionary conservation of this type of substrate recognition by Nedd4 enzymes, since human Nedd4 members have been shown to monoubiquitinate UIM-containing substrates in mammalian cells (Hoeller and Dikic, 2010). The strong correlation between the presence of a ubiquitin binding domain (e. g., UIM and CUE) in substrate sequences and the absence of polyubiqutin synthesis suggests a mechanistic model of monoubiquitination *vs.* polyubiquitination by Rsp5 and, probably Nedd4 enzymes.

The fact that Rsp5 (Nedd4) Ub-protein ligase is strongly specialized in the reaction of Rpn10 monoubiquitylation, but it is completely unable to catalyze polyubiquitylation of Rpn10, is very interesting since Rsp5 is proficient in catalyzing polyubiquititylation in other proteins substrate under similar *in vitro* reaction conditions (Kim and Huibregtse, 2009; Kim et al., 2011a). Thus, Rpn10 contains the information that drives its monoubiquitylation by Rsp5 (Nedd4). Since Nedd4 enzymes catalyze monoubiquitylation in many non-PPXY substrates *in vivo* (Hoeller et al., 2006), Rpn10 represents an experimental model for a large number of important physiological targets of monoubiquitination. Further investigation will be required for searching the factors that control processivity of Rpn10 ubiquitination. On this regard, the UIM motif contained in the substrate most likely plays an active role in the suppression of polyubiquitin synthesis in reactions catalyzed by Rsp5 and Nedd4.2 (Haglund and Stenmark, 2006; Hoeller et al., 2006; Hoeller and Dikic, 2010).

It has been shown that Ubp2 is highly active towards Rpn10-monoubiquitin isopeptide bonds and exerts a homeostatic control of mUb-Rpn10 (Figure 24B, Figure 25B and Figure 25C). It should be noted that, without mUb-Rpn10 deubiquitination, one would expect a robust accumulation of conjugated Rpn10. However this is not what we observe (Figure 24B, lanes 3 and 7; Figure 37F and G), leading us to hypothesize that other factors are also involved in the control of the ratio of Rpn10/Rpn10-mUb, and that an adaptive response may take place. A progressive increase of mUb-Rpn10 would produce a progressive inactivation of Rpn10, with the consequent induction of stress in the ubiquitin-proteasome pathway. A response counteracting this process could probably engage several machineries. One possibility could be the involvement of additional DUBs to keep the levels of mUb-Rpn10 below the threshold of stress. Other possibilities would be **1.** a decrease of Rsp5 activity to prevent excessive Rpn10-mUb since high levels of conjugated Rpn10 causes strong phenotype (Figure 36B) or **2.** an increase of Rpn10 degradation coupled with an increase of *de novo* synthesis of Rpn10.

Monoubiquitination, As A Mechanism Controlling Substrate-Proteasome Interaction And Proteasome Catalytic Rates

The so-called 'coupled-monoubiquitination' implies that the reaction product establishes an intramolecular interaction between the UIM and the linked monoubiquitin moiety, thus impairing further ubiquitination events and favoring monoubiquitination rather than polyubiquitination (Di Fiore, 2003; Woelk *et al*., 2006). In this work we have shown that the reversible monoubiquitination of proteasome subunit Rpn10/S5a, receptor of polyubiquitinated substrates, is a very powerful level of regulation of proteasome function.

We have reconstituted the reaction of Rpn10 monoubiquitination using recombinant proteins and observed that monoubiquitination can be efficiently catalyzed with either wild-type or methylated

ubiquitin, showing a pattern of multi-monoubiquitination (Figure 28A and B). MS analysis confirmed modification at four distinct lysine residues: preferentially to Lys^{84}, placed within the VWA domain, and to Lys^{268}, in the C-terminus of the sequence, and secondarily to Lys^{71} and Lys^{99} (Figure 29C). However, multi-monoubiquitination does not show an even distribution in Rpn10: major modification takes place at Lys^{84}, and secondarily al Lys^{268}. This was confirmed by mutation analysis and by quantitative proteomics (Figure 30, Figure 42, Figure 43, Figure 44 and 45).

It was previously shown that Rpn10 UIM domain binds the hydrophobic surface on ubiquitin defined by Leu^{8}, Ile^{44} and Val^{70} (Wang et al., 2005). This interaction is essential for the monoubiquitination reaction, since mutations at Rpn10 UIM or at ubiquitin I44 abrogate catalysis (Figure 27 and Figure 34B, respectively). We speculated about the possibility that the failure to obtain monoubiquitination with Ub^{I44A} *in vitro* was because the mutation prevented efficient charging of the Rsp5 ligase. However, we rejected such a possibility since Woelk et al. reported the capacity of Nedd4 to be loaded with Ub^{I44A} indicating that the mutation did not prevent efficient charging of Rsp5 ligase (Woelk et al., 2006).

Our data supports that Rpn10 and mUb-Rpn10 are two functionally distinct molecules: mUb-Rpn10 has lost the capacity exhibited by unmodified Rpn10 to bind ubiquitin conjugates (Figure 32B and Figure 33B) or unanchored polyubiquitin chains (Figure 34A), and also UBL-Dsk2 (Figure 41). This impairment is due to a UIM-ubiquitin interaction *in cis*, because the RPN10-Ub^{I44A} mutant recovers Rpn10 wild-type capacity to bind polyubiquitin. In addition, Rpn10 linked to monoubiquitin imposes a dramatic inhibition of cyclin B degradation, but simply restoring the UIM availability with the Rpn10-Ub^{I44A} mutant results in a strong rescue of Rpn10 function (Figure 35B). Therefore, Rpn10 monoubiquitination prevents binding *in trans* of degradative ligands, such as ubiquitinated cyclin B, and downregulates proteasomal protein degradation.

Is this inhibitory mechanism of proteasome activity essential for cell viability? We have tested the physiological relevance of mUb-Rpn10 by performing complementation tests with strains carrying the double gene deletion RPN10 and RAD23. We have observed that the growth defect of *rad23*Δ*rpn10*Δ (Chen and Madura, 2002) cannot be rescued by the Rpn10-Ub chimera, albeit the wild-type Rpn10 completely rescues this defect and, once more, mutant Rpn10-Ub^{I44A} partially recovers the yeast double mutant phenotype (Figure 36B). These assays suggest that a permanent form of Rpn10 monoubiquitination has a strong effect in cell proliferation. Therefore, monoubiquitination of Rpn10, by impairing the productive interaction of Rpn10 with substrates and inhibiting the proteasome, strongly decreases cell proliferation.

It is noteworthy to mention that although the C-terminal fusion is not equivalent to the modification of internal lysine, in functional assays, we have proved that the ubiquitin fusion behaves identically than monoubiquitinated Rpn10 through Lys^{84}, demonstrating that Rpn10-Ub chimeras are valuable tools for studying the functional implication of Rpn10 postsynthetic modification. Additionally, two advantages emerged of using chimeras: **1.** Rpn10-Ub represents a 100% modified form of Rpn10 and, **2.** Rpn10-Ub is stable during the course of the experiment, since it is not deubiquitinated, which is crucial for the binding experiments.

Interestingly, mUb-Rpn10 is dramatically decreased in cultures grown at low and high temperatures, and in the presence of cadmium (Figure 37A, B, C, F and G). Apparently levels of unmodified Rpn10 are not affected under proteolytic stress. According to our results, suppression of Rpn10 monoubiquitination would increase the availability of Rpn10 UIM, promoting activation of this ubiquitin receptor. Rpn10 is essential for the degradation of damaged newly synthesized proteins, which are strongly increased at low and high temperatures and in the presence of cadmium (Medicherla and Goldberg, 2008). In this scenario, Rpn10 function requires an active UIM (Elsasser et al., 2004; Verma et al., 2004). We have observed that proteasomal Rpn10 monoubiquitination is dramatically decreased in these conditions, suggesting a mechanism to increase the availability of Rpn10 UIM.

With these observations, it could be predicted that when mUb-Rpn10 levels are increased in the cell, protein targeting and degradation to the proteasome would be decreased. Cells carrying a deletion of the UBP2 gene show substantial stabilization of proteasomal mUb-Rpn10 (Figure 24B and Figure 25C), and consistently, these cells accumulate Lys^{48} ubiquitin linkages, as established in a recent study (Xu et al., 2009). This result would not be expected considering only the activity of Ubp2 on Lys^{63} ubiquitin chains (Kee et al., 2006). However, the accumulation of Lys^{48} chains fits in our model of attenuated proteasomal activity when mUb-Rpn10 levels are increased due to deletion of UBP2. The relative low abundance mUb-Rpn10 in growing cultures at standard conditions could be explained by the importance of the homeostasis of proteasome activity in the cell, yet high levels of Rpn10-Ub cause a strong phenotype (Figure 36B).

Overall, the mechanistic regulation and physiological relevance of Rpn10 monoubiquitination can be graphed as follows:

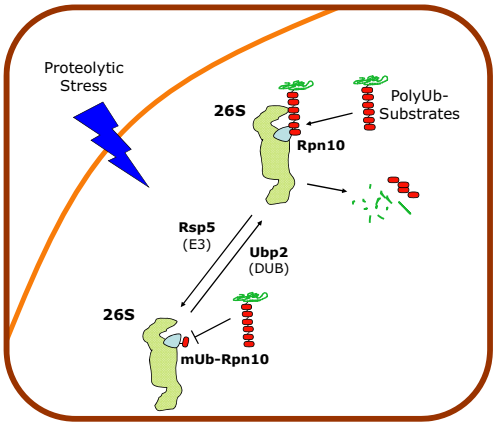

Figure 53: Graphical Abstract Of The Mechanistic Regulation And Physiological Relevance Of Rpn10 Mono-ubiquitination.

The reversal monoubiquitination of Rpn10 is an inhibitory mechanism of proteasome activity. Ubiquitination of Rpn10 inhibits its ability to bind polyubiquitinated substrates, thus regulating proteasome function and cellular protein homeostasis. Notably, down regulation of monoubiquitination is coincident with know declines in proteasome activity in response to various stress conditions.

Regulation Of The Proteasome By Associated Ubiquitin Conjugating And Deconjugating Activities

The Ub ligases that target proteins for degradation have been recognized as the primary nodes of specificity. Ubiquitin-specific proteases that disassemble Lys^{48}-linked degradation signals provide an important second level of kinetic specificity defining steady-state levels and thus, rates of degradation for ubiquitin conjugates delivered to the proteasome. The proteasome has been assumed to play a passive role in these pathways; however we have reported that regulation of the proteasome by Rpn10/S5a monoubiquitination is equally dynamic in defining long-term degradative flux in cells.

Rsp5-dependent ubiquitination of Rpn10, by impairing substrate binding, constitutes an efficient control of proteasome activity, effect that mimics the inhibition of the proteasome by Bortezomib and Carfilzomib, used as anticancer drugs. In absence of monoubiquitination, substrate recognition by Rpn10 would promote the engagement of proteasomal ubiquitin hydrolases, such as Ubp6/Usp14 or Rpn11, and chain elongating factor Hul5 (Yao and Cohen, 2002; Verma et al., 2004; Crosas, et al., 2006; Hanna et al., 2006), which define a second level of proteasome regulation. Thus, two evolutionarily conserved ubiquitin ligases, Hul5/KIAA10 and Rsp5/Nedd4.2, and their related deubiquitinating enzymes, Ubp6/Usp14 and Ubp2, respectively, regulate early steps of proteasomal mediated degradation, underscoring the relevance of associated enzymatic factors in proteasome function. This is a crucial point because the balance between mono and polyubiquitination is an emerging mechanism in cellular biology. There are very few examples of proteins regulated by this balance: p53 (Brooks and Gu, 2004), Foxo (van der Horst et al., 2006) and Pten (Trotman et al., 2007), all three tumor suppressors, suggesting that the control of proteasome activity by Rpn10 ubiquitination could represent a novel molecular model of tumor suppression.

We also note that human Nedd4.2 is downregulated in response to type 1 interferon by modification with the interferon-stimulated ISG15 ubiquitin-like protein (Malakhova and Zhang, 2008; Okumura et al., 2008). Our results predict that the enhanced degradative capacity associated with elevated levels of active Rpn10 would enhance antigen presentation during the early innate immune response of the cytokine.

A proteomics study of sumoylated proteins in human cells has detected Rpn5, a proteasome subunit of the RP, among them (Matic et al., 2010). Although that proteasome regulation by sumo signaling is completely unknown and uncharacterized, these results lead us to hypothesize whether postranslational modifications, such as monoubiquitination or sumoylation, can be an extended mechanism of proteasome pathway regulation. Currently, several examples of ubiquitin binding proteins showing monoubiquitination exist, but none of them is involved in proteasome regulation, with the exception of Rpn10. To characterize whether ubiquitin binding proteins with a role in proteasome dependent degradation, such as Rpn13 and Rad23, are also regulated by monoubiquitination, would provide us with a better understanding of proteasome regulation and its implications in physiology and molecular pathology.

Additionally, it has been published that p54, the Drosophila ortholog of Rpn10, is modified by up to four

ubiquitin groups in vivo (Lipinszki et al., 2009), resembling multiple monoubiquitination of yeast Rpn10. S5a, the human ortholog of Rpn10, also shows monoubiquitination (Danielsen et al., 2011), showing that Rpn10 monoubiquitination is conserved in higher eukaryotes. We have demonstrated that Rpn10 monoubiquitination has an antiproliferative effect, thus to examine the role of p54/S5a monoubiquitination in higher eukaryotes could represent a novel checkpoint for proliferative states or a mechanism of tumor suppression.

Monoubiquitinated Rpn10 Is Also Found In The Cytosolic Free Pool

In the present work we have shown that monoubiquitination of Rpn10 occurs at both proteasome-assembled and extraproteasomal pools (Figure 23A), which is in sharp contrast with data reported for wild-type animals. For instance, p54 protein is extensively multiubiquitinated in the cytosolic free pools, whereas only very modest modification occurs on the proteasome-bound form (Lipinszki et al., 2012).

One of the functions proposed for extraproteasomal Rpn10 is the restriction of Dsk2 access to the proteasome (Matiuhin et al., 2008) by the interaction of Rpn10-UIM and the UBL domain of Dsk2 (Zhang et al., 2009a). To study the functional impact of Rpn10 ubiquitination in a non-proteasomal context we have challenged the interaction of mUb-Rpn10 with the UBL domain of polyubiquitin receptors Dsk2. *In vitro* binding assays illustrate that the non-ubiquitinated Rpn10 bonds efficiently to recombinant 6His-Dsk2 but conjugated forms were unable to interact, indicating that ubiquitination of extraproteasomal Rpn10 drastically reduces or abolishes its affinity for the UBL domain of the extraproteasomal polyubiquitin receptors (Figure 41). Although Rpn10 UIM prefers the UBL of Dsk2 to monoubiquitin (Zhang et al., 2009a), these results show that the intramolecular Rpn10 UIM-Ub interaction prevents the intermolecular binding between Dsk2 UBL and Rpn10 UIM. This is in agreement with the data presented by Matiuhin et al. (2008) and suggests that the specific modification of Rpn10 in its extraproteasomal state participates as a shuttling factor enhancing delivery of Dsk2-dependent substrates to the proteasome. Although further *in vivo* analyses are needed to have conclusive results, we speculate that mUb-Rpn10 could couple inactivation of proteasomal Rpn10 with the enhancing of the Dsk2 pathway.

To this end several approximations can be performed in the near future: **1.** to check whether an increase of free Rpn10-mUb is detected in *dsk2Δ* strains, **2.** co-localization studies of Dsk2 to the proteasome when overexpressing Rpn10-mUb or **3.** to check the *in vivo* interaction between free UIM Rpn10 and UBL Dsk2. Ideally, single VWA domain mutations would avoid Rpn10 assembly to the RP and enrich the cytosolic pool but, eventhough the region has been mapped by Fu and colleagues (Fu et al., 1998), it has not yet been reported which exact residues of Rpn10 are responsible for its interaction with the RP.

Recently, Lipinszki et al. have reported that the most significant functional consequence of p54 ubiquitination in *Drosophila* is its inability to interact with the UBL domain of Dsk2 and Rad23. This is caused by an intramolecular interaction between the conjugated ubiquitin and the p54's UIM (Lipinszki et al., 2012), which is in agreement with the 'folding-back' model proposed in the present work.

Rpn10 Ubiquitination Differs Among Higher Eukaryotes

Our observations suggest that only the proteasomal peak of Rpn10 required a completely active UIM upon proteolytic stress, whereas that the non-associated proteasomal mUb-Rpn10 would be virtually not affected. These differences could have important functional implications and two likely hypotheses have been formulated to explore the bases of it: **1.** Rsp5 is more active in the extraproteasomal pool, **2.** Ubp2 is more active in the proteasomal context. *In vitro* assays have shown that Ubp2 is much more efficient on proteasomal than on monomeric mUb-Rpn10 (Figure 40) suggesting distinct prevalences of mUb-Rpn10 in different cellular contexts.

An evolutionary conserved feature of Rpn10 sequence, in addition to the well studied VWA domain and UIMs, is the presence of C-terminal lysines (a cluster in metazoans, a single residue in yeast) (Figure 54A). Interestingly, all studied forms of Rpn10 orthologues have shown monoubiquitination of terminal lysine residues (Danielsen et al., 2011; Lipinszki et al., 2012) (Figure 54A). Although our genetic results have illustrated that Lys^{84} is the main modified residue in Rpn10 sequence, the MS data has clearly detected Lys^{268}-diGlycine peptides (Figure 29). These observations, together with the distinct processivity of Rpn10 (Figure 38 and Figure 40), have led us to consider the functional role of Lys^{268} according Rpn10 cellular context. With that purpose, we have checked the putative effect of Lys^{84} monoubiquitination, not only on UIM, but also on the VWA domain, involved in protein degradation in a UIM-independent manner (Verma *et al.*, 2004). In addition, an integrative approach has shown that the N-terminal VWA domain of Rpn10 interacts with Rpn9 and Rpn8/Rpn11 heterodimer, so stabilizing the RP of the proteasome rather than controlling the base-lid interaction (Lasker et al., 2012). The fact that Lys^{84} is located within the VWA domain suggested that this domain could be affected by Lys^{84} monoubiquitination and that the modifications at Lys^{268} and at Lys^{84} could inhibit protein degradation with different efficiency (Figure 54B).

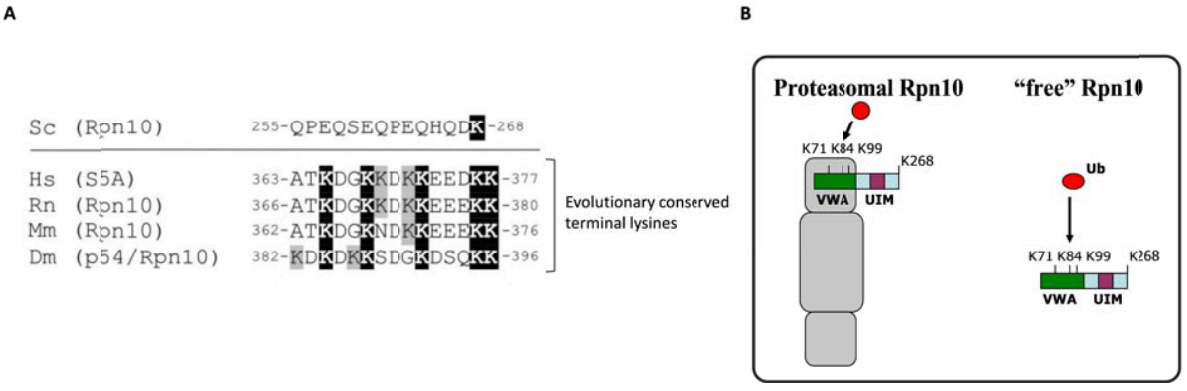

Figure 54: Characterization Of Residue-Specific Monoubiquitination of Rpn10.
(**A**) Sequence alignment of the C-terminal lysine cluster of different metazoans (human, Hs; rat, Rn; mouse, Mm; Drosophila, Dm). As a comparison, the C-terminus of the yeast (Sc) Rpn10. Adapted from Lipinszki et al., 2012. (**B**) Graphical model showing Lys^{84} as the main target of Rsp5, regardless of whether Rpn10 cellular context.

This hypothesis has been evaluated by means of a mass spectrometry method of absolute quantification

based on peptides labeled with heavy isotopes (AQUA). The quantitative proteomics analyses of *in vitro* and *in vivo* pools of Rpn10 reveal that Lys^{84} is the main target of Rsp5 ligase, regardless of Rpn10 cellular localization (Figure 54B). Therefore, Rpn10 ubiquitination differs among eukaryotes: VWA-located lysine in yeast (Figure 42, Figure 43, Figure 44, and 45) and C-terminal lysine in metazoans (Danielsen et al., 2011; Lipinszki et al., 2012). It is noteworthy to mention that we have found some difficulties in setting up the method for a rigorous quantification of modified Lys^{268}-GG. In an ideal AQUA experiment, the amount of internal standard added to a biological sample must be similar than the native peptide to obtain peak ratios around 1 (similar areas of both heavy and light peptides) and provide an accurate quantification of the protein of interest. However, Rpn10 ubiquitination is a relatively low abundant posttranslational modification, and the amount of internal standard is higher than native peptide (specifically, 2-fold more abundant in Lys^{84}-GG peptide and 50-fold in Lys^{268}-GG). As a consequence, the values obtained for Lys^{268}-GG quantification may be underestimated since the Light/Heavy peak ratio is too low. Since AQUA peptides are sequenced according specific tryptic fragments, Lys^{268}-GG internal standard has always been difficult to identify by MS. Its sequence contains 11 glutamines, being very sensitive to several deamidation reactions (an amide functional group is removed from an organic compound). This has led to a range of different monoisotopic masses that are difficult, if not impossible, to detect by proteomic methods.

Functional Analysis Of Proteins Showing Increased Ubiquitination Upon Cold-Shock In Cells Lacking RAD23 And RPN10

It is assumed in the field that physiological stresses that cause an increase of damaged and misfolded proteins require high demands of proteasomal activity. Thus, the context of these types of physiological stresses is appropriate to observe phenotypes generated by mutations of genes involved in efficient proteasome activity. Rpn10 and Rad23 are two proteasome substrate receptors showing complementary and also partially redundant functions in the proteasome: single mutations of these two genes show mild phenotypes, but double mutants show severe phenotypes. Interestingly, the double rad23-rpn10 mutants show no morphologic phenotype at permissive temperatures, but a strong sensitivity at low ones (Lambertson et al., 1999).

Independent bioinformatic analyses have been carried out with data obtained at both growth conditions. We have then compared those sites that were equally identified and quantified. Molecular biology tools are required to perform additional experiments to identify which substrates exclusively depend on the proteasomal receptor Rpn10 for targeting and degradation. In fact, the possible Rpn10-dependent candidate substrates that we may have identified in the present study would not rely exclusively on Rpn10 delivery to the proteasome, since it is more likely that substrates that use Rpn10 can also use other receptor pathways when Rpn10 is absent (Mayor et al., 2007)(Mayor et al., 2007). Working with the *rad23*Δ*rpn10*Δ double mutant, we minimize the redundancy of cellular ubiquitin receptors.

Most of the proteins that were significantly enriched after a decrease in temperature account for genes involved in metabolic (22.6%) or transport functions (27.5%) (Figure 51B). Other proteins not included in these two groups are, for example, histone H2B (Htb2), actin (Act1), endocytic ubiquitin-binding protein

Ede1, 14-3-3 protein (Bmh1), Golgi related proteins (Cpt1, Pmr1 and Aim44), ergosterol synthesis enzyme Erg11, nucleolar protein Nop1, Cullin 3 (Cul3) and Rsp5 cofactors Bul1 and Ssh4 (Figure 51A). These observations could indicate, on one hand, the need of a physiological remodeling of cell capabilities during cold-shock response and, on the other, membrane proteins that would be normally degraded in a vacuolar-dependent fashion, after a cold-shock stress, an RPN10-dependent proteasomal degradation would be highly induced. Next, we discuss some of the proteins that have mostly claimed our attention.

Ubiquitination of histones is extensively described in the literature, and indeed, H2A monoubiquitination is one of the first ubiquitin based modifications described (Goldknopf and Busch, 1977). Ubiquitination of histones has been shown to be involved in the regulation of the transcriptional status of chromatin. H2B ubiquitination at Lys^{123} participates in multiple processes, including gene activation and silencing, and H3 methylation (Sun and Allis, 2002). The machinery involved in controlling H2B monoubiquitination comprises at least Rad6 (E2), Bre1 (E3) and DUBs Ubp8 (which is part of the SAGA complex) and Ubp10. Interestingly, Tansey and collaborators described that H2B can be polyubiquitinated *in vivo*, at Lys^{123} and at Lys^{111} and that such polyubiquitination could be involved in its downregulation (Geng and Tansey, 2008). In that study, it was shown that the enzymatic factors involved in H2B polyubiquitination is distinct from the machinery that controls canonical monoubiquitination. In our analysis, we have detected both Lys^{123} and at Lys^{111} ubiquitination (Table 12, see Appendix). Lys^{123} modification was found in both PT and 16ºC cultures, with a 2.8-fold increase in *rad23*Δ*rpn10*Δ cells at 16ºC (Table 14, see Appendix). Remarkably, Lys^{111} only showed up in cold-shocked cells with a high number of spectral counts and a 9-fold increase in the double mutant cells (Table 12, see Appendix). This change in the pattern of ubiquitination, which involves differential activities of Ubp8 and Ubp10, and possibly, a ubiquitin conjugating system different than the Rad6-Bre1 one (Geng and Tansey, 2008), exemplifies very well the hypothesis of the UPS reprogramming that we suggest.

Another striking set of results include proteins integral to membrane. The levels of plasma membrane proteins involved in the transport of molecules to the interior of the cell is tightly controlled by signaling pathways that act in response to environmental conditions. The molecular events that control the fate of cargo proteins (endocytosis, sorting to the endosome, recycling to the membrane) are regulated by ubiquitination (Macgurn et al., 2012). It is generally observed that the ubiquitin ligase Rsp5 is involved in the modification of lots of plasma membrane proteins and that Rsp5 activity is required for their targeting for vacuolar degradation (Macgurn et al., 2012). Plasma membrane proteins such as Can1 and Mup1 are endocytosed upon Rsp5-dependent ubiquitination mediated by arrestin-related (ART) adaptors (Lin et al., 2008). As shown by Lin and collaborators, the N-terminal cytosolic domain is essential for this process and confers specificity to the ART adaptors. Interestingly, our study has identified ubiquitination at the N-terminal domain of 18 of 23 plasma proteins (Figure 55). Ubiquitination at C-terminal or intermediate domains was found mainly in proteins with no cytosolic N-terminal domains (such as Ctr1) or proteins with large cytosolic intermediate domains (such as Pma1 and Pmr1) (Figure 55). These results suggest that a massive internalization signaling is enhanced during response to low temparatures. The fact that these proteins all show increased ubiquitination in cells

lacking Rpn10 and Rad23 would suggest that the fate of these signaling pathway is the proteasome. This is unexpected because the canonical pathway for degradation of these proteins is the vacuole. We hypothesize that in a cold-shock response, the decrease in the functionality of plasma membrane impairs the proper sorting of plasma membrane proteins to the vacuole. In this scenario, a transfer of substrates from the vacuolar system to the proteasome would ensure proper degradation of this group of proteins. Our data also shows that Erg11 ubiquitination is highly increased (12-fold) at 16ºC in the *rad23*Δ*rpn10*Δ mutant. Erg11 encodes for lanosterol 14a-demethylase, a key enzyme in ergosterol biosynthesis, the yeast functional equivalent of cholesterol in mammalian cells. Downregulation of Erg11 would decrease the synthesis of ergosterol, which has a severe effect in the sorting plasma membrane proteins, such as the tryptophan permease Tat2 (Daicho et al., 2007). Thus, a deficient synthesis of ergosterol, induced by a hypothetical degradation of Erg11, would enhance the cellular membrane loss-of-function phenotype observed at low temperatures.

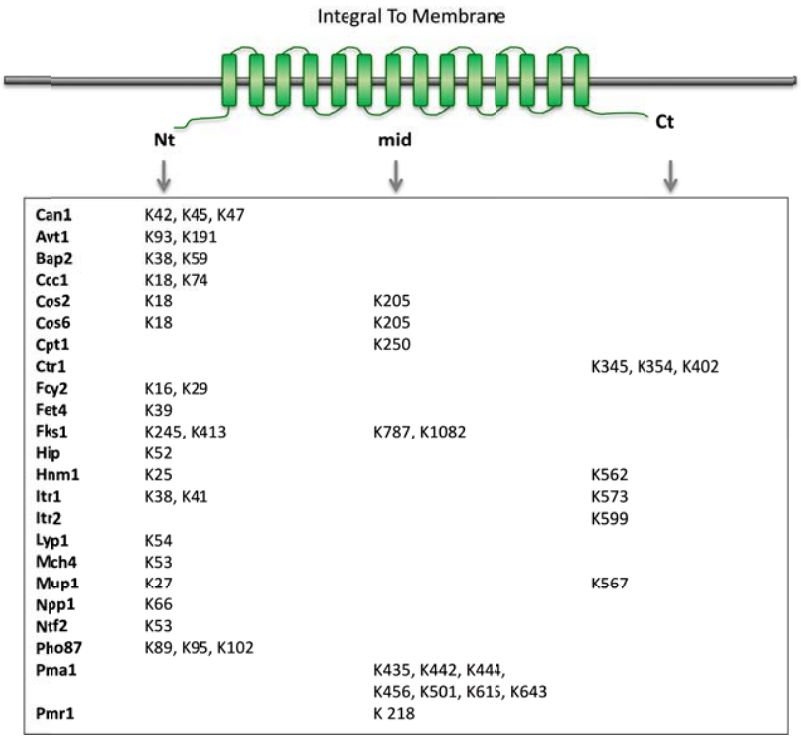

Can1	K42, K45, K47		
Avt1	K93, K191		
Bap2	K38, K59		
Ccc1	K18, K74		
Cos2	K18	K205	
Cos6	K18	K205	
Cpt1		K250	
Ctr1			K345, K354, K402
Fcy2	K16, K29		
Fet4	K39		
Fks1	K245, K413	K787, K1082	
Hip	K52		
Hnm1	K25		K562
Itr1	K38, K41		K573
Itr2			K599
Lyp1	K54		
Mch4	K53		
Mup1	K27		K567
Npp1	K66		
Ntf2	K53		
Pho87	K89, K95, K102		
Pma1		K435, K442, K444, K456, K501, K615, K643	
Pmr1		K 218	

Figure 55: Modified Sites Of The Integral To Membrane Proteins Upregulated At 16ºC.
Ubiquitinated sites of integral to membrane proteins that are enriched after temperature decrease. The 75% are modified at their N-terminal domain.

Additional hits in our analysis are worth to mention. Ubiquitinated Lys^{184} of Ack1, an uncharacterized SEL-1 domain-containing protein that acts upstream in the Pkc1 pathway, involved in cell wall integrity (Krause et al., 2008)(Krause et al., 2008), showed an increase of 25-fold in absolute spectral counts from PT to 16C (from 7 to 197 spectral counts) (Table 14, see Appendix). This is a dramatic increase that suggests that this protein is intensively ubiquitinated in a cold-shock response. Moreover, the increase

of 5-fold in *rad23*Δ*rpn10*Δ strain at 16ºC would suggest that this ubiquitination process targets Ack1 to the proteasome. Similarly, Lys^{529} of asparagine synthase 2 (Asn2) showed a 50-fold increase in spectral counts at 16ºC, and a 3-fold increase in the double mutant. Finally, Bul1 and Ssh4 proteins, adaptors of Rsp5 ubiquitin-ligase, and Cul3, were also found to be increased in ubiquitination at 16ºC in *rad23*Δ*rpn10*Δ mutant (Table 14, see Appendix).

Altogether, these data suggest that proteasome targeted degradation, more specifically, degradation dependent on the receptors rad23 and Rpn10, plays a key role in the response to cold-shock. We have obtained a comprehensive list of ubiquitinated peptides and proteins (Table 10,Table 11, Table 12 and Table 13, see Appendix), providing us with some clues to suggest a novel cold-shock response in yeast. The filtering criteria used in the selection of the counted and quantified spectra was extremely high (see *Identification And Quantification Of Ubiquitinated Substrates By Polyubiquitin Enrichment Strategies And Mass Spectrometry* section, Materials and Methods), ensuring that the ratios reported for each individual site truly reflect the fold change for peptides observed strictly in the presence of that single PTM.

The data suggest a dramatic remodeling of ubiquitination sites, probably coupled to a reprogramming of ubiquitin-dependent signaling machinery, affecting proteins involved in metabolic pathways, plasma membrane biology, chromatin regulation, mitochondrion functions, and others (Figure 51B). One of the consequences of this reprogramming would be a massive transfer of protein substrates from the vacuolar degradation system to the proteasome. Further research will be required to validate this hypothesis. By an unknown mechanism, a set of E3 ligases, maybe including Rsp5, would modify their activity to force proteins typically targeted to the vacuole to be detoured to the 26S. We hypothesize that additional factors would be required for such a profound cellular resetting. On this regard, we propose that the Cdc48 ATPase, involved in the extraction of plasma membrane proteins in the ERAD pathway, would be involved in this important functional adaptation of the cell in a cold-shock situation. In favor of this notion, Cdc48 mutants show cold sensitivity (Moir et al., 1982).

Conclusions

The aim of the present work project has been the characterization of Rpn10 monoubiquitination as a novel mechanism of proteasome regulation, using *S. cerevisiae* as a reference model. The main conclusions are as follows:

1. Rpn10 is monoubiquitinated *in vivo*. The modified form is found in both proteasomal and non-proteasomal cellular contexts.
2. Levels of Rpn10-mUb are regulated *in vivo* by Rps5, a NEDD4 ubiquitin-ligase, and Ubp2, a deubiquitinating enzyme, linking for first time Nedd4 enzymatic family with proteasome regulation.
3. We have established the direct involvement of Rsp5 in the catalysis of Rpn10 monoubiquitination by reconstituting the enzymatic reaction *in vitro*.
4. The UIM of Rpn10 is necessary for its monoubiquitination. In proteasomes containing mutations in UIM Rpn10, the monoubiquitinated form of Rpn10 drastically diminishes.
5. By means of genetic and proteomics tools we found that four sites of Rpn10 sequence are subjected to monoubiquitination by Rsp5 (Lys^{71}, Lys^{84}, Lys^{99} and Lys^{268}), but Lys^{84} within its VWA domain is the preferred one. Importantly, Rpn10 mutants that show impaired monoubiquitination, are not able to rescue Rpn10 function to WT levels, providing genetic evidence that links proteasome function with monoubiquitination of a protein.
6. *In vitro* binding assays revealed that monoubiquitination strongly inhibits the capacity of Rpn10 to bind ubiquitin conjugates (whole cell conjugates, ubiquitinated cyclin B and free ubiquitin chains) by a specific interaction *in cis* between Rpn10 UIM domain and the linked monoubiquitin.
7. Monoubiquitination of Rpn10 reduces the proteolytic activity of the proteasome, as shown by cyclib B degradation assays. Rpn10-Ub^{I44A} mutant partially restores the proteasomal activity, showing that the non-covalent ubiquitin-UIM interaction is involved in the inhibition of the UIM.
8. Notably, only the proteasomal pool of Rpn10-mUb is suppressed under perturbations that promote the proteolytic pathway, such as stress by temperature and oxidative stress; whereas other kind of stresses (DNA damage or osmostress) do not affect it.
9. We evaluated the affinity of several forms of Rpn10-mUb to Dsk2 and found that Ub-UIM interaction of Rpn10 impairs the binding of Ubl-Dsk2 domain to Rpn10, suggesting that the free pool of Rpn10-mUb may regulate Dsk2-dependent delivery of polyubiquitinated substrates to the proteasome.
10. By means of protein absolute quantification and biochemical assays it has been found that Lys^{84} is the main target of Rsp5 ligase in both proteasomal and extra-proteasomal pools of Rpn10, enhancing the role of the VWA domain in Rpn10 ubiquitination.
11. Upon cold-shock, cells lacking the proteasome substrate receptors Rad23 and Rpn10 show a remodeling of ubiquitination sites that result in an increase in the ubiquitination of a set of proteins. This group of proteins, which could be preliminarily considered proteasome substrate candidates, includes mainly metabolic enzymes and plasma membrane proteins, and certain nuclear and mitochondrial proteins.

Materials And Methods

Yeast Methods

Tetrad dissection and strain transformation were performed following standard techniques (Rose, 1990). YPD medium consisted of 1% yeast extract, 2% Bacto-Peptone, and 2% dextrose. Synthetic media consisted of 0.7% Yeast Nitrogen Base supplemented with amino acids, adenine and uracil as described (Rose, 1990), 2% dextrose (SDC) or, if necessary, 1% galactose and 1% raffinose (SGRC). For plasmid selection, synthetic media lacking leucine or uracil, or both were prepared. To remove plasmid carrying URA3 marker, 5-fluoroorotic acid (5-FOA) 0.1% w/v final was used. Images of colony spot assays were taken in the Image Service of CRAG (CID-CSIC).

Analysis Of Endogenous Rpn10

Yeast wild-type strain was grown under normal conditions and, starting at an OD_{600} of 0.5, an equivalent number of cells were taken at the indicated time points (Figure 18A and B). Cells were harvested and resuspended with buffer composed of 50 mM Tris-HCl (pH 7.8), 1 mM EDTA and 1x concentration of protease complete inhibitor cocktail (-EDTA, Roche). Cells were lysated by means of ultrasounds and by vortexing with glass beads. Supernatant was resolved by SDS-PAGE and analyzed by immunoblot against Rpn10. Fractions UR8 were obtained following the method described in Crosas *et al*., 2006. Bulk ubiquitin conjugating and deconjugating activities of UR8 fractions are shown in Figure 20.

For stress sensitivity assays (Figure 37), wild-type and *ubp2*Δ cells were cultured under normal growth conditions to an OD_{600} of 0.8-1, then cells were exposed to different stresses: cold (14ºC) and heat (37ºC) shock, oxidative stress ($CdSO_4$, final concentration of 200 μM), osmotic stress (NaCl, final concentration of 500 mM) and DNA damage stress (EMS, final concentration of 0.08%). Samples taken from growing cultures at the indicated time points were normalized by optical density at 600 nm using an Ultrospec 2000 spectrophotometer (GE Healthcare). Cells were harvested, resuspended, lysed and analyzed by Rpn10 western blotting.

Size Exclusion Chromatography

WT (Figure 23A, Figure 38), *ubp2*Δ and *ubp6Δ* strains (Figure 25C) were cultured (2L) and cells were harvested, resuspended in a 2-fold volume of 50 mM Tris-HCl pH 7.4, 1 mM EDTA, 150 mM NaCl buffer and lysed using a cell disrupter (Constant Cell Disruptor Systems). Lysate was centrifuged at 12,000xg in cold for 30 min. The supernatant was recovered and centrifugation was repeated three times. Final lysate was filtered through a 0.45 μm filter before applying it to a Superose 6 gel filtration chromatography (GE Healthcare). The eluted fractions were 10-fold concentrated by means of Microcon YM-30 (Millipore), and analyzed by western blotting against specific antibodies.

Purification Of Proteasomes

Proteasomes were purified from yeast strains carrying Rpn11-TEV-ProA tag (Leggett et al., 2002). Cells were harvested, resuspended in a 2-fold volume of 50 mM Tris-HCl (pH 8.0), 1 mM EDTA buffer, and lysed in a cell disrupter (Constant Cell Disruptor Systems). Lysate was clarified at 15,000x*g* for 25 min,

incubated with IgG resin (GE Healthcare) for 1 hr at 4°C, and the resin washed with 100 bed volumes 50 mM Tris-HCl (pH 8.0), 1 mM EDTA, 100 mM NaCl buffer. Proteasomes were eluted by equilibrating the IgG resin with 50 mM Tris-HCl (pH 8.0), 1 mM EDTA, 1 mM DTT buffer, then incubating with 1.5 volumes of the same buffer containing 100 U/ml of 6His-TEV protease at 30°C for 1 hr. TEV protease was subsequently removed from the eluate by incubation with Ni-NTA resin (Qiagen) at 4°C for 15 min. If necessary, proteasome activity was checked by the recognition of LLVY substrate (Figure 32A). The assay is based on detection of the fluorophore 7-Amino-4-methylcoumarin (AMC) after cleavage from the labeled substrate LLVY-AMC. Absorption=351nm. Emission=430nm. The free AMC fluorescence can be quantified using a 380/460 nm filter set in a fluorometer (20S Proteasome Activity Assay, Millipore). Store proteasomes at -80ºC.

Expression And Purification Of GST-Fusion Proteins In *E.coli*

In *E.coli*, glutathione S-transferase fusion vectors (pGEX-4T-3) were used to express and purify the following proteins: Rpn10, Rpn10^{K84only}, Rpn10^{K268only} Rpn10-Ub, Rpn10-Ub^{I44A}, Rsp5, Ubc4, Ubp2, Rup1-Ubp2, Ubp6, Ub and Ub^{I44A}. Ubp6^{C118A} was kindly provided by John Hanna (Finley´s lab, HMS). Bacterial cultures (2L) were grown to an OD_{600} of 0.7, induced with 500 μM isopropylthiogalactoside (IPTG) for 15 h at room temperature, resuspended with 2 volumes of 50 mM Tris-HCl pH 7.4, 1 mM EDTA, 1x concentration of protease complete inhibitor cocktail EDTA free (GE Healthcare) buffer and lysed using a cell disrupter (Constant Cell Disruptor Systems). The supernatant was mixed with Glutathione (GSH) Sepharose 4B beads at a ratio of 1 mL of 50% beads slurry to 1 L of initial culture size. The mixture was incubated at 4ºC rolling for 1 h. Beads were washed with 50 bed volumes of the previous lysis buffer supplemented with 150 mM NaCl. Proteins were eluted either with SDS loading buffer or with a reduced glutathione buffer of 50 mM Tris-HCl pH 7.4, 1 mM EDTA and 30 mM reduced glutathione. When necessary (Figure 34A and B, Figure 35B and C), GST-fused proteins were digested with biotinylated thrombin (Novagen) (1U enzyme for 10 μg target). Reactions were incubated at room temperature for 2, 4 or 8 hours. The efficiency of cleavage was determined by SDS-PAGE analysis. Thrombin was removed by benzamidine beads (Amersham Biosciences) according to the manufacturer's instructions.

Assays Of Rpn10 Ubiquitination And Deubiquitination *In Vitro*

Reactions contained 400 nM of GST-Rpn10, GST-Rpn10^{K84only}, GST-Rpn10^{K268only}, Rpn10-WT, Rpn10^{K84R}, Rpn10^{K268R} and Rpn10^{K84,268R}, 100 nM of human activating E1 (Enzo Life Sciences), 400 nM GST-Ubc4, from 400 to 1600 nM GST-Rsp5 and 2 mM ubiquitin. If required, between 100 and 400 nM of purified proteasomes (WT, Rpn10^{UIM}, *rpn10*Δ) were added instead of recombinant protein. Reactions were carried out in 100 mM Tris-HCl pH 7.4, 200 mM NaCl, 10 mM ATP, 10 mM $MgCl_2$, 1 mM DTT buffer at 37ºC for the indicated times. Different types of ubiquitins were used: wild-type, 6His-tagged, biotinylated, methylated ubiquitin (Enzo Life Sciences) or ubiquitin^{I44A}. Reactions were stopped by the addition of SDS-PAGE loading buffer and analyzed by western blotting.

Assays Of Deubiquitinating Activities

For *in vivo* deubiquitinating activities, 22.5 μg of *ubp6Δ* fractions rich in proteasomes and in mUb-Rpn10 were incubated with equimolar amounts of GST-Ubp2 (5.5 μg), GST-Ubp6 (1.8 μg) or GST-Ubp6^{C118A} (1.8 μg), in a buffer containing 100 mM Tris-HCl pH 7.4, 200 mM NaCl and 5 μM MG132. Reactions were

performed at 37ºC and stopped by the addition of SDS-PAGE loading buffer and analyzed by western blotting (Figure 25B). To obtain proteasome fractions rich in mUb-Rpn10, strains SJR125 and SBC10 (carrying the deletion of *UBP6* gene, Table 3, Appendix) were used in a standard Ni-NTA agarose chromatography. The fraction was isolated from the peak of elution of LLVY-AMC activity in an imidazole gradient elution as shown in Figure 25A.

Activity of Ubp2 and Ubp2-Rup1 complex were tested *in vitro* with deubiquitinating assays of proteasomal and recombinant Rpn10-mUb (Figure 40). Modified pools of monoubiquitinated Rpn10 were incubated at 37ºC with recombinant GST-Ubp2 and complexed GST-Rup1-Ubp2 in buffer containing 100 mM Tris-HCl pH 8.8 and 200 mM NaCl. At the indicated times, reactions were stopped by addition of SDS-PAGE buffer and analyzed by Rpn10 western blotting.

Expression And Purification Of GST-Fusion Proteins In *Saccharomyces cerevisiae*

To analyse the involvement of Rsp5 and Ubp2 in Rpn10 monoubiquitination, we used Rsp5 thermosensitive mutant (Rsp5-1), *ubp2*Δ and *rpn10*Δ *ubp2*Δ strains, all of them carrying GST-Rpn10 expressing plasmid (pEGH) (Mitchell et al., 1993). Rsp5-1 was inactivated by a temperature shift to 35ºC for 5 hours; identical cultures were grown at 28ºC to provide a control at permissive temperature (Figure 24B). To characterize the lysines of Rpn10 modified by ubiquitin, GST-Rpn10 and mutants were expressed by means of a pEGH plasmid (Mitchell *et al.*, 1992) using *ubp2*Δ*rpn10*Δ (Figure 30B-D, Lu *et al*., 2008) or *rpn10*Δ strains (Figure 24). In both cases, cells were cultured overnight in SDC-URA to an OD_{600} of 4-5, harvested, washed twice in sterile water, resupended in SGRC-URA and grown. Cells were collected, resuspended with 2 volumes of buffer composed of 50 mM Tris-HCl (pH 7.4), 1 mM EDTA, 5 mM ATP, 5 μM MG132, 1x concentration of protease complete inhibitor cocktail EDTA free (GE Healthcare) and lysated by means of ultrasounds and by vortexing with glass beads. The lysate was mixed with Glutathione (GSH) Sepharose 4B beads at a ratio of 1 mL of 50% beads slurry to 1 L of initial culture size and incubated at 4ºC rolling for 1 h. Beads were washed with 50 bed volumes of the previous lysis buffer supplemented with 150 mM NaCl. Proteins were eluted with SDS loading buffer and analyzed by immunoblot against Rpn10. To genetically characterize Rpn10 modification, GST-Rpn10 mutants were created in pEGH host vectors (Figure 30A and B). For expression and purification we followed the protocol described above.

To check that the levels of plasmid-borne RPN10 were similar to that of endogenous Rpn10, pYES2 vector containing Rpn10 WT, Rpn10-Ub and $Rpn10^{I44A}$ were expressed under galactose induction. After induction, cells were harvested, resuspended, lysed and analyzed by Rpn10 western blotting (Figure 36).

Degradation Assays Of Cyclin B1

Purified proteasomes (25 nM) lacking Rpn10 were incubated 15 min at 30ºC with *E. coli* expressed Rpn10 forms (50 nM each) and buffer containing 50 mM TrisHCl pH 7.4, 1 mM EDTA, 5 mM $MgCl_2$ and 1 mM DTT. Degradation was initiated by adding 5 μL of polyubiquitinated cyclin B1 (stock of 50 μg/mL) and 5 mM ATP. Reactions were stopped at the indicated times by the addition of SDS-PAGE loading buffer and analyzed by western blotting (Figure 35B).

Binding Experiments In GSH Sepharose

Rpn10, Rpn10-Ub and Rpn10-Ub^{I44A} were purified as GST-fusions and used as immobilized phase in the binding assays. Equal amounts of input were incubated with 30 μL of a fraction of cellular ubiquitin conjugates (Figure 33B) or 0.5 μg purified proteasomes *rpn10*Δ (Figure 35C) for 1 h at 4ºC in the presence of binding buffer containing 50 mM Tris-HCl pH 7.4, 1 mM EDTA, 100 μg mL^{-1} BSA, 1x concentration of protease complete inhibitor cocktail EDTA free (GE Healthcare). Beads were washed with 10 volumes of the previous buffer supplemented with 150 mM NaCl. Bound proteins were eluted by boiling 5 min in 2x Laemmli buffer and separated by SDS-PAGE gel for immunoblot against specific antibodies.

Binding Experiments In Ni-NTA Agarose

On one hand, fractions of ubiquitin conjugates were obtained from strain SJR125 or SBC9 (Table 3, see Appendix). Elution was performed by an increasing concentration of imidazole (from 25 mM to 1M). Total protein concentration (mg/mL) and LLVY-AMC activity were assessed for all fractions (Figure 32A). For the binding assay shown in Figure 32 the last fraction was used. Previous to binding assay, conjugate sample was incubated with 5 mM ATP and 5 μM of MG132 for 1 h at 37ºC. Then, conjugates were bound to Ni-NTA agarose beads and equilibrated with buffer containing 50 mM Tris-HCl pH 7.4, 1 mM EDTA and 1x concentration of protease complete inhibitor cocktail EDTA free (GE Healthcare), 100 μg mL^{-1} BSA, 1 μg of ubiquitin aldehyde and 1 μM of phenanthroline. Ubiquitin conjugates were then incubated at 4 ºC with equal amounts of unmodified Rpn10 and mUb-Rpn10 (20 μg). To analyze the status of mUb-Rpn10 during the binding assay, samples were taken every 30 minutes and analyzed by SDS-PAGE and immunoblot against Rpn10 (Figure 32C). After 90 minutes, beads were washed with 50 bed volumes of the previous buffer with 200 mM NaCl and then eluted with SDS-PAGE buffer. Equivalent volumes of eluate were analyzed by SDS-PAGE followed by immunoblot against anti-HIS and anti-Rpn10 antibodies. For Figure 34A, to amplify polyubiquitin, 5 μg of commercial pure ubiquitin chains (Enzo Life Sciences) were incubated 2 hours at 37ºC with 1 μg human activating E1 (Enzo Life Sciences), 2 μg Ubc4, 2.5 μg 6HISxUb (Enzo Life Sciences) and buffer consisting of 100 mM Tris-HCl pH 7.4, 200 mM NaCl, 10 mM ATP, 10 mM $MgCl_2$ and 1 mM DTT. Polyubiquitin chains were bound to Ni-NTA agarose beads and equilibrated with 50 mM Tris-HCl pH 7.4, 1 mM EDTA, 100 μg mL^{-1} BSA, 1 μg of ubiquitin aldehyde and 1 μM of phenanthroline. *In vitro* monoubiquitination reactions of Rpn10 and Rpn10^{k84only} were performed as described above. 10 μg of unmodified Rpn10, mUb-Rpn10, mUb Rpn10^{K84only}, Rpn10-Ub and Rpn10-Ub^{I44A} were used to test the affinity to ubiquitin chains. The binding assay was carried out for 90 minutes at 4ºC. Beads were washed, eluted and analyzed as described for the previous binding assay.

On the other one, binding affinities between several forms of Rpn10 and unanchored 6His-Dsk2 was tested (Figure 41). 6His-Dsk2-containing vector was kindly provided by Sharhri Raasi (University of Konstanz). Dsk2 was bacterially induced and purified following similar protocol as described for GST-fused proteins, but using equilibrated Ni-NTA beads as bait. *In vitro* monoubiquitination reactions of Rpn10, Rpn10^{k84only} and Rpn10^{K268only} were performed as described above and products were used to test the affinity to 6His-Dsk2.

Plasmid Constructions

In Table 4 (see Appendix) are listed all plasmids used in the present study. All single and multiple nucleotide mutations were performed using Quick Change Site Directed Mutagenesis kit (Stratagene). Plasmid pMIC24 was made by removing the STOP codon of pMIC26 by means of PCR amplification using *Rpn10_No TAG Fw* and *Rpn10_No TAG Rev* primers. UBI4 was derived from genomic DNA by PCR using primers *Ubi4 Fw* and *Ubi4 Rev* and cloned into *SalI* and *NotI* sites of pMIC24, generating pMIC27. To mutate isoleucine 44 of the ubiquitin group fused at the C-terminus of Rpn10 we used pMIC27 as a template. The primers used for the PCR reaction were *UbI44A Fw* and its reverse complement. Rpn10 was derived from a cloning vector and then cloned into *HindIII* and *XbaI* sites of pYES2 (Invitrogen), generating plasmid pMIC33. For the ubiquitin fusion at Ct of Rpn10 and the subsequent mutation of isoleucine 44 to alanine (pMIC15 and pMIC39, respectively), we followed the same strategy described for plasmids pMIC27 and pMIC28. pMIC71 was derived from pMIC70 by PCR amplification (primers *R84K-EcoRI Fw* and *R84K-SalI Rev*) and cloned into *EcoRI* and *SalI* cleavage sites. pMIC72 was kindly provided by Dr. I. Dikic and was used as a template to generate pMIC73. Alanine 44 of ubiquitin was mutated to isoleucine by means of a mutagenesis reaction using primers *Ub pGEX Fw* and its reverse complement.

Rpn10 WT and its lysine to arginine mutants are all cloned into pEG-KT vector described in Mitchell *et al.*, 1992. Plasmid pMIC18 was kindly provided by Dr. Heng Zhu and was used as a template for constructing pMIC20, pMIC21, pMIC48, pMIC50, pMIC52, pMIC55 and pMIC57. The primers used were *K104R Fw*, *K130-134R Fw*, *K40R Fw*, *K71R Fw*, *K268R Fw*, *K84R Fw*, *K99R Fw* and its reverse complement, respectively. pMIC30 was derived from pMIC21 using *K1045R Fw* and its reverse complement. pMIC54 was made using pMIC30 as a template and *K99R Fw* and its reverse complement. From pMIC54 we generated pMIC60 using *K268R Fw* and its reverse complement. pMIC66 was derived from pMIC60 using *K84R Fw* and its reverse complement. pMIC67 was built from pMIC66 using *K71R Fw* primer and its reverse complement. pMIC69 was made from pMIC67 using *K40R Fw* and its reverse complement. From pMIC55 we generated pMIC59 and pMIC61 using *K268R Fw*, *K71R Fw*, and its reverse complement, respectively. pMIC63 was derived from pMIC59 using *K99R Fw* and its reverse complement. pMIC65 was derived from pMIC63 using *K71R Fw* and its reverse complement. Finally, pMIC70 was derived from pMIC69 using *R84K Fw* primer and its reverse complement. Both DNA strands of cloned and mutated fragments in all plasmids described in this study were sequenced twice.

Cloning of dicistronic vector pGEX.2Rbs.Rup1-Ubp2 (pMIC101) was obtained as follows: Rup1 was derived from yeast genome using primers *Rup1-BamH1 Fw* and *Rup1-Spe1 Rev*. Both insert and vector pGEX.2Rbs (pMIC99) were double digested with BamH1 and Spe1 and ligated with T4 DNA ligase (Promega) generetin pMIC98 vector. Ubp2 (pMIC84) was amplified using Ubp2-Sac1 Fw and Ubp2-XhoI Rev and cloned into Sac1 and Xho1 sites of vector pMIC84, generating pMIC101.

Electrophoresis, Isoelectric Focusing And Immunoblot Analysis

For two-dimensional electrophoresis, the sample was applied in 8 M urea, 2% CHAPS, 0.5% ampholytes, 20 mM DTT, and 0.002% bromophenol blue**.** Isoelectric focusing extended over a pH range of 3-10 using appropriate ampholytes and strips (Invitrogen). Applied voltage was increased stepwise to 2000 V. The

second dimension, 4-12% SDS-PAGE (Invitrogen), was performed according to manufacturer's instructions. For one-dimension electrophoresis, 4-12% gradients PAGE system with 1xMES or 1xMOPS buffers were used (Invitrogen). For immunoblots, proteins were transferred to polyvinylidene difluoride membranes, which were then blocked, and incubated with antibodies using TBST buffer (50 mM Tris HCl [pH 7.4], 150 mM NaCl, 0.1% Tween 20) with 5% w/v nonfat powdered milk, and washed with TBST and with H_2O. Detection was performed by chemiluminescence, using horseradish peroxidase-conjugated donkey anti-rabbit antibodies (GE Healthcare).

Antibodies

Polyclonal antibodies to Rpn10 were raised in rabbits against full length protein and second bleed antisera was used. Anti-cyclin B antibody (Ab-2) was obtained from Neomarkers. Anti-ubiquitin and anti-HIS antibodies were obtained from Enzo Life Science. Antibody was from α7, rpn12 were kindly provided by D. Finley.

Protein Detection In Gels By Silver Staining

The gel was soaked for 10 min in fixing solution containing 40% methanol and 13.5% formaldehyde and washed twice in MilliQ water for 5 min each. Gel was incubated for 1 min in 0.02% sodium thiosulfate and washed twice, 30 seconds each, in MilliQ water. Silver solution (0.1% silver nitrate) was added, shaken for 10 min and rinsed twice with deionized water. Then the gel was rinsed shortly with the developing solution (3% sodium carbonate and 0.05% formaldehyde). The solution was discarded and a new portion of the developing solution was added. The protein image was developed by incubating the gel with the developing solution for 5 min. When the desired intensity of the bands was reached, reaction was stopped by adding 6 grams of solid citric acid and gel was shaken for 10 min. Finally, the gel was washed in MilliQ water for 30 min.

Characterization Of Modified Rpn10 Lysines By Mass Spectrometry

AQUA Stage 1: it involved the selection and standard synthesis of a peptide, which was chosen based on Rpn10 sequence and the protease to be used (Trypsin). Stable isotopes were incorporated (e.g., ^{13}C, ^{15}N, etc) at a single amino acid residue (heavy Leu in K84-GG, mass shift of 7.017 Da; heavy Pro in K268-GG, mass shift of 6.014 Da) (Table 2). AQUA internal standard peptides were then evaluated by MS to perform a Standard Reference Method (SRM) (Figure 56, see Appendix). This process provided qualitative information about peptide retention, ionization efficiency and fragmentation.

			Monoisotopic Masses-Light				Monoisotopic Masses-Heavy			
Name	**Sequence**	**Mass Add.**	(+1)	(+2)	(+3)	(+4)	(+1)	(+2)	(+3)	(+4)
K84Ox-GG	ILAGLHDTQIEGK(GG)LHM*ATALQIAQLT**L**K	7.017	3140.738	1571.376	1047.920	786.192	3147.755	1574.885	1050.259	787.946
K268-GG	QQQQQQDQPEQSEQ**P**EQHQDK(GG)	6.014	2704.171	1353.093	902.398	677.050	2710.185	1356.100	904.402	678.554

Table 2: Monoisotopic Masses of AQUA Stable Isotope Labeled Peptides.

Gly-Gly peptides were labeled with heavy Leucine (mass shift of 7.017) and Proline (mass shift of 6.014) isotopes for Lys^{84} and Lys^{268}, respectively (underlined and bold). The monoisotopic masses of the most abundant ionized forms (up to +4) are also shown for both light and heavy peptides.

AQUA stage 2: processing samples. Ubiquitination sites were identified by excising gel bands containing Rpn10 and in-gel digested with trypsin. It is important to slice the gel with a clean razor blade and to do it in a clean surface. Distain Coomassie-stained bands with 50 mM ammonium bicarbonate-50% MetOH until it is clear (switch to fresh buffer a few times). Once the bands are clear, distain them with 50 mM ammonium bicarbonate and 50% acetonitrile for 30 minutes. Then incubate it in 100% acetonitrile for 15 minutes (gel pieces become white). Dry the gel piece down in the Speed Vac. Reduce samples with 5 mM DTT at 55ºC, 30 minutes. Cool down samples and alkylate them by adding 20 mM iodoacetamide (IAA). Incubate samples in dark for 30 minutes at room temperature. Discard supernatant and repeat washings with $(NH_4)HCO_3$-MetOH, $(NH_4)HCO_3$-ACN and 100% ACN. Dry samples down in the Speed Vac and cover them with 2x volumes of tryspin solution (12.5 ng/μL Trypsin in 25 mM NH4HCO3 pH 8, freshly diluted). Incubate samples overnight at 37ºC. Make a mix of both AQUA petides (Table 2), 1 pmol each. Stop trypsin digestion by adding extraction buffer (50% ACN-5% formic acid) and AQUA peptides to the gel pieces. Vortex, spin down and take out supernatant. Repeat it twice and Speed Vac. Before performing MS/MS analysis, the peptide mixture need to be cleaned and concentrated using stop-and-go-extraction tips (StageTips). Follow manufacter´s instruction. Resuspend lyophilized peptides in 5 μL FA and use 4μL for mass spec analysis (LTQ Orbitrap; ThermoElectron). MS/MS spectra were matched to Rpn10 sequence using sequest algorithm (Yates et al., 1995) with a mass increment of 114.0429 (signature diglycine generated by trypsin digest of conjugated ubiquitin) on lysine residues.

Identification And Quantification Of Ubiquitinated Substrates By Polyubiquitin Enrichment Strategies And Mass Spectrometry

rad23rpn10 double mutant was grown in media labelled with heavy lysine (K8; lysine + 8 Da shift) up to an OD_{600} of 1. In parallel, *rad23*Δ cells were cultured in light media up to an OD_{600} of 1. Cells were mixed with an equal amount and lysed in denaturing buffer containing 8M urea, 75 mM NaCl, 50 mM Tris pH 8.2 and two tablets of protease inhibitor cocktail (complete mini, Roche) per 10 mL of lysis buffer (Villen and Gygi, 2008). Proteins were quantified by BCA protein assay (Schoel et al., 1995); the concentration should be around 10 mg ml^{-1}. Prior to trypsin digestion, lysates were diluted 1:1 with 50 mM Tris pH8 to lower urea concentration to 4M and digested with 5 ng/μL lys-C enzyme for 1 hour at room temperature. Then the mixture was diluted to a final urea concentration of 1.6M and trypsin enzyme was added at a minimum concentration of 1/200-1/250 enzyme:substrate. Samples were incubated at 37ºC overnight. Digestion was cooled down to room temperature and reaction was stopped by acidification with TFA 0.4% (vol/vol) (pH < 2). Peptides were desalted using tC18 SepPak solid-phase extraction cartridges from Waters (see manufacter´s protocol). Lyophilized peptides were resuspended in IAP buffer (50 mM MOPS pH 7.4, 10 mM Na2HPO4, 50 mM NaCl) and incubated with a-diGly antibody coupled to protein A agarose beads for 1 hour at 4ºC. Peptides were washed with IAP buffer 3x and once with PBS. Peptides were eluted twice with 50 mÑ of 1% formic acid. The eluted peptides were desaslted using C18 stage-tip method (Rappsilber et al., 2003) and resuspended in 5% FA prior to mass spec analysis. Each lysate was immunoprecipitated sequentially two times and analysed separately by mass spectrometry (Kim et al., 2011b).

Peptides were separated on 100 mm x 20 cb C18 reversed phase with a gradient of 6% to 27% ACN in 0.125% FA over 165 min (Haas et al., 2006). The twenty most intense peaks from each full MS scan

acquired in the Orbitrap were selected in linear ion trap. For protein and site quantification, SILAC ratios (Heavy: Light) were determined for each peptide in automated fashion by generating extracted ion chromatograms within 10 ppm of the observed m/z for the monoisotopic and +1 isotopes for both heavy and light isotopomers. Extracted ion chromatograms were then integrated and the sum of heavy EIC's was divided by the sum of the light EIC's to determine the SILAC ratio. Ratios for each peptide then underwent Log2 transformation. Signal-to-noise ratios were then determined for both heavy and light isotopic envelopes by comparing their observed signal intensities with the median signal intensity observed in nearby m/z ranges within several minutes of the peptide's elution. In cases where only a single isotopomer (heavy or light) was detectable, the signal-to-noise ratio was used for quantitation instead. For an individual peptide to be used for quantification of sites and proteins, it had to meet one of two conditions: (1) Both heavy and light isotopic envelopes must be detected with signal-to- noise ratios above 5.0; (2) One isotopic envelope (heavy or light) must have a signal-to-noise ratio above 10.0. The median Log2 ratio for all matching quantified peptides was taken as an estimate of the Log2 ratio for each protein or site and the standard deviation across all quantified peptides was calculated as an indication of variability. A subset of sites and proteins were identified based on peptides whose identifications were confident, but whose quantification failed to meet our minimum requirements. (Kim et al., 2011).

References

Aguilera, J., Randez-Gil, F., and Prieto, J.A. (2007). Cold response in Saccharomyces cerevisiae: new functions for old mechanisms. FEMS Microbiol Rev *31*, 327-341.

Amerik, A.Y., and Hochstrasser, M. (2004). Mechanism and function of deubiquitinating enzymes. Biochim Biophys Acta *1695*, 189-207.

Asao, H., Sasaki, Y., Arita, T., Tanaka, N., Endo, K., Kasai, H., Takeshita, T., Endo, Y., Fujita, T., and Sugamura, K. (1997). Hrs is associated with STAM, a signal-transducing adaptor molecule. Its suppressive effect on cytokine-induced cell growth. J Biol Chem *272*, 32785-32791.

Aubin-Tam, M.E., Olivares, A.O., Sauer, R.T., Baker, T.A., and Lang, M.J. (2011). Single-molecule protein unfolding and translocation by an ATP-fueled proteolytic machine. Cell *145*, 257-267.

Bache, K.G., Raiborg, C., Mehlum, A., and Stenmark, H. (2003). STAM and Hrs are subunits of a multivalent ubiquitin-binding complex on early endosomes. J Biol Chem *278*, 12513-12521.

Bajorek, M., Finley, D., and Glickman, M.H. (2003). Proteasome disassembly and downregulation is correlated with viability during stationary phase. Curr Biol *13*, 1140-1144.

Baumeister, W., Walz, J., Zuhl, F., and Seemuller, E. (1998). The proteasome: paradigm of a self-compartmentalizing protease. Cell *92*, 367-380.

Benaroudj, N., Zwickl, P., Seemuller, E., Baumeister, W., and Goldberg, A.L. (2003). ATP hydrolysis by the proteasome regulatory complex PAN serves multiple functions in protein degradation. Mol Cell *11*, 69-78.

Bennett, E.J., and Harper, J.W. (2008). DNA damage: ubiquitin marks the spot. Nat Struct Mol Biol *15*, 20-22.

Bennett, E.J., Rush, J., Gygi, S.P., and Harper, J.W. (2010). Dynamics of cullin-RING ubiquitin ligase network revealed by systematic quantitative proteomics. Cell *143*, 951-965.

Bienko, M., Green, C.M., Crosetto, N., Rudolf, F., Zapart, G., Coull, B., Kannouche, P., Wider, G., Peter, M., Lehmann, A.R*., et al.* (2005). Ubiquitin-binding domains in Y-family polymerases regulate translesion synthesis. Science *310*, 1821-1824.

Bienkowska, J.R., Hartman, H., and Smith, T.F. (2003). A search method for homologs of small proteins. Ubiquitin-like proteins in prokaryotic cells? Protein Eng *16*, 897-904.

Biggins, S., Ivanovska, I., and Rose, M.D. (1996). Yeast ubiquitin-like genes are involved in duplication of the microtubule organizing center. J Cell Biol *133*, 1331-1346.

Boersema, P.J., Raijmakers, R., Lemeer, S., Mohammed, S., and Heck, A.J. (2009). Multiplex peptide stable isotope dimethyl labeling for quantitative proteomics. Nat Protoc *4*, 484-494.

Borden, K.L., and Freemont, P.S. (1996). The RING finger domain: a recent example of a sequence-structure family. Curr Opin Struct Biol *6*, 395-401.

Braun, B.C., Glickman, M., Kraft, R., Dahlmann, B., Kloetzel, P.M., Finley, D., and Schmidt, M. (1999). The base of the proteasome regulatory particle exhibits chaperone-like activity. Nat Cell Biol *1*, 221-226.

Bremm, A., Freund, S.M., and Komander, D. (2010). Lys11-linked ubiquitin chains adopt compact conformations and are preferentially hydrolyzed by the deubiquitinase Cezanne. Nat Struct Mol Biol *17*, 939-947.

Bremm, A., and Komander, D. (2011). Emerging roles for Lys11-linked polyubiquitin in cellular regulation. Trends Biochem Sci *36*, 355-363.

Brooks, C.L., and Gu, W. (2004). Dynamics in the p53-Mdm2 ubiquitination pathway. Cell Cycle *3*, 895-899.

Burroughs, A.M., Balaji, S., Iyer, L.M., and Aravind, L. (2007). Small but versatile: the extraordinary functional and structural diversity of the beta-grasp fold. Biol Direct *2*, 18.

Burroughs, A.M., Iyer, L.M., and Aravind, L. (2009). Natural history of the E1-like superfamily: implication for adenylation, sulfur transfer, and ubiquitin conjugation. Proteins *75*, 895-910.

Burroughs, A.M., Jaffee, M., Iyer, L.M., and Aravind, L. (2008). Anatomy of the E2 ligase fold: implications for enzymology and evolution of ubiquitin/Ub-like protein conjugation. J Struct Biol *162*, 205-218.

Cadwell, K., and Coscoy, L. (2005). Ubiquitination on nonlysine residues by a viral E3 ubiquitin ligase. Science *309*, 127-130.

Catic, A., and Ploegh, H.L. (2005). Ubiquitin--conserved protein or selfish gene? Trends Biochem Sci *30*, 600-604.

Chen, L., and Madura, K. (2002). Rad23 promotes the targeting of proteolytic substrates to the proteasome. Mol Cell Biol *22*, 4902-4913.

Chen, L., Shinde, U., Ortolan, T.G., and Madura, K. (2001). Ubiquitin-associated (UBA) domains in Rad23 bind ubiquitin and promote inhibition of multi-ubiquitin chain assembly. EMBO Rep *2*, 933-938.

Chen, X., Lee, B.H., Finley, D., and Walters, K.J. (2010). Structure of proteasome ubiquitin receptor hRpn13 and its activation by the scaffolding protein hRpn2. Mol Cell *38*, 404-415.

Chiu, Y.H., Sun, Q., and Chen, Z.J. (2007). E1-L2 activates both ubiquitin and FAT10. Mol Cell *27*, 1014-1023.

Choudhary, C., and Mann, M. (2010). Decoding signalling networks by mass spectrometry-based proteomics. Nat Rev Mol Cell Biol *11*, 427-439.

Ciechanover, A., and Ben-Saadon, R. (2004). N-terminal ubiquitination: more protein substrates join in. Trends Cell Biol *14*, 103-106.

Ciechanover, A., Elias, S., Heller, H., Ferber, S., and Hershko, A. (1980). Characterization of the heat-stable polypeptide of the ATP-dependent proteolytic system from reticulocytes. J Biol Chem *255*, 7525-7528.

Ciechanover, A., Finley, D., and Varshavsky, A. (1985). Mammalian cell cycle mutant defective in intracellular protein degradation and ubiquitin-protein conjugation. Prog Clin Biol Res *180*, 17-31.

Ciechanover, A., Heller, H., Katz-Etzion, R., and Hershko, A. (1981). Activation of the heat-stable polypeptide of the ATP-dependent proteolytic system. Proc Natl Acad Sci U S A *78*, 761-765.

Clamp, M., Cuff, J., Searle, S.M., and Barton, G.J. (2004). The Jalview Java alignment editor. Bioinformatics *20*, 426-427.

Cook, W.J., Jeffrey, L.C., Carson, M., Chen, Z., and Pickart, C.M. (1992). Structure of a diubiquitin conjugate and a model for interaction with ubiquitin conjugating enzyme (E2). J Biol Chem *267*, 16467-16471.

Cox, J., and Mann, M. (2011). Quantitative, high-resolution proteomics for data-driven systems biology. Annu Rev Biochem *80*, 273-299.

Crosas, B., Hanna, J., Kirkpatrick, D.S., Zhang, D.P., Tone, Y., Hathaway, N.A., Buecker, C., Leggett, D.S., Schmidt, M., King, R.W.*, et al.* (2006). Ubiquitin chains are remodeled at the proteasome by opposing ubiquitin ligase and deubiquitinating activities. Cell *127*, 1401-1413.

Daicho, K., Maruyama, H., Suzuki, A., Ueno, M., Uritani, M., and Ushimaru, T. (2007). The ergosterol biosynthesis inhibitor zaragozic acid promotes vacuolar degradation of the tryptophan permease Tat2p in yeast. Biochim Biophys Acta *1768*, 1681-1690.

Danielsen, J.M., Sylvestersen, K.B., Bekker-Jensen, S., Szklarczyk, D., Poulsen, J.W., Horn, H., Jensen, L.J., Mailand, N., and Nielsen, M.L. (2011). Mass spectrometric analysis of lysine ubiquitylation reveals promiscuity at site level. Mol Cell Proteomics *10*, M110 003590.

Darwin, K.H. (2009). Prokaryotic ubiquitin-like protein (Pup), proteasomes and pathogenesis. Nat Rev Microbiol *7*, 485-491.

Demartino, G.N., and Gillette, T.G. (2007). Proteasomes: machines for all reasons. Cell *129*, 659-662.

Demo, S.D., Kirk, C.J., Aujay, M.A., Buchholz, T.J., Dajee, M., Ho, M.N., Jiang, J., Laidig, G.J., Lewis, E.R., Parlati, F.*, et al.* (2007). Antitumor activity of PR-171, a novel irreversible inhibitor of the proteasome. Cancer Res *67*, 6383-6391.

Deshaies, R.J., and Joazeiro, C.A. (2009). RING domain E3 ubiquitin ligases. Annu Rev Biochem *78*, 399-434.

Deveraux, Q., Ustrell, V., Pickart, C., and Rechsteiner, M. (1994). A 26 S protease subunit that binds ubiquitin conjugates. J Biol Chem *269*, 7059-7061.

Di Fiore, P.P., Polo, S., and Hofmann, K. (2003). When ubiquitin meets ubiquitin receptors: a signalling connection. Nat Rev Mol Cell Biol *4*, 491-497.

Dikic, I., Wakatsuki, S., and Walters, K.J. (2009). Ubiquitin-binding domains - from structures to functions. Nat Rev Mol Cell Biol *10*, 659-671.

Donato, P., Cacciola, F., Tranchida, P.Q., Dugo, P., and Mondello, L. (2012). Mass spectrometry detection in comprehensive liquid chromatography: Basic concepts, instrumental aspects, applications and trends. Mass Spectrom Rev.

Dunn, R., and Hicke, L. (2001). Domains of the Rsp5 ubiquitin-protein ligase required for receptor-mediated and fluid-phase endocytosis. Mol Biol Cell *12*, 421-435.

Dunn, R., Klos, D.A., Adler, A.S., and Hicke, L. (2004). The C2 domain of the Rsp5 ubiquitin ligase binds membrane phosphoinositides and directs ubiquitination of endosomal cargo. J Cell Biol *165*, 135-144.

Dupre, S., Urban-Grimal, D., and Haguenauer-Tsapis, R. (2004). Ubiquitin and endocytic internalization in yeast and animal cells. Biochim Biophys Acta *1695*, 89-111.

Eckardt, N.A. (2003). Characterization of the last subunit of the Arabidopsis COP9 signalosome. Plant Cell *15*, 580-581.

Elias, J.E., and Gygi, S.P. (2007). Target-decoy search strategy for increased confidence in large-scale protein identifications by mass spectrometry. Nat Methods *4*, 207-214.

Elsasser, S., Chandler-Militello, D., Muller, B., Hanna, J., and Finley, D. (2004). Rad23 and Rpn10 serve as alternative ubiquitin receptors for the proteasome. J Biol Chem *279*, 26817-26822.

Elsasser, S., and Finley, D. (2005). Delivery of ubiquitinated substrates to protein-unfolding machines. Nat Cell Biol *7*, 742-749.

Elsasser, S., Gali, R.R., Schwickart, M., Larsen, C.N., Leggett, D.S., Muller, B., Feng, M.T., Tubing, F., Dittmar, G.A., and Finley, D. (2002). Proteasome subunit Rpn1 binds ubiquitin-like protein domains. Nat Cell Biol *4*, 725-730.

Emanuele, M.J., Elia, A.E., Xu, Q., Thoma, C.R., Izhar, L., Leng, Y., Guo, A., Chen, Y.N., Rush, J., Hsu, P.W., *et al.* (2011). Global identification of modular cullin-RING ligase substrates. Cell *147*, 459-474.

Everley, P.A., Krijgsveld, J., Zetter, B.R., and Gygi, S.P. (2004). Quantitative cancer proteomics: stable isotope labeling with amino acids in cell culture (SILAC) as a tool for prostate cancer research. Mol Cell Proteomics *3*, 729-735.

Fallon, L., Belanger, C.M., Corera, A.T., Kontogiannea, M., Regan-Klapisz, E., Moreau, F., Voortman, J., Haber, M., Rouleau, G., Thorarinsdottir, T.*, et al.* (2006). A regulated interaction with the UIM protein Eps15 implicates parkin in EGF receptor trafficking and PI(3)K-Akt signalling. Nat Cell Biol *8*, 834-842.

Fenical, W., Jensen, P.R., Palladino, M.A., Lam, K.S., Lloyd, G.K., and Potts, B.C. (2009). Discovery and development of the anticancer agent salinosporamide A (NPI-0052). Bioorg Med Chem *17*, 2175-2180.

Finley, D. (2009). Recognition and processing of ubiquitin-protein conjugates by the proteasome. Annu Rev Biochem *78*, 477-513.

Finley, D., Bartel, B., and Varshavsky, A. (1989). The tails of ubiquitin precursors are ribosomal proteins whose fusion to ubiquitin facilitates ribosome biogenesis. Nature *338*, 394-401.

Finley, D., Ciechanover, A., and Varshavsky, A. (1984). Thermolability of ubiquitin-activating enzyme from the mammalian cell cycle mutant ts85. Cell *37*, 43-55.

Fisher, R.D., Wang, B., Alam, S.L., Higginson, D.S., Robinson, H., Sundquist, W.I., and Hill, C.P. (2003). Structure and ubiquitin binding of the ubiquitin-interacting motif. J Biol Chem *278*, 28976-28984.

Fisher, R.I., Bernstein, S.H., Kahl, B.S., Djulbegovic, B., Robertson, M.J., de Vos, S., Epner, E., Krishnan, A., Leonard, J.P., Lonial, S.*, et al.* (2006). Multicenter phase II study of bortezomib in patients with relapsed or refractory mantle cell lymphoma. J Clin Oncol *24*, 4867-4874.

Fu, H., Sadis, S., Rubin, D.M., Glickman, M., van Nocker, S., Finley, D., and Vierstra, R.D. (1998). Multiubiquitin chain binding and protein degradation are mediated by distinct domains within the 26 S proteasome subunit Mcb1. J Biol Chem *273*, 1970-1981.

Funakoshi, M., Sasaki, T., Nishimoto, T., and Kobayashi, H. (2002). Budding yeast Dsk2p is a polyubiquitin-binding protein that can interact with the proteasome. Proc Natl Acad Sci U S A *99*, 745-750.

Gabriely, G., Kama, R., Gelin-Licht, R., and Gerst, J.E. (2008). Different domains of the UBL-UBA ubiquitin receptor, Ddi1/Vsm1, are involved in its multiple cellular roles. Mol Biol Cell *19*, 3625-3637.

Gajewska, B., Kaminska, J., Jesionowska, A., Martin, N.C., Hopper, A.K., and Zoladek, T. (2001). WW domains of Rsp5p define different functions: determination of roles in fluid phase and uracil permease endocytosis in Saccharomyces cerevisiae. Genetics *157*, 91-101.

Geng, F., and Tansey, W.P. (2008). Polyubiquitylation of histone H2B. Mol Biol Cell *19*, 3616-3624.

Gerber, S.A., Rush, J., Stemman, O., Kirschner, M.W., and Gygi, S.P. (2003). Absolute quantification of proteins and phosphoproteins from cell lysates by tandem MS. Proc Natl Acad Sci U S A *100*, 6940-6945.

Gerlach, B., Cordier, S.M., Schmukle, A.C., Emmerich, C.H., Rieser, E., Haas, T.L., Webb, A.I., Rickard, J.A., Anderton, H., Wong, W.W.*, et al.* (2011). Linear ubiquitination prevents inflammation and regulates immune signalling. Nature *471*, 591-596.

Glickman, M.H., and Ciechanover, A. (2002). The ubiquitin-proteasome proteolytic pathway: destruction for the sake of construction. Physiol Rev *82*, 373-428.

Glickman, M.H., and Raveh, D. (2005). Proteasome plasticity. FEBS Lett *579*, 3214-3223.

Glickman, M.H., Rubin, D.M., Coux, O., Wefes, I., Pfeifer, G., Cjeka, Z., Baumeister, W., Fried, V.A., and Finley, D. (1998a). A subcomplex of the proteasome regulatory particle required for ubiquitin-conjugate degradation and related to the COP9-signalosome and eIF3. Cell *94*, 615-623.

Glickman, M.H., Rubin, D.M., Fried, V.A., and Finley, D. (1998b). The regulatory particle of the Saccharomyces cerevisiae proteasome. Mol Cell Biol *18*, 3149-3162.

Goldberg, A.L., Cascio, P., Saric, T., and Rock, K.L. (2002). The importance of the proteasome and subsequent proteolytic steps in the generation of antigenic peptides. Mol Immunol *39*, 147-164.

Goldberg, A.L., Stein, R., and Adams, J. (1995). New insights into proteasome function: from archaebacteria to drug development. Chem Biol *2*, 503-508.

Goldknopf, I.L., and Busch, H. (1977). Isopeptide linkage between nonhistone and histone 2A polypeptides of chromosomal conjugate-protein A24. Proc Natl Acad Sci U S A *74*, 864-868.

Gomez, T.A., Kolawa, N., Gee, M., Sweredoski, M.J., and Deshaies, R.J. (2011). Identification of a functional docking site in the Rpn1 LRR domain for the UBA-UBL domain protein Ddi1. BMC Biol *9*, 33.

Gonen, H., Bercovich, B., Orian, A., Carrano, A., Takizawa, C., Yamanaka, K., Pagano, M., Iwai, K., and Ciechanover, A. (1999). Identification of the ubiquitin carrier proteins, E2s, involved in signal-induced conjugation and subsequent degradation of IkappaBalpha. J Biol Chem *274*, 14823-14830.

Groll, M., Bajorek, M., Kohler, A., Moroder, L., Rubin, D.M., Huber, R., Glickman, M.H., and Finley, D. (2000). A gated channel into the proteasome core particle. Nat Struct Biol *7*, 1062-1067.

Groll, M., Ditzel, L., Lowe, J., Stock, D., Bochtler, M., Bartunik, H.D., and Huber, R. (1997). Structure of 20S proteasome from yeast at 2.4 A resolution. Nature *386*, 463-471.

Grossman, S.R., Deato, M.E., Brignone, C., Chan, H.M., Kung, A.L., Tagami, H., Nakatani, Y., and Livingston, D.M. (2003). Polyubiquitination of p53 by a ubiquitin ligase activity of p300. Science *300*, 342-344.

Gupta, R., Kus, B., Fladd, C., Wasmuth, J., Tonikian, R., Sidhu, S., Krogan, N.J., Parkinson, J., and Rotin, D. (2007). Ubiquitination screen using protein microarrays for comprehensive identification of Rsp5 substrates in yeast. Mol Syst Biol *3*, 116.

Guterman, A., and Glickman, M.H. (2004). Complementary roles for Rpn11 and Ubp6 in deubiquitination and proteolysis by the proteasome. J Biol Chem *279*, 1729-1738.

Haas, A.L., and Rose, I.A. (1982). The mechanism of ubiquitin activating enzyme. A kinetic and equilibrium analysis. J Biol Chem *257*, 10329-10337.

Haas, A.L., Warms, J.V., Hershko, A., and Rose, I.A. (1982). Ubiquitin-activating enzyme. Mechanism and role in protein-ubiquitin conjugation. J Biol Chem *257*, 2543-2548.

Haas, W., Faherty, B.K., Gerber, S.A., Elias, J.E., Beausoleil, S.A., Bakalarski, C.E., Li, X., Villen, J., and Gygi, S.P. (2006). Optimization and use of peptide mass measurement accuracy in shotgun proteomics. Mol Cell Proteomics *5*, 1326-1337.

Haglund, K., Di Fiore, P.P., and Dikic, I. (2003). Distinct monoubiquitin signals in receptor endocytosis. Trends Biochem Sci *28*, 598-603.

Haglund, K., and Stenmark, H. (2006). Working out coupled monoubiquitination. Nat Cell Biol *8*, 1218-1219.

Hamazaki, J., Iemura, S., Natsume, T., Yashiroda, H., Tanaka, K., and Murata, S. (2006). A novel proteasome interacting protein recruits the deubiquitinating enzyme UCH37 to 26S proteasomes. EMBO J *25*, 4524-4536.

Hamazaki, J., Sasaki, K., Kawahara, H., Hisanaga, S., Tanaka, K., and Murata, S. (2007). Rpn10-mediated degradation of ubiquitinated proteins is essential for mouse development. Mol Cell Biol *27*, 6629-6638.

Hanke, S., Besir, H., Oesterhelt, D., and Mann, M. (2008). Absolute SILAC for accurate quantitation of proteins in complex mixtures down to the attomole level. J Proteome Res *7*, 1118-1130.

Hanna, J., Hathaway, N.A., Tone, Y., Crosas, B., Elsasser, S., Kirkpatrick, D.S., Leggett, D.S., Gygi, S.P., King, R.W., and Finley, D. (2006). Deubiquitinating enzyme Ubp6 functions noncatalytically to delay proteasomal degradation. Cell *127*, 99-111.

Hanna, J., Meides, A., Zhang, D.P., and Finley, D. (2007). A ubiquitin stress response induces altered proteasome composition. Cell *129*, 747-759.

Harari-Steinberg, O., and Chamovitz, D.A. (2004). The COP9 signalosome: mediating between kinase signaling and protein degradation. Curr Protein Pept Sci *5*, 185-189.

Harper, J.W., and Schulman, B.A. (2006). Structural complexity in ubiquitin recognition. Cell *124*, 1133-1136.

Hashizume, R., Fukuda, M., Maeda, I., Nishikawa, H., Oyake, D., Yabuki, Y., Ogata, H., and Ohta, T. (2001). The RING heterodimer BRCA1-BARD1 is a ubiquitin ligase inactivated by a breast cancer-derived mutation. J Biol Chem *276*, 14537-14540.

Hatakeyama, S., Yada, M., Matsumoto, M., Ishida, N., and Nakayama, K.I. (2001). U box proteins as a new family of ubiquitin-protein ligases. J Biol Chem *276*, 33111-33120.

He, J., Kulkarni, K., da Fonseca, P.C., Krutauz, D., Glickman, M.H., Barford, D., and Morris, E.P. (2012). The structure of the 26S proteasome subunit Rpn2 reveals its PC repeat domain as a closed toroid of two concentric alpha-helical rings. Structure *20*, 513-521.

Hershko, A., and Ciechanover, A. (1998). The ubiquitin system. Annu Rev Biochem *67*, 425-479.

Hershko, A., Ciechanover, A., Heller, H., Haas, A.L., and Rose, I.A. (1980). Proposed role of ATP in protein breakdown: conjugation of protein with multiple chains of the polypeptide of ATP-dependent proteolysis. Proc Natl Acad Sci U S A *77*, 1783-1786.

Hershko, A., and Heller, H. (1985). Occurrence of a polyubiquitin structure in ubiquitin-protein conjugates. Biochem Biophys Res Commun *128*, 1079-1086.

Hesselberth, J.R., Miller, J.P., Golob, A., Stajich, J.E., Michaud, G.A., and Fields, S. (2006). Comparative analysis of Saccharomyces cerevisiae WW domains and their interacting proteins. Genome Biol *7*, R30.

Hicke, L. (2001). Protein regulation by monoubiquitin. Nat Rev Mol Cell Biol *2*, 195-201.

Hicke, L., and Dunn, R. (2003). Regulation of membrane protein transport by ubiquitin and ubiquitin-binding proteins. Annu Rev Cell Dev Biol *19*, 141-172.

Hicke, L., and Riezman, H. (1996). Ubiquitination of a yeast plasma membrane receptor signals its ligand-stimulated endocytosis. Cell *84*, 277-287.

Hirano, S., Kawasaki, M., Ura, H., Kato, R., Raiborg, C., Stenmark, H., and Wakatsuki, S. (2006). Double-sided ubiquitin binding of Hrs-UIM in endosomal protein sorting. Nat Struct Mol Biol *13*, 272-277.

Hiyama, H., Yokoi, M., Masutani, C., Sugasawa, K., Maekawa, T., Tanaka, K., Hoeijmakers, J.H., and Hanaoka, F. (1999). Interaction of hHR23 with S5a. The ubiquitin-like domain of hHR23 mediates interaction with S5a subunit of 26 S proteasome. J Biol Chem *274*, 28019-28025.

Hochstrasser, M. (2000). Evolution and function of ubiquitin-like protein-conjugation systems. Nat Cell Biol *2*, E153-157.

Hochstrasser, M. (2009). Origin and function of ubiquitin-like proteins. Nature *458*, 422-429.

Hoeller, D., Crosetto, N., Blagoev, B., Raiborg, C., Tikkanen, R., Wagner, S., Kowanetz, K., Breitling, R., Mann, M., Stenmark, H.*, et al.* (2006). Regulation of ubiquitin-binding proteins by monoubiquitination. Nat Cell Biol *8*, 163-169.

Hoeller, D., and Dikic, I. (2010). Regulation of ubiquitin receptors by coupled monoubiquitination. Subcell Biochem *54*, 31-40.

Hoeller, D., Hecker, C.M., Wagner, S., Rogov, V., Dotsch, V., and Dikic, I. (2007). E3-independent monoubiquitination of ubiquitin-binding proteins. Mol Cell *26*, 891-898.

Hofmann, K., and Falquet, L. (2001). A ubiquitin-interacting motif conserved in components of the proteasomal and lysosomal protein degradation systems. Trends Biochem Sci *26*, 347-350.

Hofmann, R.M., and Pickart, C.M. (2001). In vitro assembly and recognition of Lys-63 polyubiquitin chains. J Biol Chem *276*, 27936-27943.

Hoppe, T., Matuschewski, K., Rape, M., Schlenker, S., Ulrich, H.D., and Jentsch, S. (2000). Activation of a membrane-bound transcription factor by regulated ubiquitin/proteasome-dependent processing. Cell *102*, 577-586.

Horak, J. (2003). The role of ubiquitin in down-regulation and intracellular sorting of membrane proteins: insights from yeast. Biochim Biophys Acta *1614*, 139-155.

Huibregtse, J.M., Scheffner, M., Beaudenon, S., and Howley, P.M. (1995). A family of proteins structurally and functionally related to the E6-AP ubiquitin-protein ligase. Proc Natl Acad Sci U S A *92*, 5249.

Huibregtse, J.M., Yang, J.C., and Beaudenon, S.L. (1997). The large subunit of RNA polymerase II is a substrate of the Rsp5 ubiquitin-protein ligase. Proc Natl Acad Sci U S A *94*, 3656-3661.

Humbard, M.A., Miranda, H.V., Lim, J.M., Krause, D.J., Pritz, J.R., Zhou, G., Chen, S., Wells, L., and Maupin-Furlow, J.A. (2010). Ubiquitin-like small archaeal modifier proteins (SAMPs) in Haloferax volcanii. Nature *463*, 54-60.

Husnjak, K., and Dikic, I. (2012). Ubiquitin-binding proteins: decoders of ubiquitin-mediated cellular functions. Annu Rev Biochem *81*, 291-322.

Husnjak, K., Elsasser, S., Zhang, N., Chen, X., Randles, L., Shi, Y., Hofmann, K., Walters, K.J., Finley, D., and Dikic, I. (2008). Proteasome subunit Rpn13 is a novel ubiquitin receptor. Nature *453*, 481-488.

Hwang, G.W., Sasaki, D., and Naganuma, A. (2005). Overexpression of Rad23 confers resistance to methylmercury in saccharomyces cerevisiae via inhibition of the degradation of ubiquitinated proteins. Mol Pharmacol *68*, 1074-1078.

Ibarra-Molero, B., Loladze, V.V., Makhatadze, G.I., and Sanchez-Ruiz, J.M. (1999). Thermal versus guanidine-induced unfolding of ubiquitin. An analysis in terms of the contributions from charge-charge interactions to protein stability. Biochemistry *38*, 8138-8149.

Ikeda, F., Deribe, Y.L., Skanland, S.S., Stieglitz, B., Grabbe, C., Franz-Wachtel, M., van Wijk, S.J., Goswami, P., Nagy, V., Terzic, J.*, et al.* (2011). SHARPIN forms a linear ubiquitin ligase complex regulating NF-kappaB activity and apoptosis. Nature *471*, 637-641.

Ikeda, F., and Dikic, I. (2008). Atypical ubiquitin chains: new molecular signals. 'Protein Modifications: Beyond the Usual Suspects' review series. EMBO Rep *9*, 536-542.

Ingham, R.J., Gish, G., and Pawson, T. (2004). The Nedd4 family of E3 ubiquitin ligases: functional diversity within a common modular architecture. Oncogene *23*, 1972-1984.

Isasa, M., Katz, E.J., Kim, W., Yugo, V., Gonzalez, S., Kirkpatrick, D.S., Thomson, T.M., Finley, D., Gygi, S.P., and Crosas, B. Monoubiquitination of RPN10 regulates substrate recruitment to the proteasome. Mol Cell *38*, 733-745.

Isasa, M., Katz, E.J., Kim, W., Yugo, V., Gonzalez, S., Kirkpatrick, D.S., Thomson, T.M., Finley, D., Gygi, S.P., and Crosas, B. (2010). Monoubiquitination of RPN10 regulates substrate recruitment to the proteasome. Mol Cell *38*, 733-745.

Iyer, L.M., Burroughs, A.M., and Aravind, L. (2008). Unraveling the biochemistry and provenance of pupylation: a prokaryotic analog of ubiquitination. Biol Direct *3*, 45.

Jagannath, S., Barlogie, B., Berenson, J., Siegel, D., Irwin, D., Richardson, P.G., Niesvizky, R., Alexanian, R., Limentani, S.A., Alsina, M.*, et al.* (2004). A phase 2 study of two doses of bortezomib in relapsed or refractory myeloma. Br J Haematol *127*, 165-172.

Jin, J., Li, X., Gygi, S.P., and Harper, J.W. (2007). Dual E1 activation systems for ubiquitin differentially regulate E2 enzyme charging. Nature *447*, 1135-1138.

Johnson, E.S., Ma, P.C., Ota, I.M., and Varshavsky, A. (1995). A proteolytic pathway that recognizes ubiquitin as a degradation signal. J Biol Chem *270*, 17442-17456.

Kaiser, S.E., Riley, B.E., Shaler, T.A., Trevino, R.S., Becker, C.H., Schulman, H., and Kopito, R.R. (2011). Protein standard absolute quantification (PSAQ) method for the measurement of cellular ubiquitin pools. Nat Methods *8*, 691-696.

Kaliszewski, P., and Zoladek, T. (2008). The role of Rsp5 ubiquitin ligase in regulation of diverse processes in yeast cells. Acta Biochim Pol *55*, 649-662.

Kaminska, J., Spiess, M., Stawiecka-Mirota, M., Monkaityte, R., Haguenauer-Tsapis, R., Urban-Grimal, D., Winsor, B., and Zoladek, T. (2011). Yeast Rsp5 ubiquitin ligase affects the actin cytoskeleton in vivo and in vitro. Eur J Cell Biol *90*, 1016-1028.

Kang, R.S., Daniels, C.M., Francis, S.A., Shih, S.C., Salerno, W.J., Hicke, L., and Radhakrishnan, I. (2003). Solution structure of a CUE-ubiquitin complex reveals a conserved mode of ubiquitin binding. Cell *113*, 621-630.

Kang, Y., Chen, X., Lary, J.W., Cole, J.L., and Walters, K.J. (2007). Defining how ubiquitin receptors hHR23a and S5a bind polyubiquitin. J Mol Biol *369*, 168-176.

Katzmann, D.J., Odorizzi, G., and Emr, S.D. (2002). Receptor downregulation and multivesicular-body sorting. Nat Rev Mol Cell Biol *3*, 893-905.

Kee, Y., Lyon, N., and Huibregtse, J.M. (2005). The Rsp5 ubiquitin ligase is coupled to and antagonized by the Ubp2 deubiquitinating enzyme. EMBO J *24*, 2414-2424.

Kee, Y., Munoz, W., Lyon, N., and Huibregtse, J.M. (2006). The deubiquitinating enzyme Ubp2 modulates Rsp5-dependent Lys63-linked polyubiquitin conjugates in Saccharomyces cerevisiae. J Biol Chem *281*, 36724-36731.

Kellie, J.F., Tran, J.C., Lee, J.E., Ahlf, D.R., Thomas, H.M., Ntai, I., Catherman, A.D., Durbin, K.R., Zamdborg, L., Vellaichamy, A.*, et al.* (2010). The emerging process of Top Down mass spectrometry for

protein analysis: biomarkers, protein-therapeutics, and achieving high throughput. Mol Biosyst *6*, 1532-1539.

Kim, H.C., and Huibregtse, J.M. (2009). Polyubiquitination by HECT E3s and the determinants of chain type specificity. Mol Cell Biol *29*, 3307-3318.

Kim, H.C., Steffen, A.M., Oldham, M.L., Chen, J., and Huibregtse, J.M. (2011a). Structure and function of a HECT domain ubiquitin-binding site. EMBO Rep *12*, 334-341.

Kim, H.T., Kim, K.P., Lledias, F., Kisselev, A.F., Scaglione, K.M., Skowyra, D., Gygi, S.P., and Goldberg, A.L. (2007). Certain pairs of ubiquitin-conjugating enzymes (E2s) and ubiquitin-protein ligases (E3s) synthesize nondegradable forked ubiquitin chains containing all possible isopeptide linkages. J Biol Chem *282*, 17375-17386.

Kim, H.T., Kim, K.P., Uchiki, T., Gygi, S.P., and Goldberg, A.L. (2009). S5a promotes protein degradation by blocking synthesis of nondegradable forked ubiquitin chains. EMBO J *28*, 1867-1877.

Kim, I., Mi, K., and Rao, H. (2004). Multiple interactions of rad23 suggest a mechanism for ubiquitylated substrate delivery important in proteolysis. Mol Biol Cell *15*, 3357-3365.

Kim, T., Hofmann, K., von Arnim, A.G., and Chamovitz, D.A. (2001). PCI complexes: pretty complex interactions in diverse signaling pathways. Trends Plant Sci *6*, 379-386.

Kim, W., Bennett, E.J., Huttlin, E.L., Guo, A., Li, J., Possemato, A., Sowa, M.E., Rad, R., Rush, J., Comb, M.J*., et al.* (2011b). Systematic and quantitative assessment of the ubiquitin-modified proteome. Mol Cell *44*, 325-340.

Kirkin, V., and Dikic, I. (2007). Role of ubiquitin- and Ubl-binding proteins in cell signaling. Curr Opin Cell Biol *19*, 199-205.

Kirkpatrick, D.S., Gerber, S.A., and Gygi, S.P. (2005). The absolute quantification strategy: a general procedure for the quantification of proteins and post-translational modifications. Methods *35*, 265-273.

Kirkpatrick, D.S., Hathaway, N.A., Hanna, J., Elsasser, S., Rush, J., Finley, D., King, R.W., and Gygi, S.P. (2006). Quantitative analysis of in vitro ubiquitinated cyclin B1 reveals complex chain topology. Nat Cell Biol *8*, 700-710.

Koegl, M., Hoppe, T., Schlenker, S., Ulrich, H.D., Mayer, T.U., and Jentsch, S. (1999). A novel ubiquitination factor, E4, is involved in multiubiquitin chain assembly. Cell *96*, 635-644.

Kohler, A., Bajorek, M., Groll, M., Moroder, L., Rubin, D.M., Huber, R., Glickman, M.H., and Finley, D. (2001a). The substrate translocation channel of the proteasome. Biochimie *83*, 325-332.

Kohler, A., Cascio, P., Leggett, D.S., Woo, K.M., Goldberg, A.L., and Finley, D. (2001b). The axial channel of the proteasome core particle is gated by the Rpt2 ATPase and controls both substrate entry and product release. Mol Cell *7*, 1143-1152.

Komander, D., Clague, M.J., and Urbe, S. (2009). Breaking the chains: structure and function of the deubiquitinases. Nat Rev Mol Cell Biol *10*, 550-563.

Krause, S.A., Xu, H., and Gray, J.V. (2008). The synthetic genetic network around PKC1 identifies novel modulators and components of protein kinase C signaling in Saccharomyces cerevisiae. Eukaryot Cell *7*, 1880-1887.

Kus, B., Gajadhar, A., Stanger, K., Cho, R., Sun, W., Rouleau, N., Lee, T., Chan, D., Wolting, C., Edwards, A.*, et al.* (2005). A high throughput screen to identify substrates for the ubiquitin ligase Rsp5. J Biol Chem *280*, 29470-29478.

Lake, M.W., Wuebbens, M.M., Rajagopalan, K.V., and Schindelin, H. (2001). Mechanism of ubiquitin activation revealed by the structure of a bacterial MoeB-MoaD complex. Nature *414*, 325-329.

Lambertson, D., Chen, L., and Madura, K. (1999). Pleiotropic defects caused by loss of the proteasome-interacting factors Rad23 and Rpn10 of Saccharomyces cerevisiae. Genetics *153*, 69-79.

Lander, G.C., Estrin, E., Matyskiela, M.E., Bashore, C., Nogales, E., and Martin, A. (2012). Complete subunit architecture of the proteasome regulatory particle. Nature *482*, 186-191.

Lasker, K., Forster, F., Bohn, S., Walzthoeni, T., Villa, E., Unverdorben, P., Beck, F., Aebersold, R., Sali, A., and Baumeister, W. (2012). Molecular architecture of the 26S proteasome holocomplex determined by an integrative approach. Proc Natl Acad Sci U S A *109*, 1380-1387.

Lecker, S.H., Goldberg, A.L., and Mitch, W.E. (2006). Protein degradation by the ubiquitin-proteasome pathway in normal and disease states. J Am Soc Nephrol *17*, 1807-1819.

Lee, B.H., Lee, M.J., Park, S., Oh, D.C., Elsasser, S., Chen, P.C., Gartner, C., Dimova, N., Hanna, J., Gygi, S.P.*, et al.* (2010). Enhancement of proteasome activity by a small-molecule inhibitor of USP14. Nature *467*, 179-184.

Leggett, D.S., Hanna, J., Borodovsky, A., Crosas, B., Schmidt, M., Baker, R.T., Walz, T., Ploegh, H., and Finley, D. (2002). Multiple associated proteins regulate proteasome structure and function. Mol Cell *10*, 495-507.

Lenkinski, R.E., Chen, D.M., Glickson, J.D., and Goldstein, G. (1977). Nuclear magnetic resonance studies of the denaturation of ubiquitin. Biochim Biophys Acta *494*, 126-130.

Leon, S., Erpapazoglou, Z., and Haguenauer-Tsapis, R. (2008). Ear1p and Ssh4p are new adaptors of the ubiquitin ligase Rsp5p for cargo ubiquitylation and sorting at multivesicular bodies. Mol Biol Cell *19*, 2379-2388.

Li, W., Bengtson, M.H., Ulbrich, A., Matsuda, A., Reddy, V.A., Orth, A., Chanda, S.K., Batalov, S., and Joazeiro, C.A. (2008). Genome-wide and functional annotation of human E3 ubiquitin ligases identifies MULAN, a mitochondrial E3 that regulates the organelle's dynamics and signaling. PLoS One *3*, e1487.

Licchesi, J.D., Mieszczanek, J., Mevissen, T.E., Rutherford, T.J., Akutsu, M., Virdee, S., Oualid, F.E., Chin, J.W., Ovaa, H., Bienz, M*., et al.* (2011). An ankyrin-repeat ubiquitin-binding domain determines TRABID's specificity for atypical ubiquitin chains. Nat Struct Mol Biol *19*, 62-71.

Lin, C.H., MacGurn, J.A., Chu, T., Stefan, C.J., and Emr, S.D. (2008). Arrestin-related ubiquitin-ligase adaptors regulate endocytosis and protein turnover at the cell surface. Cell *135*, 714-725.

Lipinszki, Z., Kiss, P., Pal, M., Deak, P., Szabo, A., Hunyadi-Gulyas, E., Klement, E., Medzihradszky, K.F., and Udvardy, A. (2009). Developmental-stage-specific regulation of the polyubiquitin receptors in Drosophila melanogaster. J Cell Sci *122*, 3083-3092.

Lipinszki, Z., Kovacs, L., Deak, P., and Udvardy, A. (2012). Ubiquitylation of the Drosophila p54/Rpn10/S5a regulates its interaction with the UBA-UBL polyubiquitin receptors. Biochemistry.

Lipinszki, Z., Pal, M., Nagy, O., Deak, P., Hunyadi-Gulyas, E., and Udvardy, A. (2011). Overexpression of Dsk2/dUbqln results in severe developmental defects and lethality in Drosophila melanogaster that can be rescued by overexpression of the p54/Rpn10/S5a proteasomal subunit. FEBS J *278*, 4833-4844.

Lo, Y.C., Lin, S.C., Rospigliosi, C.C., Conze, D.B., Wu, C.J., Ashwell, J.D., Eliezer, D., and Wu, H. (2009). Structural basis for recognition of diubiquitins by NEMO. Mol Cell *33*, 602-615.

Lombaerts, M., Goeloe, J.I., den Dulk, H., Brandsma, J.A., and Brouwer, J. (2000). Identification and characterization of the rhp23(+) DNA repair gene in Schizosaccharomyces pombe. Biochem Biophys Res Commun *268*, 210-215.

Lu, J.Y., Lin, Y.Y., Qian, J., Tao, S.C., Zhu, J., Pickart, C., and Zhu, H. (2008). Functional dissection of a HECT ubiquitin E3 ligase. Mol Cell Proteomics *7*, 35-45.

Lu, P.J., Zhou, X.Z., Shen, M., and Lu, K.P. (1999). Function of WW domains as phosphoserine- or phosphothreonine-binding modules. Science *283*, 1325-1328.

Macgurn, J.A., Hsu, P.C., and Emr, S.D. (2012). Ubiquitin and membrane protein turnover: from cradle to grave. Annu Rev Biochem *81*, 231-259.

Malakhova, O.A., and Zhang, D.E. (2008). ISG15 inhibits Nedd4 ubiquitin E3 activity and enhances the innate antiviral response. J Biol Chem *283*, 8783-8787.

Masutani, C., Sugasawa, K., Yanagisawa, J., Sonoyama, T., Ui, M., Enomoto, T., Takio, K., Tanaka, K., van der Spek, P.J., Bootsma, D*., et al.* (1994). Purification and cloning of a nucleotide excision repair complex involving the xeroderma pigmentosum group C protein and a human homologue of yeast RAD23. EMBO J *13*, 1831-1843.

Mata, I.F., Lockhart, P.J., and Farrer, M.J. (2004). Parkin genetics: one model for Parkinson's disease. Hum Mol Genet *13 Spec No 1*, R127-133.

Matic, I., Schimmel, J., Hendriks, I.A., van Santen, M.A., van de Rijke, F., van Dam, H., Gnad, F., Mann, M., and Vertegaal, A.C. (2010). Site-specific identification of SUMO-2 targets in cells reveals an inverted SUMOylation motif and a hydrophobic cluster SUMOylation motif. Mol Cell *39*, 641-652.

Matiuhin, Y., Kirkpatrick, D.S., Ziv, I., Kim, W., Dakshinamurthy, A., Kleifeld, O., Gygi, S.P., Reis, N., and Glickman, M.H. (2008). Extraproteasomal Rpn10 restricts access of the polyubiquitin-binding protein Dsk2 to proteasome. Mol Cell *32*, 415-425.

Matsumoto, M.L., Wickliffe, K.E., Dong, K.C., Yu, C., Bosanac, I., Bustos, D., Phu, L., Kirkpatrick, D.S., Hymowitz, S.G., Rape, M*., et al.* (2010). K11-linked polyubiquitination in cell cycle control revealed by a K11 linkage-specific antibody. Mol Cell *39*, 477-484.

Maupin-Furlow, J.A., Humbard, M.A., Kirkland, P.A., Li, W., Reuter, C.J., Wright, A.J., and Zhou, G. (2006). Proteasomes from structure to function: perspectives from Archaea. Curr Top Dev Biol *75*, 125-169.

Mayor, T., Graumann, J., Bryan, J., MacCoss, M.J., and Deshaies, R.J. (2007). Quantitative profiling of ubiquitylated proteins reveals proteasome substrates and the substrate repertoire influenced by the Rpn10 receptor pathway. Mol Cell Proteomics *6*, 1885-1895.

Mayor, T., Lipford, J.R., Graumann, J., Smith, G.T., and Deshaies, R.J. (2005). Analysis of polyubiquitin conjugates reveals that the Rpn10 substrate receptor contributes to the turnover of multiple proteasome targets. Mol Cell Proteomics *4*, 741-751.

McLafferty, F.W., Breuker, K., Jin, M., Han, X., Infusini, G., Jiang, H., Kong, X., and Begley, T.P. (2007). Top-down MS, a powerful complement to the high capabilities of proteolysis proteomics. FEBS J *274*, 6256-6268.

Medicherla, B., and Goldberg, A.L. (2008). Heat shock and oxygen radicals stimulate ubiquitin-dependent degradation mainly of newly synthesized proteins. J Cell Biol *182*, 663-673.

Michelle, C., Vourc'h, P., Mignon, L., and Andres, C.R. (2009). What was the set of ubiquitin and ubiquitin-like conjugating enzymes in the eukaryote common ancestor? J Mol Evol *68*, 616-628.

Mitchell, D.A., Marshall, T.K., and Deschenes, R.J. (1993). Vectors for the inducible overexpression of glutathione S-transferase fusion proteins in yeast. Yeast *9*, 715-722.

Moir, D., Stewart, S.E., Osmond, B.C., and Botstein, D. (1982). Cold-sensitive cell-division-cycle mutants of yeast: isolation, properties, and pseudoreversion studies. Genetics *100*, 547-563.

Mora, J.F., Van Berkel, G.J., Enke, C.G., Cole, R.B., Martinez-Sanchez, M., and Fenn, J.B. (2000). Electrochemical processes in electrospray ionization mass spectrometry. J Mass Spectrom *35*, 939-952.

Morano, K.A., Grant, C.M., and Moye-Rowley, W.S. (2011). The Response to Heat Shock and Oxidative Stress in Saccharomyces cerevisiae. Genetics.

Morrione, A., Plant, P., Valentinis, B., Staub, O., Kumar, S., Rotin, D., and Baserga, R. (1999). mGrb10 interacts with Nedd4. J Biol Chem *274*, 24094-24099.

Nalepa, G., Rolfe, M., and Harper, J.W. (2006). Drug discovery in the ubiquitin-proteasome system. Nat Rev Drug Discov *5*, 596-613.

Ng, J.M., Vermeulen, W., van der Horst, G.T., Bergink, S., Sugasawa, K., Vrieling, H., and Hoeijmakers, J.H. (2003). A novel regulation mechanism of DNA repair by damage-induced and RAD23-dependent stabilization of xeroderma pigmentosum group C protein. Genes Dev *17*, 1630-1645.

Nijman, S.M., Luna-Vargas, M.P., Velds, A., Brummelkamp, T.R., Dirac, A.M., Sixma, T.K., and Bernards, R. (2005). A genomic and functional inventory of deubiquitinating enzymes. Cell *123*, 773-786.

Nikko, E., Sullivan, J.A., and Pelham, H.R. (2008). Arrestin-like proteins mediate ubiquitination and endocytosis of the yeast metal transporter Smf1. EMBO Rep *9*, 1216-1221.

Nishio, K., Kim, S.W., Kawai, K., Mizushima, T., Yamane, T., Hamazaki, J., Murata, S., Tanaka, K., and Morimoto, Y. (2009). Crystal structure of the de-ubiquitinating enzyme UCH37 (human UCH-L5) catalytic domain. Biochem Biophys Res Commun *390*, 855-860.

Nunoura, T., Takaki, Y., Kakuta, J., Nishi, S., Sugahara, J., Kazama, H., Chee, G.J., Hattori, M., Kanai, A., Atomi, H.*, et al.* (2011). Insights into the evolution of Archaea and eukaryotic protein modifier systems revealed by the genome of a novel archaeal group. Nucleic Acids Res *39*, 3204-3223.

Okumura, A., Pitha, P.M., and Harty, R.N. (2008). ISG15 inhibits Ebola VP40 VLP budding in an L-domain-dependent manner by blocking Nedd4 ligase activity. Proc Natl Acad Sci U S A *105*, 3974-3979.

Orlowski, R.Z., and Kuhn, D.J. (2008). Proteasome inhibitors in cancer therapy: lessons from the first decade. Clin Cancer Res *14*, 1649-1657.

Ortolan, T.G., Chen, L., Tongaonkar, P., and Madura, K. (2004). Rad23 stabilizes Rad4 from degradation by the Ub/proteasome pathway. Nucleic Acids Res *32*, 6490-6500.

Park, S., Roelofs, J., Kim, W., Robert, J., Schmidt, M., Gygi, S.P., and Finley, D. (2009a). Hexameric assembly of the proteasomal ATPases is templated through their C termini. Nature *459*, 866-870.

Park, Y., Yoon, S.K., and Yoon, J.B. (2009b). The HECT domain of TRIP12 ubiquitinates substrates of the ubiquitin fusion degradation pathway. J Biol Chem *284*, 1540-1549.

Pathare, G.R., Nagy, I., Bohn, S., Unverdorben, P., Hubert, A., Korner, R., Nickell, S., Lasker, K., Sali, A., Tamura, T.*, et al.* (2012). The proteasomal subunit Rpn6 is a molecular clamp holding the core and regulatory subcomplexes together. Proc Natl Acad Sci U S A *109*, 149-154.

Pelzer, C., Kassner, I., Matentzoglu, K., Singh, R.K., Wollscheid, H.P., Scheffner, M., Schmidtke, G., and Groettrup, M. (2007). UBE1L2, a novel E1 enzyme specific for ubiquitin. J Biol Chem *282*, 23010-23014.

Penengo, L., Mapelli, M., Murachelli, A.G., Confalonieri, S., Magri, L., Musacchio, A., Di Fiore, P.P., Polo, S., and Schneider, T.R. (2006). Crystal structure of the ubiquitin binding domains of rabex-5 reveals two modes of interaction with ubiquitin. Cell *124*, 1183-1195.

Peng, J., Schwartz, D., Elias, J.E., Thoreen, C.C., Cheng, D., Marsischky, G., Roelofs, J., Finley, D., and Gygi, S.P. (2003). A proteomics approach to understanding protein ubiquitination. Nat Biotechnol *21*, 921-926.

Persaud, A., and Rotin, D. (2011). Use of proteome arrays to globally identify substrates for E3 ubiquitin ligases. Methods Mol Biol *759*, 215-224.

Pickart, C.M. (2001). Mechanisms underlying ubiquitination. Annu Rev Biochem *70*, 503-533.

Pickart, C.M., and Fushman, D. (2004). Polyubiquitin chains: polymeric protein signals. Curr Opin Chem Biol *8*, 610-616.

Pickart, C.M., and Rose, I.A. (1985). Functional heterogeneity of ubiquitin carrier proteins. J Biol Chem *260*, 1573-1581.

Piva, R., Ruggeri, B., Williams, M., Costa, G., Tamagno, I., Ferrero, D., Giai, V., Coscia, M., Peola, S., Massaia, M*., et al.* (2008). CEP-18770: A novel, orally active proteasome inhibitor with a tumor-selective pharmacologic profile competitive with bortezomib. Blood *111*, 2765-2775.

Plant, P.J., Lafont, F., Lecat, S., Verkade, P., Simons, K., and Rotin, D. (2000). Apical membrane targeting of Nedd4 is mediated by an association of its C2 domain with annexin XIIIb. J Cell Biol *149*, 1473-1484.

Plant, P.J., Yeger, H., Staub, O., Howard, P., and Rotin, D. (1997). The C2 domain of the ubiquitin protein ligase Nedd4 mediates Ca2+-dependent plasma membrane localization. J Biol Chem *272*, 32329-32336.

Rabl, J., Smith, D.M., Yu, Y., Chang, S.C., Goldberg, A.L., and Cheng, Y. (2008). Mechanism of gate opening in the 20S proteasome by the proteasomal ATPases. Mol Cell *30*, 360-368.

Raiborg, C., and Stenmark, H. (2009). The ESCRT machinery in endosomal sorting of ubiquitylated membrane proteins. Nature *458*, 445-452.

Rani, N., Aichem, A., Schmidtke, G., Kreft, S.G., and Groettrup, M. (2012). FAT10 and NUB1L bind to the VWA domain of Rpn10 and Rpn1 to enable proteasome-mediated proteolysis. Nat Commun *3*, 749.

Rappsilber, J., Ishihama, Y., and Mann, M. (2003). Stop and go extraction tips for matrix-assisted laser desorption/ionization, nanoelectrospray, and LC/MS sample pretreatment in proteomics. Anal Chem *75*, 663-670.

Ravid, T., and Hochstrasser, M. (2007). Autoregulation of an E2 enzyme by ubiquitin-chain assembly on its catalytic residue. Nat Cell Biol *9*, 422-427.

Reyes-Turcu, F.E., Horton, J.R., Mullally, J.E., Heroux, A., Cheng, X., and Wilkinson, K.D. (2006). The ubiquitin binding domain ZnF UBP recognizes the C-terminal diglycine motif of unanchored ubiquitin. Cell *124*, 1197-1208.

Reyes-Turcu, F.E., Ventii, K.H., and Wilkinson, K.D. (2009). Regulation and cellular roles of ubiquitin-specific deubiquitinating enzymes. Annu Rev Biochem *78*, 363-397.

Richardson, P.G., Barlogie, B., Berenson, J., Singhal, S., Jagannath, S., Irwin, D., Rajkumar, S.V., Srkalovic, G., Alsina, M., Alexanian, R.*, et al.* (2003). A phase 2 study of bortezomib in relapsed, refractory myeloma. N Engl J Med *348*, 2609-2617.

Riedinger, C., Boehringer, J., Trempe, J.F., Lowe, E.D., Brown, N.R., Gehring, K., Noble, M.E., Gordon, C., and Endicott, J.A. (2010). Structure of Rpn10 and its interactions with polyubiquitin chains and the proteasome subunit Rpn12. J Biol Chem *285*, 33992-34003.

Roelofs, J., Park, S., Haas, W., Tian, G., McAllister, F.E., Huo, Y., Lee, B.H., Zhang, F., Shi, Y., Gygi, S.P.*, et al.* (2009). Chaperone-mediated pathway of proteasome regulatory particle assembly. Nature *459*, 861-865.

Rose, M.D., Winston, F., and Hieter, P. (1990). Methods in Yeast Genetics, A Laboratory Course Manual. Cold Spring Harbor Laboratory, Cold Spring Harbor, NY.

Rotin, D., and Kumar, S. (2009). Physiological functions of the HECT family of ubiquitin ligases. Nat Rev Mol Cell Biol *10*, 398-409.

Ryabov, Y., and Fushman, D. (2006). Interdomain mobility in di-ubiquitin revealed by NMR. Proteins *63*, 787-796.

Sadygov, R.G., Cociorva, D., and Yates, J.R., 3rd (2004). Large-scale database searching using tandem mass spectra: looking up the answer in the back of the book. Nat Methods *1*, 195-202.

Saeki, Y., Saitoh, A., Toh-e, A., and Yokosawa, H. (2002a). Ubiquitin-like proteins and Rpn10 play cooperative roles in ubiquitin-dependent proteolysis. Biochem Biophys Res Commun *293*, 986-992.

Saeki, Y., Sone, T., Toh-e, A., and Yokosawa, H. (2002b). Identification of ubiquitin-like protein-binding subunits of the 26S proteasome. Biochem Biophys Res Commun *296*, 813-819.

Saeki, Y., Toh, E.A., Kudo, T., Kawamura, H., and Tanaka, K. (2009). Multiple proteasome-interacting proteins assist the assembly of the yeast 19S regulatory particle. Cell *137*, 900-913.

Sahara, T., Goda, T., and Ohgiya, S. (2002). Comprehensive expression analysis of time-dependent genetic responses in yeast cells to low temperature. J Biol Chem *277*, 50015-50021.

Sakata, E., Bohn, S., Mihalache, O., Kiss, P., Beck, F., Nagy, I., Nickell, S., Tanaka, K., Saeki, Y., Forster, F.*, et al.* (2012). Localization of the proteasomal ubiquitin receptors Rpn10 and Rpn13 by electron cryomicroscopy. Proc Natl Acad Sci U S A *109*, 1479-1484.

Saksena, S., Sun, J., Chu, T., and Emr, S.D. (2007). ESCRTing proteins in the endocytic pathway. Trends Biochem Sci *32*, 561-573.

Schauber, C., Chen, L., Tongaonkar, P., Vega, I., Lambertson, D., Potts, W., and Madura, K. (1998). Rad23 links DNA repair to the ubiquitin/proteasome pathway. Nature *391*, 715-718.

Scheffner, M., Nuber, U., and Huibregtse, J.M. (1995). Protein ubiquitination involving an E1-E2-E3 enzyme ubiquitin thioester cascade. Nature *373*, 81-83.

Schlesinger, D.H., Goldstein, G., and Niall, H.D. (1975). The complete amino acid sequence of ubiquitin, an adenylate cyclase stimulating polypeptide probably universal in living cells. Biochemistry *14*, 2214-2218.

Schoel, B., Welzel, M., and Kaufmann, S.H. (1995). Quantification of protein in dilute and complex samples: modification of the bicinchoninic acid assay. J Biochem Biophys Methods *30*, 199-206.

Schrader, E.K., Harstad, K.G., and Matouschek, A. (2009). Targeting proteins for degradation. Nat Chem Biol *5*, 815-822.

Schreiner, P., Chen, X., Husnjak, K., Randles, L., Zhang, N., Elsasser, S., Finley, D., Dikic, I., Walters, K.J., and Groll, M. (2008). Ubiquitin docking at the proteasome through a novel pleckstrin-homology domain interaction. Nature *453*, 548-552.

Schulman, B.A., and Harper, J.W. (2009). Ubiquitin-like protein activation by E1 enzymes: the apex for downstream signalling pathways. Nat Rev Mol Cell Biol *10*, 319-331.

Schwarz, S.E., Rosa, J.L., and Scheffner, M. (1998). Characterization of human hect domain family members and their interaction with UbcH5 and UbcH7. J Biol Chem *273*, 12148-12154.

Schwechheimer, C. (2004). The COP9 signalosome (CSN): an evolutionary conserved proteolysis regulator in eukaryotic development. Biochim Biophys Acta *1695*, 45-54.

Seeger, M., Hartmann-Petersen, R., Wilkinson, C.R., Wallace, M., Samejima, I., Taylor, M.S., and Gordon, C. (2003). Interaction of the anaphase-promoting complex/cyclosome and proteasome protein complexes with multiubiquitin chain-binding proteins. J Biol Chem *278*, 16791-16796.

Seo, S.R., Lallemand, F., Ferrand, N., Pessah, M., L'Hoste, S., Camonis, J., and Atfi, A. (2004). The novel E3 ubiquitin ligase Tiul1 associates with TGIF to target Smad2 for degradation. EMBO J *23*, 3780-3792.

Seong, K.M., Baek, J.H., Ahn, B.Y., Yu, M.H., and Kim, J. (2007). Rpn10p is a receptor for ubiquitinated Gcn4p in proteasomal proteolysis. Mol Cells *24*, 194-199.

Seron, K., Blondel, M.O., Haguenauer-Tsapis, R., and Volland, C. (1999). Uracil-induced down-regulation of the yeast uracil permease. J Bacteriol *181*, 1793-1800.

Sharp, P.M., and Li, W.H. (1987). Ubiquitin genes as a paradigm of concerted evolution of tandem repeats. J Mol Evol *25*, 58-64.

Shekhtman, A., and Cowburn, D. (2002). A ubiquitin-interacting motif from Hrs binds to and occludes the ubiquitin surface necessary for polyubiquitination in monoubiquitinated proteins. Biochem Biophys Res Commun *296*, 1222-1227.

Shih, H.M., Chang, C.C., Kuo, H.Y., and Lin, D.Y. (2007). Daxx mediates SUMO-dependent transcriptional control and subnuclear compartmentalization. Biochem Soc Trans *35*, 1397-1400.

Shih, S.C., Prag, G., Francis, S.A., Sutanto, M.A., Hurley, J.H., and Hicke, L. (2003). A ubiquitin-binding motif required for intramolecular monoubiquitylation, the CUE domain. EMBO J *22*, 1273-1281.

Shih, S.C., Sloper-Mould, K.E., and Hicke, L. (2000). Monoubiquitin carries a novel internalization signal that is appended to activated receptors. EMBO J *19*, 187-198.

Sloper-Mould, K.E., Jemc, J.C., Pickart, C.M., and Hicke, L. (2001). Distinct functional surface regions on ubiquitin. J Biol Chem *276*, 30483-30489.

Smith, D.M., Chang, S.C., Park, S., Finley, D., Cheng, Y., and Goldberg, A.L. (2007). Docking of the proteasomal ATPases' carboxyl termini in the 20S proteasome's alpha ring opens the gate for substrate entry. Mol Cell *27*, 731-744.

Somesh, B.P., Sigurdsson, S., Saeki, H., Erdjument-Bromage, H., Tempst, P., and Svejstrup, J.Q. (2007). Communication between distant sites in RNA polymerase II through ubiquitylation factors and the polymerase CTD. Cell *129*, 57-68.

Song, L., and Rape, M. (2008). Reverse the curse--the role of deubiquitination in cell cycle control. Curr Opin Cell Biol *20*, 156-163.

Sowa, M.E., Bennett, E.J., Gygi, S.P., and Harper, J.W. (2009). Defining the human deubiquitinating enzyme interaction landscape. Cell *138*, 389-403.

Springael, J.Y., and Andre, B. (1998). Nitrogen-regulated ubiquitination of the Gap1 permease of Saccharomyces cerevisiae. Mol Biol Cell *9*, 1253-1263.

Stadtmueller, B.M., Ferrell, K., Whitby, F.G., Heroux, A., Robinson, H., Myszka, D.G., and Hill, C.P. (2010). Structural models for interactions between the 20S proteasome and its PAN/19S activators. J Biol Chem *285*, 13-17.

Stadtmueller, B.M., and Hill, C.P. Proteasome activators. Mol Cell *41*, 8-19.

Stamenova, S.D., Dunn, R., Adler, A.S., and Hicke, L. (2004). The Rsp5 ubiquitin ligase binds to and ubiquitinates members of the yeast CIN85-endophilin complex, Sla1-Rvs167. J Biol Chem *279*, 16017-16025.

Staub, O., Dho, S., Henry, P., Correa, J., Ishikawa, T., McGlade, J., and Rotin, D. (1996). WW domains of Nedd4 bind to the proline-rich PY motifs in the epithelial Na+ channel deleted in Liddle's syndrome. EMBO J *15*, 2371-2380.

Stawiecka-Mirota, M., Pokrzywa, W., Morvan, J., Zoladek, T., Haguenauer-Tsapis, R., Urban-Grimal, D., and Morsomme, P. (2007). Targeting of Sna3p to the endosomal pathway depends on its interaction with Rsp5p and multivesicular body sorting on its ubiquitylation. Traffic *8*, 1280-1296.

Steen, H., Jebanathirajah, J.A., Springer, M., and Kirschner, M.W. (2005). Stable isotope-free relative and absolute quantitation of protein phosphorylation stoichiometry by MS. Proc Natl Acad Sci U S A *102*, 3948-3953.

Stephen, A.G., Trausch-Azar, J.S., Ciechanover, A., and Schwartz, A.L. (1996). The ubiquitin-activating enzyme E1 is phosphorylated and localized to the nucleus in a cell cycle-dependent manner. J Biol Chem *271*, 15608-15614.

Su, V., and Lau, A.F. (2009). Ubiquitin-like and ubiquitin-associated domain proteins: significance in proteasomal degradation. Cell Mol Life Sci *66*, 2819-2833.

Sun, Z.W., and Allis, C.D. (2002). Ubiquitination of histone H2B regulates H3 methylation and gene silencing in yeast. Nature *418*, 104-108.

Szlanka, T., Haracska, L., Kiss, I., Deak, P., Kurucz, E., Ando, I., Viragh, E., and Udvardy, A. (2003). Deletion of proteasomal subunit S5a/Rpn10/p54 causes lethality, multiple mitotic defects and overexpression of proteasomal genes in Drosophila melanogaster. J Cell Sci *116*, 1023-1033.

Taylor, S.V., Kelleher, N.L., Kinsland, C., Chiu, H.J., Costello, C.A., Backstrom, A.D., McLafferty, F.W., and Begley, T.P. (1998). Thiamin biosynthesis in Escherichia coli. Identification of ThiS thiocarboxylate as the immediate sulfur donor in the thiazole formation. J Biol Chem *273*, 16555-16560.

Thompson, D., Hakala, K., and DeMartino, G.N. (2009). Subcomplexes of PA700, the 19 S regulator of the 26 S proteasome, reveal relative roles of AAA subunits in 26 S proteasome assembly and activation and ATPase activity. J Biol Chem *284*, 24891-24903.

Thrower, J.S., Hoffman, L., Rechsteiner, M., and Pickart, C.M. (2000). Recognition of the polyubiquitin proteolytic signal. EMBO J *19*, 94-102.

Tian, G., Park, S., Lee, M.J., Huck, B., McAllister, F., Hill, C.P., Gygi, S.P., and Finley, D. (2011). An asymmetric interface between the regulatory and core particles of the proteasome. Nat Struct Mol Biol *18*, 1259-1267.

Tomko, R.J., Jr., and Hochstrasser, M. (2011). Incorporation of the Rpn12 subunit couples completion of proteasome regulatory particle lid assembly to lid-base joining. Mol Cell *44*, 907-917.

Trotman, L.C., Wang, X., Alimonti, A., Chen, Z., Teruya-Feldstein, J., Yang, H., Pavletich, N.P., Carver, B.S., Cordon-Cardo, C., Erdjument-Bromage, H*., et al.* (2007). Ubiquitination regulates PTEN nuclear import and tumor suppression. Cell *128*, 141-156.

Ulrich, H.D., and Walden, H. (2010). Ubiquitin signalling in DNA replication and repair. Nat Rev Mol Cell Biol *11*, 479-489.

Upadhya, S.C., and Hegde, A.N. (2003). A potential proteasome-interacting motif within the ubiquitin-like domain of parkin and other proteins. Trends Biochem Sci *28*, 280-283.

van der Horst, A., de Vries-Smits, A.M., Brenkman, A.B., van Triest, M.H., van den Broek, N., Colland, F., Maurice, M.M., and Burgering, B.M. (2006). FOXO4 transcriptional activity is regulated by monoubiquitination and USP7/HAUSP. Nat Cell Biol *8*, 1064-1073.

van Nocker, S., Sadis, S., Rubin, D.M., Glickman, M., Fu, H., Coux, O., Wefes, I., Finley, D., and Vierstra, R.D. (1996). The multiubiquitin-chain-binding protein Mcb1 is a component of the 26S proteasome in Saccharomyces cerevisiae and plays a nonessential, substrate-specific role in protein turnover. Mol Cell Biol *16*, 6020-6028.

Ventii, K.H., and Wilkinson, K.D. (2008). Protein partners of deubiquitinating enzymes. Biochem J *414*, 161-175.

Verma, R., Aravind, L., Oania, R., McDonald, W.H., Yates, J.R., 3rd, Koonin, E.V., and Deshaies, R.J. (2002). Role of Rpn11 metalloprotease in deubiquitination and degradation by the 26S proteasome. Science *298*, 611-615.

Verma, R., Oania, R., Graumann, J., and Deshaies, R.J. (2004). Multiubiquitin chain receptors define a layer of substrate selectivity in the ubiquitin-proteasome system. Cell *118*, 99-110.

Villen, J., and Gygi, S.P. (2008). The SCX/IMAC enrichment approach for global phosphorylation analysis by mass spectrometry. Nat Protoc *3*, 1630-1638.

Virdee, S., Ye, Y., Nguyen, D.P., Komander, D., and Chin, J.W. (2010). Engineered diubiquitin synthesis reveals Lys29-isopeptide specificity of an OTU deubiquitinase. Nat Chem Biol *6*, 750-757.

Volker, C., and Lupas, A.N. (2002). Molecular evolution of proteasomes. Curr Top Microbiol Immunol *268*, 1-22.

Wagner, S., Carpentier, I., Rogov, V., Kreike, M., Ikeda, F., Lohr, F., Wu, C.J., Ashwell, J.D., Dotsch, V., Dikic, I.*, et al.* (2008). Ubiquitin binding mediates the NF-kappaB inhibitory potential of ABIN proteins. Oncogene *27*, 3739-3745.

Wagner, S.A., Beli, P., Weinert, B.T., Nielsen, M.L., Cox, J., Mann, M., and Choudhary, C. (2011). A proteome-wide, quantitative survey of in vivo ubiquitylation sites reveals widespread regulatory roles. Mol Cell Proteomics *10*, M111 013284.

Wang, G., McCaffery, J.M., Wendland, B., Dupre, S., Haguenauer-Tsapis, R., and Huibregtse, J.M. (2001). Localization of the Rsp5p ubiquitin-protein ligase at multiple sites within the endocytic pathway. Mol Cell Biol *21*, 3564-3575.

Wang, G., Yang, J., and Huibregtse, J.M. (1999). Functional domains of the Rsp5 ubiquitin-protein ligase. Mol Cell Biol *19*, 342-352.

Wang, Q., Young, P., and Walters, K.J. (2005). Structure of S5a bound to monoubiquitin provides a model for polyubiquitin recognition. J Mol Biol *348*, 727-739.

Wang, T., Yin, L., Cooper, E.M., Lai, M.Y., Dickey, S., Pickart, C.M., Fushman, D., Wilkinson, K.D., Cohen, R.E., and Wolberger, C. (2009). Evidence for bidentate substrate binding as the basis for the K48 linkage specificity of otubain 1. J Mol Biol *386*, 1011-1023.

Watkins, J.F., Sung, P., Prakash, L., and Prakash, S. (1993). The Saccharomyces cerevisiae DNA repair gene RAD23 encodes a nuclear protein containing a ubiquitin-like domain required for biological function. Mol Cell Biol *13*, 7757-7765.

Wei, N., and Deng, X.W. (2003). The COP9 signalosome. Annu Rev Cell Dev Biol *19*, 261-286.

Wenzel, D.M., Stoll, K.E., and Klevit, R.E. (2011). E2s: structurally economical and functionally replete. Biochem J *433*, 31-42.

Wickliffe, K., Williamson, A., Jin, L., and Rape, M. (2009). The multiple layers of ubiquitin-dependent cell cycle control. Chem Rev *109*, 1537-1548.

Wilkins, M.R., Pasquali, C., Appel, R.D., Ou, K., Golaz, O., Sanchez, J.C., Yan, J.X., Gooley, A.A., Hughes, G., Humphery-Smith, I.*, et al.* (1996). From proteins to proteomes: large scale protein identification by two-dimensional electrophoresis and amino acid analysis. Biotechnology (N Y) *14*, 61-65.

Wilkinson, C.R., Seeger, M., Hartmann-Petersen, R., Stone, M., Wallace, M., Semple, C., and Gordon, C. (2001). Proteins containing the UBA domain are able to bind to multi-ubiquitin chains. Nat Cell Biol *3*, 939-943.

Woelk, T., Oldrini, B., Maspero, E., Confalonieri, S., Cavallaro, E., Di Fiore, P.P., and Polo, S. (2006). Molecular mechanisms of coupled monoubiquitination. Nat Cell Biol *8*, 1246-1254.

Wolfe, K.H., and Li, W.H. (2003). Molecular evolution meets the genomics revolution. Nat Genet *33 Suppl*, 255-265.

Xie, Y., and Varshavsky, A. (2000). Physical association of ubiquitin ligases and the 26S proteasome. Proc Natl Acad Sci U S A *97*, 2497-2502.

Xu, P., Duong, D.M., Seyfried, N.T., Cheng, D., Xie, Y., Robert, J., Rush, J., Hochstrasser, M., Finley, D., and Peng, J. (2009). Quantitative proteomics reveals the function of unconventional ubiquitin chains in proteasomal degradation. Cell *137*, 133-145.

Yang, B., and Kumar, S. (2010). Nedd4 and Nedd4-2: closely related ubiquitin-protein ligases with distinct physiological functions. Cell Death Differ *17*, 68-77.

Yao, T., and Cohen, R.E. (2002). A cryptic protease couples deubiquitination and degradation by the proteasome. Nature *419*, 403-407.

Yao, T., Song, L., Xu, W., DeMartino, G.N., Florens, L., Swanson, S.K., Washburn, M.P., Conaway, R.C., Conaway, J.W., and Cohen, R.E. (2006). Proteasome recruitment and activation of the Uch37 deubiquitinating enzyme by Adrm1. Nat Cell Biol *8*, 994-1002.

Yates, J.R., 3rd, Eng, J.K., and McCormack, A.L. (1995). Mining genomes: correlating tandem mass spectra of modified and unmodified peptides to sequences in nucleotide databases. Anal Chem *67*, 3202-3210.

Ye, Y., and Rape, M. (2009). Building ubiquitin chains: E2 enzymes at work. Nat Rev Mol Cell Biol *10*, 755-764.

Zhang, D., Chen, T., Ziv, I., Rosenzweig, R., Matiuhin, Y., Bronner, V., Glickman, M.H., and Fushman, D. (2009a). Together, Rpn10 and Dsk2 can serve as a polyubiquitin chain-length sensor. Mol Cell *36*, 1018-1033.

Zhang, N., Wang, Q., Ehlinger, A., Randles, L., Lary, J.W., Kang, Y., Haririnia, A., Storaska, A.J., Cole, J.L., Fushman, D*., et al.* (2009b). Structure of the s5a:k48-linked diubiquitin complex and its interactions with rpn13. Mol Cell *35*, 280-290.

Ziv, I., Matiuhin, Y., Kirkpatrick, D.S., Erpapazoglou, Z., Leon, S., Pantazopoulou, M., Kim, W., Gygi, S.P., Haguenauer-Tsapis, R., Reis, N*., et al.* (2011). A perturbed ubiquitin landscape distinguishes between ubiquitin in trafficking and in proteolysis. Mol Cell Proteomics *10*, M111 009753.

Resum de la Tesi en Català

Introducció

La molécula d'Ubicuitina i la seva versatilitat en la senyalització cel·lular

Les proteïnes d'una cèl·lula eucariota es sotmeten a una gran varietat de modificacions post-traduccionals. Aquestes augmenten en gran mesura la diversitat funcional i la dinàmica del proteoma. Les proteïnes poden ser modificades per petites molècules com ara grups fosfat, metil o acetil, o per a certes proteïnes, com per exemple la ubicuitina. La molècula d'ubicuitina es va descriure a finals dels 70 -principis dels 80- i des de llavors, la investigació dedicada a la ubicuitina (Ub) i a les seves proteïnes relacionades (UBLS, Ubiquitin Like Proteins) ha aconseguit desxifrar el seu rol en múltiples rutes biològiques, fent de la ubicuitina una de les molècules més versàtils de la cèl·lula.

El sistema d'ubicuitina es troba en tots els organismes eucariotes i participa en la regulació de múltiples i diversos processos cel·lulars, com ara la degradació de proteïnes mitjançant el proteasoma, processament d'antígens, apoptosi, biogènesi d'orgànuls, divisió i cicle cel·lular, transcripció i reparació de l'ADN, diferenciació i desenvolupament, sistema immunitari, degeneració neuronal i muscular, morfogènesi de les xarxes neuronals, regulació dels receptors de superfície cel·lular, resposta estrès i biogènesi dels ribosomes.

El sistema Ubicuitina Proteasoma

La ubicuitina és una proteïna de 76 aminoàcids (8,5 KDa) altament conservada en sistemes eucariotes que té la propietat de formar conjugats covalents amb altres proteïnes o amb sí mateixa. En la seva forma funcional, és la glicina situada a l'extrem C-terminal (Gly76) la que estableix un enllaç iso-peptídic amb el grup ε-amino d'una lisina de la proteïna receptora. Perquè aquest fet tingui lloc es requereix la reacció coordinada de tres enzims. En primer lloc, un enzim activador d'ubicuitina (E1) que hidrolitza l'ATP i adenila una molècula d'Ub. Després aquesta és transferida al lloc actiu de la cisteïna d'E1, coincidint amb l'adenilació d'una segona Ub. Aquesta ubicuitina adenilada és transferida a un enzim conjugador d'Ub (o E2) i finalment és un membre de la família de les ubicuitina lligasa (o E3) que reconeix la proteïna substrat i catalitza la transferència d'Ub des de l'E2 a la proteïna receptora. Si aquesta cascada enzimàtica es produeix cíclicament, es generen proteïnes poliubicuitinades que seran reconegudes per l'UPS. Així, és l'enzim E3 qui confereix l'especificitat del substrat al sistema. Existeixen un gran nombre d'E3 diferents en humans, indicant la gran quantitat de proteïnes possibles a ser degradades pel sistema ubicuitina proteasoma (UPS). A més, també existeix un grup de proteïnes capaces de poliubicuitinar substrats prèviament ubicuitinats anomenats E4. Tot i que no es coneix amb precisió la funció d'aquests enzims es postula que són factors potenciadors de la degradació.

El sistema d'Ub segueix una estructura jeràrquica on un nombre molt reduït d'E1 interacciona amb un major nombre d'E2. Aquest últim grup d'enzims pot interaccionar amb un gran ventall d'enzims E3, els quals, poden reconèixer diferents proteïnes substrats amb motius de reconeixement d'ubicuitina idèntics o similars. De totes maneres, aquesta jerarquització no es pot representar mitjançant una

simple estructura piramidal, sinó més aviat com una xarxa complexa d'interaccions superposades entre els seus múltiples components.

Enzims activadors d'Ubicuitina (E1)

La unió covalent de la molècula d'Ubicuitina a un substrat requereix de la seva activació mitjançant un enzim E1. En humans, s´han descrit dos enzims E1: UBA1 i UBA6, tot i que durant vàries dècades es va considerar UBA1 com l'únic membre d'aquesta família. S´ha descrit que cèl·lules portadores de mutacions termosensibles d'UBA1 aturen el seu cicle cel·lular entre les fases G2-M i mostren una disminució significativa de conjugats ubicuitinats. El mecanisme catalític de l'enzim UBA1 és el següent: el C-terminal de la ubicuitina, invariablement ocupat per una glicina en totes les seqüències d'ubicuitina, és adenilat i els adductes d'ubicuitina-AMP romanen units a l'enzim. En una segona etapa, l'adenilat d'Ub és atacat per la Cys catalítica d'UBA1, produint una unió covalent entre el tioéster sulfhidril de la Cys d'UBA1 i l'extrem C-terminal de la ubicuitina. Posteriorment, UBA1 catalitza la adenilació d'una segona molècula d'ubicuitina i es carrega asimètricament amb dues molècules d'ubicuitina. Finalment, UBA1 interactua físicament amb un E2 i es transfereix un tioéster, assegurant que el C-termianl de la Ub es transfereix a la Cys catalítica d'E2.

Enzims conjugadors d'Ubicuitina (E2)

Els E2 representen un grup conservat d'enzims que tenen un paper essencial per a la correcta conjugació d'Ub. L'activitat d'E2 influencia directament en el tipus de lisines que conformen les cadenes poluybiquitinades, per tant, en el destí cel·lular de la proteïna modificada. Els membres d'aquesta família es caracteritzen per la presència d'un domini de conjugació d'Ub (ubicuitin-conjugating catalytic, UBC) el qual actua de plataforma per a la unió entre E1, E3 i l'Ub prèviament activada.

Enzims d'Ubicuitina lligasa (E3)

A l'últim pas de la cascada enzimàtica, el complex E2-Ub s'associa amb un E3, el qual determinarà l'especificació amb el substrat. Els enzims d'Ub lligasa es poden bàsicament catalogar en dues subfamílies d'enzims: HECT (Homologous to E6AP C-Terminus) i RING (Really Interesting New Gene). Els enzims de la família HECT contenen una Cys activa la qual, previament a la lligació Ub i substrat, es carrega amb Ub mitjançant l'E2. En canvi, les RING lligases no contenen un residu actiu i uneixen simultàniament el conjunt E2-Ub i el substrat per promocionar la lligació.

HECT és un domini a C-terminal d'aproximadament 350 amino àcids i que es va descriure per primera vegada en el virus del papil·loma humà. El domini HECT consisteix en dos lòbuls, l'N- i C-terminal. El primer lòbul, l'N-terminal, representa dos terços del domini i està involucrat en la interacció amb l'E2. En canvi, el lòbul C-terminal conté la Cys activa que interacciona amb la molècula d'Ub. Junt amb el domini HECT, dos dominis a N-terminal defineixen la família de les lligases Nedd4: C2 i WW. El primer domini s'uneix amb molècules de calci, mentre que el segon reconeix motius PY (residus fosfo-serina/treonina) de la proteïna substrat.

La família de Nedd4 és el grup de lligases més intensament estudiat. Estan involucrades en diverses i múltiples funcions cel·lulars, en part, degut a la seva capacitat de mono- i poliubicuitinar una llarga llista

de substrats. El llevat S*accharomyces cerevisiae* expressa un únic membre de la familia de les lligases Nedd4: Rsp5. Rsp5 comparteix la mateixa arquitectura modular que altres lligases HECT: un domini C2 a N-terminal, tres dominis centrals WWW i un domini HECT a C-terminal. Rsp5 participa en múltiples funcions cel·lulars, com per exemple herència mitocondrial, ruta metabòlica dels àcids grassos, regulació transcriptòmica i endocítica, entre d'altres. La deleció del gen de Rsp5 és letal en llevat. S'ha descrit que Ubp2 és l'enzim que contrarresta l'activitat de Rsp5 *in vivo*.

Enzims de desubicuitinació (Dubs)

De la mateixa manera que els enzims E3 regulen la senyalització per Ub, també ho fan els enzims encarregats de regular el procés invers, anomenats enzims de desubicuitinació (Dubs). Els Dubs són proteases isopeptídiques que tallen específicament molècules d'Ub conjugades a un determinat substrat. Diferenciem dos grups segons els seu mecanisme enzimàtic: els que contenen un residu actiu de Cys i els que contenen un residu actiu de Zn.

Diferents productes d'ubicuitinació generen una àmplia senyal·lització cel·lular

La ubicuitinació inclou la modificació posttraduccional causada per una sola mol·lècula d'Ub, procés conegut com a monoubicuitinació, o per la formació de cadenes d'Ub unides a un determinat substrat, també conegut com a poliubicuitinació. Aquestes cadenes es poden propagar per enllaços successius en qualsevol de les 7 lisines que conté la seqüència d'Ub (Lys^{6}, Lys^{11}, Lys^{27}, Lys^{29}, Lys^{33}, Lys^{48} and Lys^{63}) o bé a través de la metionina de l'extrem N-terminal (M1).

Aquesta complexitat genera un model on el destí de les proteïnes modificades depèn del tipus i longitud del senyal de les cadenes de poliubicuitina, incloent-hi la monoubicuitinació com un senyal diferent. Dues evidències suporten aquest model. En primer lloc, cada tipus de cadena mostra una topologia i conformació diferent. Així, les cadenes ençallades a través de les Lys^{11} i Lys^{48} adopten una conformació més rígida, amb una elevada compactació dels monòmers d'Ub. En canvi, les cadenes enllaçades a través de la Lys63 mostren una conformació molt més relaxada i extesa. En segon lloc, les cèl·lules posseeixen motius o dominis capaços de reconèixer de manera específica cada tipus d'enllaç. Així, el senyal canònic de degradació el conformen cadenes que es propaguen per enllaços successius en la lisina 48 de la ubicuitina, de manera que les proteïnes que pateixin aquesta modificació seran senyalitzades cap al proteasoma i posteriorment, degradades. També s'han observat cadenes enllaçades per altres lisines (Lys^{63}) que constitueixen un tipus no canònic de poliubicuitinació, les quals estan involucrades en funcions com l'activació de les quinases IKK, la reparació de DNA o l'endocitosi. Recentment, s'ha descrit el rol de les cadenes enllaçades a través de la Lys^{11} en la regulació del cicle cel·lular.

La monoubicuitinació és una modificació no proteolítica reversible en què les proteïnes apareixen conjugades per una única molècula d'Ub. S'ha descrit que la monoubicuitilació és una modificació post-traduccional que controla la funció de proteïnes implicades en processos tals com l'endocitosi, regulació d'histones, reparació de DNA, expressió gènica i selecció proteica. A més, s'ha descrit que la presència del motiu UIM és essencial per a la monoubicuitinació de moltes proteïnes.

Superfícies d'interacció amb Ubicuitina

Hi ha diversos factors que estan involucrats en el reclutament de proteïnes poliubicuitinades. En la literatura científica s'han descrit els següents motius d'unió amb Ub: UBA (*Ubicuitin Associated*), UIM (*Ubicuitin Interacting Motif*), CUE (*Cuel-Homologous*), IUIM (*Inverted UIM*), ZnF-UBP i PRU (*Pleckstrin-like receptor*) de la subunitat proteasomal Rpn13. També s'ha descrit que la presència del motiu UIM funcional és essencial per a la monoubicuitilació acoblada de moltes proteïnes. S'ha descrit que hi ha 20 residus dins de la seqüència del motiu UIM que convergeixen per a un gran grup de proteïnes, sobretot el nucli hidrofòbic format per Φ-X-X-Ala-X-X-X-Ser-X-X-Ac on *Φ* representa un residu altament hidrofòbic i *Ac* un d'àcid. Mitjançant tècniques de ressonància magnètica nuclear i mutagènesi, s'ha demostrat que la regió hidrofòbica de la molècula d'ubicuitina constituïda pels aminoàcids Leucina[8], Isoleucina[44] i Valina[70] és important per a la interacció amb el motiu UIM. La superfície hidrofòbica de la molècula d'Ub, la Isoleucina[44], interacciona amb el grup metil d'una Alanina altament conservada del motiu UIM.

El proteasoma: element central de la fisiologia cel·lular

El destí d'una gran fracció de proteïnes ubicuitinades és el proteasoma, el complex on resideix l'activitat proteolítica. El proteasoma 26S és un complex multiproteic de més de 2,0 MDa present en nucli i citoplasma de totes les cèl·lules eucariotes i *Archaebacteria*. És el responsable del 80 % de la proteòlisi intracel·lular i representa un important mecanisme pel qual les cèl·lules controlen la concentració de determinades proteïnes mitjançant la seva degradació. El sistema ubicuitina-proteasoma (UPS) no només està relacionat amb la degradació de proteïnes malmeses o parcialment desnaturalitzades, sinó que també està involucrat en processos tan diversos com el control del cicle cel·lular, tràfic de proteïnes, regulació de la transcripció, patologies neurodegeneratives, apoptosi o oncogènesi, i probablement en molts altres processos.

El proteasoma (26S) està format per una partícula nucli (PN, 20S) i dues partícules regulatòries (19S). El nucli conté una cavitat tancada on les proteïnes són degradades i consta de 4 anells heptamèrics apilats, compostos per dos tipus diferents de subunitats; les subunitats α i les subunitats β. Els dos anells exteriors estan compostos de subunitats α que serveixen d'ancoratge a les partícules regulatòries i de "canal", evitant l'entrada desregulada de proteïnes a la cavitat interior. Els dos anells interns, compostos de subunitats β, contenen els llocs actius de les proteases que realitzen les reaccions catalítiques. Les partícules regulatòries (PR) o 19S consisteixen de com a mínim 17 proteïnes integrals, les quals es poden dividir en dos grups; una base de 9 proteïnes, que s'uneix directament a l'anell α exterior del nucli 20S i una "tapa" de 8 proteïnes (Rpn3, Rpn5-Rpn9, Rpn11-Rpn12). De les 9 proteïnes de la base, 6 són ATPases de la família AAA i tres no ATPases, Rpn1, Rpn2 i Rpn10. Les subunitats ATPases exhibeixen activitat *unfoldasa*, capaç de desplegar les proteïnes, actuant de manera similar, però inversa, a les xaperones. Simultàniament al procés de *unfolding*, es dóna la translocació de la proteïna a la partícula nucli.

Des què una proteïna és modificada per una cadena poliubicuitinada fins que és degradada pel proteasoma es donen uns passos, la regulació dels quals és crítica per a una correcta proteòlisi: (**i.**) unió del substrat poliubicuitinat a la PR del 26S, (**ii.**) desubicuitinació i desdoblament del substrat i (es

desconeix quin dels dos passos és el limitant en la reacció de proteòlisi) (**iii.**) translocació a la PN i posterior degradació de la proteïna en pèptids curts.

Rpn10: diferents funcions segons la seva localització cel·lular

La subunitat no ATPasa Rpn10 o S5a (llevat de gemmació i humans, respectivament) presenta el motiu UIM (*Ubicuitin-Interacting Motif*) d'unió a cadenes poliubicuitinades. Aquest fet li confereix un paper important en el reconeixement i posterior degradació de proteïnes poliubicuitinades. Tanmateix, la mutació nul·la de Rpn10 en llevat no és letal i mostra fenotips poc severs en estrès proteolític, manifestant que Rpn10 no és l'únic lloc d'ancoratge de proteïnes poliubicuitinades. Un segon grup de proteïnes d'unió de cadenes PUb són les proteïnes adaptadores que poden intervenir proporcionant llocs de reclutament alternatius, com per exemple, Rad23 i Dsk2. Aquestes són conegudes com a proteïnes UBA-UBL ja que tenen la propietat dual d'unir-se a poliubicuitina mitjançant el domini UBA (*Ubicuitin-Associated*) i a receptors del 26S, com Rpn1, mitjançant el domini UBL (*Ubicuitin-Like*). Així, les proteïnes UBA-UBL exerceixen de mediadors entre proteïnes poliubicuitinades i el proteasoma, suggerint un possible nivell de regulació del procés de degradació. També es coneix la capacitat de Rpn13 i Rpt5, una de les sis ATPases de la base de la PR d'unir ubicuitina. Un cop la proteïna ubicuitinada és reconeguda pel 19S serà desubicuitinada per enzims de desubicuitilació, tals com Rpn11 i Ubp6, i translocada a l'interior de la PN per tal de ser degradada.

Una altra propietat de Rpn10 és que a part de ser una subunitat intrínseca del proteasoma, també es troba en fraccions citosòliques. La fracció soluble de Rpn10 impedeix la formació de forquilles de cadenes de Ub no-degradables i, en conseqüència, estimula la degradació de certs substrats. A més a més, la fracció extra-proteasomal de Rpn10 també inhibeix l'accés de Dsk2 al proteasoma.

Objectius

La regulació del proteasoma és un aspecte biològic fonamental relacionat amb múltiples processos cel·lulars. La finalitat d'aquest projecte és la comprensió de la ubicuitinació *en* i *del* proteasoma ja que pot ser crucial a l'hora d'entendre patologies on hi hagi una implicació del sistema ubicuitina-proteasoma, tals com el càncer i algunes malalties neurodegeneratives en què es formen agregats proteics rics en proteasoma i ubicuitina (Parkinson, Alzheimer, esclerosi lateral amiotròfica, malalties priòniques i de poliQ).

Cobrir el significat biològic de la monoubicuitinació de Rpn10 (Rpn10-mUb) ha estat l'eix central d'aquest treball. Aquest objectiu s'ha desglossat en els punts següents:

1. Caracterització de Rpn10 ubicuitinat segons la seva localització cel·lular.
2. Esbrinar els enzims ubicuitina lligasa i de desubicuitinació involucrats en la reacció de monoubicuitinació de Rpn10. Establir la participació d'amdós enzims i reproduir la reacció de monoubicuitinació de Rpn10 *in vitro*.
3. Definir el paper del motiu UIM en la monoubicuitinació de Rpn10.
4. Determinar la/les lisina/es de Rpn10 modificades per Ub mitjançant espectrometria de masses i l'expressió de Rpn10 WT i varis mutants en *Saccharomyces cerevisiae*.

5. Caracteritzar el rol i l'efecte de la monoubicuitinació de Rpn10 en un context proteasomal.
6. Definir la rellevància fisiològica i la distribució cel·lular de Rpn10-mUb sota diverses condicions d'estrès proteolític.
7. Caracterització dels residus específics de la monoubicuitinació diferencial de Rpn10 segons la seva localització cel·lular.
8. Establir estratègies d'enriquiment de poliubicuitinació seguides d'espectrometria de masses quantitativa per a identificar i quantificar substrats estabilitzats per la deleció de RPN10.
9. Comparar les proteïnes ubicuitinades i els seus residus modificats per Ub en el el doble mutant rad23 rpn10 sota condicions de creixement normal i de baixa temperatura.

Resultats i Discussió

Rpn10 està monoubicuitinat in vivo

En un estudi recent, s'ha demostrat que Rpn10 és degradat pel proteasoma i que Hul5 és la lligasa que està involucrada en aquest procés. Amb l'objectiu d'estudiar la significància fisiològica de la ubicuitinació de Rpn10 es va analitzar el seu estat en cultius de creixement exponencial. En anàlisis directes d'extractes cel·lulars es va detectar una banda immunorreactiva addicional amb una mobilitat menor, suggerint una modificació post-traduccional per ubicuitina. Posteriorment, es va purificar Rpn10 expressat d'un vector induïble i del seu propi locus cromosomal. En anàlisis de western blot, la mateixa banda i una segona banda es van tornar a observar.

Aquestes bandes van ser analitzades per espectròmetre de masses qualitativa. Comparant la recopilació de les seqüències obtingudes amb les d'una base de dades, es va comprovar que les bandes analitzades corresponien únicament a Rpn10 i Ub, i es va poder resoldre fins el 80% de la seqüència de Rpn10 (ràtio entre la seqüència teòrica i els pèptids assenyalats en verd), i el 100% de la seqüència d'ubicuitina. Per tant, mitjançant MS, es confirmà de manera inequívoca que la mostra de menor mobilitat electroforètica eren una espècie formada pels polipèptids de Rpn10 i Ub, la qual cosa indicava que Rpn10 està monoubicuitinat *in* vivo.

Rpn10 monoubicuitinat es troba en ambdós contextos proteasomal i no-proteasomal

Donat que una fracció significativa de Rpn10 no està unida al proteasoma, es va voler determinar el context cel·lular de Rpn10-mUb. Es van aillar fraccions riques en factors enzimàtics del sistema ubicuitina-proteasoma, així com de conjugats ubicuitinats i de Rpn10. Es va observar un patró complex d'ubicuitinació de Rpn10 que incloïa una forma abundant de Rpn10 monoubicuitinat, Rpn10 diubicuitinat i diverses bandes de Rpn10 poliubicuitinat. Es va repetir l'assaig amb fraccions que provenien d'una soca hul5Δ i les espècies de Rpn10 amb més de dos grups de ubicuitina van disminuir dràsticament. En canvi, les formes mono i diubicuitinades de Rpn10 es mantenien al mateix nivell que les mostres WT. Aquests resultats indicaven que la monoubicuitinació de Rpn10 era independent de Hul5 i, per tant, els conjugats d´ubicuitina de Rpn10 eren generats, com a mínim, per dues activitats conjugadores d´ubicuitina: una desconeguda que catalitzaria la síntesi de Rpn10 mono- i diubicuitilat, i una altra depenent de Hul5, que sintetitzaria els conjugats més llargs.

Per tal de corroborar la observació de la monoubicuitinació fisiològica de Rpn10, es va dur a terme un fraccionament d'extractes totals mitjançant cromatografia d'exclusió molecular. Les fraccions es van analitzar per immunodetecció de Rpn10 i d'altres subunitats del proteasoma com Rpn12 (subunitat de la tapa de la PR) i α7 (proteïna de la PN). Es va detectar la forma modificada de Rpn10 en fraccions proteasomals i citosòliques.

La ubicuitina lligasa Rsp5 i l'enzim de desubicuitinació Ubp2 regulen la reacció de monoubicuitinació de Rpn10

A més d'una interacció funcional amb el proteasoma, una característica de l'enzim E3 que buscàvem era una catàlisi eficient en reaccions de monoubicuitinació. Una E3 que s'ajusta a aquest segon requisit és Rsp5, ortòleg de NEDD4.2 en mamífers, que està implicat en molts processos cel·lulars en *Saccharomyces cerevisiae* i forma part d'una gran família de proteïnes que controlen processos anàlegs en cèl·lules de mamífer. Rsp5 forma un complex amb el l'enzim de desubicuitinació Ubp2. En una cerca proteòmica de substrats de Rsp5, Rpn10 va donar positiu. En conseqüència es va analitzar la suposada participació dels enzims Rsp5 i Ubp2 en la monoubicuitinació de Rpn10. Es va comparar l'estat de Rpn10 en les soques següents: salvatge, mutant termosensible de *rsp5-1* i la doble deleció de Rsp5 i Ubp2. Es va observar com la presència de Rpn10-mUb era completament dependent de l'activitat de Rsp5, suggerint que Rsp5 era la principal lligasa *in vivo*. A més a més, en absència d'Ubp2, els nivells de Rpn10-mUb augmentaven significativament.

Amb l'objectiu d'aprofundir en l'activitat desubicuitinasa d'Ubp2, també es va considerar la possible activitat d'Ubp6 (enzim relacionat amb Hul5 i associat amb desubicuitinació de substrats en el 26S) sobre la mUb de Rpn10. Es varis assajos bioquímics es va comprovar com la forma mUb de Rpn10 era processada per ambdós enzims Ubp2 i Ubp6, però el primer era molt més eficient en la reacció.

Monoubicuitinació de Rpn10 in vitro

Per establir la participació directa de Rsp5 en la catàlisi de Rpn10 monoubicuitinat es va reconstituir la reacció enzimàtica *in vitro*. Es van incubar les formes recombinants i proteasomals de Rpn10 amb E1, Ubc4, Rsp5, Ub i ATP, obtenint com a producte majoritari de la reacció Rpn10-mUb i, en segon terme, la seva forma diubicuitinada (Rpn10-Ub_2).

El motiu UIM és necessari per a la monoubicuitinació de Rpn10

La família de la Ub lligasa Nedd4 detecta substrats que contenen motius PPY i UIM. Aquesta última interacció proteïna-proteïna normalment requereix un motiu UIM funcional i promou el que s'anomena "monoubicuitinacio acoblada". Al realitzar reaccions d'ubicuitinació *in vitro* es va trobar que en proteasomes en què l'UIM apareixia mutat, la monoubicuitilació de Rpn10 disminuia dràsticament. En conseqüència, la ubicuitinació de Rpn10 és depenent del motiu UIM.

Identificació de les lisines de Rpn10 modificades per ubicuitina

Es va optimitzar la reacció *in vitro* de monoubicuitinació de Rpn10 per tal d'obtenir elevades quantitats de Rpn10-mUb i poder analitzar-ho per espectrometria de masses (MS). L'anàlisi proteòmic va revelar que la mUb de Rpn10 tenia lloc a les lisines 71, 84 i 99 i 268 de la seqüència de Rpn10. Les tres primeres

lisines es localitzen al domini VWA, mentre que la última es troba a l'extrem C-terminal de Rpn10. La lisina 84 fou la majoritària amb un 52% dels pètids modificats per diglicina (Gly-Gly). Per a una caracterització més profunda, es va dur a terme un estudi genètic amb diferents mutants de Rpn10. En el mutant K84R, es va observar una dràstica disminució de Rpn10-mUb, reforçant els resultats obtinguts per per proteòmica.

Rpn10 monoubicuitinat mostra una baixa afinitat pels conjugats ubicuitinats

Amb l'objectiu de comprendre la funció biològica de la monoubicuitilació de Rpn10 es va plantejar si la presència d'un grup d'ubicuitina lligat covalentment a Rpn10 podria imposar alguna restricció en la seva capacitat per interaccionar amb substrats. La nostra hipòtesi de partida va ser que la monoubicuitilació de Rpn10 podia influenciar negativament en el reclutament de substrats poliubicuitilats al proteasoma, ja que la molècula d'ubicuitina unida a Rpn10 podria competir avantatjosament amb els substrats per l'accessibilitat al motiu UIM de Rpn10. Mitjançant assajos de fixació, es van comparar les capacitats de interacció de vàries formes de Rpn10-mUb amb cadenes pures d'Ub i conjugats ubicuitinats. En tots els casos es comprovà com la forma salvatge de Rpn10 tenia una gran afinitat per les formes ubicuitinades, mentre que Rpn10-mUb era incapaç d'interactuar. Cal subratllar que la interacció entre la molècula d'Ub i el motiu UIM de Rpn10 recau en la butxaca hidrofòbica de la superfície d'Ub (Leu8, Ile44, Val70) i l'alanina 231 de Rpn10. Així, el mutant de la forma ubicuitilada de Rpn10 (Rpn10-Ub^{I44A}) era un bon control per a l'esmentada reacció de fixació ja que havia de recuper la funció de la forma salvatge de Rpn10. Mitjançant assajos de fixació *in vitro*, es va poder comprovar que existeix una interacció en *cis* entre la molècula d'ubicuitina i el motiu UIM de Rpn10 i que aquesta unió inhibeix la capacitat de Rpn10 per a reclutar substrats poliubicuitilats al proteasoma 26S.

La monoubicuitinació de Rpn10 disminueix la capacitat proteolítica del proteasoma

En aquest punt, havíem demostrat que Rpn10-mUb exhibia una reduïda afinitat per cadenes de poliubicuitina i substrats poliubicuitinats, però no havíem provat el seu efecte en l'activitat del proteasoma. Per adreçar aquesta qüestió es va dur a terme la monitorització de la degradació del substrat poliubucuitinat ciclina B, afegint quantitats equimolars de Rpn10 i Rpn10-Ub en proteasomes rpn10Δ. Altra vegada, es va comprovar com la velocitat de degradació de la ciclina B es va incrementar significativament amb la presència de Rpn10, una mica quan es va afegir el mutant Rpn10-Ub^{I44A} i substancialment inhibida en absència de Rpn10 o l'addició de Rpn10-mUb. Aquests assajos ens van permetre concloure que la forma monoubicuitinada de Rpn10 no només era incapaç d'interaccionar amb substrats poliubicuitinats però també tenia un efecte directe sobre l'activitat proteolítica del 26S.

La forma monoubicuitinada de Rpn10 es redueix sota condicions d'estrès proteolític

Els resultats mostrats fins ara suggerien que la mUb de Rpn10 regulava la seva capacitat per unir substrats ubicuitinats. Ens vam preguntar si els nivells de Rpn10-mUb es podien veure afectats sota condicions d'estrès proteolític, on una elevada activitat proteolítica és necessària. Es va detectar una disminució dràstica de Rpn10-mUb en cèl·lules sotmeses a estrès per calor (37ºC) i fred (14ºC), així com per l'addició de cadmi (compost que promou l'estrès proteolític). En canvi, sota xocs osmòtics o de dany al DNA, la forma mUb de Rpn10 no es va veure afectada.

Només la forma proteasomal de Rpn10-mUb es veu afectada sota condicions d'estrès proteolític

S'ha demostrat que la forma mUb de Rpn10 es perd sota determinades condicions d'estrès, quan es requereix l'activitat de Rpn10. No obstant això, es desconeixia si la pèrdua de Rpn10-mUb afectava a ambdues fraccions cel·lulars de la proteïna. Així, es va dur a terme un fraccionament d'extractes totals sotmesos a diferents condicions d'estrès, on es van detectar dos patrons cel·lulars ben diferenciats. Patró 1: estrès no proteolític (xoc osmòtic) en què Rpn10-mUb es manté constant en ambdues fraccions. Patró 2: estrès proteolític (xoc tèrmic a baixa temperatura) en què la fracció proteasomal de Rpn10-mUb desapareix, mentre que la citosòlica es manté. Aquests resultats van suggerir que ambdues fraccions de Rpn10-mUb estaven regulades diferencialment.

La forma monoubicuitinada de Rpn10 no es pot unir al domini UBL de Dsk2

La forma extraproteasomal de Rpn10 restringeix l'accés de Dsk2 al proteasoma, mantenint el correcte funcionament del sistema ubicuitina-proteasoma. S'ha descrit que el domini Dsk2 té més afinitat per la monoubicuitina que Rpn10, i que aquest últim prefereix interaccionar amb el domini UBL de Dsk2 que no pas amb la monoubicuitina. Amb aquestes premises, mitjançant assajos de fixació es va voler esbrinar si el motiu UBL de Dsk2 podria competir amb l'UIM de Rpn10-mUb. Es va demostrar que Rpn10 Ub no podia unir-se a UBL-Dsk2.

Caracterització dels residus específics de la monoubicuitinació diferencial de Rpn10 segons la seva localització cel·lular

Rpn10 es poli-monoubicuitina a les lisines 71, 84, 99 (localitzades al domini VWA) i 268 (a l'extrem C-terminal de la proteïna), sent la Lys^{84} la diana principal de Rsp5. Donat que sota condicions d'estrès s'observen diferents patrons de Rpn10-Ub i que la Lys^{84} es localitza en el domini VWA (responsable de la interacció de Rpn10 amb altres subunitats del proteasoma), fou del nostre interès esbrinar si hi havia una selecció negativa de la utilització de les lisines 84 i 268 degut a una reduïda accessibilitat de la Lys^{84} al proteasoma. Aquest objectiu es va plantejar a través de la unió de les tècniques existents de biologia molecular i de proteòmica quantitativa, en particular AQUA. AQUA ens va permetre revelar la quantitat d'ambdues Lys^{84} i Lys^{268} en les diferents fraccions de Rpn10. Es va demostrar que, independentment de la localització cel·lular de Rpn10, la Lys^{84} era el residu majoritari en Rpn10-mUb, reforçant el paper del domini VWA en aquesta modificació.

Desxifrar els substrats de Rpn10 mitjançant estratègies d'enriquiment de poliubicuitina

Un dels reptes per a desxifrar la biologia de la Ub és esquematitzar les xarxes de substrats i lligands dels components de l'UPS. Per tal d'esbrinar l'amplitud del paper de Rpn10 en la degració proteïca depenent del 26S, es van combinar tècniques d'enriquiment de l'ubicuitinoma cel·lular amb aproximacions de proteòmica quantitativa. Per adreçar aquest estudi es van comparar dues soques marcades metabòlicament amb isòtops pesats (SILAC): el doble mutant *rad23Δrpn10Δ* i *rad23Δ*. En total, més de 380 candidats ubicuitinats van ser identificats, dels quals 230 es van poder quantificar. S'han distribuït els substrats ubicuitinats en diferents funcions biològiques, éssent les proteïnes implicades en el processament de l'ARN les més abundants. Actualment estem combinant eines de biologia molecular i anàlisi bioinformatic per elucidar quines proteïnes són substrats de Rpn10 front les que no ho són.

Conclusions

1. Rpn10 és modificat per Ub *in vivo*. La forma monoubicuitilada de Rpn10 existeix en el propi proteasoma i en la seva fracció citosòlica, indicant que la forma Rpn10-Ub_1 és una forma genèrica i abundant en les cèl·lules de *S. cerevisiae*.
2. La ubicuitina lligasa Rsp5 i l'enzim de desubicuitinació Ubp2 regulen la reacció de monoubicuitinació de Rpn10. Aquesta reacció és independent de les activitats dels enzims lligasa Hul5 i de desubicuitinació Ubp6.
3. La reacció de monoubicuitilació de Rpn10 en el proteasoma i en la seva forma recombinant es reconstitueix molt eficientment *in vitro*. La forma no modificada de Rpn10 és molt inestable en el proteasoma. Aquesta pot ser fortament neutralitzada per la reacció de monoubicuitilació.
4. En reaccions d'ubicuitilació *in vitro* s'ha trobat que la ubicuitilació de Rpn10 és dependent del motiu UIM. En proteasomes on l'UIM està mutat, la forma mono-ubicuitilada de Rpn10 disminueix dràsticament.
5. Mitjançant espectrometria de masses i estudis genètics de Rpn10 s'ha trobat que Rpn10 es modificat per ubicuitina en les lisines 71, 84 i 99, localitzades al domini VWA, i 268, situada a l'extrem C-terminal de la seva seqüència.
6. Mitjançant assajos de fixació *in vitro*, es comprova que existeix una interacció en *cis* entre la molècula d'ubicuitina i el motiu UIM de Rpn10. Aquesta unió inhibeix la capacitat de Rpn10 per a reclutar substrats poliubicuitilats al proteasoma.
7. La forma modificada de Rpn10 disminueix la capacitat proteolítica del proteasoma. Amb el mutant Rpn10-Ub^{I44A} es recupera parcialment la seva activitat, demostrant que la monoubicuitinació de Rpn10 és un nou mecanisme de regulació de l'UPS.
8. La forma monoubicuitilada de Rpn10 disminueix dràsticament sota estressos proteolítics, mostrant la rellevància fisiològica d'aquesta modificació. Només la fracció de Rpn10-mUb unida al proteasoma es veu afectada per condicions d'estrès proteolític. Sota les mateixes condicions, la fracció citosòlica de Rpn10-mUb es manté constant.
9. Rpn10-mUb no pot unir-se al domini UBL de Dsk2, demostrant que la interacció Ub-UIM de Rpn10 no competeix amb el domini UBL de Dsk2.
10. Mitjançant tècniques quantitatives d'espectrometria de masses basades en el marcatge de pèptids amb isòtops pesats (AQUA) es determina que la Lys^{84} és la diana principal de Rsp5. Mitjançant AQUA es determina que no hi ha una selecció negativa de les Lys^{84} i Lys^{268} en funció de la localització cel·lular de Rpn10.
11. S'usen tècniques d'enriquiment de substrats poliubicuitinats i proteòmica quantitativa per elucidar els substrats que s'estabilitzen en cèl·lules on el gen de RPN10 està delecionat. S'han de dur a terme assajos bioquímics addicionals per descartar aquells substrats poliubicuitinats la degradació del quals no és dependent de Rpn10.

Appendix

Strain	Genotype	Reference
SUB62	***MATa lys2-801 leu2-3, 2-112 ura3-52 his3-Δ200 trp1-1***	**Finley *et al*., 1987**
Sub62 based strains (relevant genotype):		
SDL133	*rpn11::RPN11-TEVProA (HIS3)*	Leggett *et al*., 2002
SDL145	*rpn11::RPN11-TEVProA (HIS3) ubp6::URA3*	Leggett *et al*., 2002
SBC6	*rpn11::RPN11-TEVProA (HIS3) hul5::kanMX4*	Crosas *et al*., 2006
SBC50	*rpn11::RPN11-TEVProA (HIS3) Ubr1::kanMX4*	This study
SBC51	*rpn11::RPN11-TEVProA (HIS3) ufd4::kanMX4*	This study
SJR125	*[am] ubi1-Δ1::TRP1 ubi2-Δ2::ura3 ubi3-Δub-2 ubi4-Δ2::LEU2 arg4::HYG pdr5::ura3 [pUB221] [pUB100]*	Crosas *et al*., 2006
SBC9	*[am] ubi1-Δ1::TRP1 ubi2-Δ2::ura3 ubi3-Δub-2 ubi4-Δ2::LEU2 arg4::HYG pdr5::ura3 hul5::kanMX4 [pUB221] [pUB100]*	Crosas *et al*., 2006
SBC10	*[am] ubi1-Δ1::TRP1 ubi2-Δ2::ura3 ubi3-Δub-2 ubi4-Δ2::LEU2 arg4::HYG pdr5::ura3 Ubp6::kanMX4 [pUB221] [pUB100]*	This study
SY74	*rpt1::HIS3 rpn10::rpn10-uim-natMX pEL36 (TRP1)*	S. Elsasser
sJH177	*ubp6::URA3 rpn11::RPN11-TEV-ProA (HIS3) [pJH60]*	J. Hanna
SDL73	*MATα rpn11::RPN11-TEVProA (HIS3)*	Leggett *et al*., 2002
SY36	*rpt1::HIS3 pEL36 (TRP1)*	S. Elsasser
SBC52	*Rpn10::natMX*	This study
SBC53	*Rad23::KanMX4*	This study
SBC54	*Rpn10::natMX Rad23::KanMX4*	This study
YDS124	*Rsp5Δ::HIS3MX [Ycplac33pRSP5 URA3]*	Siepe and Jentsch, 2009
BY4741	***MATa his3Δ1 leu2Δ0 lys2Δ0 ura3Δ0***	**Brachmann *et al*., 1998**
BY4741 based strains (relevant genotype):		
SBC55	*ubp2::kanMX4*	Euroscarf
SBC56	*rpn10::RPN10-TAP (HIS3)*	Euroscarf
FY56	***MATa ura3-52 his4-912σR5 lys2Δ 128***	**Huibregtse *et al.*, 1997**
FY56 based strains:		
FW1808	*MATa rsp5-1 ura3-52 his4-912σR5 lys2Δ 128*	Huibregtse *et al.,* 1997
JYL01	*MATa ura3-52 his4-912σR5 lys2Δ 128 RPN10::URA3*	Lu *et al*., 2008
JYL02	*MATa rsp5-1 ura3-52 his4-912σR5 lys2Δ 128 RPN10::URA3*	Lu *et al*., 2008
JYL19	*MATa ura3-52 his4-912σR5 lys2Δ 128 RPN10::URA3 ubp2Δ::KanMX*	Lu *et al*., 2008
JYL20	*MATa rsp5-1 ura3-52 his4-912σR5 lys2Δ 128 RPN10::URA3 ubp2Δ::KanMX*	Lu *et al*., 2008

Table 3: Strains Used In This Study

Plasmid	Details	Reference
pMIC15	Ubiquitin fused at Ct of Rpn10 (pYES2)	This study
pMIC18	Rpn10 WT (pEG-KT)	Provided by Dr. H. Zhu
pMIC20	GST-Rpn10 K104R (pEG-KT)	This study
pMIC21	GST-Rpn10 K130, 133, 134R (pEG-KT)	This study
pMIC24	GST-Rpn10 NoStop (pGEX-4T-3)	This study
pMIC26	GST-Rpn10 Stop (pGEX-4T-3)	Crosas et al., 2006
pMIC27	Ubiquitin fused at Ct of GST-Rpn10 (pGEX-4T-3)	This study
pMIC28	Ubiquitin I44A fused at Ct of GST-Rpn10 (pGEX-4T-3)	This study
pMIC30	GST-Rpn10 K104, 130, 133, 134R (pEG-KT)	This study
pMIC33	Rpn10 WT (pYES2)	This study
pMIC39	Ubiquitin I44A fused at Ct of Rpn10 (pYES2)	This study
pMIC48	GST-Rpn10 K40R (pEG-KT)	This study
pMIC50	GST-Rpn10 K71R (pEG-KT)	This study
pMIC52	GST-Rpn10 K268R (pEG-KT)	This study
pMIC54	GST-Rpn10 K99, 104, 130, 133, 134R (pEG-KT)	This study
pMIC55	GST-Rpn10 K84R (pEG-KT)	This study
pMIC57	GST-Rpn10 K99R (pEG-KT)	This study
pMIC59	GST-Rpn10 K84, 268R (pEG-KT)	This study
pMIC60	GST-Rpn10 K99, 104, 130, 133, 134, 268R (pEG-KT)	This study
pMIC61	GST-Rpn10 K71, 84R (pEG-KT)	This study
pMIC63	GST-Rpn10 K84, 99, 268R (pEG-KT)	This study
pMIC65	GST-Rpn10 K71, 84, 99, 268R (pEG-KT)	This study
pMIC66	GST-Rpn10 K84, 99, 104, 130, 133, 134, 268R (pEG-KT)	This study
pMIC67	GST-Rpn10 K71, 84, 99, 104, 130, 133, 134, 268R (pEG-KT)	This study
pMIC69	GST-Rpn10 K40, 71, 84, 99, 104, 130, 133, 134, 268R (pEG-KT)	This study
pMIC70	GST-Rpn10 K84only (pEG-KT)	This study
pMIC72	GST-Ubiquitin I44A (pGEX-4T-1)	Provided by Dr. I. Dikic
pMIC73	GST.Ubiquitin (pGEX-4T-1)	This study
pMIC88	GST-Rpn10 K268only (pEG-KT)	This study
pMIC120	GST-Rpn10 K84, 268R (pGEX-4T-3)	This study
pMIC121	GST-Rpn10 K268R (pGEX-4T-3)	This study
pMIC98	GST-Rup1 (pGEX6p-2rbs)	This study
pMIC101	GST-Rup1-Ubp2 (pGEX6p-2rbs)	This study
pMIC109	6His-Dsk2 (pET21b)	Provided by Dr. S. Raasi

Table 4: Plasmid Vectors Used In This Study

Name	Sequence
Rpn10_NoTAG Fw	CGT AGG TAC CGA ATT CCA TGG TAT TGG AAG CTA CAG TG
Rpn10_NoTAG Fw	GCA TGT CGA CCT ATT TGT CTT GGT GTT GTT CAG G
Ubi4 FW	CTG AGT CGA CAT GCA GAT TTT CGT CAA GAC TTT G
Ubi4 Rev	CGA TGC GGC CGC CTA ACC ACC TCT TAG CCT TAG CAC AAG
UbI44A Fw	TCC AGA TCA ACA AAG ATT GGC CTT TGC CGG TAA GCA GCT A
K40R Fw	TCA TAT TTC AAG CCA GGA GAA ACA GCA ATC C
K71R Fw	CCG CCG AGT TTG GGA GGA TTC TTG CTG GAC T
K84R Fw	CGC AGA TCG AGG GTA GGC TGC ATA TGG CCA C
K99R Fw	CTC AGC ATC GCC AGA ATA GGG TCC AAC ATC AAA GGA TT
K104R Fw	TTG AAG CAT CGC CAG AAT AGG GTC CAA CAT CAA AGG ATT
K130-134R Fw	TTG ATC AGA TTG GCA AGA ACA CTG AGA AGG AAT AAT GTT GCC GTG
K268R Fw	AGC CTG AAC AAC ACC AAG ACA GAT AGC ATG GCA ATT CCC GGG
R84K Fw	GAC ACG CAG ATC GAG GGT AAG CTG CAT ATG GCC ACT GCG
R84K-EcoR1 Fw	CGT ACC GAA TTC CAT GGT ATT GGA AGC TAC AGT G
R84K-Sal1 Rev	CGC TAG TCG ACC TAT CTG TCT TGG TGT TGT TCA
Ub pGEX Fw	CTG ATC AAC AAA GAT TGA TCT TTG CCG GTA AGC AGC
Rup1-BamH1 Fw	CGT ACG GAT CCA TGA TGG ATA ATC AGG CTG TAA AG
Rup1-SpeI Rev	CGG TAA CTA GTC TAA TTA TCA GAA TCG ATG TCA TC
Ubp2-Sac1 Fw	CGT ACG AGC TCA TGC CGA ACG AAG ATA ATG AAC
Ubp2-XhoI Rev	CGG TAC TCG AGC TAC TTT AGA ATT CTT TTC AAT GG

Table 5: Oligonucleotide Primers Used In The Present Study.
Only forward sequences of mutagenic primers are shown.

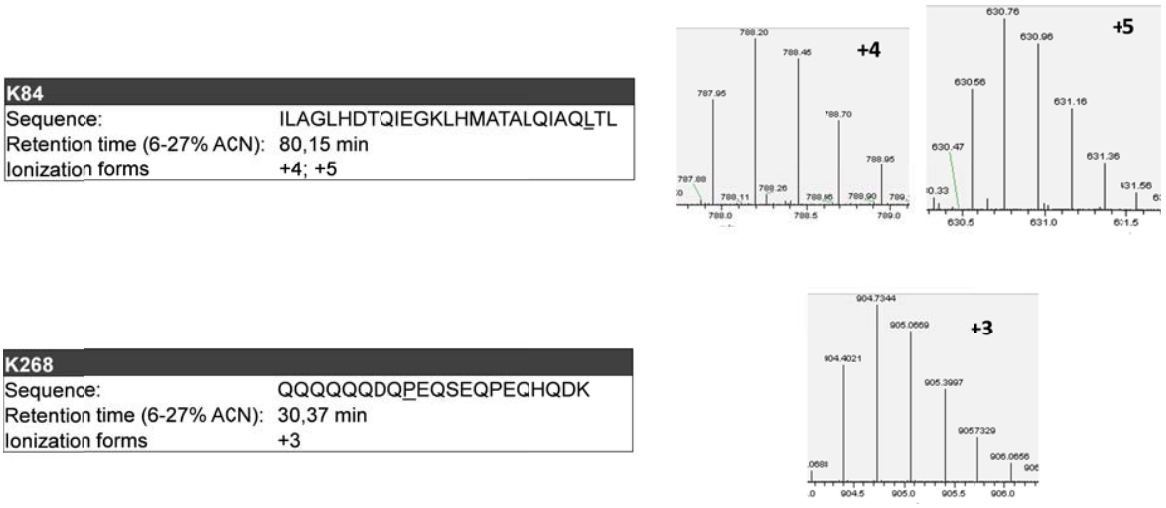

Figure 56: Setting Up An AQUA Reference Method.

Lyophilized AQUA internal standard peptides were resuspended in formic acid and evaluated by MS. The peptides were separated on 100 µm x 20 cm C18 reversed phase (Maccel C18 3 µ 200Å, The Nest Group, Inc.) with a gradient of 6% to 27% acetonitrile in 0.125% formic acid over 90 min . This process provided qualitative information about peptide retention, ionization efficiency and fragmentation.

		GST-Rpn10												
		K268 (+3)				K84 (+4)				K84 (+5)				
		1000 fmol				4000 fmol				4000 fmol				
		rt (min)	ma	ratio(L/H)	fmol	rt (min)	ma	ratio(L/H)	fmol	rt (min)	ma	ratio(L/H)	fmol	
IS	Heavy	33.66	7.0E+08	-	-	82.12	2.9E+06			82.12	3.1E+06			
	Light	-	-	-	-									
Rxn1-A	Heavy	30.52	9.2E+07	0.01	**5.55**	80.18	2.6E+08	0.03	**102.12**	80.18	2.0E+08	0.02	**78.90**	**90.51**
	Light	30.52	5.1E+05			80.22	6.6E+06			80.25	4.0E+06			
Rxn2-A	Heavy	28.05	1.4E+08	0.01	**8.92**	81.07	3.2E+08	0.04	**178.02**	81.06	2.3E+08	0.04	**141.22**	**159.62**
	Light	28.05	1.2E+06			81.07	1.4E+07			81.04	8.3E+06			
Rxn1-B	Heavy	31.41	9.9E+07	0.03	**27.87**	79.70	2.1E+08	0.55	**2217.57**	79.70	1.7E+08	0.60	**2415.35**	**2316.46**
	Light	31.41	2.8E+06			79.70	1.2E+08			79.70	1.1E+08			
Rxn2-B	Heavy	32.91	1.2E+08	0.03	**29.70**	81.26	3.1E+08	0.64	**2543.56**	81.26	2.7E+08	0.76	**3024.87**	**2784.22**
	Light	32.91	3.6E+06			81.26	2.0E+08			81.26	2.0E+08			
Rxn1-C	Heavy	29.19	1.1E+08	0.06	**63.25**	80.44	1.5E+08	0.55	**2206.77**	80.44	1.4E+08	0.47	**1899.96**	**2053.36**
	Light	29.19	7.0E+06			80.44	8.4E+07			80.44	6.8E+07			
Rxn2-C	Heavy	29.21	1.4E+07	0.06	**59.53**	82.90	2.7E+07	0.90	**3605.28**	82.90	1.8E+07	0.88	**3503.49**	**3554.38**
	Light	29.21	8.2E+05			82.90	2.4E+07			82.94	1.5E+07			
Rxn1-D	Heavy	30.49	1.1E+08	0.09	**86.77**	82.51	1.8E+08	0.23	**917.36**	82.51	1.5E+08	0.21	**835.78**	**876.57**
	Light	30.49	1.0E+07			82.51	4.0E+07			82.52	3.1E+07			
Rxn2-D	Heavy	30.37	1.0E+08	0.08	**83.50**	81.71	1.8E+08	0.36	**1452.57**	81.71	1.3E+08	0.39	**1567.24**	**1509.90**
	Light	30.37	8.7E+06			81.71	6.6E+07			81.71	5.1E+07			

Table 6: Quantification Of Ub-Modified Lys^{84} and Lys^{268} Of Recombinant Rpn10

For each sample, the amount of modified Lys^{84} and Lys^{268} has been calculated measuring the mass area under the curve. For Lys^{84} the average of the two most abundant ionized forms has been calculated.

		26S WT												
		K268 (+3)				K84 (+4)				K84 (+5)				
		1000 fmol				4000 fmol				4000 fmol				
		rt (min)	ma	ratio(L/H)	fmol	rt (min)	ma	ratio(L/H)	fmol	rt (min)	ma	ratio(L/H)	fmol	
IS	Heavy	33.66	7.0E+08	-	-	82.12	2.9E+06			82.12	3.1E+06			
	Light	-	-	-	-									
26S WT-E	Heavy	22.10	1.2E+07	-	-	76.25	8.8E+07	-	-	76.25	1.1E+08	0.00	12.39	**12.39**
	Light	-	-	-	-	-	-	-	-	76.25	3.3E+05			
Rxn3-F	Heavy	27.02	2.8E+05	-	-	72.48	6.0E+07	0.44	**1767.31**	72.48	6.4E+07	0.36	**1450.85**	**1609.08**
	Light	-	-	-	-	72.48	2.7E+07			72.48	2.3E+07			
Rxn4-G	Heavy	22.39	1.2E+06	0.03	**25.64**	73.21	7.1E+07	0.17	**666.08**	73.21	7.3E+07	0.21	**836.55**	**751.32**
	Light	22.39	3.0E+04			73.21	1.2E+07			73.21	1.5E+07			

Table 7: Quantification Of Ub-Modified Lys^{84} and Lys^{268} Of Proteasomal Rpn10

For each sample, the amount of modified Lys^{84} and Lys^{268} has been calculated measuring the mass area under the curve. For Lys^{84} the average of the two most abundant ionized forms has been calculated.

		Whole Cell Lysates Fractionation Assays												
		K268 (+3)				K84 (+4)				K84 (+5)				
		1000 fmol				4000 fmol				4000 fmol				
		rt (min)	ma	ratio(L/H)	fmol	rt (min)	ma	ratio(L/H)	fmol	rt (min)	ma	ratio(L/H)	fmol	
IS	Heavy	33.66	7.0E+08	-	-	82.12	2.9E+06			82.12	3.1E+06			
	Light	-	-	-	-									
Frac. 1 - 26S	Heavy	26.49	1.4E+08	0.01	6.14	81.83	1.5E+07	0.01	22.36	81.83	1.7E+07	0.00	12.75	17.55
	Light	26.47	8.4E+05			81.87	8.2E+04			81.76	5.4E+04			
Frac. 1 - Free	Heavy	26.70	1.3E+08	0.01	6.61	81.83	2.8E+07	0.01	21.36	81.94	3.8E+07	0.01	24.82	23.09
	Light	26.70	8.6E+05			81.94	1.7E+05			81.83	2.7E+05			
Frac. 2 - 26S	Heavy	22.61	1.1E+08	0.01	6.74	82.14	3.8E+08	0.01	29.09	82.14	4.2E+08	0.01	26.22	27.66
	Light	22.59	7.3E+05				2.8E+06				2.8E+06			
Frac. 2 - Free	Heavy	25.69	1.1E+08	0.01	6.35	81.55	4.1E+07	0.01	29.72	81.55	5.6E+07	0.01	33.16	31.44
	Light	25.83	6.9E+05			0.00	3.0E+05			0.00	4.6E+05			

Table 8: Quantification Of Ub-Modified Lys^{84} and Lys^{268} Of Proteasomal and Cytosolic Rpn10

Fractionations of wild-type cell lysates were performed. Fractions corresponding to both proteasomal and free pool of Rpn10 were subjected to ubiquitin remnant profiles assays. For each Rpn10 pool, the amount of modified Lys^{84} and Lys^{268} has been calculated measuring the mass area under the curve. For Lys^{84} the average of the two most abundant ionized forms has been calculated.

Sample	Peptide	Ub-Lys	XCorr	PPM
Rpn10-Ub1	R.LIFAGK#QLEDGR.T	K48	3.397	-1.66
	K.TLTGK#TITLEVEPSDTIENVK.A	K11	2.897	0.08
	R.TLSDYNIQK#ESTLHLVLR.L	K63	2.155	-0.49
	R.TLSDYNIQK#ESTLHLVLR.L	K63	2.095	-0.36
	R.TLSDYNIQK#ESTLHLVLR.L	K63	2.038	-0.49
	R.TLSDYNIQK#ESTLHLVLR.L	K63	1.919	-0.66
	R.TLSDYNIQK#ESTLHLVLR.L	K63	1.715	-0.57
	K.TLTGK#TITLEVEPSDTIENVK.A	K11	1.682	0.41
Rpn10-Ub2	R.TLSDYNIQK#ESTLHLVLR.L	K63	4.114	-0.67
	R.LIFAGK#QLEDGR.T	K48	3.131	-0.73
	R.TLSDYNIQK#ESTLHLVLR.L	K63	2.669	-0.35
	R.LIFAGK#QLEDGR.T	K48	2.617	-1.36
	R.TLSDYNIQK#ESTLHLVLR.L	K63	2.57	-1.11
	R.TLSDYNIQK#ESTLHLVLR.L	K63	1.812	-0.59
	R.TLSDYNIQK#ESTLHLVLR.L	k63	1.68	-0.29
	R.TLSDYNIQK#ESTLHLVLR.L	K63	1.62	-0.55
	R.TLSDYNIQK#ESTLHLVLR.L	K63	1.595	-0.79
	R.TLSDYNIQK#ESTLHLVLR.L	K63	1.463	-1.26
	K.TLTGK#TITLEVEPSDTIENVK.A	K11	1.446	-0.02
	R.TLSDYNIQK#ESTLHLVLR.L	K63	1.42	-0.87
	R.TLSDYNIQK#ESTLHLVLR.L	K63	1.284	-0.56
Ron10-Ubn	R.LIFAGK#QLEDGR.T	K48	-0.56	3.146
	R.TLSDYNIQK#ESTLHLVLR.L	K63	-0.2	2.493
	R.TLSDYNIQK#ESTLHLVLR.L	K63	-1.17	2.441
	R.LIFAGK#QLEDGR.T	K48	-1.4	2.396
	K.TLTGK#TITLEVEPSDTIENVK.A	K11	0.26	2.278
	R.TLSDYNIQK#ESTLHLVLR.L	K63	-1.06	2.009
	R.TLSDYNIQK#ESTLHLVLR.L	K63	-0.63	1.878
	R.TLSDYNIQK#ESTLHLVLR.L	K63	-0.41	1.867
	R.TLSDYNIQK#ESTLHLVLR.L	K63	-0.34	1.865
	R.TLSDYNIQK#ESTLHLVLR.L	K63	-1.68	1.849
	K.TLTGK#TITLEVEPSDTIENVK.A	K11	0.02	1.81
	R.TLSDYNIQK#ESTLHLVLR.L	K63	-2.14	1.797
	R.TLSDYNIQK#ESTLHLVLR.L	K63	-1.26	1.791
	R.TLSDYNIQK#ESTLHLVLR.L	K63	-0.89	1.776
	R.TLSDYNIQK#ESTLHLVLR.L	K63	-0.44	1.716
	R.TLSDYNIQK#ESTLHLVLR.L	K63	-0.78	1.716
	R.TLSDYNIQK#ESTLHLVLR.L	K63	0.29	1.673
	R.TLSDYNIQK#ESTLHLVLR.L	K63	-1.74	1.574

Table 9: Identification Of Lysine-Linkage Specificity In Rpn10 Oligoubiquitination.

Ubiquitin chains linked through Lys^{11}, Lys^{48} and Lys^{63} were detected in Rpn10 oligoubiquitination. Lys^{63}-linked chains were the most abundant ones. The peptide sequence, Sequest score (XCorr) and mass deviation (PPM) are shown. Ubiquitinated lysines are indicated by K#

.

Sites that were highly enriched in the double mutant *rad23Δrpn10Δ* strain sites under normal growth conditions (Log2 (H:L) > 2):

Gene Symbol	Site Position	Motif Peptide	RT Spectral Counts	RT Num Quant	RT Median	RT Standard Deviation	Biological Function
AFT2	378	IATNLGKERNENF	2	1	2.159	0	Transcription
ALD6	342	VGNPFDKANFQGA	3	2	2.618	0.053514285	Metabolic
ALY2	629	TIFNSAKLKSNIY	3	1	2.214	0	Endocytosis
BMH1	125	SKVFYYKMKGDYH	4	4	3.420	0.353096358	Growth/Cell Cycle
BUD4	886	PPPSIRKQPIAPD	2	1	2.143	0	Cytokinesis
CBF5	267	TLLVGYKRIVVKD	2	2	2.412	0.144856752	Growth/Cell Cycle
CDC4	202	PLAKTTKTINNNN	2	2	2.675	0.006665759	Growth/Cell Cycle
CIT2	215	IYRNVFKDGKMGE	1	1	3.182	0	Metabolic
CIT2	239	VNLIGSKDEDFVD	2	1	2.596	0	
CPR6	223	KAIETVKNIGTEQ	6	2	2.112	0.880463699	Translation
DOT6	606	NRTPNSKNPQDIA	3	2	2.675	0.212471243	Chromatin
ERB1	127	DPNIYSKYADGSD	16	2	4.009	0.117739793	Translation
FAA4	496	DLGYFAKNNQGEL	5	2	2.211	0.205512509	Metabolic
FAA4	541	IAEWTPKGQVKII	8	4	2.143	0.156186965	
FIR1	711	HNFIEEKRSIKNL	1	1	2.892	0	Translation
FKS1	245	RNMSLGKLSRKAR	2	2	3.091	0.340880528	Metabolic
GCD11	479	ARVVAVKADMARL	1	1	2.321	0	Translation
GDH1	404	RVDQELKRIMINC	5	4	3.512	0.352281973	Metabolic
GDH1	371	VWYGPPKAANLGG	35	1	2.230	0	
HHF1	32	NIQGITKPAIRRL	2	2	2.909	0.400265471	Chromatin
HHT1	80	EIAQDFKTDLRFQ	2	2	4.217	0.141690665	Chromatin
HHT1	57	EIRRFQKSTELLI	4	4	3.825	0.54629522	
HOF1	467	DSQRFAKSWNSSN	3	1	3.604	0	Actin
HSC82	178	VLRLFLKDDQLEY	5	2	2.360	0.086912417	Stress Response
HSP12	18	KASEALKPDSQKS	1	1	2.023	0	Stress Response
LSB5	115	NSGSGEKYEPRII	4	1	2.672	0	Actin
LSB5	157	QLGQTVKQRYSKS	2	1	2.626	0	
MDH2	180	RIMGVTKLDIVRA	6	2	5.654	0.602762648	Metabolic
MMR1	257	FVQYGLKGNNNNN	4	2	3.066	0.043127387	Mitochondrion
NHP2	32	AVLPFAKPLASKK	1	1	2.934	0	Translation
NOP10	28	ESGEITKSAHPAR	8	4	3.176	0.155662556	Translation
PCL1	237	NDLRRLKDVTNIA	6	1	2.516	0	Cellular Wall Biogenesis
PGK1	351	KFAAGTKALLDEV	6	2	2.296	1.195686406	Metabolic
PHM7	990	DYEPEAKKxxxxx	6	2	2.596	0.250938643	Cellular Wall Biogenesis
PNO1	154	DPGALQKGADFIK	1	1	2.941	0	Translation
PUP3	70	NEMFRYKTNLYKL	2	2	2.108	0.106974565	UPS
RNR1	849	EVPAPTKNEEKAA	20	6	3.380	1.092254791	Growth/Cell Cycle
RPB2	99	GKIYVTKPMVNES	8	1	3.850	0	Transcription

Gene Symbol	Site Position	Motif Peptide	RT Spectral Counts	RT Num Quant	RT Median	RT Standard Deviation	Biological Function
RPL12B	48	VGEDIAKATKEFK	6	4	2.143	0.207053838	Translation
RPL13B	45	RAARAAKIAPRPL	5	4	4.029	0.307651217	Translation
RPL13B	64	VRAPTVKYNRKVR	2	2	3.820	0.255021172	
RPL15A	47	RPTRPDKARRLGY	1	1	2.642	0	Translation
RPL15A	83	KGATYGKPTNQGV	5	2	2.477	0.215195548	
RPL15A	93	QGVNELKYQRSLR	9	2	2.274	0.027633364	
RPL16A	114	IPPPYDKKKRVVV	11	3	3.861	0.475995499	Translation
RPL16B	65	KATAFNKTRGPFH	5	5	3.425	0.363213036	Translation
RPL16B	31	QVLNGQKIVVVRA	5	2	3.289	0.047847999	
RPL16B	24	LASTIAKQVLNGQ	7	4	3.062	0.141804663	
RPL16B	133	RLKPGRKYTTLGK	1	1	2.916	0	
RPL16B	113	IPPPYDKKKRVVV	7	3	2.846	0.326585313	
RPL16B	169	SAEYYAKKRAFTK	1	1	2.823	0	
RPL17A	105	AANAEAKGLDATK	8	2	2.288	0.079518011	Translation
RPL18B	72	RIARALKQEGAAN	7	4	3.011	0.116164148	Translation
RPL18B	133	LAVRAPKGQNTLI	4	3	2.206	0.07450717	
RPL19B	46	AIRKLVKNGTIVK	6	6	2.702	0.24756451	Translation
RPL19B	146	EHIIQAKADAQRE	19	5	2.665	0.066302656	
RPL20A	38	SNEVIAKSRYWYF	8	3	5.669	0.253676148	Translation
RPL20A	141	VKRQYVKQFLTKD	8	4	3.844	0.516228668	
RPL20A	149	FLTKDLKFPLPHR	9	2	2.434	0.011584597	
RPL20A	166	TKTFSYKRPSTFY	4	1	2.210	0	
RPL21A	129	GVAVQLKRQPAQP	4	3	2.863	0.585153925	Translation
RPL21A	43	GDIVDIKANGSIQ	3	1	2.661	0	
RPL21A	35	TYLKVYKVGDIVD	1	1	2.481	0	
RPL21B	35	TYLKIYKVGDIVD	3	2	2.564	0.11937076	Translation
RPL24A	35	FRFQNSKSASLFK	8	4	3.154	0.38600929	Translation
RPL24A	41	KSASLFKQRKNPR	5	3	2.785	0.120998143	
RPL24A	77	RSRKTVKAQRPIT	4	1	2.167	0	
RPL27A	111	SQREEAKKVVKKA	14	4	3.721	0.07887926	Translation
RPL27A	133	NQWFFSKLRFxxx	4	2	3.287	0.099413642	
RPL27A	9	KFLKAGKVAVVVR	5	3	2.346	0.096156435	
RPL28	132	KARFVSKLAEEKI	3	2	2.842	0.02373077	Translation
RPL2A	68	VFRDPYKYRLREE	3	2	4.761	0.244801462	Translation
RPL2A	177	GGGRVDKPLLKAG	1	1	4.581	0	
RPL2A	46	YIRGIVKQIVHDS	2	2	4.550	0.181549586	
RPL2A	155	RLPSGAKKVISSD	4	4	4.545	0.340539457	
RPL2A	28	LRQGAAKLRTLDY	2	2	4.407	0.451033791	
RPL2A	92	QFIYAGKKASLNV	5	2	2.751	0.193635864	
RPL2A	145	HNPDENKTRVRLP	12	4	2.614	0.113819717	
RPL2A	234	GAVSGQKAGLIAA	4	2	2.574	0.064881309	

Gene Symbol	Site Position	Motif Peptide	RT Spectral Counts	RT Num Quant	RT Median	RT Standard Deviation	Biological Function
RPL2A	119	VSNVEEKPGDRGA	7	1	2.569	0	
RPL2A	156	LPSGAKKVISSDA	1	1	2.141	0	
RPL2A	10	VIRNQRKGAGSIF	1	1	2.083	0	
RPL33A	31	PNVSLIKIEGVAT	1	1	3.790	0	Translation
RPL33A	47	AQFYLGKRIAYVY	21	4	2.469	0.059040846	
RPL33B	47	AQFYLGKRIAYVY	11	4	2.049	0.218064772	Translation
RPL34A	106	IVKKVVKEQTEAA	4	3	2.916	0.544906164	Translation
RPL34A	67	QYATVSKTHKTVS	4	3	2.109	0.926665993	
RPL35B	32	KELAELKVQKLSR	1	1	2.180	0	Translation
RPL38	21	TRRADVKTATVKI	8	6	2.014	0.126744634	Translation
RPL6A	139	ERVEDQKVVDKAL	7	6	2.392	0.499264611	Translation
RPL6A	108	NVEYFAKEKLTKK	12	4	2.292	0.110982468	
RPL6B	19	EDVAAPKKTRKAV	1	1	2.716	0	Translation
RPL6B	139	ERVEDQKVVDKAL	6	4	2.155	0.451844212	
RPO21	1246	CRVVRPKSLDAET	2	2	2.478	0.134917538	Translation
RPS11B	46	LGFKTPKTAIEGS	10	2	3.421	0.074791954	Translation
RPS11B	56	EGSYIDKKCPFTG	4	3	3.224	0.653336834	
RPS11B	43	NAGLGFKTPKTAI	8	4	2.605	0.148130454	
RPS17B	23	IERYYPKLTLDFQ	4	1	2.027	0	Translation
RPS1B	55	NKSTGLKNASDAL	3	2	2.067	0.091738501	Translation
RPS22A	88	KIGDIEKWTANLL	4	1	2.143	0	Translation
RPS23A	50	GGSSHAKGIVLEK	1	1	2.523	0	Translation
RPS23A	56	KGIVLEKLGIESK	4	4	2.416	0.320283727	
RPS23A	114	GRKGKAKGDIPGV	3	2	2.385	0.078623365	
RPS23A	39	LLGTAFKSSPFGG	5	3	2.276	0.194257569	
RPS25A	90	EKEGIIKPISKHS	2	2	2.670	0.039247908	Translation
RPS25A	94	IIKPISKHSKQAI	1	1	2.093	0	
RPS31	29	IDNVKSKIQDKEG	50	3	2.459	0.131795254	Translation
RPS31	6	xMQIFVKTLTGKT	15	8	2.361	0.188448159	
RPS31	48	RLIFAGKQLEDGR	267	17	2.153	0.450713373	
RPS4B	122	DEEASYKLGKVKK	6	4	4.119	0.296882027	Translation
RPS4B	211	FDLVHIKDSLDNT	11	3	4.085	0.970283826	
RPS4B	161	KVNDTVKIDLASG	6	4	3.863	0.492807436	
RPS4B	198	IGTIVHKERHDGG	4	2	3.538	0.01635054	
RPS4B	106	RLVYDVKGRFAVH	6	4	3.220	0.126647356	
RPS4B	174	KITDFIKFDAGKL	10	4	3.013	0.241176124	
RPS4B	155	YPDPNIKVNDTVK	24	7	2.912	0.106620312	
RPS4B	53	FLRNRLKYALNGR	1	1	2.900	0	
RPS4B	168	IDLASGKITDFIK	19	6	2.862	0.120448706	
RPS4B	233	VIGEQGKPYISLP	6	2	2.252	0.024952628	
RPS6B	131	TDTTVPKRLGPKR	9	2	2.304	0.032087088	Translation

Gene Symbol	Site Position	Motif Peptide	RT Spectral Counts	RT Num Quant	RT Median	RT Standard Deviation	Biological Function
RPS6B	214	YAQLLAKRLSERK	6	2	2.039	0.221806978	
RPS7B	175	FQAVYNKLTGKQI	5	1	2.095	0	Translation
RPS8A	37	RQPANTKIGAKRI	2	1	3.009	0	Translation
RPS8A	74	ASEGISKKTRIAG	23	5	2.831	0.49343147	
RPS9B	115	LQTQVYKLGLAKS	1	1	3.079	0	Translation
RPT1	282	GSELVQKYVGEGA	2	2	2.965	0.088584394	Translation
RPT2	255	GSELIQKYLGDGP	4	2	2.428	0.037919548	UPS
SEC11	116	ISLYANKKIYLNK	2	2	2.683	0.152289591	Endocytosis
SIC1	36	GQKTPQKPSQNLV	1	1	2.989	0	Growth/Cell Cycle
SSA1	54	LIGDAAKNQAAMN	10	2	3.037	0.052354425	Stress Response
SWI5	227	PQFLSPKRKISPA	5	2	2.121	0.055912526	Growth/Cell Cycle
TEF2	154	LIVAVNKMDSVKW	1	1	2.206	0	Translation
TUB3	402	FDLMYAKRAFVHW	1	1	3.178	0	Growth/Cell Cycle
TYE7	251	TSTKLNKSMILEK	1	1	4.367	0	Transcription
TYE7	225	VGDSVKKQDEDGA	1	1	3.142	0	
TYE7	166	KTNLDAKETKKRA	1	1	2.778	0	
UBC6	188	TEDPFTKAAKEKV	3	1	2.084	0	UPS
VHS2	50	DPSYLYKTVSNNA	2	2	4.514	0.334394862	Growth/Cell Cycle
VHS2	310	NQQYLLKQQRSPS	5	2	2.208	0.642152329	
WBP1	85	IIVFPTKGGKNLA	4	2	2.055	0.063110249	Endocytosis
YDR186C	667	LLNDTSKKQKFLN	3	3	2.310	0.207813998	Unknown
YDR261C-D	568	DFYWVSKKYLLPS	3	1	2.917	0	Unknown
YDR261C-D	1199	RDTWNTKNMRSLE	3	1	2.047	0	
YEF3	295	KLLPGLKSNFATI	2	2	2.602	0.012750081	Translation
YEF3	196	ATAAMTKATETVD	2	1	2.387	0	
YIL108W	518	SKYGFSKNVQGIK	7	4	2.024	0.027031842	Unknown
YKL068W-A	28	LFSQTQKQGSFQK	2	1	3.115	0	Unknown

Table 10: Highly Enriched Sites Under Normal Growth Conditions, Log2 (H:L) > 2.
For each identified ubiquitinated site the following items are shown: gene symbol, site position, motif peptide, the number of identified spectral counts, the number of quantified spectral counts (RT Num Quant), the median (equivalent to the Log2 H:L ratio), its standard deviation and biological function.

Sites that were enriched in the single mutant *rad23Δ* strain sites under normal growth conditions (Log2 (H:L) < 1):

Gene Symbol	Site Position	Motif Peptide	RT Spectral Counts	RT Num Quant	RT Median	RT Standard Deviation	Biological Function
COS2	18	VDVLSFKQLESQK	10	3	-1.299	0.155164447	Metabolic
FCY2	29	SSLENEKKVAASE	20	9	-1.389	0.247592229	Transmembrane Transport
FKS1	1082	PILGDGKSDNQNH	2	2	-2.090	3.424152692	Metabolic
HTA2	22	SQSRSAKAGLTFP	2	1	-1.532	0	Chromatin
PEP4	60	YLTQFEKANPEVV	4	2	-3.827	0.485659471	Endocytosis
PRE8	108	GEYPPTKLLVSEV	3	2	-1.360	0.561696462	UPS
RAX1	274	VGVTNEKSNRSRG	3	2	-1.139	0.202840595	Cellular Wall Biogenesis
RPL1B	18	HVKELLKYSNETK	3	2	-1.920	0.739306213	Translation
RPO31	1240	VFPEGYKAKSIST	2	2	-1.053	0.007653996	Translation
RPS20	8	SDFQKEKVEEQEQ	11	4	-3.072	3.852956596	Translation
RPT6	402	TAISVAKLFKxxx	3	1	-1.503	0	UPS
SSB2	194	GAGKSEKERHVLI	1	1	-1.413	0	Stress Response
SSB2	497	KVTAVEKSTGKSS	1	1	-4.094	0	
STE2	337	SINNDAKSSLRSR	15	2	-2.179	0.089394281	Growth/Cell Cycle
URA1	46	AGAFITKSATTLE	7	2	-1.326	0.17332558	Metabolic
YCF1	504	KLYAWEKPYREKL	1	1	-1.125	0	Transmembrane Transport

Table 11: Depleted Sites Under Normal Growth Conditions, Log2 (H:L) < -1.
For each identified ubiquitinated site the following items are shown: gene symbol, site position, motif peptide, the number of identified spectral counts, the number of quantified spectral counts (RT Num Quant), the median (equivalent to the Log2 H:L ratio), its standard deviation and biological function.

Sites that were highly enriched in the double mutant *rad23Δrpn10Δ* strain sites under a cold-shock stress (Log2 (H:L) > 2):

Gene Symbol	Site Position	Motif Peptide	16C Spectral Counts	16C Num Quant	16C Median	16C Standard Deviation	Biological Function
ACK1	184	SRILQEKVYRTEE	197	16	2.257	0.225104962	Cell Wall Biogenesis
ACT1	326	LAPSSMKVKIIAP	18	8	2.445	0.345186397	Actin
ADE13	273	RLLANLKEVEEPF	35	3	2.392	0.044077168	Metabolism
ADE6	1336	SWYPEGKYEEWGG	1	1	2.537	0	Metabolism
ALD6	474	VPFGGVKQSGYGR	7	2	2.623	0.060475404	Metabolism
ASC1	46	KTLISWKLTGDDQ	12	5	3.030	0.109653413	AA biosynthesis
ASN2	529	AYWYRLKFDAWFP	53	6	2.397	0.109846924	AA biosynthesis

Gene Symbol	Site Position	Motif Peptide	16C Spectral Counts	16C Num Quant	16C Median	16C Standard Deviation	Biological Function
AVT1	191	MDSIVVKRVEGVD	13	4	2.909	0.307880666	Transmembrane Transport
BAP2	59	RFADSFKRAEGST	3	1	2.720	0	Transmembrane Transport
BMH1	51	LLSVAYKNVIGAR	2	2	3.298	0.958135302	Growth/Cell Cycle
BUL1	578	VNYNDLKLGHDLD	1	1	4.157	0	Transmembrane Transport
CAN1	42	RGSIPLKDEKSKE	1	1	3.840	0	Transmembrane Transport
CAN1	45	IPLKDEKSKELYP	11	2	2.794	0.336300697	
CBR1	86	KANINGKDITRSY	2	2	2.522	1.611799516	Metabolism
CCC1	74	SPMSVGKDNRNGD	5	1	4.571	0	Transmembrane Transport
CCC1	18	TLIQKAKGSGGTS	2	1	3.253	0	
CCT8	15	PNAGLFKQGYNSY	5	2	2.931	0.445042388	Actin
CDC48	594	ELDSIAKARGGSL	20	4	2.186	0.049964552	Growth/Cell Cycle
CDC60	830	YALTNYKNALKYG	3	3	3.772	0.70612756	Growth/Cell Cycle
CIT2	176	SESKFAKAYAQGI	6	3	4.697	0.062180572	Metabolism
CPR1	29	YNDIVPKTAENFR	11	2	5.286	0.243248813	Stress Response
CPR1	151	SPSGATKARIVVA	2	1	2.130	0	
CPR6	231	IGTEQFKKQNYSV	16	4	3.143	0.106652066	Translation
CPT1	250	YESQSTKSATPSK	10	4	3.279	3.36734372	Metabolism
CRM1	50	NPDAWQKADQILQ	5	3	4.261	0.68979079	Translation
CTR1	402	NLLPAEKFTHNxx	5	3	4.163	0.068471393	Transmembrane Transport
CTR1	345	EKNNESKVAISEN	5	4	3.940	0.393377037	
CTR1	354	ISENNQKKTPTQE	7	2	3.768	0.021516676	
CUE4	37	RTVQDAKPAPSVA	8	2	3.313	0.174170688	UPS
CUE5	295	DLSQGGKNSRPQQ	12	6	3.144	0.197767686	UPS
CUL3	718	LTPSILKRSIQLL	10	2	4.188	0.090097295	UPS
CUL3	688	IIVRIMKTEGKLS	2	2	3.150	0.514902785	
CYS3	154	PTNPTLKVTDIQK	4	2	4.202	2.120777769	Metabolism
DED1	588	GWGSDSKSSGWGN	1	1	3.071	0	Translation
DSE1	553	EDIVFTKRMYSVN	1	1	2.315	0	Cell Wall Biogenesis
EDE1	1318	QQPIPLKNDPIVD	6	2	3.098	0.595414934	Endocytosis
EDE1	1329	VDASLSKGPIVNR	10	4	2.791	0.177077913	
EFB1	109	IAAYNAKKAAKPA	1	1	2.290	0	Translation
EFT2	171	LELQVSKEDLYQT	8	2	2.073	0.033684115	Translation
ENO2	195	EVYHNLKSLTKKR	25	4	2.150	0.095768181	Metabolism
ERG11	215	SRSLLGKEMRAKL	5	4	3.666	0.33143875	Metabolism
FAS2	1736	SLTFNSKNIQSKD	5	2	3.550	1.716169499	Metabolism
FAS2	37	TQDVFLKDFNTER	2	2	2.989	0.027154017	
FAS2	1741	SKNIQSKDSYINA	3	2	2.769	0.207519568	
FBA1	27	NLFTYAKEHKFAI	5	1	2.140	0	Metabolism

Gene Symbol	Site Position	Motif Peptide	16C Spectral Counts	16C Num Quant	16C Median	16C Standard Deviation	Biological Function
FKS1	1082	PILGDGKSDNQNH	3	3	2.003	0.303910999	Cell Wall Biogenesis
GDH1	371	VWYGPPKAANLGG	3	1	2.709	0	AA biosynthesis
GLN1	273	IEQAIEKLSKRHA	22	5	3.496	0.246044993	AA biosynthesis
GLN1	283	RHAEHIKLYGSDN	8	4	2.770	0.311715666	
GLN1	324	IPRSVAKEGYGYF	14	2	2.661	0.156324116	
GLN1	77	DSDIYLKPVAYYP	2	1	2.322	0	
GLT1	896	SWQLYVKKEMEAI	2	2	2.319	0.054894456	AA biosynthesis, Stress Response
GLY1	228	VLVGNLKFVKKAT	2	1	2.349	0	AA biosynthesis
GNP1	57	EVEYFEKTVEKTI	3	2	2.833	0.10952491	Transmembrane Transport
GNP1	34	VSHYEMKEIQPKE	4	4	2.657	0.314180967	
HNM1	562	EHVPWGKKxxxxx	4	1	2.650	0	Transmembrane Transport
HOF1	467	DSQRFAKSWNSSN	25	6	3.303	0.41503843	Cytokinesis
HTB2	112	LPGELAKHAVSEG	11	3	3.171	0.537233173	Chromatin
HTB2	124	GTRAVTKYSSSTQ	1	1	2.099	0	
IPP1	74	PIIQDTKKGKLRF	4	4	3.661	0.343745222	Metabolism
ITR1	41	SPSKRGKITLESH	7	2	3.853	0.766425176	Transmembrane Transport
ITR2	599	AAHHKLKFEPTQE	7	2	2.859	0.04808264	Transmembrane Transport
KHA1	562	LSVIDEKLTPFEG	5	4	6.122	1.684287266	Transmembrane Transport
KRE6	316	DTPDTAKTREAMD	4	3	4.131	0.420783479	Metabolism
KRE6	104	KGVSDYKGYYSRN	8	4	3.266	0.099401996	
LSB5	115	NSGSGEKYEPRII	10	1	3.971	0	Actin
LSB5	251	DEEATSKFIQARA	1	1	2.634	0	
LYP1	54	PYSIDEKQYNTKK	5	4	2.146	0.27438947	Transmembrane Transport
MCH4	53	AADAILKKNSDQV	12	5	2.197	0.425560075	Transmembrane Transport
MTH1	301	AVMNLSKPEWRNI	7	6	2.585	0.279305036	Transcription
MUP1	567	NIIEHYKSEQEKS	6	1	2.810	0	Metabolism
NOP1	109	EDLLVTKNMAPGE	3	2	4.813	0.05011761	Translation
NOP1	102	VYIARGKEDLLVT	1	1	4.134	0	
OLE1	461	LGKDATKAFSGGV	1	1	2.045	0	Metabolism
OSH3	548	ETPLLGKSDQNEF	2	2	2.050	0.226927929	Metabolism
PDC1	562	TAATNAKQxxxxx	4	1	2.799	0	Metabolism
PDR5	825	RGVLTEKNANDPE	5	1	2.262	0	Transmembrane Transport
PFK1	98	SQGALLKIRLVMS	9	3	2.433	3.564841969	Metabolism
PGK1	244	MAFTFKKVLENTE	9	1	4.070	0	
PGK1	258	GDSIFDKAGAEIV	5	3	3.362	0.06101486	
PGK1	351	KFAAGTKALLDEV	4	1	2.447	0	

Gene Symbol	Site Position	Motif Peptide	16C Spectral Counts	16C Num Quant	16C Median	16C Standard Deviation	Biological Function
PIL1	130	QYRLTLKSIRDIE	2	1	3.709	0	Endocytosis
PIL1	29	PPPSTTKGRFFGK	5	3	3.643	0.292314166	
PIN3	80	GLKPGDKVQLLEK	1	1	3.592	0	Prion Formation
PIN3	76	DGDLGLKPGDKVQ	5	2	2.989	0.255085064	
PMA1	615	EVFPQHKYRVVEI	2	2	4.281	0.099285885	Transmembrane Transport
PMA1	643	NDAPSLKKADTGI	1	1	2.815	0	
PMR1	218	TSQTIEKSSFNDQ	6	2	2.428	0.118707711	Transmembrane Transport
RNR1	849	EVPAPTKNEEKAA	3	1	2.142	0	Metabolism
RPL11B	49	QTPVQSKARYTVR	4	1	3.551	0	Translation
RPL16B	95	HKTARGKAALERL	6	4	3.702	0.278280749	Translation
RPL16B	169	SAEYYAKKRAFTK	1	1	2.739	0	
RPL16B	133	RLKPGRKYTTLGK	4	1	2.588	0	
RPL16B	113	IPPPYDKKKRVVV	2	2	2.250	0.164110782	
RPL16B	31	QVLNGQKIVVVRA	1	1	2.180	0	
RPL17A	89	WPAKSVKFVQGLL	2	2	3.333	0.349588401	Translation
RPL17A	13	TSTNPAKSASARG	2	2	2.928	0.326734106	
RPL17A	153	ELVVTEKEEAVAK	2	2	2.833	0.264868765	
RPL18B	72	RIARALKQEGAAN	1	1	3.718	0	Translation
RPL18B	133	LAVRAPKGQNTLI	2	2	3.405	0.04816115	
RPL19B	108	LRRLLAKYRDAGK	6	2	3.253	0.095189539	Translation
RPL19B	21	VGVGKRKVWLDPN	2	2	3.202	0.092216749	
RPL20A	141	VKRQYVKQFLTKD	3	2	2.553	0.138477584	Translation
RPL21A	129	GVAVQLKRQPAQP	4	2	2.446	0.020101773	Translation
RPL22A	99	IRFVSTKTNEYRL	2	1	2.237	0	Translation
RPL2A	46	YIRGIVKQIVHDS	3	1	3.743	0	Translation
RPL3	39	PKDDRSKPVALTS	2	1	2.463	0	Translation
RPL33A	10	SHRLYVKGKHLSY	6	3	2.019	0.155787797	Translation
RPL34A	106	IVKKVVKEQTEAA	1	1	2.471	0	Translation
RPL35B	25	SQLVDLKKELAEL	8	3	3.673	0.319441655	Translation
RPL37B	84	FQTGSAKATSAxx	4	2	3.717	0.390188919	Translation
RPL6A	108	NVEYFAKEKLTKK	10	4	2.446	0.159722728	Translation
RPL9A	84	MITGVTKGYKYKM	2	2	2.418	0.46448054	Translation
RPO21	1350	GRAALYKEVYNVI	4	3	2.198	0.006540732	Translation
RPO21	789	TLPHFSKDDYSPE	6	4	2.079	0.101081048	
RPS10B	52	LQSLTSKGYVKTQ	6	4	3.368	0.13112061	Translation
RPS11B	36	RTKRWYKNAGLGF	6	1	2.173	0	Translation
RPS11B	15	SERAFQKQPHIFN	5	4	2.009	0.093111367	
RPS13	76	KIMRILKSNGLAP	2	2	4.107	0.296218204	Translation
RPS13	39	VIEQIVKYARKGL	2	2	2.467	0.178128731	
RPS15	64	KKLRAAKLAAPEN	1	1	2.982	0	Translation

Gene Symbol	Site Position	Motif Peptide	16C Spectral Counts	16C Num Quant	16C Median	16C Standard Deviation	Biological Function
RPS17B	23	IERYYPKLTLDFQ	1	1	3.381	0	Translation
RPS18A	49	SNLVCKKADVDLH	2	1	6.747	0	Translation
RPS1B	55	NKSTGLKNASDAL	2	1	2.489	0	Translation
RPS1B	248	KKVSGFKDEVLET	2	2	2.137	0.079919418	
RPS20	101	APVQIVKRITQIT	4	1	2.987	0	Translation
RPS22A	88	KIGDIEKWTANLL	1	1	2.519	0	Translation
RPS31	33	KSKIQDKEGIPPD	3	1	2.300	0	Translation
RPS4B	174	KITDFIKFDAGKL	1	1	3.449	0	Translation
RPS4B	198	IGTIVHKERHDGG	2	1	2.170	0	
RPT6	402	TAISVAKLFKxxx	2	1	2.680	0	UPS
RTT101	791	CITRSVKSERNGL	1	1	2.588	0	UPS
SSH4	99	LHSLFGKKHSGIL	2	2	2.936	0.414890605	UPS
SSL2	624	YALKMGKPFIYGS	1	1	2.278	0	Transcription
STT3	56	FNYRATKYLVNNS	2	1	3.757	0	Metabolism
TDH3	213	SSTGAAKAVGKVL	1	1	2.961	0	Cell Wall Biogenesis

Table 12: Highly Enriched Sites Under Cold-Shock Stress, Log2 (H:L) > 2.
For each identified ubiquitinated site the following items are shown: gene symbol, site position, motif peptide, the number of identified spectral counts, the number of quantified spectral counts (RT Num Quant), the median (equivalent to the Log2 H:L ratio), its standard deviation and biological function.

Sites that were highly enriched in the single mutant *rad23Δ* strain sites under cold-shock stress (Log2 (H:L) < 1):

Gene Symbol	Site Position	Motif Peptide	16C Spectral Counts	16C Num Quant	16C Median	16C Standard Deviation	Biological Function
RPL17A	89	WPAKSVKFVQGLL	7	1	-1.152	0	Translation
RPL17A	46	ELTKAQKYLEQVL	1	1	-1.012	0	
RPL17B	46	ELTKAQKYLDQVL	17	7	-1.204	0.076025017	Translation
RPS31	11	VKTLTGKTITLEV	2	1	-5.217	0	Translation
RPS31	63	SDYNIQKESTLHL	12	3	-4.592	3.414822818	
RPS31	48	RLIFAGKQLEDGR	2	1	-4.124	0	
RPS31	6	xMQIFVKTLTGKT	2	1	-4.124	0	
RPS31	27	DTIDNVKSKIQDK	5	1	-3.766	0	
RPS31	29	IDNVKSKIQDKEG	4	2	-3.621	0.125150885	
RPS31	33	KSKIQDKEGIPPD	1	1	-2.613	0	
YMR253C	40	TRSLSPKESNSNE	4	1	-1.242	0	Unknown

Table 13: Depleted Sites Under Cold-Shock Stress, Log2 (H:L) < -1.

For each identified ubiquitinated site the following items are shown: gene symbol, site position, motif peptide, the number of identified spectral counts, the number of quantified spectral counts (RT Num Quant), the median (equivalent to the Log2 H:L ratio), its standard deviation and biological function.

Lits of proteins containing quantified sites at both growth conditions:

			PERMISSIVE TEMPERATURE				COLD-SHOCK			
Gene Symbol	**Site Position**	**Motif Peptide**	**PT Spectral Counts**	**PT Num Quant**	**PT Median**	**PT St. Dev.**	**16C Spectral Counts**	**16C Num Quant**	**16C Median**	**16C St. Dev.**
ACC1	1813	MSYVPAKRNMPVP	1	1	0.2278	0.0000	14	3	1.3895	0.1955
ACC1	1311	LSNFNIKPIFTDN	3	2	1.0512	0.2600	74	16	0.6895	1.0919
ACK1	184	SRILQEKVYRTEE	7	3	-0.1177	0.0813	197	16	2.2566	0.2251
ACT1	326	LAPSSMKVKIIAP	7	2	0.5219	0.1052	18	8	2.4451	0.3452
AFT2	378	IATNLGKERNENF	2	1	2.1593	0.0000	11	2	0.6470	0.0113
AIM44	605	ARIQNYKSNVVYM	3	2	0.1571	0.1089	18	4	1.9225	0.0543
ALD6	474	VPFGGVKQSGYGR	3	1	1.0904	0.0000	7	2	2.6227	0.0605
ALD6	342	VGNPFDKANFQGA	3	2	2.6181	0.0535	6	2	1.7784	0.0722
AQR1	29	LTREYTKPDGQTK	2	2	-0.1700	0.1550	4	3	0.3063	0.0340
ASC1	161	RVVPNEKADDDSV	6	2	0.0818	0.0228	1	1	0.5787	0.0000
ASC1	46	KTLISWKLTGDDQ	1	1	1.6596	0.0000	12	5	3.0297	0.1097
ASN2	529	AYWYRLKFDAWFP	1	1	0.5393	0.0000	53	6	2.3972	0.1098
BAP2	59	RFADSFKRAEGST	2	2	1.2804	0.0964	3	1	2.7198	0.0000
BMH1	51	LLSVAYKNVIGAR	2	1	0.8959	0.0000	2	2	3.2980	0.9581
BUL1	578	VNYNDLKLGHDLD	2	1	0.5862	0.0000	1	1	4.1574	0.0000
CAN1	42	RGSIPLKDEKSKE	1	1	0.3057	0.0000	1	1	3.8396	0.0000
CBR1	86	KANINGKDITRSY	2	2	-0.4069	0.1150	2	2	2.5221	1.6118
CCC1	74	SPMSVGKDNRNGD	5	2	0.0313	0.0174	5	1	4.5708	0.0000
CCC1	18	TLIQKAKGSGGTS	3	2	0.3627	0.1046	2	1	3.2533	0.0000
CDC19	135	DYKNITKVISAGR	4	2	0.7363	0.0088	19	5	-0.2505	0.1325
CDC48	594	ELDSIAKARGGSL	4	2	1.6867	0.1552	20	4	2.1856	0.0500
CIT2	176	SESKFAKAYAQGI	3	1	1.9249	0.0000	6	3	4.6972	0.0622
CIT2	239	VNLIGSKDEDFVD	2	1	2.5964	0.0000	44	7	0.8377	0.0305
CIT2	215	IYRNVFKDGKMGE	1	1	3.1815	0.0000	8	1	0.5592	0.0000
COS2	18	VDVLSFKQLESQK	10	3	-1.2989	0.1552	31	6	0.7543	0.7742
COS2	205	KLFNTEKSWSPVG	11	3	-0.4405	0.1253	17	4	0.4128	0.0212
COS6	18	VDVLSVKQLESQK	3	1	-0.9552	0.0000	8	2	0.7471	0.0083
CPR1	29	YNDIVPKTAENFR	5	2	1.3989	0.0850	11	2	5.2863	0.2432
CPR1	158	ARIVVAKSGELxx	1	1	1.2425	0.0000	10	2	1.5839	0.0331
CPR1	87	FPDENFKKHHDRP	6	2	1.2604	0.0488	1	1	0.8425	0.0000
CPR1	151	SPSGATKARIVVA	1	1	1.1919	0.0000	2	1	2.1303	0.0000
CPT1	250	YESQSTKSATPSK	4	2	1.2503	0.0722	10	4	3.2791	3.3673
CTR1	345	EKNNESKVAISEN	6	1	-0.6332	0.0000	5	4	3.9403	0.3934

			PERMISSIVE TEMPERATURE				COLD-SHOCK			
Gene Symbol	Site Position	Motif Peptide	PT Spectral Counts	PT Num Quant	PT Median	PT St. Dev.	16C Spectral Counts	16C Num Quant	16C Median	16C St. Dev.
CTR1	354	ISENNQKKTPTQE	1	1	-0.5199	0.0000	7	2	3.7678	0.0215
CUL3	688	IIVRIMKTEGKLS	2	1	0.8206	0.0000	2	2	3.1500	0.5149
DSE1	553	EDIVFTKRMYSVN	9	4	1.9008	0.0272	1	1	2.3146	0.0000
EDE1	1329	VDASLSKGPIVNR	5	2	0.2364	0.0261	10	4	2.7910	0.1771
EFB1	109	IAAYNAKKAAKPA	1	1	-0.3019	0.0000	1	1	2.2904	0.0000
EFT2	87	MSDEDVKEIKQKT	2	2	0.5545	0.2334	8	2	1.6673	0.0613
ENA5	523	LSQHNEKPGSAQF	5	1	0.9787	0.0000	1	1	0.8936	0.0000
ENO2	195	EVYHNLKSLTKKR	5	3	-0.1067	0.0221	25	4	2.1502	0.0958
ERB1	127	DPNIYSKYADGSD	16	2	4.0092	0.1177	4	1	1.3604	0.0000
ERG1	289	IKSWMIKDVQPFI	13	3	1.6909	0.2684	5	2	1.2705	0.0018
ERG11	215	SRSLLGKEMRAKL	5	4	0.0980	0.4953	5	4	3.6664	0.3314
ERG13	305	TCKLVTKSYGRLL	3	3	0.2344	0.0837	14	4	0.5573	0.0320
FAS1	887	VPTLEAKRDYIIS	4	3	0.5515	0.3308	4	3	0.7808	0.6970
FAS2	37	TQDVFLKDFNTER	3	1	0.5505	0.0000	2	2	2.9886	0.0272
FAS2	1632	YPSKTLKTDGVRA	1	1	0.8353	0.0000	7	5	0.9202	0.2876
FAS2	999	PELKPYKQVKQIA	1	1	0.9799	0.0000	12	3	1.5596	0.0793
FBA1	27	NLFTYAKEHKFAI	13	2	0.8066	0.6250	5	1	2.1396	0.0000
FCY2	29	SSLENEKKVAASE	20	9	-1.3895	0.2476	5	2	1.9585	0.0791
FCY2	16	EIQDLEKRSPVIG	6	2	-0.5390	0.0508	8	3	-0.3913	0.0335
FET4	39	GDSNDYKNDDVVR	6	2	-0.5739	0.0254	1	1	0.9080	0.0000
FIR1	711	HNFIEEKRSIKNL	1	1	2.8916	0.0000	6	3	1.1869	0.1472
FKS1	245	RNMSLGKLSRKAR	2	2	3.0907	0.3409	2	2	0.7100	0.0920
FKS1	1082	PILGDGKSDNQNH	2	2	-2.0900	3.4242	3	3	2.0030	0.3039
GDH1	371	VWYGPPKAANLGG	35	1	2.2305	0.0000	3	1	2.7090	0.0000
GLN1	273	IEQAIEKLSKRHA	1	1	0.1440	0.0000	22	5	3.4963	0.2460
GLY1	228	VLVGNLKFVKKAT	25	5	1.0710	0.1904	2	1	2.3492	0.0000
GPM1	175	KDLLSGKTVMIAA	5	2	-0.6615	0.0449	8	2	1.6689	0.0117
GPM1	71	ANIALEKADRLWI	2	2	-0.6796	0.0625	2	1	1.8600	0.0000
GPM1	109	KKFGEEKFNTYRR	1	1	0.1620	0.0000	5	2	1.5007	0.1370
GPM1	57	DVLYTSKLSRAIQ	2	2	-0.1154	0.4392	2	2	0.7521	0.0497
GRX2	139	KLAEILKPVFQxx	4	2	-0.4714	0.0410	5	2	1.1051	0.0212
GSG1	687	APRPSEKNLTRTS	6	5	1.4343	0.1908	17	7	-1.2037	0.0760
HHT1	57	EIRRFQKSTELLI	4	4	3.8252	0.5463	6	2	0.1552	0.1550
HIP1	52	AFPLSSKDSPGIN	23	4	-0.6840	0.0566	6	2	0.1627	0.1024
HNM1	562	EHVPWGKKxxxxx	2	1	0.2360	0.0000	4	1	2.6500	0.0000
HNM1	25	SNASMHKRDLRVE	7	2	-0.1022	0.0268	23	4	1.3157	0.6431
HOF1	467	DSQRFAKSWNSSN	3	1	3.6037	0.0000	25	6	3.3026	0.4150
HTB2	124	GTRAVTKYSSSTQ	19	2	0.5812	0.0460	1	1	2.0993	0.0000
IPP1	74	PIIQDTKKGKLRF	4	2	1.2271	0.9132	4	4	3.6614	0.3437
ITR1	41	SPSKRGKITLESH	1	1	-0.3849	0.0000	7	2	3.8527	0.7664

			PERMISSIVE TEMPERATURE				COLD-SHOCK			
Gene Symbol	Site Position	Motif Peptide	PT Spectral Counts	PT Num Quant	PT Median	PT St. Dev.	16C Spectral Counts	16C Num Quant	16C Median	16C St. Dev.
ITR2	599	AAHHKLKFEPTQE	8	2	-0.5092	0.0183	7	2	2.8590	0.0481
KRE6	104	KGVSDYKGYYSRN	2	2	0.3761	0.0433	8	4	3.2662	0.0994
KRS1	241	LDLIMNKDARNRF	3	2	-0.7907	0.1449	3	1	1.7685	0.0000
LSB5	157	QLGQTVKQRYSKS	2	1	2.6257	0.0000	8	1	0.4702	0.0000
LSB5	115	NSGSGEKYEPRII	4	1	2.6720	0.0000	10	1	3.9709	0.0000
LYP1	54	PYSIDEKQYNTKK	7	2	-0.3704	0.0110	5	4	2.1463	0.2744
MCH4	53	AADAILKKNSDQV	3	2	1.0108	0.1259	12	5	2.1971	0.4256
MDH2	180	RIMGVTKLDIVRA	6	2	5.6540	0.6028	9	1	1.8905	0.0000
MDM34	293	QSFPQPKSSTVSS	13	2	0.4858	0.0640	4	2	-0.0946	0.0501
MUP1	567	NIIEHYKSEQEKS	13	2	1.0592	0.1239	6	1	2.8098	0.0000
NHP2	32	AVLPFAKPLASKK	1	1	2.9335	0.0000	1	1	-0.5505	0.0000
NOP1	102	VYIARGKEDLLVT	2	2	1.4522	0.1394	1	1	4.1335	0.0000
NOP1	109	EDLLVTKNMAPGE	6	2	1.6335	0.1858	3	2	4.8135	0.0501
NPP1	66	IVIGDAKDSRDGS	4	2	0.4810	0.2499	3	1	1.7859	0.0000
NTF2	53	AKDIVEKLVSLPF	3	1	0.4907	0.0000	3	2	1.9396	0.0581
NYV1	202	VSLLVDKTSQLNS	6	2	0.5973	0.0107	18	2	1.1436	0.0371
OSH3	548	ETPLLGKSDQNEF	12	1	0.2368	0.0000	2	2	2.0498	0.2269
PAB1	105	LNYTPIKGRLCRI	4	2	0.4958	0.0676	6	2	0.8218	0.0373
PDC1	562	TAATNAKQxxxxx	4	2	0.5785	0.0602	4	1	2.7993	0.0000
PDC1	269	YVGTLSKPEVKEA	2	1	0.1206	0.0000	4	1	1.2655	0.0000
PDR17	49	SEDQNEKYRAVLR	9	2	0.3823	0.1096	4	1	1.9431	0.0000
PDR5	825	RGVLTEKNANDPE	3	2	0.0782	0.1125	5	1	2.2620	0.0000
PGK1	258	GDSIFDKAGAEIV	14	2	-0.1335	0.0206	5	3	3.3623	0.0610
PGK1	351	KFAAGTKALLDEV	6	2	2.2958	1.1957	4	1	2.4475	0.0000
PGK1	244	MAFTFKKVLENTE	3	1	0.7561	0.0000	9	1	4.0701	0.0000
PHM7	990	DYEPEAKKxxxxx	6	2	2.5963	0.2509	1	1	1.8735	0.0000
PHO87	89	RKLFGSKTPSGSK	2	1	-0.2038	0.0000	7	1	1.8933	0.0000
PIN3	80	GLKPGDKVQLLEK	8	2	0.0309	0.0578	1	1	3.5924	0.0000
PIN3	76	DGDLGLKPGDKVQ	2	1	-0.0226	0.0000	5	2	2.9892	0.2551
PMA1	643	NDAPSLKKADTGI	8	2	-0.7440	0.0536	1	1	2.8145	0.0000
PMA1	444	DALTKYKVLEFHP	5	3	0.3407	0.1942	1	1	-0.0189	0.0000
PMR1	218	TSQTIEKSSFNDQ	6	2	0.0493	0.0057	6	2	2.4278	0.1187
PNO1	154	DPGALQKGADFIK	1	1	2.9409	0.0000	13	2	1.4640	0.0447
PUP3	70	NEMFRYKTNLYKL	2	2	2.1080	0.1070	6	4	0.6329	0.2088
RAS2	196	QTSQDTKGSGANS	4	2	0.5869	0.0711	7	2	0.8607	0.1545
RAX1	274	VGVTNEKSNRSRG	3	2	-1.1389	0.2028	7	1	-0.2891	0.0000
RNQ1	84	TLMADSKGSSQTQ	29	5	-0.3800	1.4225	3	1	0.8073	0.0000
RNR1	849	EVPAPTKNEEKAA	20	6	3.3799	1.0923	3	1	2.1417	0.0000
RPB2	344	GTALGIKKEKRIQ	1	1	1.8526	0.0000	4	2	1.2917	0.0569
RPL10	183	DRPEYLKKREAGE	3	2	-0.1941	0.0126	1	1	0.8881	0.0000

			PERMISSIVE TEMPERATURE				COLD-SHOCK			
Gene Symbol	Site Position	Motif Peptide	PT Spectral Counts	PT Num Quant	PT Median	PT St. Dev.	16C Spectral Counts	16C Num Quant	16C Median	16C St. Dev.
RPL11B	49	QTPVQSKARYTVR	11	2	0.5496	0.0469	4	1	3.5514	0.0000
RPL11B	164	DTVSWFKQKYDAD	4	2	0.9393	0.0773	1	1	-0.9365	0.0000
RPL12B	48	VGEDIAKATKEFK	6	4	2.1426	0.2071	2	1	0.3599	0.0000
RPL13B	81	FTLAEVKAAGLTA	16	4	1.4647	0.0801	12	2	-0.1875	0.1245
RPL13B	64	VRAPTVKYNRKVR	2	2	3.8195	0.2550	4	1	0.8328	0.0000
RPL14B	50	VLIDGPKAGVPRQ	1	1	1.1607	0.0000	1	1	1.2309	0.0000
RPL16A	114	IPPPYDKKKRVVV	11	3	3.8610	0.4760	4	2	0.9325	0.1086
RPL16B	31	QVLNGQKIVVVRA	5	2	3.2889	0.0478	1	1	2.1800	0.0000
RPL16B	133	RLKPGRKYTTLGK	1	1	2.9156	0.0000	4	1	2.5881	0.0000
RPL16B	113	IPPPYDKKKRVVV	7	3	2.8462	0.3266	2	2	2.2504	0.1641
RPL16B	169	SAEYYAKKRAFTK	1	1	2.8235	0.0000	1	1	2.7390	0.0000
RPL16B	65	KATAFNKTRGPFH	5	5	3.4254	0.3632	4	1	2.8928	0.0000
RPL17A	89	WPAKSVKFVQGLL	32	4	0.9395	0.0541	2	2	3.3329	0.3496
RPL17A	13	TSTNPAKSASARG	3	2	1.0664	0.1206	2	2	2.9281	0.3267
RPL17A	153	ELVVTEKEEAVAK	8	2	1.7598	0.1160	2	2	2.8329	0.2649
RPL17B	46	ELTKAQKYLDQVL	2	2	1.8756	0.0270	2	1	1.6538	0.0000
RPL18B	72	RIARALKQEGAAN	7	4	3.0106	0.1162	1	1	3.7182	0.0000
RPL18B	133	LAVRAPKGQNTLI	4	3	2.2059	0.0745	2	2	3.4052	0.0482
RPL19B	146	EHIIQAKADAQRE	19	5	2.6651	0.0663	1	1	0.3295	0.0000
RPL19B	108	LRRLLAKYRDAGK	2	2	1.9182	0.4477	6	2	3.2532	0.0952
RPL1B	18	HVKELLKYSNETK	3	2	-1.9199	0.7393	8	2	0.4872	0.0176
RPL20A	149	FLTKDLKFPLPHR	9	2	2.4343	0.0116	1	1	0.5130	0.0000
RPL20A	38	SNEVIAKSRYWYF	8	3	5.6692	0.2537	6	4	0.6047	0.0588
RPL20A	141	VKRQYVKQFLTKD	8	4	3.8437	0.5162	3	2	2.5535	0.1385
RPL21A	60	HKFYQGKTGVVYN	5	2	1.7892	0.1557	1	1	0.5820	0.0000
RPL21A	129	GVAVQLKRQPAQP	4	3	2.8634	0.5852	4	2	2.4463	0.0201
RPL24A	41	KSASLFKQRKNPR	5	3	2.7846	0.1210	1	1	1.6277	0.0000
RPL24A	77	RSRKTVKAQRPIT	4	1	2.1671	0.0000	4	3	0.2495	0.1429
RPL25	74	TSETAMKKVEDGN	37	10	1.9157	2.0004	3	2	-0.2888	0.1060
RPL27A	111	SQREEAKKVVKKA	14	4	3.7209	0.0789	8	6	0.5244	0.1190
RPL27A	126	ERHQAGKNQWFFS	1	1	0.2268	0.0000	4	2	0.9512	0.0720
RPL28	126	NVPVIVKARFVSK	7	3	1.4555	0.0751	6	4	0.6926	0.1222
RPL28	96	YLKSASKETAPVI	3	2	0.2815	0.1244	2	2	1.1791	0.2943
RPL2A	145	HNPDENKTRVRLP	12	4	2.6136	0.1138	5	2	0.9392	0.1508
RPL2A	92	QFIYAGKKASLNV	5	2	2.7511	0.1936	3	2	1.6044	0.0672
RPL2A	155	RLPSGAKKVISSD	4	4	4.5455	0.3405	8	2	0.4872	0.0299
RPL2A	46	YIRGIVKQIVHDS	2	2	4.5505	0.1815	3	1	3.7429	0.0000
RPL2A	177	GGGRVDKPLLKAG	1	1	4.5812	0.0000	4	4	1.0095	0.2807
RPL3	287	KIYRVGKGDDEAN	6	2	1.0541	0.1588	3	2	1.5022	0.7088
RPL30	83	LGTAVGKLFRVGV	12	2	1.6687	0.0495	4	3	1.7102	0.0384

			PERMISSIVE TEMPERATURE				COLD-SHOCK			
Gene Symbol	Site Position	Motif Peptide	PT Spectral Counts	PT Num Quant	PT Median	PT St. Dev.	16C Spectral Counts	16C Num Quant	16C Median	16C St. Dev.
RPL33A	92	RNNLPAKTFGASV	7	4	1.3633	0.0468	2	1	-0.6098	0.0000
RPL33A	12	RLYVKGKHLSYQR	3	2	1.9522	0.1373	1	1	1.1647	0.0000
RPL33A	10	SHRLYVKGKHLSY	4	2	1.8329	0.0506	6	3	2.0188	0.1558
RPL34A	106	IVKKVVKEQTEAA	4	3	2.9156	0.5449	1	1	2.4708	0.0000
RPL35B	25	SQLVDLKKELAEL	11	6	1.6978	0.2385	8	3	3.6732	0.3194
RPL38	21	TRRADVKTATVKI	8	6	2.0140	0.1267	2	2	0.5388	0.0016
RPL6A	19	EDVAALKKTRKAA	9	2	1.8240	0.0612	2	1	0.2642	0.0000
RPL6A	139	ERVEDQKVVDKAL	7	6	2.3922	0.4993	3	2	-0.2376	0.0310
RPL6A	108	NVEYFAKEKLTKK	12	4	2.2923	0.1110	10	4	2.4457	0.1597
RPL7A	14	TPESQLKKSKAQQ	1	1	0.2869	0.0000	4	2	-0.0827	0.0438
RPL9A	84	MITGVTKGYKYKM	21	5	1.3261	0.2300	2	2	2.4176	0.4645
RPO21	738	LAEVNLKDLNNVK	1	1	1.6215	0.0000	1	1	-0.2940	0.0000
RPO31	1249	SISTSAKEPSEND	1	1	-0.4146	0.0000	8	2	-0.8364	0.0342
RPS0B	52	HVINVGKTWEKLV	4	2	-0.1913	0.0243	5	1	1.6697	0.0000
RPS0B	88	GQRAVLKFAAHTG	3	2	0.9335	0.0945	2	1	0.4842	0.0000
RPS10B	52	LQSLTSKGYVKTQ	8	3	0.4053	0.1608	6	4	3.3678	0.1311
RPS11B	43	NAGLGFKTPKTAI	8	4	2.6051	0.1481	3	1	0.1648	0.0000
RPS11B	36	RTKRWYKNAGLGF	5	4	1.7161	0.7079	6	1	2.1730	0.0000
RPS11B	15	SERAFQKQPHIFN	1	1	1.0086	0.0000	5	4	2.0095	0.0931
RPS15	64	KKLRAAKLAAPEN	18	6	1.5450	1.9959	1	1	2.9823	0.0000
RPS16B	30	AGKGLIKVNGSPI	9	2	0.7729	0.1830	6	1	0.7236	0.0000
RPS17B	23	IERYYPKLTLDFQ	4	1	2.0271	0.0000	1	1	3.3813	0.0000
RPS17B	59	YTTHLMKRIQKGP	4	3	1.6512	0.0873	2	1	-0.4044	0.0000
RPS18A	96	NDITDGKDYHTLA	2	1	0.7706	0.0000	2	2	1.4666	0.1399
RPS1A	248	KKVTGFKDEVLET	1	1	-0.5721	0.0000	3	3	1.6184	0.3218
RPS1A	55	NKSTGLKSASDAL	4	2	1.6887	0.0426	2	1	-0.1695	0.0000
RPS1B	55	NKSTGLKNASDAL	3	2	2.0674	0.0917	2	1	2.4891	0.0000
RPS1B	248	KKVSGFKDEVLET	2	2	1.6859	0.3759	2	2	2.1365	0.0799
RPS1B	50	GKTLVNKSTGLKN	2	2	1.8820	0.0243	5	2	0.1878	0.0024
RPS2	33	PRNTEEKGWVPVT	16	4	-0.0940	0.0177	5	3	0.2796	0.0370
RPS20	43	VSSNIVKNAEQHN	11	3	0.1008	0.0825	4	2	1.6432	0.0052
RPS20	101	APVQIVKRITQIT	2	2	0.2626	0.1909	4	1	2.9867	0.0000
RPS21B	80	QNDGLLKNVWSYS	6	1	0.2828	0.0000	3	2	-0.0326	0.6295
RPS22A	88	KIGDIEKWTANLL	4	1	2.1427	0.0000	1	1	2.5188	0.0000
RPS25A	46	VILDQEKYDRILK	7	2	1.8744	0.0028	1	1	0.3945	0.0000
RPS31	6	xMQIFVKTLTGKT	15	8	2.3610	0.1884	4	2	0.7955	0.2024
RPS31	27	DTIDNVKSKIQDK	2	2	1.0047	0.0728	1	1	0.7051	0.0000
RPS31	29	IDNVKSKIQDKEG	50	3	2.4586	0.1318	1	1	0.6469	0.0000
RPS4B	198	IGTIVHKERHDGG	4	2	3.5382	0.0164	2	1	2.1696	0.0000
RPS4B	174	KITDFIKFDAGKL	10	4	3.0133	0.2412	1	1	3.4487	0.0000

			PERMISSIVE TEMPERATURE				COLD-SHOCK			
Gene Symbol	Site Position	Motif Peptide	PT Spectral Counts	PT Num Quant	PT Median	PT St. Dev.	16C Spectral Counts	16C Num Quant	16C Median	16C St. Dev.
RPS4B	134	KVQLGKKGVPYVV	3	2	1.8379	0.1071	2	1	0.5729	0.0000
RPS7B	83	LTRELEKKFPDRH	3	3	0.0643	0.0421	1	1	0.1836	0.0000
RPS7B	157	KVLLDSKDVQQID	2	2	0.7376	0.2061	1	1	0.0484	0.0000
RPT1	282	GSELVQKYVGEGA	2	2	2.9649	0.0886	1	1	1.7936	0.0000
RPT6	402	TAISVAKLFKxxx	3	1	-1.5032	0.0000	2	1	2.6799	0.0000
RVS167	242	NRLQDMKIPYFDL	16	2	-0.1137	0.0089	2	1	0.1463	0.0000
SAM3	63	EQTEQEKIQWKLA	2	1	-0.0384	0.0000	2	1	0.1744	0.0000
SNC1	63	LTSIEDKADNLAV	6	2	0.4587	0.1084	3	1	0.0400	0.0000
SNC2	62	LTSIEDKADNLAI	11	5	-0.2248	0.1899	1	1	-0.1860	0.0000
SSA2	504	ITITNDKGRLSKE	4	3	0.7552	0.3052	1	1	0.7433	0.0000
SSA2	497	GTGKSNKITITND	2	2	0.5657	0.0101	2	1	1.2333	0.0000
SSB2	497	KVTAVEKSTGKSS	1	1	-4.0941	0.0000	3	1	0.7286	0.0000
SSH4	99	LHSLFGKKHSGIL	3	2	0.3508	0.0138	2	2	2.9356	0.4149
SUP45	331	TIRYTFKDAEDNE	18	6	1.8954	0.1014	2	1	-0.4862	0.0000
SWI5	227	PQFLSPKRKISPA	5	2	2.1213	0.0559	4	2	-0.9469	0.2116
TDH3	213	SSTGAAKAVGKVL	18	4	1.6309	0.0638	1	1	2.9606	0.0000
TUB3	402	FDLMYAKRAFVHW	1	1	3.1782	0.0000	2	2	0.6861	0.0210
YDR261C-D	1199	RDTWNTKNMRSLE	3	1	2.0475	0.0000	2	1	-4.1235	0.0000
YDR261C-D	207	IPTVNGKPVRQIT	10	2	1.2316	0.0818	2	1	-4.1235	0.0000
YIL108W	518	SKYGFSKNVQGIK	7	4	2.0244	0.0270	1	1	0.6499	0.0000

Table 14: Sites That Have Been Quantified In Both Growth Conditions And Are Upregulated At Cold-shock

Sites that have been identified and quantified in both growth conditions and that are highly enriched after cold-shock stress. For each ubiquitinated site and its corresponding gene are shown the following items: the motif sequence, the number of identified spectral counts, the quantified number of spectral counts, the median (Log2 (H:L) ratio) and its corresponding standard deviation.